BOURDON TUBE STUDIES

BOURDON TUBE STUDIES

by

Edward Tong Lee, B.A.Sc.

A Thesis

Submitted to the Faculty of Graduate Studies

in Partial Fulfilment of the Requirements

for the Degree

Master of Engineering

McMaster University

May 1970

MASTER OF ENGINEERING (1970) McMASTER UNIVERSITY
Hamilton, Ontario

TITLE : BOURDON Tube Studies

AUTHOR : Edward Tong Lee, B.A.Sc. (U.B.C.)

SUPERVISOR : Professor G. KARDOS

NUMBER OF PAGES: xiii, 160

SCOPE AND CONTENTS

The objective of this study is to elucidate as much as possible the theory and analysis of BOURDON tubes. Both thick-walled and thin-walled tubes are considered.

Three papers, representative of the state-of-the-art of BOURDON tube analysis, are reviewed (References 1, 2, and 6):

1. WUEST, W., "Theory of High-Pressure BOURDON Tubes"
2. ANDREEVA, L.E., "Elastic Elements of Instruments"
3. DRESSLER, R., "Elastic Shell-Theory Formulation for BOURDON Tubes"

Reanalysis of (3) above, with a different approach (Appendix A) checked and completed the general formulation by DRESSLER. The final forms of all necessary equations, boundary conditions, etc. to the solution of the three governing equations of the BOURDON tube with an elliptical cross-section are given.

Comparison of results of ANDREEVA's sensitivity equation with test data of KARDOS, MASON and EXLINE (References 3, 4 and 5) using a qualitative approach as set out by KARDOS (References 3 and 17) showed good correlation.

The study concludes with recommendations for the approach of future research and preliminary design procedures for BOURDON tubes.

ACKNOWLEDGEMENT

Throughout the report suitable acknowledgement to works consulted or adopted has been made by references, but the author's chief debt is to Professor G. KARDOS of McMaster University who influenced the selections of this study and provided guidance to the completion of this thesis. The author is grateful to Professor G.A. ORAVAS of McMaster University and Professor R. DRESSLER of The City University of New York, Graduate Engineering School for their valuable suggestions. To his wife MARY, the author is indebted for her persevering support and encouragement in his completion of this study. Finally to Mrs. B. EHRICH the author gives thanks for her careful typing of this thesis.

CONTENTS

ILLUSTRATIONS

TABLES

CHAPTER 1

THE BOURDON TUBE

1.1 Introduction

Since E. BOURDON of PARIS, FRANCE (in 1852) introduced the pressure gage various approximative analyses have been suggested to predict the tube's performance. These analyses, however, showed differences between test data by as much as ±50%. It is therefore the objective of this study to elucidate as much as possible reasons for these discrepancies and the theory and analysis of BOURDON tubes.

1.2 Scope

In this thesis, methods representative of the state-of-the-art of BOURDON tube analysis are presented. Both thick and thin-walled tubes, with flat-oval and/or elliptic cross-sections, are considered.

The methods of analysis may be divided into three groups:

1. Empirical or Qualitative
2. Approximation
3. Exact

Currently, the first two methods are predominantly

used (References 1, 2, 3, 4, 5 and 17). It is only recently (due to the advances of the electronic computer) that the third method (Reference 6) of analysis can be conceived as a possibility.

Chapters 2, 3 and 4 reviews the methods of BOURDON tube analysis of the following papers (References 1, 2 and 6):

1. WUEST, W., "Theory of High-Pressure BOURDON Tubes"
2. ANDREEVA, L.E., "Elastic Elements of Instruments"
3. DRESSLER, R., "Elastic Shell-Theory Formulation for BOURDON Tubes"

Comparison of ANDREEVA's thin-walled tube analysis with experimental data of KARDOS, MASON and EXLINE (References 3, 4 and 5) using a qualitative approach (Reference 17) is discussed in Chapter 5. Supporting matters of the above with detailed analysis, computer program and data are given in the Appendices.

The final chapter concludes the findings of this study with recommendations for future research and preliminary design procedures for BOURDON tubes.

CHAPTER 2

THICK-WALLED TUBE ANALYSIS

2.1 W. WUEST - "Theory of High-Pressure BOURDON Tubes"

In Herr von W. WUEST's "Theory of High-Pressure BOURDON Tubes" (Reference 1), the characteristic ratio λ of the tube must fulfill the following requirement:

$$\lambda = \frac{a^2}{dR_o} < 1 \qquad (2.1)$$

where, a denotes the average semi-major axis of the oval cross-section

d denotes the wall thickness

R denotes the mean or tube radius of curvature

For then the deformation of the tube cross-section can be calculated without considering the effect or reaction of the annular stress $\Delta\sigma_x$ (composed of the tensile stress and the bending) at the very start. After that, a mere superposition of the effect of $\Delta\sigma_x$ is made when the change of curvature/or sensitivity is calculated.

With thick-walled BOURDON tubes (Figure 2.1), this requirement is always fulfilled.

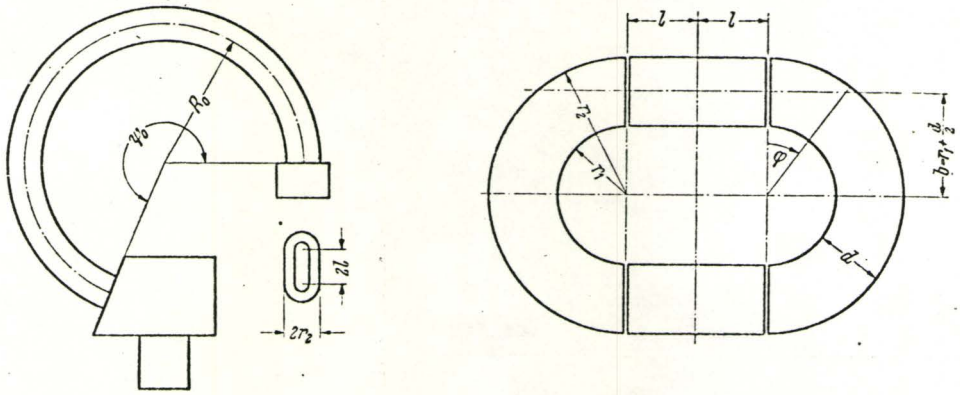

Figure 2.1 - WUEST's Flat-oval BOURDON Tube

Figure 2.2 illustrates the coordinate system used by

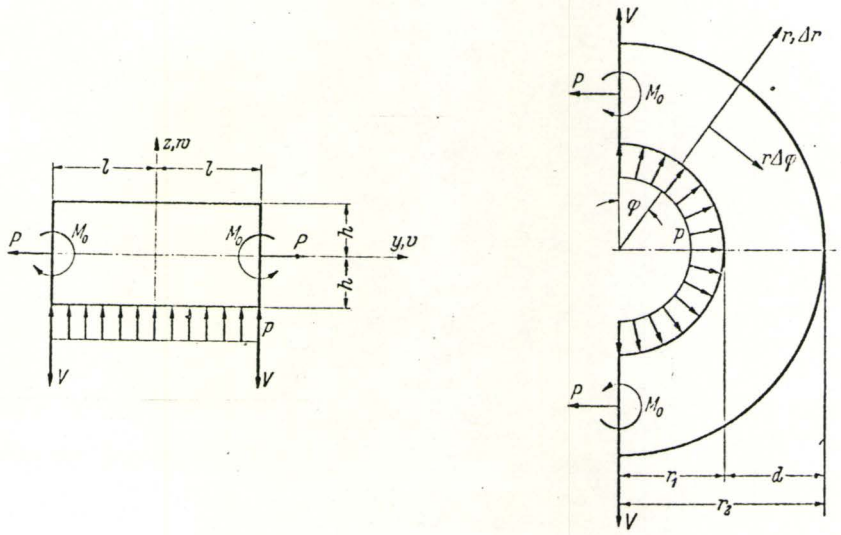

Figure 2.2 - Breakdown of Flat-oval BOURDON Tube, coordinate system (x, y, z), and forces and moments in the rectangular section and end arcs

WUEST and the breakdown of the flat-oval cross section, to determine w, into:

(a) a rectangular part

(b) and the two end arcs.

Thus based on this, the development simplifies to the solution of the biharmonic equations for the deformation or deflection w of the tube cross-sections as if the tube was straight (excluding torsion of the tube) and under a plane strain condition[1].

As the expressions for the deformation are not required at this time, they will not be presented here. Reference to their forms and development may be obtained in WUEST's paper, formulas (14), (14a) and (35).

2.2 Change of Curvature

Because of the curvature of the BOURDON tube, the deformation w produces "annular stresses". Expressing the "annular" strain of the tube as[2],

$$\varepsilon_x = \frac{w}{R_o} - \frac{\omega}{R_o}\,\bar{z} \qquad (2.2)$$

---

[1] c.f. C.T.WANG, "Applied Elasticity, McGraw-Hill, 1953 pp. 43, 44 - the plane strain equations

[2] c.f. this with ANDREEVA's "Elastic Elements of Instruments", Reference (2). Note that at this stage of WUEST's development the state of plane strain imposed previously is suspended, then $\sigma_x = \mu(\sigma_z+\sigma_y) + E\varepsilon_x$

with $\bar{z}$ designating the distance from the line of symmetry, see Figure 2.2

or $\bar{z} = z + r_1 + \frac{d}{2}$ in the straight section

$\bar{z} = r \cos \phi$ in the curved section

Then, the resulting moment over the cross section of the tube is

$$M = \iint_{F_1} \sigma_x' \, \bar{z} \, d F$$

where σ_x' denotes the net "annular" stress.

For zero external moment and $\sigma_x' = E\varepsilon_x$,

$$M = \iint_{F_1} \frac{w}{R_o} \bar{z} \, d F - \frac{\omega}{R_o} \bar{z}^2 \, d F = 0 \qquad (2.3)$$

From this the change of curvature ω is,

$$\omega = \frac{\int\int w \, \bar{z} \, d F}{\int\int \bar{z}^2 \, d F} \qquad (2.4)$$

Observe that when substituting the value of w as determined previously (for the case of a straight tube under a plane strain condition), the reaction or effect of that part of the annular stress $\Delta\sigma_x$ on the deformation of the cross section does not yet exist. However since $\lambda<1$, this effect can be merely appended to the above expression for ω .

Therefore, to evaluate ω^* the curvature change due

to the reaction of $\Delta\sigma_x = E\Delta\varepsilon_x$, consider $\Delta\varepsilon_x$ as

$$\Delta\varepsilon_x = \frac{\beta\bar{z}}{E} + \frac{\gamma}{E} \tag{2.5}$$

where $\beta = \omega E/R_o$ the bending stress of $\Delta\sigma_x$

$\gamma = (1-2\mu)(F_o/F_1)p$ the tensile stress of $\Delta\sigma_x$

$F_o = r_1^2\pi + 4\ell r_1$ the internal surface

$F_1 = (r_2^2-r_1^2)\pi + 4\ell(r_2-r_1)$ the cross-sectional area

μ = POISSON's ratio

Then its reaction in the transverse direction (using POISSON's ratio):

$$\Delta\varepsilon_y = \frac{\partial v^*}{\partial y} = -\mu(\Delta\varepsilon_x)$$
$$\Delta\varepsilon_z = \frac{\partial w^*}{\partial z} = -\mu(\Delta\varepsilon_x) \tag{2.6}$$

From these expressions and appropriate boundary conditions (see page 11 of WUEST's "Theory of High Pressure BOURDON Tubes") the deflection w^* may be determined. Then since change of curvature is defined as,

$$\omega^* = \frac{\int\int w^*\,\bar{z}\,d\,F}{\int\int \bar{z}\,d\,F} = -\frac{\mu\gamma}{E}\,J/J$$

where $J = 4/3\ \ell(r_2^3-r_1^3) + \pi/4\ (r_2^4-r_1^4)$, the moment of inertia of the cross-sectional area about the major axis,

$$\omega^* = - \frac{\mu\gamma}{E} \qquad (2.7)$$

Thus the change of curvature ω of the Flat-oval thick-walled BOURDON tube becomes:

$$\omega = \frac{\iint w\, \bar{z}\, d\, F}{\iint \bar{z}^2\, d\, F} + \omega^* \qquad (2.8)$$

2.3 Sensitivity Ratio: $\Delta R/R_o\ E/p$

In terms of the sensitivity ratio $\omega E/p \doteq \Delta R/R_o\ E/p$, equation (2.8) when evaluated becomes: (WUEST's equation (37))

$$\frac{\omega E}{p} = \frac{1}{J}\left\{\frac{4\ell^5 b}{d^2}\left[-0.819 - 0.5266\left(\frac{d}{\ell}\right)^2 + 0.0561\left(\frac{d}{\ell}\right)^4 - 0.0325\left(\frac{d}{\ell}\right)^4 \frac{r_1}{b} - 0.0379\left(\frac{d}{\ell}\right)^4 \frac{d}{b}\right] + \frac{4M_o}{pd^2}\ell^3 b\left[1.82-0.5\left(\frac{d}{\ell}\right)^2\right] + 4c_o bd\ell + \frac{1.3\pi}{p}\left[-\frac{(r_2^2-r_1^2)}{2} c_1 + 0.200\,(r_2^4-r_1^4)\, c_2 + (0.200(r_2^4 \ln r_2 - r_1^4 \ln r_1) + 0.0500(r_2^4-r_1^4))\, c_3 - (0.59982(r_2^5-r_1^5) + 1.7542\, r_1^2 r_2^2 (r_2-r_1))\, c_4\right]\right\} - \frac{\mu\gamma}{p} \qquad (2.9)$$

where $b = r_1 + d/2$, the average semi-minor axis

$$c_1 = 1/N[2r_1^2r_2^2 \ln(r_2/r_1)(r_1r_2p - 2M_o) - r_1^2r_2^2(r_2^2-r_1^2)p]$$

$$c_2 = 1/N\left\{-\frac{1}{2}\left[r_2^2-r_1^2+2(r_2^2 \ln r_2 - r_1^2 \ln r_1)\right](pr_1r_2-2M_o) + (1+2 \ln r_2)r_1^2r_2^2 \ln(r_2/r_1)p + r_1^2/2\,(r_2^2-r_1^2)p\right\}$$

$$c_3 = 1/N[(r_2^2-r_1^2)(pr_1r_2-2M_o) - 2r_1^2r_2^2 \ln(r_2/r_1)p]$$

$$N = (r_2^2-r_1^2)^2 - 4r_1^2r_2^2 \ln^2(r_2/r_1) \qquad (20)$$

WUEST's equations

$$c_4 = -\frac{p\,\ell}{2[(r_1^2+r_2^2)\ln(r_2/r_1) - (r_2^2-r_1^2)]} \qquad (25)$$

WUEST's equation

$$\frac{M_o}{d^2} = \frac{3.64(\ell/d)^3 - F\,\ell/d + G}{10.92\,\ell/d + H}\,p$$

$$d = 2h = r_2 - r_1$$

$$F = 0.026 + \frac{6.24(r_2^2-r_1^2) + 1.04(r_1^2+r_2^2)\ln(r_2/r_1)}{2[(r_1^2+r_2^2)\ln(r_2/r_1) - (r_2^2-r_1^2)]}$$

$$G = \frac{1.82\pi}{N}[(r_2^2-r_1^2)r_1r_2 - 2r_1^2r_2^2 \ln(r_2/r_1)] \qquad (29)$$

WUEST's equations

$$H = \frac{3.64\pi}{N} d^2(r_2^2-r_1^2)$$

$$c_o = [2.275(\ell/d)^4 + 1.384(\ell/d)^2 - 0.05043]d$$

$$- [5.46(\ell/d)^2 - 0.5]d\,M_o/(pd^2) + \left\{-\frac{\ln(r_2/r_1)}{r_2-r_1}c_1\right.$$

$$+ 0.4(r_1+r_2)c_2 + \left[\frac{0.4(r_2^2 \ln r_2 - r_1^2 \ln r_1)}{r_2-r_1}\right.$$

$$\left.\left. - 0.7(r_1+r_2)\right]c_3\right\} \times 1.3/p - 5.71(r_1^2+r_2^2)c_4/p$$

(35)

WUEST's equations

The following Table 2.1 (WUEST's Table 2) results from the evaluation of the sensitivity formula $\omega E/p$.

TABLE 2.1 Sensitivity, $\omega E/p$

$\frac{\ell}{d}$ \ $\frac{r_1}{d}$	0.25	0.50	1.00	1.50	2.00	2.50
0	0.1210	0.3425	0.8267	1.3005	1.7610	2.2087
0.1	0.2329	0.5312	1.2115	1.9014	2.6367	3.4183
0.25	0.5551	0.9943	1.9554	3.0309	4.2817	5.5675
0.5	1.3753	2.1305	3.7581	5.5394	7.8004	10.136
0.75	2.7650	4.1099	6.4126	9.2333	12.450	16.093
1.0	4.9370	6.6148	10.118	14.075	18.561	23.622
1.25	8.1309	10.389	15.084	20.339	26.903	32.911
1.5	12.613	15.522	21.533	28.238	37.755	44.158
2	26.642	30.915	39.849	49.801	60.974	73.347
3	85.431	91.074	105.726	123.110	142.794	176.398
4	205.878	210.281	227.162	251.215	280.040	353.199

Observe that the above curvature change or sensitivity expression does not depend on the tube's radius of curvature R_o . This is due to the straight tube approximation used in the analysis which is valid for thick-walled high pressure tubes with $\lambda<1$.

2.4 Corrections to the Curvature Change or Sensitivity Equation

Next WUEST incorporates corrections to the curvature change (equation 2.8) or sensitivity (equations 2.9) expres-

sion. The corrections are for:

(1) Eccentricity effect or deformation of the cross-sectional area during manufacturing

(2) the lengthening of the tube when under pressure.

In evaluating the correction for eccentricity, a simplifying assumption that the deformation of the tube should occur in an ideal plastic fashion is made. Therefore

$$\varepsilon_y = -\frac{1}{2}\,\varepsilon_x \qquad , \qquad \varepsilon_z = -\frac{1}{2}\,\varepsilon_x$$

with $\varepsilon_x = \bar{z}/R_o$, $\varepsilon_y = \partial v/\partial y$, $\varepsilon_z = \partial w/\partial z$.

From these relations and suitable boundary conditions, v and w may be determined - see WUEST's equations (38). Then after some operation WUEST gives the correction for the additional change in curvature, caused by the deformation of the cross-sectional area during production with the flat-oval BOURDON tube under pressure as (WUEST's equation (42)):

$$\omega_1 = -(1-2\mu)\,\frac{[M(r_2,\ell)-M(r_1,\ell)]\,\frac{F_o}{F_1} - M(r_1,\ell)}{J}\,R_o\,\frac{p}{E} \qquad (2.10)$$

With the moment of the surface of the deformed flat-oval cross-sectional area referred to the old axis of symmetry,

$$M(r,\ell) = \frac{1}{R_o}\left[\frac{r\ell^3}{3} - \ell r^2 + \frac{\pi}{4}\,r^2(\ell^2-r^2)\right] \quad , \quad r=r_1 \text{ or } r_2$$

Table 2.2 (WUEST's Table 3) shows numerical values for $-\omega_1 \frac{E}{p}$

TABLE 2.2 Eccentricity Correction, $-\omega_1 E/p$

$\frac{\ell}{d}$ \ $\frac{r_1}{d}$	0.25	0.5	1.0	1.5	2.0	2.5
0	0.0160	0.0450	0.1067	0.1654	0.2215	0.2759
0.1	0.0216	0.0518	0.1098	0.1722	0.2282	0.2925
0.25	0.0279	0.0601	0.1228	0.1814	0.2374	0.2918
0.50	0.0344	0.0697	0.1349	0.1945	0.2511	0.3056
0.75	0.0377	0.0754	0.1435	0.2050	0.2624	0.3178
1.00	0.0387	0.0771	0.1495	0.2144	0.2718	0.3281
1.25	0.0382	0.0792	0.1530	0.2188	0.2793	0.3368
1.50	0.0367	0.0784	0.1551	0.2230	0.2852	0.3441
2.00	0.0313	0.0735	0.1547	0.2270	0.2930	0.3547
3.00	0.0153	0.0545	0.1418	0.2222	0.2952	0.3634
4.00	-0.0043	0.0304	0.1190	0.2094	0.2852	0.3593

The second correction which WUEST suggests is the correction for the lengthening of the tube when it is under pressure. Via HOOK's law the lengthening correction, which is precisely the tensile strain due to the (internal) pressure acting against the face of the "end plug", is

$$E\varepsilon_x = \sigma_x - \mu(\sigma_y + \sigma_z)$$

$$= \gamma = (1-2\mu)\, F_o/F_1 p$$

or

$$\frac{\varepsilon_x E}{p} = (1-2\mu)\,\frac{F_o}{F_1} \qquad (2.11)$$

where F_o and F_1 are the internal surface and the cross-sectional areas respectively (see equations (2.5)).

Table 2.3 (WUEST's Table 4) shows the numerical values of equation (2.11) as a function of r_1/d and ℓ/d

TABLE 2.3 Correction for Length $\varepsilon_x E/p$

$\frac{\ell}{d}$ \ $\frac{r_1}{d}$	0.25	0.5	1.0	1.5	2.0	2.5
0	0.0167	0.0500	0.1333	0.2250	0.3200	0.4167
0.1	0.0232	0.0590	0.1442	0.2366	0.3319	0.4288
0.25	0.0313	0.0706	0.1589	0.2526	0.3487	0.4461
0.50	0.0415	0.0862	0.1800	0.2765	0.3742	0.4726
0.75	0.0491	0.0985	0.1977	0.2973	0.3970	0.4968
1.00	0.0549	0.1084	0.2128	0.3155	0.4174	0.5188
1.25	0.0596	0.1165	0.2258	0.3317	0.4359	0.5390
1.50	0.0633	0.1233	0.2371	0.3462	0.4527	0.5575
2.00	0.0691	0.1340	0.2558	0.3709	0.4820	0.5905
3.00	0.0766	0.1485	0.2827	0.4082	0.5279	0.6436
4.00	0.0810	0.1577	0.3012	0.4350	0.5622	0.6845

Hence with the two corrections the sensitivity or curvature change expression appears as

$$\text{SENSITIVITY} = \frac{\omega E}{P} + \frac{\omega_1 E}{P} - \frac{\varepsilon_x E}{P}$$

or

$$\frac{\omega_c E}{P} = \frac{(\omega_k - \varepsilon_x)E}{P} \qquad (2.12)$$

where ω_c denotes the curvature change with the corrections applied $(= \omega_k - \varepsilon_x)$

$\omega_k = \omega + \omega_1$

ω as defined in equation (2.9)

ω_1 as defined in equation (2.10)

ε_x as defined in equation (2.11)

Note that by incorporating the correction for length the assumption (as opposed to thin-walled analysis[3]) that the tube axis extends after deformation is involved. Therefore,

$$R\psi - R_o\psi_o = \varepsilon_x R_o\psi_o \qquad (2.13)$$

where R_o denotes the mean radius of curvature before deformation

ψ_o denotes the tube angle before deformation

R denotes the mean radius of curvature after deformation

ψ denotes the tube angle after deformation

---

[3] c.f. References (3), (4) and (5) where the relation is assumed: $R\psi = R_o\psi_o$ (with $R = \Delta R + R_o$, $\psi = \Delta\psi + \psi_o$) and therefore $-\Delta\psi/\psi_o = \Delta R/R_o$

ε_x denotes the lengthening of the tube in the direction of its axis

Further, since $R = R_o + \Delta R$ and defining ω_k (the curvature corrected for the effect of eccentricity) as

$$\omega_k = \omega + \omega_1 \sim \frac{\Delta R}{R_o}$$

then, $$R = R_o(1 + \omega_k) \qquad (2.14)$$

Substituting (2.14) into (2.13), ψ becomes:

$$\psi = \psi_o \frac{(1 + \varepsilon_x)}{(1 + \omega_k)} \qquad (2.15)$$

Since $1/(1 + \omega_k) \sim 1 - \omega_k$ and retaining only first order terms,

$$\psi \sim \psi_o(1 + \varepsilon_x - \omega_k)$$

With $\Delta\psi = \psi - \psi_o$, the change in angular movement,

then, $\Delta\psi = \psi_o(\varepsilon_x - \omega_k)$

or $-\Delta\psi = \psi_o(\omega_k - \varepsilon_x)$

Substituting $\omega_k = \omega + \omega_1$

$$-\frac{\Delta\psi}{\psi_o} = \omega + \omega_1 - \varepsilon_x$$

In terms of the sensitivity:

$$-\frac{\Delta\psi}{\psi_o}\frac{E}{p} = \omega\frac{E}{p} + \omega_1\frac{E}{p} - \varepsilon_x\frac{E}{p} \qquad (2.16)$$

Observe that the term $\Delta\psi = \psi - \psi_o$ is a negative quantity, as $\psi < \psi_o$ after uncoiling - c.f. with equation (2.12). Further observe that without the corrections for eccentricity ω_1 and for lengthening of the tube ε_x equation (2.16) reduces to that of the thin-walled tube analysis - $-\Delta\psi/\psi_o\ E/p = \Delta R/R_o\ E/p$, see footnote No. 3.

Figure 2.3 (or WUEST's Figure 11) illustrates $\omega E/p$ (solid lines) and $-\Delta\psi/\psi_o\ E/p$ (dashed lines) as a function of ℓ/d and r_1/d .

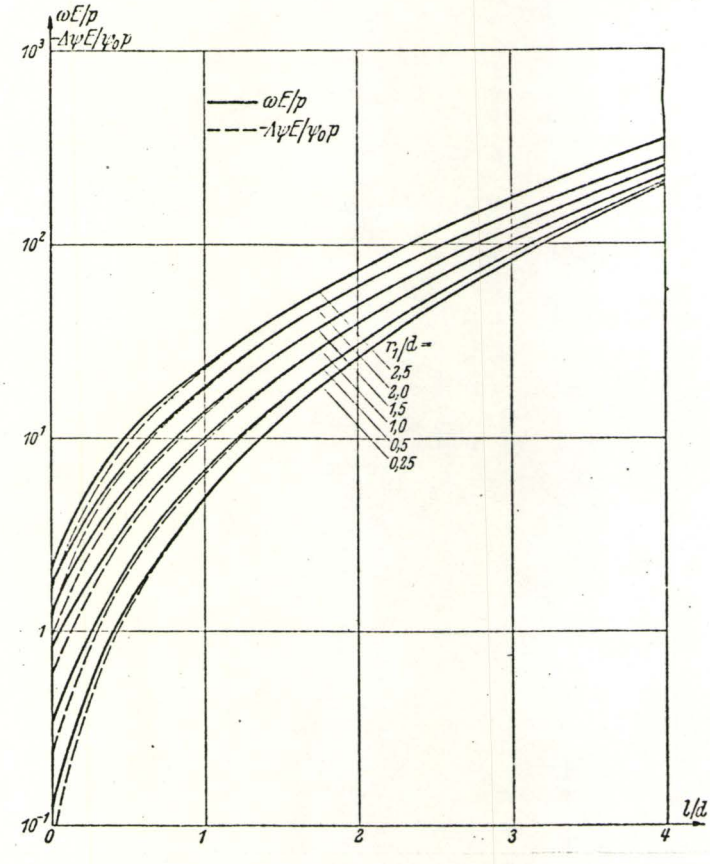

Figure 2.3 - Sensitivities $\omega E/p$ (solid curves) and $-\Delta\psi/\psi_o\ E/p$ (dashed lines) as a function of ℓ/d and r_1/d

It can be seen that the difference between the two curves is noticeable only for values of $\ell/d < 1$.

2.5 Deflection of Tube End

Two approaches to the determination of the deflection of the tube end are discussed next by WUEST. The first of these involves evaluating initial and final coordinates of the tube end[4]. Then

$$S = \sqrt{(x_E - x_{E_o})^2 + (y_E - y_{E_o})^2}$$

where x_{E_o} = initial x-coordinate of the tube end before deformation

$= -R_o \sin \psi_o$

y_{E_o} = initial y-coordinate of the tube end before deformation

$= R_o(1 - \cos \psi_o)$

x_E = final x-coordinate after deformation

$= -R \sin \psi$

y_E = final y-coordinate after deformation

$= R(1 - \cos \psi)$

with R as defined in equation (2.14)

ψ as defined in equation (2.15)

---

[4] c.f. MASON, H.L., "Sensitivity and Life Data on BOURDON Tubes", ASME paper No. 54-A-169

or,

$$S = R_o\omega_k\left[(2 + \psi_o^2 - 2\psi_o \sin\psi_o - 2\cos\psi_o) - 2\frac{\varepsilon_x}{\omega_k}(\psi_o^2 - \psi_o\sin\psi_o) + (\frac{\varepsilon_x}{\omega_k})^2 \psi_o^2\right]^{\frac{1}{2}} \qquad (2.17)$$

Equation (2.17) thus determines the tube end deflection - the tube end, to which this formula refers, is the theoretical tip of the tube.

However, as WUEST states that in practical application the tube end is not usually taken from the theoretical tip of the tube, it is more correct to calculate the path of the tube from the relation:

$$S = k' \Delta\psi$$

where k' denotes the pole ray, a distance measured from the polar point (a point about which a plane fastened to the tip of the tube turns for small changes in pressure) to the actual place at which the movement is measured.

$\Delta\psi$ as determined from Figure 2.3.

To determine the pole ray k' , the coordinates of the polar point (x_{p_o} , y_{p_o}) must first be calculated. These are given by WUEST as:

$$x_{p_o} = - R_o \frac{1 - \cos\psi_o}{\psi_o} \frac{\omega_k}{\omega_k - \varepsilon_x}$$

$$y_{p_o} = R_o \left(1 - \frac{\sin \psi_o}{\psi_o} \frac{\omega_k}{\omega_k - \varepsilon_x}\right) \tag{2.18}$$

Then either graphically or analytically, k' may be determined.

Figure 2.4 shows various position of the polar point as a function of ψ_o and ε_x/ω_k.

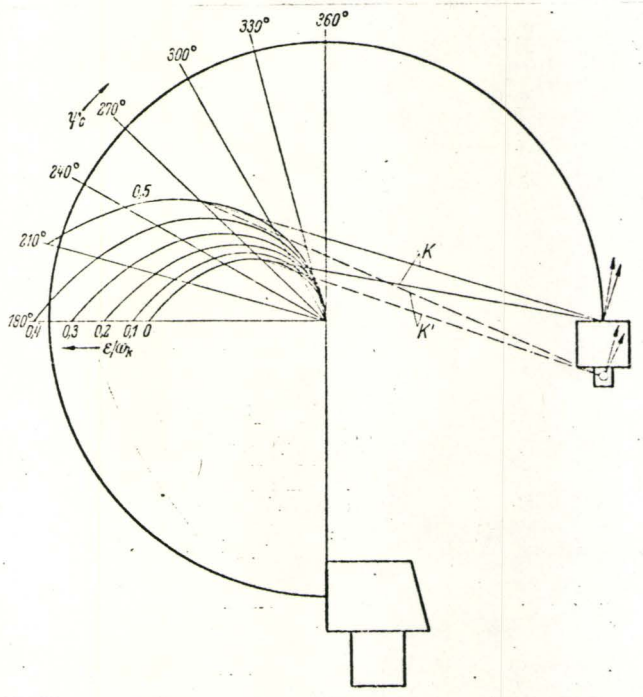

Figure 2.4 - Position of the Polar Point as a Function of ψ_o and ε_x/ω_k

As an example, for $\psi_o = 270°$ and $\varepsilon_x/\omega_k = 0$ and 0.5, the pole rays k (measured to the theoretical tip of the tube) and k' (measured to the actual tip of the tube) may be located.

2.6 WUEST's Results

Finally, WUEST compares his theory of high pressure BOURDON tubes with two examples. Table 2.4 and 2.5 give the data.

TABLE 2.4 U-shaped Steel Tube

R_o = 44mm ; k' = 75mm ; $\psi_o = \pi$; E = 2.1×10^6 kg/cm^2

p kg/cm^2	d mm	r_1 mm	ℓ mm	σ_v kg/mm	$\frac{\Delta\psi}{\psi}\frac{E}{p}$	$\frac{\Delta\psi}{\psi} 10^3$	S (calc.) mm	S (meas.) mm
800	2	1.80	2.75	111	18.0	6.86	1.62	1.58
1000	2.25	1.85	2.65	113	11.8	5.62	1.32	1.65
1600	2.5	2.00	2.45	152	8.4	6.40	1.48	1.58
2000	2.75	2.10	2.25	155	5.8	5.52	1.30	1.44

TABLE 2.5 Highest Pressure Tubes

R_o = 92mm ; k' = 120mm ; ψ = 250° = 4.36 ; E = 2.1×10^6 kg/cm^2

p kg/cm^2	d mm	r_1 mm	ℓ mm	σ_v kg/mm	$\frac{\Delta\psi}{\psi}\frac{E}{p}$	$\frac{\Delta\psi}{\psi} 10^3$	S (calc.) mm	S (meas.) mm
6000	5.2	0.95	2.35	300	0.82	2.34	1.22	1.14
6000	7.0	1.65	2.35	278	0.88	2.52	1.32	0.98
6000	7.0	1.65	2.35	278	0.88	2.52	1.32	1.05
8000	4.85	0.78	1.77	354	0.57	2.17	1.13	0.84
8000	5.1	0.65	2.00	386	0.50	1.90	1.00	1.05
8000	6.4	0.85	2.49	383	0.54	2.05	1.07	1.00

It can be observed from Tables 2.4 and 2.5 that there is a percentage error of approximately 9% to 30% between the measured and calculated values[5].

Also presented by WUEST is an example of a very thick-walled tube of a circular cross-section. Equations for this special case are derived (see WUEST's equations 46-49) and results showed a reduction of the error by 70%.

---

[5] σ_v denotes maximum stress of the tube (see WUEST's equations (30) - (33) for its derivation.

CHAPTER 3

THIN-WALLED TUBE ANALYSIS, APPROXIMATION METHOD

3.1 L.E.ANDREEVA - "Elastic Elements of Instruments"

In L.E.ANDREEVA's theory of thin-walled BOURDON tubes (Reference 2), both elliptical and flat-oval cross-sections are considered. The analysis is based on the minimization of the total potential energy of the BOURDON gage in accordance with the RITZ's method. The total potential energy here, is defined as the sum of the potential energy of deformation and the energy of position of the external forces.

3.2 Assumptions and Hypothesis

To determine the total potential energy of the gage the following hypotheses and assumptions are utilized:

(1) All tube elements, cut off by cross-sections normal to the central axis, operate under identical conditions. The influence of the end connections is neglected.

(2) The hypotheses used in the theory of shells, which assumes no transverse compression and a constant normal, are assumed to be valid.

(3) It is assumed that the axis of the tube is not

stretched.

(4) The tube wall thickness is small compared with the minor semi-axis of the cross-section (h<<b) , and the semi-axis b is small compared with the radius of curvature R of the central axis (b<<R) . (see Figure 3.1)

(5) The tube section is symmetrical relative to the x and y axes.

(6) The tube cross-section is assumed to deform in approximately the same way as is the contour of a straight tube subjected to internal pressure.

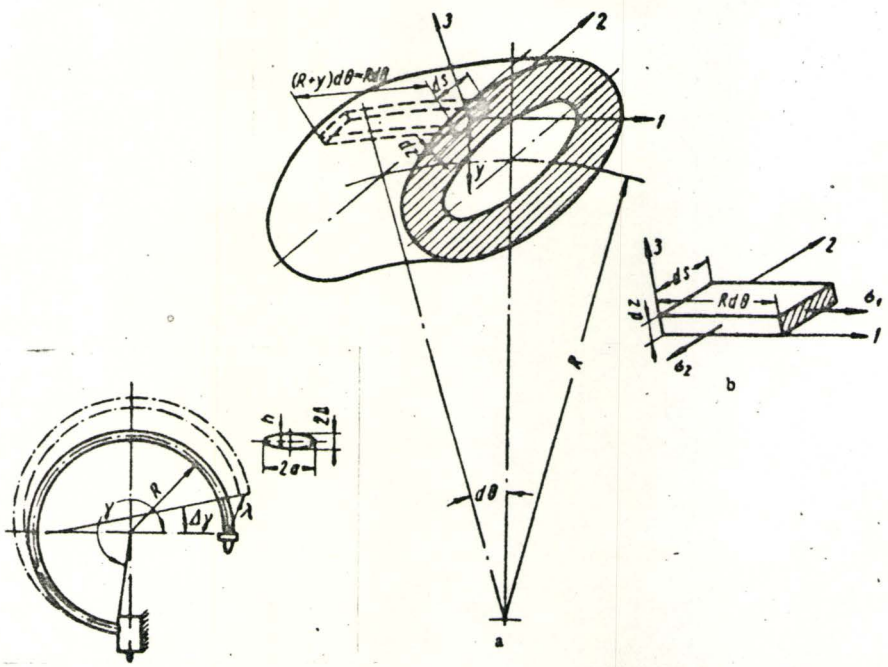

Figure 3.1 - Coordinate System and Stress System

(7) The deformations due to the stretching of the mean contour as a whole are neglected since they are small compared with the bending deformations.

3.3 Total Potential Energy

From the above conditions it can be seen that the specific potential energy u, expressed through the deformation components, is a result of a biaxial stress system:

$$u = \frac{E}{2(1-\mu^2)} (\varepsilon_1^2 + \varepsilon_2^2 + 2\mu\varepsilon_1\varepsilon_2) \qquad (3.1)$$

where ε_1 denotes the longitudinal strain

ε_2 denotes the lateral strain

E denotes elastic modulus of the tube material

μ denotes the POISSON's ratio

Then with the strains ε_1 and ε_2 expressed as (see Reference 2 for derivation)

$$\varepsilon_1 = \frac{w - y\frac{\Delta\gamma}{\gamma}}{R} \quad ; \quad \varepsilon_2 = z\,\Delta x \qquad (3.2)$$

where w = projection of displacement of the cross-section on the y-axis

γ = central angle of the tube

$\frac{\Delta\gamma}{\gamma}$ = relative angle of rotation of the end section

Δx = curvature change of contour of cross-section

and the energy of position of the external forces,

$$T = p\,\Delta V \quad , \quad \Delta V = \Delta f\, R\gamma$$

where ΔV is the volume change of the tube cavity,

Δf is the change in the area delimited by the mean contour of the cross-section,

p is the internal pressure

the total potential energy of the gage becomes:

$$W = u\,dv + (-T)$$

where $dv = R\,d\theta\;ds\;dz$ (due to assumption (4); c.f. in shell theory LOVE's First Approximation).

Therefore after integration with respect to z :

$$W = \frac{Eh\gamma}{2R(1-\mu^2)} \int_0^S \left[(w - y\,\frac{\Delta\gamma}{\gamma})^2 + \frac{R^2h^2}{12}\,(\Delta x)^2\right] ds - p\Delta f\, R\gamma \qquad (3.3)$$

To reduce the number of unknowns in equation (3.3), ANDREEVA establishes a relationship between three of the unknowns:

w = the deflection in the direction of the minor axis of the cross section of an arbitrary point on the section contour

Δx = the change in the curvature at an arbitrary point on the mean contour of the cross section

Δf = the change in the area delimited by the mean contour

in accordance with the assumption, that the BOURDON tube

cross section is deformed in approximately the same way as is the contour of a straight tube subjected to internal pressure - for a detail analysis see Reference 2, page 322. After some operations the expression for the total potential energy becomes,

$$W = \frac{2Eha\gamma}{R(1-\mu^2)} \left[\frac{w_o^2}{m^2} A_1 - 2b \frac{w_o}{m} \frac{\Delta\gamma}{\gamma} A_2 + b^2 \left(\frac{\Delta\gamma}{\gamma}\right)^2 A_3 + \frac{x^2}{12} \frac{w_o^2}{m^2} n \right]$$

$$- 2p \frac{w_o}{m} a \left(1 - \frac{b^2}{a^2}\right) n R \gamma \qquad (3.4)$$

where x = the principal parameter of the BOURDON tube

$= \frac{Rh}{a^2}$ (c.f. WUEST's $\lambda = \frac{a^2}{Rh}$)

A_1 , A_2 , A_3 , m , n are parameters depending on the shape of the BOURDON tube cross section - elliptic or flat-oval (Reference 2, page 324)

The two unknowns w_o , the increase in the length of the minor semiaxis of the cross section, and $\Delta\gamma/\gamma$, the relative angle of rotation of the end section, are then determined from the condition of minimum total potential energy in accordance with the RITZ's method:

$$\frac{\partial W}{\partial w_o} = 0 \quad ; \quad \frac{\partial W}{\partial \left(\frac{\Delta\gamma}{\gamma}\right)} = 0 \qquad (3.5)$$

3.4 Sensitivity Equation for Thin-Walled Tubes

Simultaneous solution of equation (3.5) gives the relative angle of rotation of the tube end under pressure p :

$$\frac{\Delta\gamma}{\gamma} = p \frac{(1-\mu^2)}{E} \frac{R^2}{bh} \left(1 - \frac{b^2}{a^2}\right) \frac{\alpha}{\beta+x^2} \qquad (3.6)$$

where α and β are functions of the parameters A_1 , A_2 , A_3 , m and n ; x is the principal parameter of the BOURDON tube $= Rh/a^2$.

Numerical values of the coefficients α and β for various axis-length ratio a/b are given in TABLE (3.1) for tubes with elliptical and flat-oval cross-sections.

The tube sensitivity is then obtained by solving for $\Delta\gamma/\gamma \; E/p(1-\mu^2)$ from equation (3.6). Observe that the factor $(1-\mu^2)$ is included in the sensitivity in this case so that the right-hand side of the expression is a function of the tube geometry only. Therefore,

$$\frac{\Delta\gamma}{\gamma} \frac{E}{p(1-\mu^2)} = \frac{R^2}{bh} \left(1 - \frac{b^2}{a^2}\right) \frac{\alpha}{\beta+x^2} \qquad (3.7)$$

TABLE 3.1 Coefficients α , β

Cross section shape	$\frac{a}{b}$	1	1.5	2	3	4	5	6	7	8	9	10	∞
Flattened 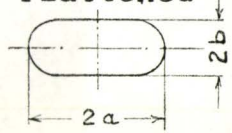	α	0.637	0.594	0.548	0.480	0.437	0.408	0.388	0.372	0.360	0.350	0.343	0.267
	β	0.096	0.110	0.115	0.121	0.121	0.121	0.121	0.120	0.119	0.119	0.118	0.114
Elliptical 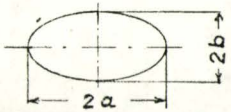	α	0.750	0.636	0.566	0.493	0.452	0.430	0.416	0.406	0.400	0.395	0.390	0.368
	β	0.083	0.062	0.053	0.045	0.044	0.043	0.042	0.042	0.042	0.042	0.042	0.042

For flat-oval BOURDON tubes that do not satisfy the condition that the wall thickness h is considerably smaller than the length b of the minor semiaxis of the section, ANDREEVA suggests the possible use of a thick-walled (with a very flat elongated cross section) tube formula as obtained by FEODOS'EV[1] by applying the energy method:

$$\frac{\Delta\gamma}{\gamma} = p\,\frac{1-\mu^2}{E}\,\frac{R^2}{bh}\,\frac{1-\varkappa}{\varkappa + \frac{h^2}{12b^2}} \qquad (3.8)$$

The coefficient $\varkappa$ is defined as

$$\varkappa = \frac{1}{ca}\,\frac{sh^2\,ca + \sin^2 ca}{sh\,ca \cdot ch\,ca + \sin ca \cdot \cos ca}$$

where a = the major semiaxis

$$c = \sqrt[4]{\frac{3}{R^2h^2}}$$

3.5 Deflection of the Tube End

To calculate the deflection of the BOURDON tube, ANDREEVA employs the simplification that the tube end deflects in a manner similar to that of a curved beam. Then with the aid of the MOHR integral (see Reference 2 pp. 327-328) the

---

[1] FEODOS'EV, V.I., "Uprugie elementy tochnogo priborostroeniya" (The Use of Elastic Elements in Manufacture of Precision Instruments) - Oborongiz 1949.

tube end deflection becomes:

$$\lambda = \frac{\Delta\gamma}{\gamma} R \Gamma \qquad (3.9)$$

where $\Gamma = \sqrt{(1-\cos\gamma)^2 + (\gamma-\sin\gamma)^2}$

$\frac{\Delta\gamma}{\gamma}$ = equation (3.6) or (3.8)

3.6 ANDREEVA's Comparison with Experimental Results

Table 3.2 illustrates some results of MASON's experimental compilation (Reference 4) and those obtained by use of formula (3.7) for thin-walled flat-oval tubes and formula (3.8) for thick-walled flat-oval tubes. ANDREEVA observes that equation (3.7) for thin-walled flat-oval tubes gives satisfactory correlation with the experimental results for tubes which satisfy the condition that: $h \ll b$. Therefore tubes No. 47, 50 and 252 to 256 are not applicable as this condition is not satisfied. On the other hand, the calculations using equation (3.8) gives reasonable results only for the last four tubes, since in these tubes: $h \ll b$ (thick-walled) and $a/b > 8$ (a rather flat cross section).

TABLE 3.2

Comparison of the experimental and calculated values of Bourdon tube sensitivities

Sample No. according to /96/	p, kg/cm²	Material	R_1, mm	γ^0	h_1, mm	a_1, mm	b_1, mm	$\frac{a}{b}$	$\frac{h}{b}$	Sensitivity $\frac{\Delta\gamma}{\gamma}\frac{E}{p(1-\mu^2)}$				
										Experimental	Calculated by formula ( )	Error, %	Calculated by formula ( )	Error, %
22	2.11	Phosphor bronze	52.3	241	0.381	10.4	3.05	3.40	0.125	7200	5870	18.5	4550	37
25	4.22		41.1	228	0.431	10.4	3.02	3.44	0.143	4000	3380	15.5	2760	31
26	4.22		52.3	241	0.534	10.4	3.17	3.28	0.168	3800	3340	12.1	2210	42
29	7.03		41.1	228	0.534	10.5	3.12	3.36	0.171	2400	2460	−2.5	1860	22.5
30	7.03		52.3	241	0.660	10.5	3.22	3.26	0.205	2300	2280	0.87	1620	30
46	141	Beryllium bronze	18.3	245	0.559	3.30	0.914	3.62	0.612	230	250	−8.7	153	33.5
47	98.5		18.0	250	0.559	3.42	0.584	5.85	0.957	360	402	−11.7	275	29
50	352		18.3	250	0.812	3.04	0.890	3.42	0.913	57	66	−15.8	39	31
51	352		18.8	250	0.812	2.92	1.17	2.50	0.694	39	44	−12.8	27	30
53	281		20.8	300	0.762	2.97	1.22	2.44	0.625	53	54	−2.3	32	39
250	7.03	Phosphor bronze	19.9	1800	0.305	4.70	0.685	6.86	0.443	3440	3240	5.8	2470	28.2
251	14.06		19.9	1800	0.407	4.70	0.635	7.40	0.639	1890	1980	−4.8	1410	25.4
252	28.12		19.9	1800	0.508	4.62	0.584	7.91	0.869	1030	1260	−22.4	864	16.3
253	42.18		19.9	1800	0.610	4.57	0.508	9.00	1.20	665	880	−17.3	584	12.2
255	56.24	Stainless steel	19.9	1800	0.407	4.57	0.381	12.0	1.07	2335	2900	−24.2	1980	15.2
256	56.25		19.9	1800	0.610	4.44	0.508	8.74	1.20	654	810	−23.8	542	16.9

CHAPTER 4

THIN-SHELL TUBE ANALYSIS

4.1 R.DRESSLER "Elastic Shell-Theory Formulation for BOURDON Tubes"

A formulation for BOURDON tube with an elliptical cross-section (Reference 6) by R. DRESSLER essentially uses the linear shell equations as derived by LOVE (Reference 7), with the exception of one expression - the twist, in which he favours E. REISSNER's twist equation[1], as it is symmetrical. From an overall view, the formulation of the problem is adequately complete, considering the limited space allotted in a paper. However there still remain a considerable task in order to arrive at the final expressions such as (A.51) or Table A.1 and the boundary conditions. Therefore in the sections that follows, a detailed analysis and comment on DRESSLER's approach to the problem, approximations and assumptions used, and a check of his expressions as compared with the directed derivative/vector method (Appendix A) will be made.

---

[1] E.REISSNER, "New Derivation of the Equations for Deformation of Elastic Shells", American Journal of Mathematics, Vol. 63, 1941.

4.2 Geometry of Toroidal Surface

A general description of the BOURDON gage is presented (refer to Figure A.7) - defining the parameters α and β, the radius of the torus ρ and the semidiameters of the ellipse $\bar{a}$ and $\bar{b}$ [2]. From these, the parametric equations which define the lines of principal curvature on the central shell surface are given: (c.f. with equations (A.1))

$$\begin{aligned} X &= (\rho + \bar{a}\cos\alpha)\cos\beta \\ Y &= (\rho + \bar{a}\cos\alpha)\sin\beta \\ Z &= \bar{b}\sin\alpha \end{aligned} \qquad (4.1)$$

The orthogonality condition and the classification of the parametric lines α and β as lines of principal curvature are next discussed according to the vanishing of the quantities F and M from the first and second fundamental forms respectively:

$$ds^2 = A^2 d\alpha^2 + 2F d\alpha d\beta + B^2 d\beta^2$$

where
$$\begin{aligned} A(\alpha) &= (\bar{a}^2\sin^2\alpha + \bar{b}^2\cos^2\alpha)^{\frac{1}{2}} \\ B(\alpha) &= \rho + \bar{a}\cos\alpha \\ F &= 0 \end{aligned} \qquad (4.2)$$

From
$$HM = (\bar{r}_1 \times \bar{r}_2) \cdot \bar{r}_{12} \quad , \quad M = 0 \qquad (4.3)$$

---

[2] For a compact discussion of differential geometry refer to: C.T.WANG, "Applied Elasticity", McGraw-Hill, 1953, pages 310 to 322.

where, $H^2 = A^2B^2 - F^2$

$\frac{\partial r}{\partial \alpha}$, $\frac{\partial r}{\partial \beta}$, and $\frac{\partial^2 \bar{r}}{\partial \alpha \partial \beta}$ are denoted by $\bar{r}_1$, $\bar{r}_2$, and $\bar{r}_{12}$ respectively.

$\bar{r}$ is defined as the radius vector.

Observe the following equivalence (c.f. equations (A.21) to (A.23)):

$$A(\alpha) = |\bar{g}_\alpha| \quad , \quad B(\alpha) = |\bar{g}_\beta| \quad , \quad F = g_{\beta\alpha}$$

$\bar{r}_1$, $\bar{r}_2 = \bar{g}_\alpha$, $\bar{g}_\beta$ respectively

$\bar{r} = \bar{r}^0$ the position vector to the middle surface

$M = K_i^{(t)}$ $(i = 1, 2)$

The radii of principal curvature R_α and R_β are calculated from:

$$R_\alpha(\alpha) = \frac{A^2}{\bar{a}\ \bar{b}} \qquad (4.4)$$

$$R_\beta(\alpha) = \frac{AB}{\bar{b}\ \cos\alpha}$$

(The above are equal to $1/K_\alpha^{(n)}$ and $1/K_\beta^{(n)}$ respectively - c.f. equations (A.23))

Thence, the following relations are given:

(a) $k_1 = \frac{1}{R_\alpha}$, $k_2 = \frac{1}{R_\beta}$ (defined as "principal curvatures")

(b) $\frac{1}{A} = a$, $\frac{1}{B} = b$, $\frac{1}{AB} = p$

The above, therefore, illustrates the differential geometry of the shell surface as presented in Reference (6). In terms of these symbols then, the analysis in elastic shell theory proceeds.

4.3 Elastic-Shell Theories

In order to compare formulas with the directed vector method (Appendix A), differences in coordinate systems and conventions will first be discussed. Figure 4.1 shows the two local or moving coordinate systems and the positive

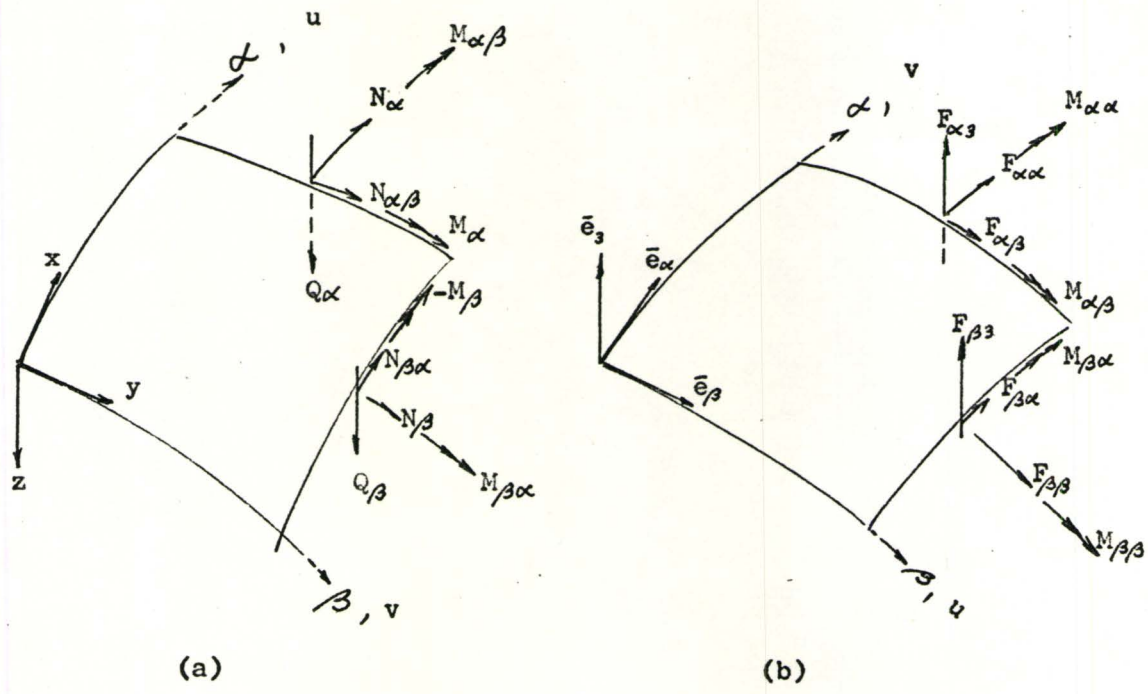

Figure 4.1 - Local or Moving Coordinate Systems:
(a) DRESSLER-LOVE's System
(b) Directed Vector System

directions of the stress resultants and stress couples: (a) DRESSLER-LOVE's system (b) Directed vector system. Observe that LOVE considered the displacement w to be positive if it was directed along the interior normal (i.e., toward the centre of curvature for the case of a sphere); whereas the directed vector method (Appendix A) considered the positive displacement w in the direction of the exterior normal (i.e., from the centre of curvature for the case of a sphere - this particular case denotes a shell with positive Gaussian curvature k_g ; see equation (A.24). Because of LOVE's convention, DRESSLER's displacements u and v will correspond to v and u , respectively, of the directed vector method. Further, from Figure 4.1(a) and (b) the correspondence between the stress couples can be determined. This correspondence is set out in Table 4.1. The difference in subscripts of the stress couples is due to LOVE's naming

DIRECTED VECTOR METHOD	DRESSLER-LOVE's SYSTEM
M_{11}	$M_{\beta\alpha}$
M_{12}	$-M_{\beta\beta}$
M_{21}	$M_{\alpha\alpha}$
M_{22}	$M_{\alpha\beta}$

TABLE 4.1 Correspondence between Stress Couples

of the stress couples in the manner: (c.f. equations (A.41))

$$M_{ij} = \int_{\alpha_3} \alpha_3 \sigma_{ij}(1 + \alpha_3 k_{rr}) d\alpha_3$$

Therefore when formulas of Reference (6) are compared with those of the directed vector method (Appendix A) the following are to be noted: Signs for the displacement w ; the transverse stress resultants Q_α and Q_β ; and the correspondence (Table 4.1) between the stress couples.

Thus having defined the local coordinate system (x,y,z) and the positive directions of the stress resultants N_{ij} and stress couples M_{ij} , DRESSLER presents LOVE's equations for strains as a function of the Z-coordinate in a linear form (i.e., LOVE's First Approximation):

$$\begin{aligned} \varepsilon_\alpha &= \varepsilon_{\alpha^0} - ZK_\alpha \\ \varepsilon_\beta &= \varepsilon_{\beta^0} - ZK_\beta \\ \varepsilon_{\alpha\beta} &= \varepsilon_{\alpha\beta^0} - 2ZK_{\alpha\beta} \end{aligned} \qquad (4.5)$$

where ε_{α^0} , ε_{β^0} , and $\varepsilon_{\alpha\beta^0}$ are the strains at the middle surface of the shell

K_α , K_β are the curvature changes

$K_{\alpha\beta}$ is the twist

Observe that the above strain equations are comparable to those of equations (A.25) and (A.26). Apart from the negative

sign associated with the variable z-coordinate, the only difference is DRESSLER's definition of $\varepsilon_{\alpha\beta^0}$ which LOVE (Reference 7, pages 517 and 529) defines as ϖ

or,

ϖ = cosine of the angle χ between tangents of the curve α and β or the shearing strain at the middle surface

Therefore it should be noted that DRESSLER's (total shearing strain) $\varepsilon_{\alpha\beta}$ is equal to twice that of the (tensorial) strain component as defined in equations (A.25) or (A.26); or (to avoid confusion) consider γ to represent the shearing strain

$$\gamma = \varpi - z\ 2\ K_{\alpha\beta}$$

Then since $$\varepsilon_{\alpha\beta} = \frac{1}{2}\gamma$$

$$\frac{1}{2}\gamma = \frac{1}{2}(\varpi - z\ 2\ K_{\alpha\beta})$$

or $$\varepsilon_{\alpha\beta} = \frac{1}{2}\varpi - z\ K_{\alpha\beta}$$

$$= \varepsilon^0_{\alpha\beta} - z\ K_{\alpha\beta}$$

This final expression then is comparable to that as shown in equations (A.25) or (A.26).

Next in terms of the rotation components,

$$\omega_\alpha = b\ w,_\beta + k_2 v$$

$$\omega_\beta = -\ a\ w,_\alpha - k_1 u \qquad (4.6)$$

the curvature changes and twist are given:

$$K_\alpha = - a\omega_{\beta,\alpha} + p\, A,_\beta \omega_\alpha$$

$$K_\beta = b\omega_{\alpha,\beta} - p\, B,_\alpha \omega_\beta \qquad (4.7)$$

$$2K_{\alpha\beta} = a\, B(b\omega_\alpha),_\alpha - A\, b(a\omega_\beta),_\beta$$

Observe (after adjustments for sign) that equations (4.6) are identical to the rotation expressions ϕ_{i3} (i = 1,2) as set out in equations (A.27). Upon expansion the curvatures (4.7) become:

$$K_\alpha = -(\bar{a}^2-\bar{b}^2)\sin\alpha\cos\alpha/A^4\, w,_\alpha + \frac{1}{A^2} w,_{\alpha\alpha} - 3\bar{a}\,\bar{b}(\bar{a}^2-\bar{b}^2)\sin\alpha\cos\alpha/A^6$$
$$u + \frac{k_1}{A} u,_\alpha$$

$$K_\beta = \frac{1}{B^2} w,_{\beta\beta} + \frac{k_2}{B} v,_\beta - \frac{\bar{a}\sin\alpha}{(A^2B)} w,_\alpha - \frac{k_1\bar{a}\sin\alpha}{(A\,B)} u \qquad (4.8)$$

$$K_{\alpha\beta} = \frac{\bar{a}\sin\alpha}{(A\,B^2)} w,_\beta + \frac{1}{(A\,B)} w,_{\beta\alpha} + \frac{\bar{a}\sin\alpha\, k_2}{(A\,B)} v + \frac{(k_2 v),_\alpha}{A}$$
$$+ \frac{(k_1 u),_\beta}{B}$$

At the middle surface (when z = 0) the strains are:

$$\varepsilon_{\alpha^0} = a\, u,_\alpha + p\, A,_\beta v - k_1 w$$

$$\varepsilon_{\beta^0} = b\, v,_\beta + p\, B,_\alpha u - k_2 w \qquad (4.9a)$$

$$\varepsilon_{\alpha\beta^0} = A\, b(a\, u),_\beta + a\, B(b\, v),_\alpha$$

or
$$\varepsilon_{\alpha^0} = \frac{1}{A} u,_\alpha - k_1 w$$
$$\varepsilon_{\beta^0} = \frac{1}{B} v,_\beta - \frac{a \sin\alpha}{AB} u - k_2 w \qquad (4.9b)$$
$$\varepsilon_{\alpha\beta^0} = \frac{1}{B} u,_\beta + \frac{\bar{a} \sin\alpha}{(AB)} v + \frac{1}{A} v,_\alpha$$

Note that equations (4.9) are equivalent to equations (A.30), with the exception of $\varepsilon_{\alpha\beta^0}$ as stated.

As stated previously, the above equations are due to LOVE (Reference 7) with the exception of the twist expression $K_{\alpha\beta}$ of REISSNER which DRESSLER favoured due to its symmetrical appearance. However, for a general theory of thin elastic shells KOITER in Reference 8 showed that REISSNER's twist can not be correct - "significant terms in which the rotation around the normal occurs, divided by a radius of curvature or torsion" are missing. On comparing $K_{\alpha\beta}$, equations (4.7):

$$2K_{\alpha\beta} = - \frac{1}{B} \omega_{\beta,\beta} + \frac{1}{A} \omega_{\alpha,\alpha} + \frac{\bar{a} \sin\alpha}{(AB)} \omega_\alpha \qquad (4.10)$$

and $\delta K_{\alpha\beta}$, equations (A.31):

$$2\delta K_{\beta\alpha} = -(g_{\beta\beta})^{-\frac{1}{2}} \phi_{23,\beta} - (g_{\alpha\alpha})^{-\frac{1}{2}} \phi_{13,\alpha} - k_\beta^{(g)} \phi_{13}$$
$$- k_\beta^{(n)} \phi_{12} - K_\alpha^{(n)} \phi_{21} \qquad (4.11)$$

it can be seen that the rotations around the normal, divided by a curvature, $(-k_\beta^{(n)} \phi_{12} - k_\alpha^{(n)} \phi_{21})$, are missing in REISSNER's $K_{\alpha\beta}$ expression (4.10).

However, when ARON's Approximations are applicable, observe that REISSNER's twist $K_{\alpha\beta}$ and $\delta K_{\alpha\beta}$ are equal. Therefore since the walls of BOURDON tubes are thin and the loading is by internal pressure only, ARON's Approximations will be incorporated in the analysis (see Reference 14, page 336 and Reference 13, page 89).

In the case when ARON's Approximations are not applicable it is suggested that LOVE's twist expression (Reference 7, page 524, equations (26)) be used - see also the paper by KOITER (Reference 8):

$$K_{\alpha\beta} = \frac{1}{A}\left(\frac{1}{B} w,_{\beta} + k_2 v\right),_{\alpha} - \frac{1}{(A^2 B)} A,_{\beta} w,_{\alpha} - \frac{1}{(AR_1)} v,_{\alpha} \qquad (4.12)$$

or the twist as presented in the directed vector method (Appendix A): (adjusted into DRESSLER's coordinate system)

$$2\delta K_{\alpha\beta} = \frac{2}{(|\bar{g}_{\alpha}||\bar{g}_{\beta}|)} w,_{\beta\alpha} + \frac{2\, k_{\beta}^{(g)}}{(g_{\beta\beta})^{\frac{1}{2}}} w,_{\beta} + \frac{(k_{\beta}^{(n)} - k_{\alpha}^{(n)})}{(g_{\alpha\alpha})^{\frac{1}{2}}} v,_{\alpha} + \frac{(k_{\alpha}^{(n)} - k_{\beta}^{(n)})}{(g_{\beta\beta})^{\frac{1}{2}}} u,_{\beta} + \frac{(k_{\beta}^{(n)}),_{\alpha}}{(g_{\alpha\alpha})^{\frac{1}{2}}} v \qquad (4.13a)$$

or,

$$2K_{\alpha\beta} = \frac{2}{(AB)} w,_{\beta\alpha} + 2\bar{a}\frac{\sin\alpha}{(AB^2)} w,_{\beta} + \frac{(k_2 - k_1)}{A} v,_{\alpha} + \frac{(k_1 - k_2)}{B} u,_{\beta} + \frac{k_2,_{\alpha}}{A} v \qquad (4.13b)$$

From one of the following methods, (1) Bidimensional analysis of a shell element, (2) Minimization of the strain energy, the equilibrium equations may be obtained:

$$\left.\begin{aligned}
&(BN_\alpha)_{,\alpha} + (AN_{\beta\alpha})_{,\beta} + A_{,\beta}N_{\alpha\beta} - B_{,\alpha}N_\beta - ABk_1Q_\alpha = -ABF_\alpha \\
&(AN_\beta)_{,\beta} + (BN_{\alpha\beta})_{,\alpha} + B_{,\alpha}N_{\beta\alpha} - A_{,\beta}N_\alpha - ABk_2Q_\beta = -ABF_\beta \\
&(BQ_\alpha)_{,\alpha} + (AQ_\beta)_{,\beta} + ABk_1N_\alpha + ABk_2N_\beta = -ABF_z \\
&(BM_{\alpha\beta})_{,\alpha} - (AM_\beta)_{,\beta} + A_{,\beta}M_\alpha - B_{,\alpha}M_{\beta\alpha} + ABQ_\beta = 0 \\
&(AM_{\beta\alpha})_{,\beta} + (BM_\alpha)_{,\alpha} - B_{,\alpha}M_\beta - A_{,\beta}M_{\alpha\beta} - ABQ_\alpha = 0
\end{aligned}\right\} \quad (4.14)$$

where F_α , F_β , F_z denote external forces per unit area. For the BOURDON tube $F_\alpha = F_\beta = 0$, $F_z = -p$ (the internal fluid pressure), and the external moments per unit area are zero. Upon expansion of equations (4.14):

<u>α-component force equation</u>

$$\left.\begin{aligned}
&\frac{1}{B}N_{\beta\alpha,\beta} + \frac{1}{A}N_{\alpha,\alpha} + \left(-\frac{1}{(AB)}B_{,\alpha}\right)(N_\beta - N_\alpha) - k_1Q_\alpha + F_\alpha = 0 \\
&\underline{\beta\text{-component force equation}} \\
&\frac{1}{B}N_{\beta,\beta} + \frac{1}{A}N_{\alpha\beta,\alpha} + \left(\frac{1}{(AB)}B_{,\alpha}\right)(N_{\alpha\beta} + N_{\beta\alpha}) - k_2Q_\beta + F_\beta = 0 \\
&\underline{z\text{-component force equation}} \\
&\frac{1}{B}Q_{\beta,\beta} + \frac{1}{A}Q_{\alpha,\alpha} + \left(\frac{1}{(AB)}B_{,\alpha}\right)Q_\alpha + k_2N_\beta + k_1N_\alpha + F_z = 0
\end{aligned}\right\} \quad (4.15) \text{ cont'd.}$$

α-component moment equation

$$- \frac{1}{B} M_{\beta,\beta} + \frac{1}{A} M_{\alpha\beta,\alpha} + (- \frac{1}{(AB)} B_{,\alpha})(M_{\beta\alpha}-M_{\alpha\beta}) + Q_{\beta} = 0$$

β-component moment equation

$$\frac{1}{B} M_{\beta\alpha,\beta} + \frac{1}{A} M_{\alpha,\alpha} + (\frac{1}{(AB)} B_{,\alpha})(M_{\alpha}-M_{\beta}) - Q_{\alpha} = 0 \qquad (4.15)$$

Observe that with Figure 4.1 and Table 4.1, equations (4.15) will transform to expressions (A.49).

To the above expressions, may be added a sixth equilibrium equation (or the third moment equilibrium equation about the normal) - c.f. the analysis in Appendix A, note that there is no direct counterpart, as the third moment equilibrium equation can be shown to be an identity:

$$N_{12} - N_{21} - k_1 M_{\beta\alpha} - k_2 M_{\alpha\beta} - k_{12}(-M_{\beta\beta} + M_{\alpha\alpha}) = 0 \qquad (4.16)$$

Since for the BOURDON gage $k_{21} = k_{12} = 0$ (i.e., the orthogonal parametric lines α_1 and α_2 are coincident with the lines of principal curvature), equation (4.16) simplifies to:

$$N_{12} - N_{21} - k_1 M_{\beta\alpha} - k_2 M_{\alpha\beta} = 0 \qquad (4.17)$$

Due to the symmetry of the stress tensor $\bar{\bar{\sigma}}$ (i.e., $\sigma_{ij}=\sigma_{ji}$) and N_{12} , N_{21} , $M_{\beta\alpha}$ and $M_{\alpha\beta}$ as defined by:

$$\left.\begin{aligned} N_{12} &= \int_{-h}^{h} \sigma_{12}(1 - zk_2)dz \qquad N_{21} = \int_{-h}^{h} \sigma_{21}(1 - zk_1)dz \\ M_{\beta\alpha} &= \int_{-h}^{h} z\sigma_{12}(1 - zk_2)dz \qquad M_{\alpha\beta} = -\int_{-h}^{h} z\sigma_{21}(1 - zk_1)dz \end{aligned}\right\} \quad (4.18)$$

are substituted into equation (4.17), it can be shown to vanish identically:

$$\int \sigma_{12}(1 - zk_2)dz - \int \sigma_{21}(1 - zk_1)dz - k_1\left[\int z\sigma_{12}(1 - zk_2)dz\right]$$

$$- k_2\left[-\int z\sigma_{21}(1 - zk_1)dz\right] \equiv 0$$

Observe when LOVE's First Approximation is used, the identity is also satisfied. Also note,

$$\left.\begin{aligned} N_{\beta\alpha} &= N_{\alpha\beta} \\ M_{\beta\alpha} &= -M_{\alpha\beta} \end{aligned}\right\} \quad (4.19)$$

With shell thickness $2h$, POISSON's ratio σ, modulus of elasticity E, the stress resultants and stress-couples are next presented by DRESSLER:

$$\left.\begin{aligned} N_\alpha &= C(\varepsilon_{\alpha o} + \sigma\varepsilon_{\beta o}) \\ N_\beta &= C(\varepsilon_{\beta o} + \sigma\varepsilon_{\alpha o}) \\ N_{\alpha\beta} &= J\,\varepsilon_{\alpha\beta o} \\ M_\alpha &= -D(K_\alpha + \sigma K_\beta) \end{aligned}\right\} \quad (4.20) \text{ cont'd.}$$

$$\left.\begin{aligned} M_\beta &= -D(K_\beta + \sigma K_\alpha) \\ M_{\alpha\beta} &= I\, K_{\alpha\beta} \end{aligned}\right\} \qquad (4.20)$$

where the constants are

$$C = \frac{2Eh}{(1-\sigma^2)} \qquad J = \frac{Eh}{(1+\sigma)}$$

$$D = \frac{2Eh^3}{3(1-\sigma^2)} \qquad I = D(1-\sigma)$$

Substituting equations (4.8) and (4.9) into equations (4.20), the stress resultants and stress-couples (with ARON's Approximations) become:

Stress resultants

$$\left.\begin{aligned} N_\alpha &= \frac{2Eh}{(1-\sigma^2)}\left[\frac{1}{A}u_{,\alpha} - k_1 w + \sigma\left(\frac{1}{B}v_{,\beta} - \frac{\bar{a}\sin\alpha}{(AB)}u - k_2 w\right)\right] \\ N_\beta &= \frac{2Eh}{(1-\sigma^2)}\left[\frac{1}{B}v_{,\beta} - \frac{\bar{a}\sin\alpha}{(AB)}u - k_2 w + \sigma\left(\frac{1}{A}u_{,\alpha} - k_1 w\right)\right] \\ N_{\alpha\beta} &= \frac{Eh}{(1+\sigma)}\left[\frac{1}{B}u_{,\beta} + \frac{\bar{a}\sin\alpha}{(AB)}v + \frac{1}{A}v_{,\alpha}\right] \end{aligned}\right\} \qquad (4.21)$$

Stress-couples

$$M_\alpha = \frac{-2Eh^3}{(3(1-\sigma^2))}\left[-(\bar{a}^2-\bar{b}^2)\sin\alpha\cos\alpha/A^4\, w_{,\alpha} + \frac{1}{A^2}w_{,\alpha\alpha} + \sigma\left(\frac{1}{B^2}w_{,\beta\beta} - \frac{\bar{a}\sin\alpha}{(A^2 B)}w_{,\alpha}\right)\right]$$

$$M_\beta = \frac{-2Eh^3}{(3(1-\sigma^2))}\left[\frac{1}{B^2}w_{,\beta\beta} - \frac{\bar{a}\sin\alpha}{(A^2 B)}w_{,\alpha} + \sigma\left(\frac{-(\bar{a}^2-\bar{b}^2)\sin\alpha\cos\alpha}{A^4}w_{,\alpha} + \frac{1}{A^2}w_{,\alpha\alpha}\right)\right] \qquad (4.22)$$

cont'd.

$$M_{\alpha\beta} = \frac{2Eh^3}{(3(1+\sigma))}\left[\frac{\bar{a}\sin\alpha}{(A\,B^2)}\,w,_{\beta} + \frac{1}{(AB)}\,w,_{\beta\alpha}\right] \qquad (4.22)$$

which are in agreement with equation (A.47) and (A.48) when corrected for signs (see Table 4.1), and noting that the thickness is $2h$.

In terms of displacements u , v , w (by using equations (4.6), (4.8), (4.9) and (4.20)) and the shear resultants Q_α , Q_β DRESSLER displays equations (4.14) in the form of a "listing" of coefficients. To designate the coefficient of each derivative in the i^{th} equation, the symbol ℓ_{mn}^{iq} is employed. The superscript q represents u , v , or w . The subscripts m and n denote the m^{th} and n^{th} derivatives of α and β respectively. For example, the coefficient of $w,_{\alpha\alpha\beta}$ in the second equation of (4.14) is ℓ_{21}^{2w} . Thus, for equations (4.14):

x-component force equation

$$\ell_{20}^{1u} = CaB$$

$$\ell_{02}^{1u} = JAb$$

$$\ell_{10}^{1u} = C(Ba'+\sigma BB'p + (1-\sigma)B'a)$$

$$\ell_{00}^{1u} = C(\sigma B(B'p'+B''p) - (1-\sigma)(B')^2p)$$

$$\ell_{11}^{1v} = C\sigma + J \qquad (4.23a)\ \text{cont'd.}$$

$$\ell_{01}^{1v} = \sigma CBb' - (1-\sigma)CB'b - JAB'p$$

$$\ell_{10}^{1w} = -CB(k_1 + \sigma k_2)$$

$$\ell_{00}^{1w} = (1-\sigma)CB'(k_2-k_1) - CB(k_1'+\sigma k_2')$$

$$\ell_{00}^{1Q_\alpha} = -ABk_1 \qquad (4.23a)$$

$$\text{Right side} = -ABF_\alpha$$

y-component force equation

$$\ell_{11}^{2u} = J + \sigma C$$

$$\ell_{01}^{2u} = JBb' + 2JB'b + CAB'p$$

$$\ell_{20}^{2v} = JaB$$

$$\ell_{02}^{2v} = CAb$$

$$\ell_{10}^{2v} = J(B(a'-B'p) + 2aB') \qquad (4.23b)$$

$$\ell_{00}^{2v} = -J(B'p' + B''p) + 2(B')^2p)$$

$$\ell_{01}^{2w} = -CA(k_2 + \sigma k_1)$$

$$\ell_{00}^{2Q_\beta} = -ABk_2$$

$$\text{Right side} = -ABF_\beta$$

z-component force equation

$$\ell_{10}^{3u} = CB(k_1 + \sigma k_2)$$

$$\ell_{00}^{3u} = CB'(k_2 + \sigma k_1) \qquad (4.23c)$$

cont'd.

$$\ell_{01}^{3v} = CA(k_2 + \sigma k_1)$$

$$\ell_{00}^{3w} = -CAB(k_1^2 + 2\sigma k_1 k_2 + k_2^2)$$

$$\ell_{10}^{3Q_\alpha} = B \qquad (4.23c)$$

$$\ell_{00}^{3Q_\alpha} = B'$$

$$\ell_{01}^{3Q_\beta} = A$$

$$\text{Right side} = -ABF_z$$

x-component moment equation

$$\ell_{11}^{4u} = \sigma D k_1 + \tfrac{1}{2} I k_1$$

$$\ell_{01}^{4u} = D(AB'pk_1 + \sigma k_1') + \tfrac{1}{2} IB(bk_1)' + IB'bk_1$$

$$\ell_{20}^{4v} = \tfrac{1}{2} IBak_2$$

$$\ell_{02}^{4v} = DAbk_2 \qquad (4.23d)\ \text{cont'd.}$$

$$\ell_{10}^{4v} = \tfrac{1}{2} IB((ak_2)' + aB(bk_2)') + IaB'k_2$$

$$\ell_{00}^{4v} = \tfrac{1}{2} IB((aB)(bk_2)')' + IaBB'(bk_2)'$$

$$\ell_{21}^{4w} = \sigma Da + Ia$$

$$\ell_{03}^{4w} = DAb^2$$

$$\ell_{11}^{4w} = D(B'p + \sigma a') + IB(p' + ab') + 2IB'p$$

$$\ell_{01}^{4w} = IB(ab')' + 2IB'ab'$$

$$\ell_{00}^{4Q_\beta} = AB \qquad (4.23d)$$

Right side = 0

y-component moment equation

$$\ell_{20}^{5u} = -DaBk_1$$

$$\ell_{02}^{5u} = -\tfrac{1}{2}IAbk_1$$

$$\ell_{10}^{5u} = -D(Ba'k_1 + 2Bak_1' + B'ak_1)$$

$$\ell_{00}^{5u} = -D(B(ak_1')'+\sigma BB'p'k_1+\sigma aB''k_1+B'ak_1'-(1-\sigma)(B')^2pk_1)$$

$$\ell_{11}^{5v} = -\sigma Dk_2 - \tfrac{1}{2}Ik_2$$

$$\ell_{01}^{5v} = -D(\sigma Bb'k_2+\sigma k_2'-B'(1-\sigma)bk_2)-\tfrac{1}{2}IB(bk_2)'$$

$$\ell_{20}^{5w} = -Da^2B$$

$$\ell_{12}^{5w} = -\sigma Db-Ib \qquad (4.23e)$$

$$\ell_{20}^{5w} = -Da(3a'B+aB')$$

$$\ell_{02}^{5w} = -D(2\sigma b'-(1-\sigma)B'b^2)-Ib'$$

$$\ell_{10}^{5w} = -D(B(aa')'+\sigma B(apB')'+(1-\sigma)B'aa'-(1-\sigma)(B')^2ap)$$

$$\ell_{00}^{5Q_\alpha} = -AB$$

Right side = 0

Observe that in the moment equations (4.23d) and (4.23e) REISSNER's twist expression (4.8) is employed. However since ARON's Approximations are valid for thin-walled BOURDON tube analysis, coefficients of ℓ^{4u}, ℓ^{4v}, and ℓ^{5u}, ℓ^{5v} shall be equated to zero.

Further, DRESSLER in addition to using ARON's Approximations introduces simplifications as may be found in "shallow shell" theory:

(1) $\omega_\alpha = b\, w,_\beta$ and $\omega_\beta = -a\, w,_\alpha$ - as for plate theory

(2) the absence of the transverse shear terms in the first two equilibrium equations

However as the curvature is large at the extremeties of the BOURDON tube the moment effect on the transverse shear may be significant (see also Reference 9), these additional approximations will not be employed in the analysis that follows. Therefore expressions (4.23) when expanded become:

x-component force equation

$$\ell^{1u}_{20} = \frac{2Eh}{(A^2(1-\sigma^2))}$$

$$\ell^{1u}_{02} = \frac{Eh}{(B^2(1+\sigma))}$$

$$\ell^{1u}_{10} = \frac{2Eh}{(1-\sigma^2)}\left[\frac{-(\bar{a}^2-\bar{b}^2)\sin\alpha\cos\alpha}{A^4} - \frac{\bar{a}\sin\alpha}{(A^2\,B)}\right] \qquad \text{(4.24a) cont'd.}$$

$$\ell^{1u}_{00} = \frac{2Eh}{(1-\sigma^2)}\left[\frac{\sigma\bar{a}\sin\alpha}{(A^3B)}(\bar{a}^2-\bar{b}^2)\sin\alpha\cos\alpha - \frac{\bar{a}^2\sin^2\alpha}{(A^2\,B^2)} - \frac{\sigma\bar{a}\cos\alpha}{(A^2\,B)}\right]$$

$$\ell_{11}^{1v} = \frac{Eh}{((1-\sigma)AB)}$$

$$\ell_{01}^{1v} = -\frac{Eh}{(1-\sigma^2)}\frac{\bar{a}\sin\alpha}{(A\,B^2)}(\sigma-3) \qquad (4.24a)$$

$$\ell_{10}^{1w} = -\frac{2Eh}{(A(1-\sigma^2))}(k_1 + \sigma k_2)$$

$$\ell_{00}^{1w} = -\frac{2Eh}{(1-\sigma)}\frac{\bar{a}\sin\alpha}{(AB)}(k_2+\sigma k_1) + \frac{2Eh}{(1-\sigma^2)}\frac{\bar{a}\sin\alpha}{(AB)k_1} + \frac{2Eh\sigma}{(A(1-\sigma^2))}$$

$$\frac{\bar{b}\sin\alpha}{(AB)} + \frac{2Eh}{(A(1-\sigma^2))}(\bar{a}^2-\bar{b}^2)\sin\alpha\cos\alpha\left[\frac{3\bar{a}\bar{b}}{A^5} + \frac{\sigma\bar{b}\cos\alpha}{(A^3B)}\right]$$

$$\ell_{00}^{1Q_\alpha} = -k_1$$

Right side = $-F_\alpha$

<u>y-component force equation</u>

$$\ell_{11}^{2u} = \frac{Eh}{((1-\sigma^2)AB)}(1+\sigma)$$

$$\ell_{01}^{2u} = \frac{Eh}{(1-\sigma^2)}\frac{\bar{a}\sin\alpha}{(A\,B^2)}(\sigma-3)$$

$$\ell_{20}^{2v} = \frac{Eh}{(A^2(1+\sigma))}$$

$$\ell_{02}^{2v} = \frac{2Eh}{(B^2(1-\sigma^2))} \qquad (4.24b)$$

$$\ell_{10}^{2v} = -\frac{Eh}{(A(1+\sigma))}\left[\frac{\bar{a}\sin\alpha}{(AB)} + \frac{(\bar{a}^2-\bar{b}^2)\sin\alpha\cos\alpha}{A^3}\right]$$

$$\ell_{00}^{2v} = \frac{Eh}{(1+\sigma)}\left[\frac{\bar{a}\cos\alpha}{(A^2\,B)} - \frac{\bar{a}^2\sin^2\alpha}{(A^2\,B^2)} - \frac{\bar{a}\sin\alpha}{(AB)}\frac{(\bar{a}^2-\bar{b}^2)\sin\alpha\cos\alpha}{A^3}\right]$$

$$\ell_{01}^{2w} = -\frac{2Eh}{(B(1-\sigma^2))}(k_2+\sigma k_1)$$

$$\ell_{00}^{2Q_\beta} = -k_2 \qquad \text{Right side} = -F_\beta$$

z-component force equation

$$\ell_{10}^{3u} = \frac{2Eh}{(A(1-\sigma^2))}(k_1 + \sigma k_2)$$

$$\ell_{00}^{3u} = -\frac{2Eh}{(1-\sigma^2)}\frac{\bar{a}\sin\alpha}{(AB)}(k_2 + \sigma k_1)$$

$$\ell_{01}^{3v} = \frac{2Eh}{(B(1-\sigma^2))}(k_2 + \sigma k_1)$$

$$\ell_{00}^{3w} = -\frac{2Eh}{(1-\sigma^2)}(k_1^2 + 2\sigma k_1 k_2 + k_2^2) \qquad (4.24c)$$

$$\ell_{10}^{3Q_\alpha} = \frac{1}{A}$$

$$\ell_{00}^{3Q_\alpha} = -\frac{\bar{a}\sin\alpha}{(AB)}$$

$$\ell_{01}^{3Q_\beta} = \frac{1}{B}$$

Right side = $-F_z$

x-component moment equation

$$\ell_{21}^{4w} = \frac{D}{(A^2B)}$$

$$\ell_{03}^{4w} = \frac{D}{B^3}$$

$$\ell_{11}^{4w} = -\frac{D}{(AB)}\left[\frac{\bar{a}\sin\alpha}{(AB)} + \frac{(\bar{a}^2-\bar{b}^2)\sin\alpha\cos\alpha}{A^3}\right] \qquad (4.24d)$$

$$\ell_{01}^{4w} = -\frac{D(1-\sigma)}{(A^2B)}\left[\frac{\bar{a}\sin\alpha}{(AB)}\frac{(\bar{a}^2-\bar{b}^2)\sin\alpha\cos\alpha}{A} - \frac{\bar{a}\cos\alpha}{B}\right]$$

$$\ell_{00}^{4Q_\beta} = 1$$

Right side = 0

y-component moment equation

$$\ell_{30}^{5w} = -\frac{D}{A^3}$$

$$\ell_{12}^{5w} = -\frac{D}{(AB^2)}$$

$$\ell_{20}^{5w} = \frac{D}{A^2}\left[\frac{\bar{a}\sin\alpha}{(AB)} + \frac{3(\bar{a}^2-\bar{b}^2)\sin\alpha\cos\alpha}{A^3}\right]$$

$$\ell_{02}^{5w} = -\frac{2D\,\bar{a}\sin\alpha}{(AB^3)} \qquad (4.24e)$$

$$\ell_{10}^{5w} = \frac{D}{A}\left[\frac{(\bar{a}^2-\bar{b}^2)(\cos^2\alpha-\sin^2\alpha)}{A^4} - \frac{\bar{a}\sin\alpha}{(AB)}\,\frac{(\bar{a}^2-\bar{b}^2)\sin\alpha\cos\alpha(1+\sigma)}{A^3}\right.$$
$$\left. + \frac{\bar{a}^2\sin^2\alpha}{(A^2\,B^2)} - \frac{4(\bar{a}^2-\bar{b}^2)^2\sin^2\alpha\cos^2\alpha}{A^6} + \frac{\sigma\bar{a}\cos\alpha}{(A^2\,B)}\right]$$

$$\ell_{00}^{5Q_\alpha} = -1$$

Right side = 0

Again, allowing for differences in signs (see Figure 4.1 and Table 4.1) the foregoing listing of the equilibrium equations can be verified with those of expressions (A.51).

By solving for Q_β and Q_α in the moment equilibrium equations (4.24d) and (4.24e) and substituting into the force equilibrium equations (after carrying out some wieldly operations), the results may be tabulated as in Table (4.2) - for a more graphical presentation, the metric coefficients and curvatures are shown. This Table is comparable with the one which appears in the Appendix (Table A.1) when signs are adjusted.

Table 4.2 - Governing Equations of the BOURDON Gage

$u(\alpha,\beta)$	$v(\alpha,\beta)$	$w(\alpha,\beta)$	Free Terms
$\frac{E'(1-\nu)}{2g_{\beta\beta}}\frac{\partial^2}{\partial\beta^2}+\frac{E'}{g_{\alpha\alpha}}\frac{\partial^2}{\partial\alpha^2}+\left[-\frac{E'k_\beta^{(g)}}{\bar g_\alpha}-\frac{E'(\bar a^2-\bar b^2)\sin\alpha\cos\alpha}{(g_{\alpha\alpha})^2}\right]\frac{\partial}{\partial\alpha}-\left[E'k_\beta^{(g)}k_\beta^{(g)}+\frac{E'\nu}{\bar g_\alpha}\left\{\frac{\bar a\cos\alpha}{\bar g_\alpha\bar g_\beta}-\frac{K_\beta^{(g)}(\bar a^2-\bar b^2)\cdot\sin\alpha\cos\alpha}{g_{\alpha\alpha}}\right\}\right]$	$\frac{E'(1+\nu)}{2\bar g_\alpha\bar g_\beta}\frac{\partial^2}{\partial\alpha\partial\beta}-\frac{E'k_\beta^{(g)}(\nu-3)}{2\bar g_\beta}\frac{\partial}{\partial\beta}$	$+\frac{D\,k_\alpha^{(n)}}{(g_{\alpha\alpha})^{3/2}}\frac{\partial^3}{\partial\alpha^3}+\frac{D\,k_\alpha^{(n)}}{\bar g_\alpha g_{\beta\beta}}\frac{\partial^3}{\partial\beta^2\partial\alpha}+\frac{2D\,k_\alpha^{(n)}k_\beta^{(g)}}{g_{\beta\beta}}\frac{\partial^2}{\partial\beta^2}-\frac{D\,k_\alpha^{(n)}}{g_{\alpha\alpha}}\left[k_\beta^{(g)}+\frac{3(\bar a^2-\bar b^2)\sin\alpha\cos\alpha}{(g_{\alpha\alpha})^{3/2}}\right]\frac{\partial^2}{\partial\alpha^2}-\left[\frac{E'}{\bar g_\alpha}(k_\alpha^{(n)}+\nu k_\beta^{(n)})+\frac{D\,k_\alpha^{(n)}}{\bar g_\alpha}\left\{\frac{(\bar a^2-\bar b^2)(\cos^2\alpha-\sin^2\alpha)}{(g_{\alpha\alpha})^2}-\frac{k_\beta^{(g)}(1+\nu)(\bar a^2-\bar b^2)\cdot\sin\alpha\cos\alpha}{(g_{\alpha\alpha})^{3/2}}+k_\beta^{(g)}k_\beta^{(g)}-\frac{4(\bar a^2-\bar b^2)^2\sin^2\alpha\cos^2\alpha}{(g_{\alpha\alpha})^3}+\frac{\nu\,\bar a\cos\alpha}{g_{\alpha\alpha}\bar g_\beta}\right\}\cdot\right]\frac{\partial}{\partial\alpha}-\left[E'k_\beta^{(g)}(k_\beta^{(n)}+\nu k_\alpha^{(n)})-E'k_\beta^{(g)}k_\alpha^{(n)}-\frac{E'\nu\,\bar b\sin\alpha}{g_{\alpha\alpha}\bar g_\beta}-\frac{E'(\bar a^2-\bar b^2)\sin\alpha\cos\alpha}{\bar g_\alpha}\left\{\frac{3\bar a\,\bar b}{(g_{\alpha\alpha})^{5/2}}+\frac{\nu\,k_\beta^{(n)}}{g_{\alpha\alpha}}\right\}\right]$	F_α
$\frac{E'(1+\nu)}{2\bar g_\alpha\bar g_\beta}\frac{\partial^2}{\partial\beta\partial\alpha}+\frac{E'k_\alpha^{(g)}}{2\bar g_\beta}(\nu-3)\frac{\partial}{\partial\beta}$	$\frac{E'}{g_{\beta\beta}}\frac{\partial^2}{\partial\beta^2}+\frac{E'(1-\nu)}{2g_{\alpha\alpha}}\frac{\partial^2}{\partial\alpha^2}-\frac{E'(1-\nu)}{2\bar g_\alpha}\cdot\left[k_\beta^{(g)}+\frac{(\bar a^2-\bar b^2)\sin\alpha\cos\alpha}{(g_{\alpha\alpha})^{3/2}}\right]\frac{\partial}{\partial\alpha}+\frac{E'(1-\nu)}{2}\cdot\left[\frac{\bar a\cos\alpha}{g_{\alpha\alpha}\bar g_\beta}-k_\beta^{(g)}k_\beta^{(g)}-\frac{k_\alpha^{(g)}(\bar a^2-\bar b^2)\sin\alpha\cos\alpha}{(g_{\alpha\alpha})^{3/2}}\right]$	$+\frac{D\,k_\beta^{(n)}}{(g_{\beta\beta})^{3/2}}\frac{\partial^3}{\partial\beta^3}+\frac{D\,k_\beta^{(n)}}{g_{\alpha\alpha}\bar g_\beta}\frac{\partial^3}{\partial\beta\partial\alpha^2}-\frac{D\,k_\beta^{(n)}}{\bar g_\alpha\bar g_\beta}\left[k_\beta^{(g)}+\frac{(\bar a^2-\bar b^2)\sin\alpha\cos\alpha}{(g_{\alpha\alpha})^{3/2}}\right]\frac{\partial^2}{\partial\alpha\partial\beta}-\left[\frac{E'}{\bar g_\beta}(k_\beta^{(n)}+\nu k_\alpha^{(n)})+\frac{D(1-\nu)k_\beta^{(n)}}{g_{\alpha\alpha}\bar g_\beta}\cdot\left\{k_\beta^{(g)}\frac{(\bar a^2-\bar b^2)\sin\alpha\cos\alpha}{\bar g_\alpha}-\frac{\bar a\cos\alpha}{\bar g_\beta}\right\}\right]\frac{\partial}{\partial\beta}$	F_β
$-\frac{E'}{\bar g_\alpha}(k_\alpha^{(n)}+\nu k_\beta^{(n)})\frac{\partial}{\partial\alpha}+E'k_\beta^{(g)}\cdot(k_\beta^{(n)}+\nu k_\alpha^{(n)})$	$-\frac{E'}{\bar g_\beta}(k_\beta^{(n)}+\nu k_\alpha^{(n)})\frac{\partial}{\partial\beta}$	$+\frac{D}{(g_{\beta\beta})^2}\frac{\partial^4}{\partial\beta^4}+\frac{D}{(g_{\alpha\alpha})}\frac{\partial^4}{\partial\alpha^4}+\frac{2D}{g_{\alpha\alpha}g_{\beta\beta}}\frac{\partial^4}{\partial\beta^2\partial\alpha^2}-\frac{2D}{g_{\beta\beta}}\left[\frac{(\bar a^2-\bar b^2)\sin\alpha\cos\alpha}{(g_{\alpha\alpha})^2}-\frac{k_\beta^{(g)}}{\bar g_\alpha}\right]\frac{\partial^3}{\partial\beta^2\partial\alpha}-\frac{D}{(g_{\alpha\alpha})^{3/2}}\cdot\left[\frac{6(\bar a^2-\bar b^2)\sin\alpha\cos\alpha}{(g_{\alpha\alpha})^{3/2}}+2k_\beta^{(g)}\right]\frac{\partial^3}{\partial\alpha^3}-\left[\frac{D\,k_\beta^{(g)}(3-\nu)(\bar a^2-\bar b^2)}{(g_{\alpha\alpha})^{3/2}g_{\beta\beta}}\cdot\sin\alpha\cos\alpha-\frac{2D\,k_\beta^{(g)}k_\beta^{(g)}(2+3\nu)}{g_{\beta\beta}}-\frac{D(3-\nu)\bar a\cos\alpha}{g_{\alpha\alpha}(g_{\beta\beta})^{3/2}}\right]\cdot\frac{\partial^2}{\partial\beta^2}-\left[\frac{D\,k_\beta^{(g)}k_\beta^{(g)}}{g_{\alpha\alpha}}+\frac{D\,\bar a\cos\alpha(1+\nu)}{(g_{\alpha\alpha})^{5/2}\bar g_\beta}-\frac{D\,k_\beta^{(g)}(\bar a^2-\bar b^2)}{(g_{\alpha\alpha})^{5/2}}\cdot\sin\alpha\cos\alpha\,(7+\nu)+\frac{4D(\bar a^2-\bar b^2)}{(g_{\alpha\alpha})^3}(\cos^2\alpha-\sin^2\alpha)-\frac{19D(\bar a^2-\bar b^2)^2\sin^2\alpha\cos^2\alpha}{(g_{\alpha\alpha})^4}\right]\frac{\partial^2}{\partial\alpha^2}-\left[-\frac{3D\,k_\beta^{(g)}k_\beta^{(g)}}{(g_{\alpha\alpha})^2}(\bar a^2-\bar b^2)\cdot\sin\alpha\cos\alpha+\frac{D\,k_\beta^{(g)}k_\beta^{(g)}k_\beta^{(g)}}{\bar g_\alpha}+\frac{2D\,k_\beta^{(g)}(\bar a^2-\bar b^2)\sin^2\alpha(1+\nu)}{(g_{\alpha\alpha})^{5/2}}-\frac{D\,k_\beta^{(g)}(\bar a^2-\bar b^2)\cos^2\alpha(3+5\nu)}{(g_{\alpha\alpha})^{5/2}}+\frac{D\,k_\beta^{(g)}\bar a\cos\alpha(1+\nu)}{(g_{\alpha\alpha})^{3/2}\bar g_\beta}+\frac{D\,k_\beta^{(g)}(\bar a^2-\bar b^2)^2\sin^2\alpha\cos^2\alpha}{(g_{\alpha\alpha})^{7/2}}(9+5\nu)+\frac{D}{\bar g_\alpha}\left\{-\frac{4(\bar a^2-\bar b^2)}{(g_{\alpha\alpha})^{5/2}}\cdot\sin\alpha\cos\alpha-\frac{13(\bar a^2-\bar b^2)^2\sin\alpha\cos\alpha(\cos^2\alpha-\sin^2\alpha)}{(g_{\alpha\alpha})^{7/2}}+\frac{28(\bar a^2-\bar b^2)^3\sin^3\alpha\cos^3\alpha}{(g_{\alpha\alpha})^{9/2}}-\frac{D\,k_\beta^{(g)}\nu}{(g_{\alpha\alpha})^{3/2}}\right]\frac{\partial}{\partial\alpha}+E'\left[k_\alpha^{(n)}k_\alpha^{(n)}+k_\beta^{(n)}k_\beta^{(n)}+2\nu k_\alpha^{(n)}k_\beta\right]$	F_z

The tabulated expressions (Table 4.2) are then the governing three partial differential equations of the BOURDON gage with an elliptical cross-section.

4.4 Summary of the Geometrical and Vectorial Properties of the BOURDON Gage with an Elliptical Cross-Section as Illustrated in Table 4.2

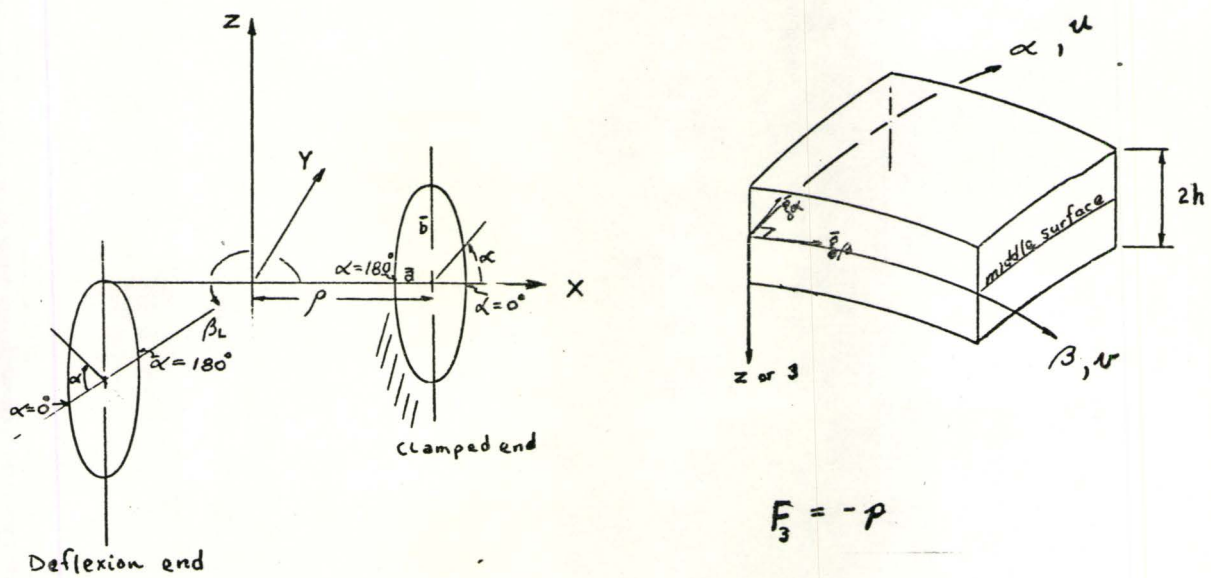

Figure 4.2 - BOURDON Gage with an Elliptical Cross-Section

Metric Coefficients

$$|\bar{g}_\beta| = (g_{\beta\beta})^{\frac{1}{2}} = \rho + \bar{a}\cos\alpha$$

$$|\bar{g}_\alpha| = (g_{\alpha\alpha})^{\frac{1}{2}} = (\bar{a}^2\sin^2\alpha + \bar{b}^2\cos^2\alpha)^{\frac{1}{2}}$$

$$g_{\beta\alpha} = g_{\alpha\beta} = 0$$

$\bar{b}$ = semi-major axis

$\bar{a}$ = semi-minor axis

Curvatures

a. Lineβ: $K_\beta^{(n)} = \bar{b}\cos\alpha/(|\bar{g}_\alpha||\bar{g}_\beta|)$

$K_\beta^{(g)} = \bar{a}\sin\alpha/(|\bar{g}_\alpha||\bar{g}_\beta|)$

b. Lineα: $K_\alpha^{(n)} = \bar{a}\,\bar{b}/(g_{\alpha\alpha})^{3/2}$

For thickness 2h

$$E' = \frac{2Eh}{(1-\nu^2)}$$

$$D = \frac{2Eh^3}{3(1-\nu^2)}$$

E = Elastic Modulus
ν = Poisson's Ratio

4.5 Boundary Conditions for BOURDON Tube

In this section DRESSLER gives a rather extensive formulation of the edge conditions - particularly at the plug or deflection end. The conditions at the edges $\alpha = 0$, π and $\beta = 0$ are the familiar force and/or displacement boundary conditions:

(1) u or N_α prescribed

(2) v or "effective" tangential shear $N_{\alpha\beta eff}$ prescribed

(3) w or "effective" transverse shear $Q_{\alpha eff}$ prescribed

(4) ω_α or M_α prescribed

At $\beta = \beta_L$, the end conditions are based on the conditions of continuity at the junction of two shells (i.e., the rigid plug and the BOURDON shell). For comparison a

simplified approach to this edge condition will also be presented.

As shown in Appendix A, because of curvature, the twisting moment can be resolved into equivalent vertical and horizontal force components. These are then combined vectorially with the stress resultants $N_{\alpha\beta}$ and Q_{α} to produce an "effective" tangential shear $N_{\alpha\beta eff}$ and an "effective" transverse shear $Q_{\alpha eff}$.

Thus in accordance with the procedure as set out in Appendix A, $N_{\alpha\beta eff}$ and $Q_{\alpha eff}$ appear as follows:

$$N_{\alpha\beta eff} = N_{\alpha\beta} - M_{\alpha\beta}/R_{\beta}$$

$$Q_{\alpha eff} = Q_{\alpha} - b\, M_{\alpha\beta,\beta}$$

Similarly along the boundary β = constant,

$$N_{\beta\alpha eff} = N_{\beta\alpha} + M_{\beta\alpha}/R_{\alpha}$$

$$Q_{\beta eff} = Q_{\beta} + a\, M_{\beta\alpha,\alpha}$$

However, since LOVE's First Approximation is employed it can be proved that,

$$N_{\alpha\beta eff} = N_{\alpha\beta}$$

$$N_{\beta\alpha eff} = N_{\beta\alpha}$$

With equations (4.22), (4.24d), and (4.24e), the ef-

fective transverse shears may be expressed in terms of displacements - using geometrical and vectorial properties as in Table 4.2:

$$-Q_{\alpha eff} = \frac{D}{(g_{\alpha\alpha})^{3/2}} w,_{\alpha\alpha\alpha} + \frac{D(2-\nu)}{(|\bar{g}_\alpha| g_{\beta\beta})} w,_{\beta\beta\alpha} + \frac{D(3-\nu)k_\beta^{(g)}}{g_{\beta\beta}} w,_{\beta\beta}$$
$$- \frac{D(k_\beta^{(g)} + 3(\bar{a}^2-\bar{b}^2)\sin\alpha\cos\alpha/(g_{\alpha\alpha})^{3/2})}{g_{\alpha\alpha}} w,_{\alpha\alpha} - \frac{D}{|\bar{g}_\alpha|}$$
$$\left[\frac{(\bar{a}^2-\bar{b}^2)(\cos^2\alpha-\sin^2\alpha)}{(g_{\alpha\alpha})^2} - k_\beta^{(g)}(1+\nu)\frac{(\bar{a}^2-\bar{b}^2)\sin\alpha\cos\alpha}{(g_{\alpha\alpha})^{3/2}}\right.$$
$$\left. + k_\beta^{(g)} k_\beta^{(g)} - \frac{4(\bar{a}^2-\bar{b}^2)^2\sin^2\alpha\cos^2\alpha}{(g_{\alpha\alpha})^3} + \frac{\nu\bar{a}\cos\alpha}{(g_{\alpha\alpha}|\bar{g}_\beta|)}\right] w,_\alpha \qquad (4.25a)$$

$$-Q_{\beta eff} = \frac{D}{(g_{\beta\beta})^{3/2}} w,_{\beta\beta\beta} + \frac{D(2-\nu)}{(g_{\alpha\alpha}|\bar{g}_\beta|)} w,_{\beta\alpha\alpha} - \frac{D}{(|\bar{g}_\alpha||\bar{g}_\beta|)}$$
$$\left[k_\beta^{(g)}(2\nu-1) + \frac{(\bar{a}^2-\bar{b}^2)\sin\alpha\cos\alpha(2-\nu)}{(g_{\alpha\alpha})^{3/2}}\right] w,_{\beta\alpha} - \frac{2D(1-\nu)}{|\bar{g}_\beta|}$$
$$\left[k_\beta^{(g)}\frac{(\bar{a}^2-\bar{b}^2)\sin\alpha\cos\alpha}{(g_{\alpha\alpha})^{3/2}} - \frac{\bar{a}\cos\alpha}{(g_{\alpha\alpha}|\bar{g}_\beta|)} - k_\beta^{(g)} k_\beta^{(g)}\right] w,_\beta \qquad (4.25b)$$

Therefore, specifically, the boundary conditions of the BOURDON tube are:

At $\beta = 0°$ - the clamped or fixed end

(i) $u = 0$ (iii) $w = 0$

(ii) $v = 0$ (iv) $\omega_\alpha = 0$ (4.26)

or in terms of displacement, $w_{,\beta} = 0$

At $\alpha = 0°$ and $180°$ (from symmetry conditions)

(i) $u = 0$

(ii) $N_{\alpha\beta eff} = N_{\alpha\beta} = 0$

or in terms of displacement, $v_{,\alpha} = 0$

(iii) $Q_{\alpha eff} = 0$

or in terms of displacement, $w_{,\alpha\alpha\alpha} = 0$

(iv) $\omega_{\beta} = 0$

or in terms of displacement, $w_{,\alpha} = 0$ (4.27)

At $\beta = \beta_L$ - the plug or deflection end

(a) DRESSLER's simplified approach - based on the familiar "free-end" condition[3]:

(i) N_{β} = P/circumference

where P = resultant normal force from fluid pressure on the end

= (fluid pressure p)×(area of ellipse)

or $P = p \pi \bar{a} \bar{b}$

circumference = circumference of ellipse = $2\pi\sqrt{\frac{(\bar{a}^2+\bar{b}^2)}{2}}$

(ii) $M_{\beta} = 0$

(iii) $N_{\beta\alpha eff} = N_{\beta\alpha} = 0$ (4.28) cont'd.

---

[3] For a more realistic simplified approach, reasoned along a geometrical and physical basis, to the edge conditions at $\beta = \beta_L$ refer to Appendix A.

$$\text{(iv)} \quad Q_{\beta\text{eff}} = 0 \tag{4.28}$$

(b) DRESSLER's exact edge conditions at $\beta = \beta_L$

For the exact boundary conditions at $\beta = \beta_L$, the conditions at the junction of two shells (the BOURDON shell at $\beta = \beta_L$ and the rigid end plug) must be considered. DRESSLER, in this section, formulates these conditions only. Complete and/or necessary equations are not presented; however they may be obtained easily by making the necessary adjustment of signs and conventions to the derived expressions as presented in Appendix A. They are (in DRESSLER's coordinate system):

$$\begin{aligned}
&\text{(i)} \quad u = -\frac{\bar{a}\sin\alpha}{|\bar{g}_\alpha|}\cos\beta_L U_o - \frac{\bar{a}\sin\alpha}{|\bar{g}_\alpha|}\sin\beta_L V_o \\
&\text{(ii)} \quad v = -\sin\beta_L U_o + \cos\beta_L V_o + (\rho+\bar{a}\cos\alpha)\phi_z^o \\
&\text{(iii)} \quad w = -\frac{\bar{b}\cos\alpha}{|\bar{g}_\alpha|}\cos\beta_L U_o - \frac{\bar{b}\cos\alpha}{|\bar{g}_\alpha|}\sin\beta_L V_o \\
&\text{(iv)} \quad -(g_{\beta\beta})^{-\frac{1}{2}}\frac{\partial w}{\partial\beta} - k_\beta^{(n)} v = -\frac{\bar{b}\cos\alpha}{|\bar{g}_\alpha|}\phi_z^o
\end{aligned} \tag{4.29}$$

The constants U_o, V_o and ϕ_z^o of the end plug are determined with the following additional relations (based upon equilibrium and symmetry conditions of the end plug):

$$(1) \qquad \int_0^{\pi} |\bar{g}_\alpha| + N_{\beta\alpha eff}\,\bar{\ell}_1 + Q_{\beta 3 eff}\,\bar{\ell}_2\, d\alpha = 0 \qquad @\ \beta = \beta_L$$

$$(2) \quad \text{(Area ellipse)} \quad p - 2\int_0^{\pi} |\bar{g}_\alpha| N_\beta\, d\alpha = 0 \qquad @\ \beta = \beta_L \tag{4.30}$$

$$(3) \qquad \int_0^{\pi} |\bar{g}_\alpha| \left[-M_{\beta\beta}\,\bar{m}_1 + N_\beta\,\bar{a}\cos\alpha\right] d\alpha = 0 \qquad @\ \beta = \beta_L$$

Where the direction cosines, (see Appendix A and Reference 6)

$$\bar{\ell}_1 = -\frac{\bar{a}\sin\alpha}{|\bar{g}_\alpha|}$$

$$\bar{m}_1 = \frac{\bar{b}\cos\alpha}{|\bar{g}_\alpha|} \tag{4.31}$$

$$\bar{\ell}_2 = -\frac{\bar{b}\cos\alpha}{|\bar{g}_\alpha|}$$

The above, then, represents the edge conditions (simplified or exact) of the boundary-value problem for the shell equations of the BOURDON tube with an elliptical cross-section. With an appropriate numerical method it is hoped that more accurate solutions can be effected.

CHAPTER 5

DISCUSSION AND COMPARISON WITH EXPERIMENTAL RESULTS

5.1 Forms of Comparison

Appendix B includes experimental data of KARDOS, EX-LINE, and MASON (Reference 3, 4, 5). These data will be used for comparison with theoretical values from formulas derived in ANDREEVA's thin-walled BOURDON tube analysis.

Two forms of graphical presentation will be noted. They are on log-log graph paper:

(1) $\frac{\Delta R}{R}\frac{E}{p}\frac{bh^3}{a^4}$ vs $\frac{Rh}{a^2}$ with the axis ratio $\frac{b}{a}$ as a third parameter.

(2) $\frac{\Delta R}{R}\frac{E}{p}$ vs $\frac{Rh}{a^2}$ with the ratio grouping: $\frac{b}{a}$ and $\frac{a}{R}$ as the third and fourth parameters.

The first graphical form has been used in theoretical work of WOLF, WUEST, and CLARK, et. al.[1]. The second has been suggested by KARDOS (Reference 3). This latter form was

---

[1] WOLF, A., "An Elementary Theory of the BOURDON GAGE", Journal of Applied Mechanics, Vol. 13 (1946) p. A207.
CLARK, GILROY, REISSNER, "Stresses and Deformations of Toroidal shells of Elliptical Cross Sections", Journal of Applied Mechanics, Vol. 74 March 1952, pp. 37-48.

recently used by EXLINE (Reference 5); however not without error - the ratio grouping: $\frac{b}{a}$ and $\frac{a}{R}$ was not considered. As a result considerable scatter was exhibited. Recently KARDOS (Reference 17) confirmed the use of the ratio grouping.

In the sections following, tabular and graphical comparisons are made for flat-oval and elliptical BOURDON tubes (tubes with central angle $\leq 360°$). Example computer program listing may be seen in Appendix C.

5.2 Flat-Oval BOURDON Tubes

Table 5.1 through Table 5.4 tabulate data of KARDOS and EXLINE with the common ratio grouping: $\frac{b}{a}$ and $\frac{a}{R}$. The average values of the ratio grouping shown in the tables are those used to calculate the theoretical curves using ANDREEVA's thin-walled flat-oval tube formula (3.6):

$$\frac{\Delta R}{R} \frac{E}{p(1-\mu^2)} = \frac{R^2}{bh} \left(1-\frac{b^2}{a^2}\right) \frac{\alpha}{\beta+x^2}$$

where $x = \frac{Rh}{a^2}$ (c.f. WUEST's $\lambda = \frac{a^2}{Rh}$)

α , β are functions of the tube shape and $\frac{a}{b}$ ratio (see Table 3.1)

Figure 5.1 through 5.4 are the corresponding log-log plots of $\frac{\Delta R}{R} \frac{E}{p}$ vs $\frac{Rh}{a^2}$ with the ratio grouping: $\frac{b}{a}$ and $\frac{a}{R}$. Good correlation can be observed. A median line drawn through

the experimental points will vary at approximately ±15% from the theoretical curve.

Figure 5.4(b) illustrates the plot of $\frac{\Delta R}{R}\frac{E}{p}\frac{bh^3}{a^4}$ vs $\frac{Rh}{a^2}$ using EXLINE's data[2] with $.2 \leq \frac{b}{a} < .32$. Although a little more scatter (as compared with Figure 5.4(a)) can be noted, the experimental points curves along with results of ANDREEVA's formula for thin-walled flat-oval BOURDON tube - Observe that the theoretical curves (solid line and dashed line) are determined by using average values of $\frac{b}{a}$ as shown in Table 5.4 or Figure 5.4(a).

5.3 Elliptical BOURDON Tubes

Table 5.5 tabulates a set of MASON's elliptical tube data with a common ratio grouping[3]: $\frac{b}{a}$ and $\frac{a}{R}$. Figure 5.5(a) and 5.5(b) are the graphical presentation of $\frac{\Delta R}{R}\frac{E}{p}$ vs $\frac{Rh}{a^2}$ and $\frac{\Delta R}{R}\frac{E}{p}\frac{bh^3}{a^4}$ vs $\frac{Rh}{a^2}$ respectively. As to be expected, deviation from the theoretical formula of ANDREEVA for elliptic tubes is large considering the nonuniformity of tests/and methods used by different manufacturers. However in the graph of $\frac{\Delta R}{R}\frac{E}{p}$ vs $\frac{Rh}{a^2}$ with the same ratio grouping: $\frac{b}{a}$ and $\frac{a}{R}$, the

---

[2] KARDOS (Reference 3) plotting his data in this form showed also considerable scatter. Therefore in this study, KARDOS data was not illustrated in this form of graphical presentation.

[3] There were insufficient data for other values of the ratio grouping; therefore they were not plotted.

test points follow the theoretical curve with a uniform difference.

5.4 Graphical vs Tabular Comparison

Thus it should be observe from the above graphical comparisons that the plot of $\frac{\Delta R}{R}\frac{E}{p}$ vs $\frac{Rh}{a^2}$ with the ratio grouping: $\frac{b}{a}$ and $\frac{a}{R}$, provides a better correlation than the other form of graphical presentation. Also note that a mere tabular comparison of the data of KARDOS, EXLINE, or MASON will provide an unsatisfactory method of correlation with theoretical formulas. (see Tables 5.6 to 5.9) In these tables, calculations from both thin-walled and thick-walled equations as derived in ANDREEVA's analysis are presented. Random scattered results can be observed for tubes with $\frac{a}{R} > 0.20$. KARDOS in Reference 17 reported similar observations.

Further from these observed scattered results, ANDREEVA's claim that the use of the thick-walled expression (3.8) will give a better correlation for tubes with $h \ll b$ and $\frac{a}{b} > 8$ does not seem to be justified.

TABLE 5.1 Flat-Oval Tube Data - KARDOS

Tube No.	Experimental $\Delta R/R$ E/p	$\lambda = Rh/a^2$	b/a	a/R
1001	70.5	1.736	.2480	.1566
1101	83.5	1.628	.2520	.1572
1103	87.1	1.694	.2886	.1536
1501	94.8	1.584	.2886	.1539
1502	110.0	1.526	.2480	.1572
2802	256.0	1.0530	.2348	.1583
4303	144.0	1.3216	.2937	.1561
4304	155.0	1.2791	.2500	.1588
1003	86.4	1.6695	.2087	.1604
3001	911.0	.66420	.2037	.1673
3102	493.0	.7883	.2080	.1667
3202	2560.0	.4498	.2574	.1635
4305	192.0	1.2593	.2287	.1600
1204	602.0	.8007	.2299	.1732
1602	5400.0	.3110	.2326	.1787
1701	939.0	.6165	.2701	.1717
1702	1210.0	.5959	.2353	.1751
2001	1840.0	.4647	.2593	.1768
2103	2890.0	.4066	.2857	.1757
2105	3415.0	.3853	.2103	.1790

Average Values: $\frac{b}{a} = 0.242$, $\frac{a}{R} = 0.166$

used for theoretical calculation with ANDREEVA's equation

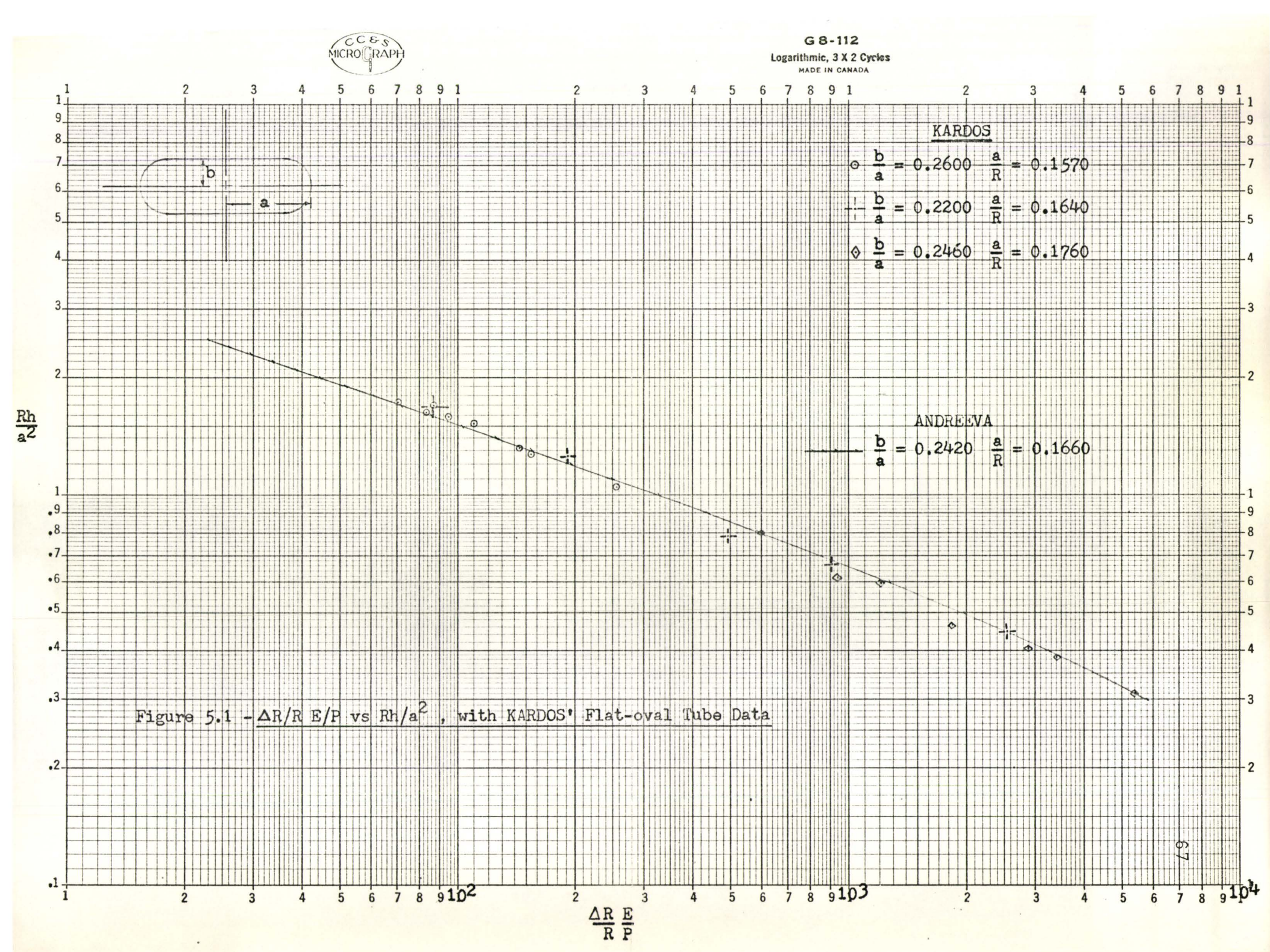

Figure 5.1 - $\Delta R/R\ E/P$ vs Rh/a^2 , with KARDOS' Flat-oval Tube Data

TABLE 5.2 Flat-Oval Tube Data - KARDOS

Tube No.	Experimental $\Delta R/R$ E/p	$\lambda = Rh/a^2$	b/a	a/R
1102	122.50	1.5429	.1953	.1620
1205	743.0	.7788	.1835	.1755
2801	309.0	1.0492	.1970	.1588
3002	1112.0	.6569	.1679	.1667
3101	793.0	.7685	.1403	.1685
3201	3175.0	.4165	.1866	.1690
3203	4890.0	.3912	.1062	.1751
3301	2500.0	.5143	.1489	.1724
3302	1838.0	.5415	.1884	.1673
4306	225.5	1.1862	.1692	.1648

Average Values: $\frac{b}{a} = 0.168$, $\frac{a}{R} = 0.168$

TABLE 5.3 Flat-Oval Tube Data - KARDOS

Tube No.	Experimental $\Delta R/R$ E/p	$\lambda = Rh/a^2$	b/a	a/R
1201	342.0	.9335	.3828	.1590
1202	379.0	.8934	.3473	.1623
1601	3570.0	.3397	.3212	.1719
2002	1468.0	.4782	.3002	.1742
2107	1992.0	.4309	.3272	.1706
4301	102.5	1.4271	.3852	.1493
4302	122.0	1.3798	.3468	.1520

Average Values: $\frac{b}{a} = 0.345$, $\frac{a}{R} = 0.163$

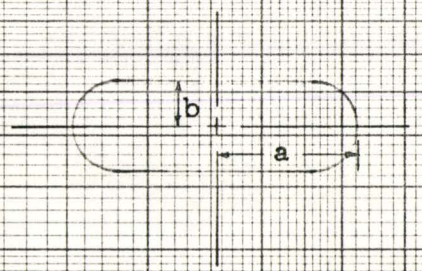

$\frac{b}{a} = 0.1680 \quad \frac{a}{R} = 0.1680$

ANDREEVA's curve

$\frac{Rh}{a^2}$

$\frac{\Delta R}{R}\frac{E}{P}$

Figure 5.2 - $\Delta R/R\ E/P$ vs Rh/a^2, with KARDOS' Flat-oval Tube Data

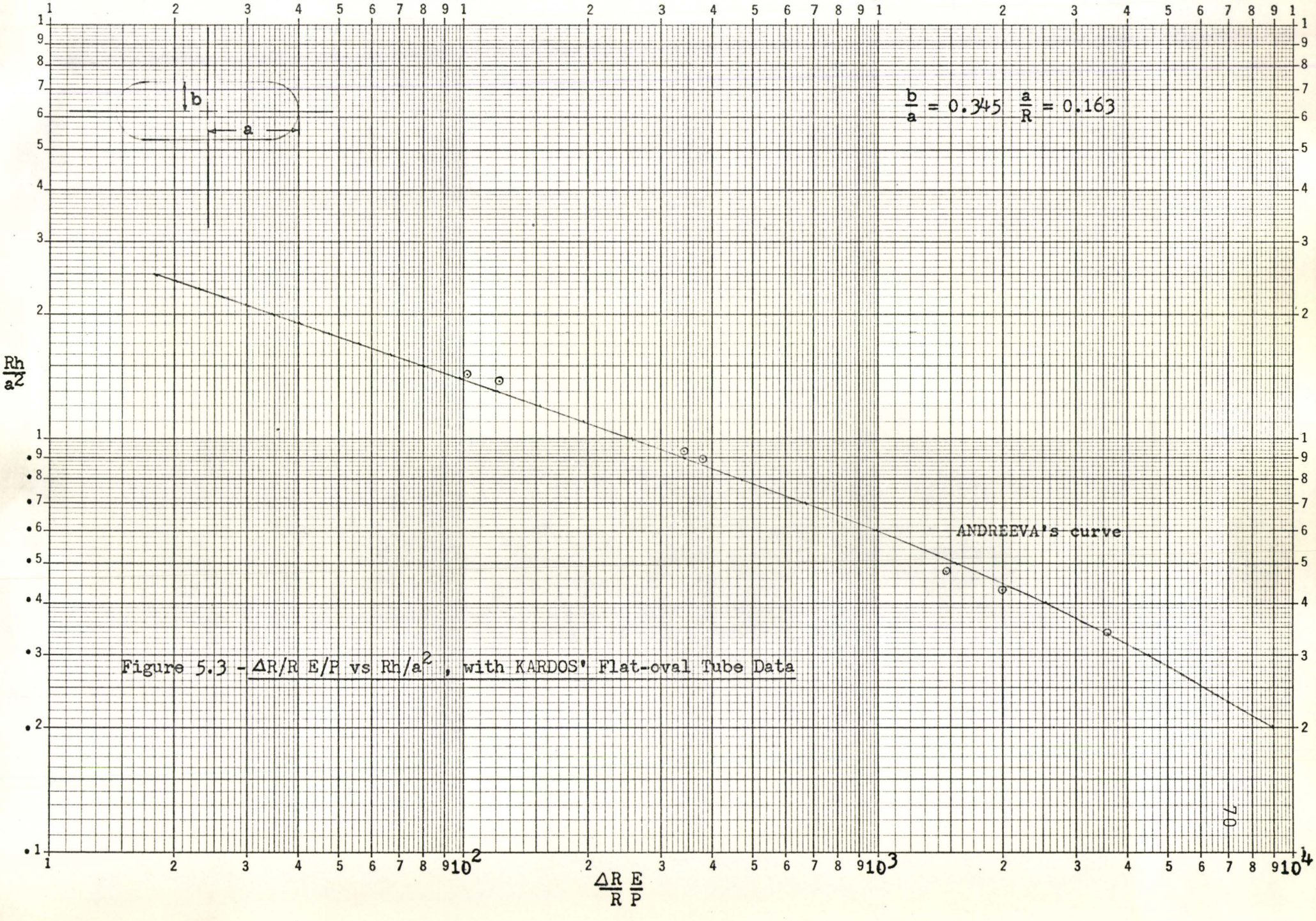

Figure 5.3 - $\Delta R/R\ E/P$ vs Rh/a^2, with KARDOS' Flat-oval Tube Data

TABLE 5.4 Flat-Oval Tube Data - EXLINE

Tube No.	Experimental $\Delta R/R\ E/p$	$\lambda = Rh/a^2$	b/a	a/R	Experimental $\Delta R/R\ E/p\ bh^3/a^4$
12	2190.0	.4247	.324	.1626	.241
13	3100.0	.3759	.310	.1619	.217
14	4070.0	.3320	.302	.1632	.196
51	1100.0	.5541	.324	.1660	.276
61	2130.0	.4496	.319	.1624	.265
71	1400.0	.5219	.312	.1655	.282
81	1740.0	.4784	.325	.1639	.274
20	6160.0	.2839	.310	.1605	.179
24	1400.0	.5526	.318	.1651	.337
25	3500.0	.3558	.308	.1665	.225
27	775.0	.6452	.300	.1691	.303
Average values: $\frac{b}{a} = 0.314$, $\frac{a}{R} = 0.1642$					
11	6510.0	.2664	.282	.1626	.149
29	3490.0	.3546	.273	.1653	.192
35	2730.0	.4613	.202	.1656	.244
Average values: $\frac{b}{a} = 0.275$, $\frac{a}{R} = 0.165$					

In addition to the above, test values of $\frac{\Delta R}{R}\frac{E}{p}\frac{bh^3}{a^4}$ from EXLINE's experimental data: Tube No. 1, 2, 3, 4, 8, 9, 10, 19, 28, 30, 41 having $0.2<b/a<0.32$ are plotted (with the symbol x) in Figure 5.4(b) - $\frac{\Delta R}{R}\frac{E}{p}\frac{bh^3}{a^4}$ vs $\frac{Rh}{a^2}$, EXLINE's flat-oval tube data.

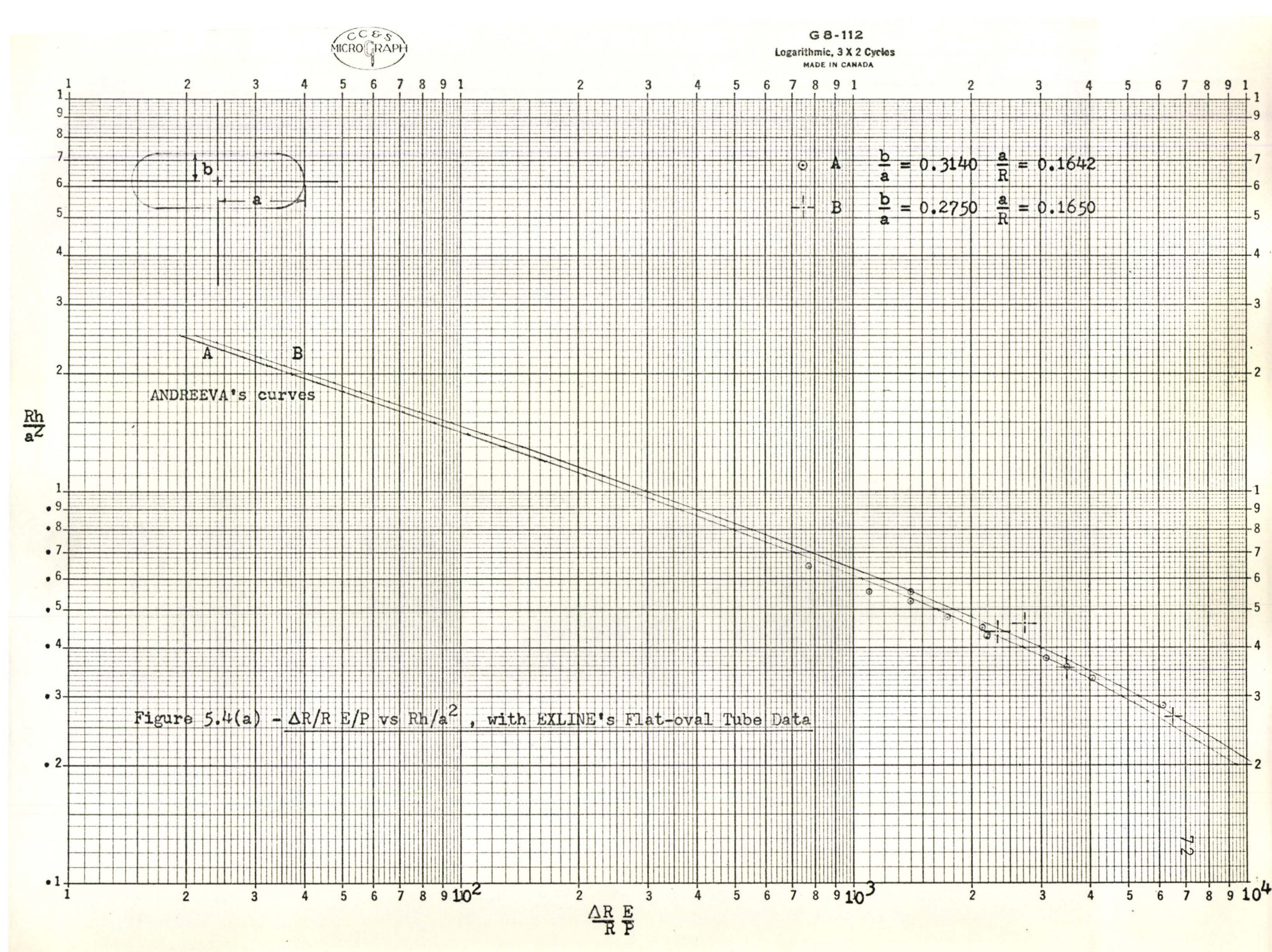

Figure 5.4(a) - $\Delta R/R$ E/P vs Rh/a^2, with EXLINE's Flat-oval Tube Data

G 8-112
Logarithmic, 3 X 2 Cycles
MADE IN CANADA

Figure 5.4(b) - $\Delta R/R\ E/P\ bh^3/a^4$ vs Rh/a^2, with EXLINE's Flat-oval Tube Data

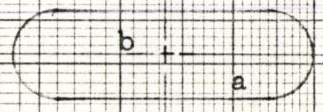

A
B
ANDREEVA's curves

$\frac{\Delta R}{R}\frac{E}{P}\frac{bh^3}{a^4}$

Rh/a^2

TABLE 5.5 Elliptic Tube Data - MASON

Tube No.	Experimental $\Delta R/R\ E/p$	$\lambda = Rh/a^2$	b/a	a/R	Experimental $\Delta R/R\ E/p\ bh^3/a^4$
60	14000	.2391	.3278	.1613	.2618
85	4420	.3434	.3149	.1609	.2365
86	4400	.3415	.3140	.1613	.2367
194	190	1.0560	.3413	.1667	.3610
195	190	1.0822	.3351	.1671	.3743
226	180	1.0691	.3406	.1631	.4104
227	150	1.1484	.3425	.1622	.3420
228	170	1.1484	.3425	.1622	.4862
229	130	1.2603	.3435	.1604	.3718
230	150	1.2636	.3361	.1613	.4200
Average values:		$\frac{b}{a} = 0.3338$,		$\frac{a}{R} = 0.1626$	
137	480	.9475	.3333	.1547	.4992
138	480	.9421	.3381	.1551	.5088
139	430	.9343	.3401	.1542	.4300
140	400	.9717	.3401	.1542	.452
141	480	.9290	.3448	.1547	.4848
Average values:		$\frac{b}{a} = 0.3393$,		$\frac{a}{R} = 0.1546$	

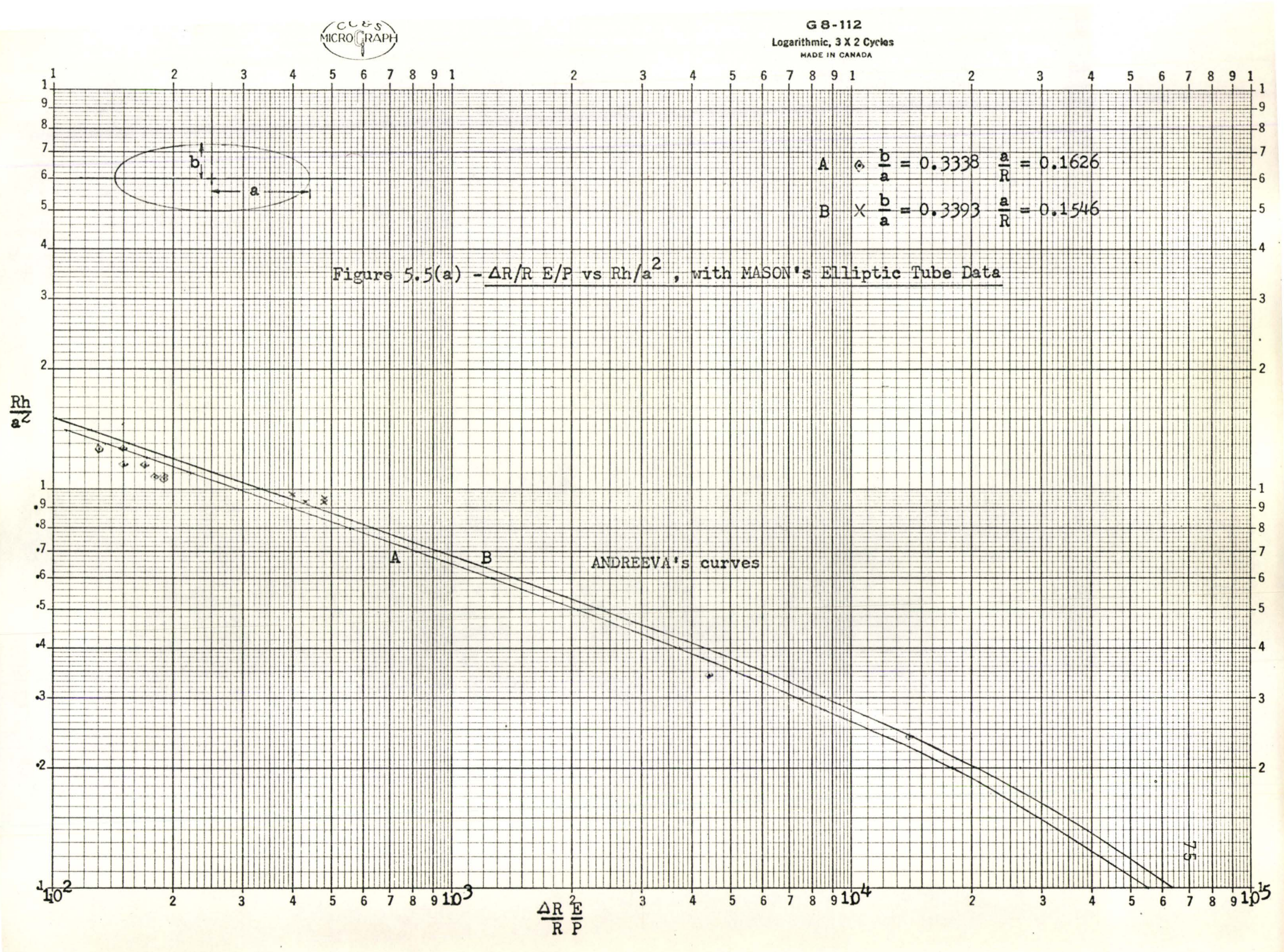
G 8-112
Logarithmic, 3 X 2 Cycles
MADE IN CANADA
b
a
A ◇ b/a = 0.3338 a/R = 0.1626
B X b/a = 0.3393 a/R = 0.1546
Figure 5.5(a) - ΔR/R E/P vs Rh/a², with MASON's Elliptic Tube Data
Rh/a²
A
B
ANDREEVA's curves
ΔR/R E/P
10²
10³
10⁴
10⁵

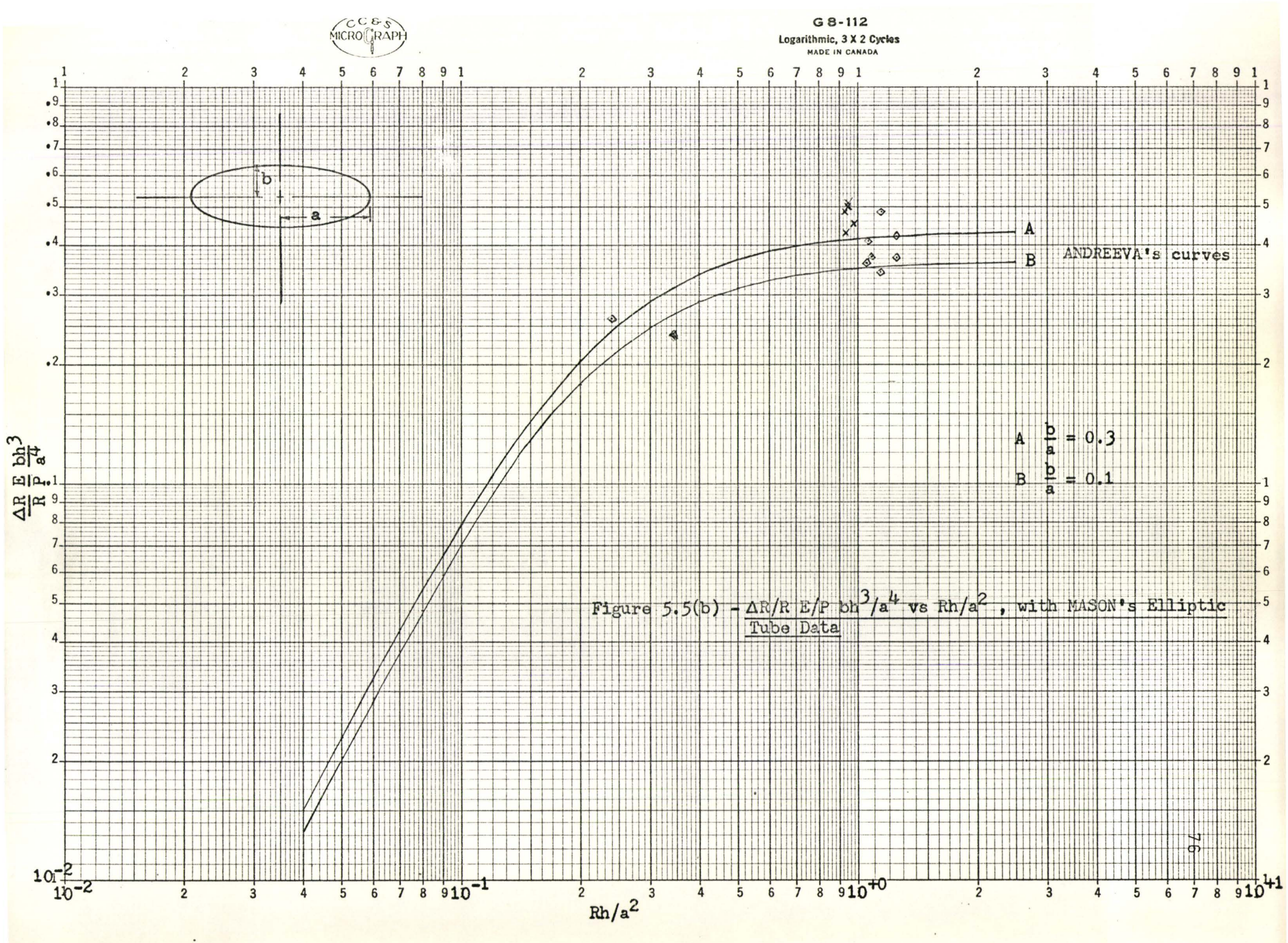

Figure 5.5(b) - $\Delta R/R\ E/P\ bh^3/a^4$ vs Rh/a^2, with MASON's Elliptic Tube Data

TABLE 5.6 Tabular Comparison of Sensitivity with KARDOS' Flat-Oval Tube Data

Symbols used in Table

FORTRAN	THEORY
P	Pressure, psi
H	Wall thickness, h ($\times 10^{-3}$ inch)
R	Tube radius, inches
DEG	Degree
B	Semi-Major axis, inch
A	Semi-Minor axis, inch
DEFLEC	Deflection of tube end (equation 3.9), inch
EXP SENS	Sensitivity $\frac{\Delta R}{R}\frac{E}{p}$ (experimental)
CAL SENS	Sensitivity (equation 3.7)
DEVIATION	Percent deviation of CAL SENS from EXP SENS
NSENS2	Sensitivity (thick-walled equation 3.8)
DEVIA2	Percent deviation of NSENS2 from EXP SENS
BR	The ratio B/R

TABLE 5.6

TUBE	P	H	R	EXECUTIØN DEG	B	A	A/B	DEFLEC	EXP SENS	CAL SENS	DEVIATIØN	NSENS2	DEVIA2	A/R	H/A	B/A	RH/B**2	BR
1001	100	34.0	0.798	217	0.125	0.0310	0.2480	0.001	70	78	10.6	46	-34.8	0.039	1.097	4.03	1.7364	0.1566
1003	100	34.0	0.792	192	0.127	0.0265	0.2087	0.001	86	94	8.8	55	-36.3	0.033	1.283	4.79	1.6695	0.1604
1101	100	32.0	0.795	221	0.125	0.0315	0.2520	0.001	83	92	10.2	55	-34.1	0.040	1.016	3.97	1.6282	0.1572
1102	100	32.0	0.790	224	0.128	0.0250	0.1953	0.002	122	121	-1.2	72	-41.2	0.032	1.280	5.12	1.5430	0.1620
1103	100	32.0	0.801	217	0.123	0.0355	0.2886	0.001	87	79	-9.3	46	-47.2	0.044	0.901	3.46	1.6942	0.1536
1201	100	19.0	0.805	220	0.128	0.0490	0.3828	0.004	342	301	-12.0	185	-45.9	0.061	0.388	2.61	0.9335	0.1590
1202	100	19.0	0.807	223	0.131	0.0455	0.3473	0.005	379	351	-7.4	216	-43.0	0.056	0.418	2.88	0.8935	0.1623
1204	100	19.0	0.791	236	0.137	0.0315	0.2299	0.008	602	552	-8.3	355	-41.0	0.040	0.603	4.35	0.8007	0.1732
1205	100	19.0	0.792	228	0.139	0.0255	0.1835	0.009	743	684	-7.9	451	-39.3	0.032	0.745	5.45	0.7788	0.1755
1301	100	21.0	0.793	236	0.114	0.0300	0.2632	0.003	256	234	-8.6	144	-43.8	0.038	0.700	3.80	1.2814	0.1438
1302	100	21.0	0.786	217	0.116	0.0255	0.2198	0.004	312	283	-9.3	178	-42.9	0.032	0.824	4.55	1.2267	0.1476
1401	100	25.0	0.791	204	0.112	0.0270	0.2411	0.002	159	144	-9.4	88	-44.7	0.034	0.926	4.15	1.5765	0.1416
1402	100	25.0	0.797	216	0.110	0.0320	0.2909	0.002	126	117	-7.1	70	-44.4	0.040	0.781	3.44	1.6467	0.1380
1501	100	30.0	0.799	223	0.123	0.0355	0.2886	0.001	94	95	0.2	57	-39.9	0.044	0.845	3.46	1.5844	0.1539
1502	100	30.0	0.795	237	0.125	0.0310	0.2480	0.002	110	113	2.7	68	-38.2	0.039	0.968	4.03	1.5264	0.1572
1601	100	8.0	0.797	229	0.137	0.0440	0.3212	0.044	3570	3247	-9.0	2151	-39.7	0.055	0.182	3.11	0.3397	0.1719
1602	100	8.0	0.806	191	0.144	0.0335	0.2326	0.050	5400	4496	-16.7	3159	-41.5	0.042	0.239	4.30	0.3110	0.1787
1701	100	14.5	0.798	238	0.137	0.0370	0.2701	0.014	939	984	4.8	631	-32.8	0.046	0.392	3.70	0.6165	0.1717
1702	100	14.5	0.794	234	0.139	0.0327	0.2353	0.016	1210	1130	-6.6	740	-38.8	0.041	0.443	4.25	0.5959	0.1751
2001	100	11.5	0.792	231	0.140	0.0363	0.2593	0.025	1840	1839	-0.1	1210	-34.2	0.046	0.317	3.86	0.4647	0.1768
2002	100	11.5	0.792	225	0.138	0.0417	0.3022	0.021	1468	1581	7.7	1017	-30.7	0.053	0.276	3.31	0.4783	0.1742
2101	100	10.0	0.790	227	0.143	0.0350	0.2448	0.036	3000	2691	-10.3	1820	-39.3	0.044	0.286	4.09	0.3863	0.1810
2102	100	10.0	0.783	235	0.148	0.0250	0.1689	0.051	4900	3727	-23.9	2702	-44.9	0.032	0.400	5.92	0.3575	0.1890
2103	100	10.0	0.797	226	0.140	0.0400	0.2857	0.031	2890	2326	-19.5	1528	-47.1	0.050	0.250	3.50	0.4066	0.1757
2105	100	10.0	0.810	218	0.145	0.0305	0.2103	0.042	3415	3157	-7.6	2193	-35.8	0.038	0.328	4.75	0.3853	0.1790
2106	100	10.0	0.791	236	0.152	0.0190	0.1250	0.069	5610	4940	-11.9	3728	-33.5	0.024	0.526	8.00	0.3424	0.1922
2107	100	10.0	0.797	208	0.136	0.0445	0.3272	0.024	1992	1983	-0.5	1279	-35.8	0.056	0.225	3.06	0.4309	0.1706
2202	100	13.5	0.782	241	0.156	0.0135	0.0865	0.042	21100	2942	-86.1	2595	-87.7	0.017	1.000	11.56	0.4338	0.1995
2401	100	9.0	0.806	239	0.195	0.0195	0.1000	0.118	12100	8141	-32.7	7108	-41.3	0.024	0.462	10.00	0.1908	0.2419
2402	100	9.0	0.806	231	0.197	0.0145	0.0736	0.124	14300	8875	-37.9	9316	-34.9	0.018	0.621	13.59	0.1869	0.2444
2801	100	22.0	0.831	224	0.132	0.0260	0.1970	0.010	309	385	24.6	247	-20.1	0.031	0.846	5.08	1.0492	0.1588
2802	100	22.0	0.834	226	0.132	0.0310	0.2348	0.009	256	335	30.9	211	-17.6	0.037	0.710	4.26	1.0530	0.1583
3001	100	15.0	0.807	226	0.135	0.0275	0.2037	0.028	911	1103	21.1	733	-19.5	0.034	0.545	4.91	0.6642	0.1673
3002	100	15.0	0.822	228	0.137	0.0230	0.1679	0.034	1112	1338	20.3	912	-18.0	0.028	0.652	5.96	0.6569	0.1667
3101	100	18.0	0.825	222	0.139	0.0195	0.1403	0.025	793	990	24.8	669	-15.6	0.024	0.923	7.13	0.7686	0.1685
3102	100	18.0	0.822	223	0.137	0.0285	0.2080	0.018	493	700	42.0	457	-7.3	0.035	0.632	4.81	0.7883	0.1667
3201	100	10.0	0.840	226	0.142	0.0265	0.1866	0.091	3175	3488	9.9	2454	-22.7	0.032	0.377	5.36	0.4166	0.1690
3202	100	10.0	0.832	199	0.136	0.0350	0.2574	0.056	2560	2519	-1.6	1668	-34.8	0.042	0.286	3.89	0.4498	0.1635
3203	100	10.0	0.834	211	0.146	0.0155	0.1062	0.135	4890	5659	15.7	4274	-12.6	0.019	0.645	9.42	0.3913	0.1751
3204	100	10.0	0.847	224	0.148	0.0105	0.0709	0.179	6130	6887	12.3	6122	-0.1	0.012	0.952	14.10	0.3867	0.1747
3301	100	12.5	0.818	205	0.141	0.0210	0.1489	0.055	2500	2436	-2.6	1723	-31.1	0.026	0.595	6.71	0.5143	0.1724
3302	100	12.5	0.825	224	0.138	0.0260	0.1884	0.050	1838	1954	6.3	1338	-27.2	0.032	0.481	5.31	0.5415	0.1673
3401	100	23.5	0.849	231	0.264	0.0337	0.1277	0.043	1320	1610	22.0	1186	-10.2	0.040	0.697	7.83	0.2863	0.3110
3402	100	23.5	0.844	195	0.266	0.0282	0.1060	0.041	1709	1867	9.2	1374	-19.6	0.033	0.833	9.43	0.2803	0.3152
3501	100	13.5	0.850	211	0.352	0.0330	0.0937	0.085	7420	3501	-52.8	5085	-31.5	0.039	0.409	10.67	0.0926	0.4141
3502	100	13.5	0.855	236	0.353	0.0280	0.0793	0.116	7780	4185	-46.2	5931	-23.8	0.033	0.482	12.61	0.0926	0.4129
3601	100	10.5	0.863	215	0.351	0.0410	0.1168	0.123	9320	4862	-47.8	6491	-30.4	0.048	0.256	8.56	0.0736	0.4067
3602	100	10.5	0.875	266	0.354	0.0307	0.0867	0.166	8960	5272	-41.2	8752	-2.3	0.035	0.342	11.53	0.0733	0.4046
3604	100	10.5	0.867	186	0.360	0.0170	0.0472	0.199	17650	9432	-46.6	14421	-18.3	0.020	0.618	21.18	0.0702	0.4152
3702	100	28.5	0.827	210	0.363	0.0637	0.1755	0.022	1020	938	-8.0	760	-25.5	0.077	0.447	5.70	0.1789	0.4389
3801	100	22.5	0.831	223	0.342	0.0427	0.1249	0.045	2060	1761	-14.5	1537	-25.4	0.051	0.527	8.01	0.1599	0.4116
3802	100	22.5	0.834	226	0.346	0.0327	0.0945	0.047	2330	1805	-22.5	1950	-16.3	0.039	0.688	10.58	0.1567	0.4149
3803	100	22.5	0.823	224	0.350	0.0217	0.0620	0.068	2718	2696	-0.8	2548	-6.3	0.026	1.037	16.13	0.1512	0.4253
3804	100	22.5	0.828	233	0.336	0.0540	0.1607	0.038	1671	1426	-14.7	1213	-27.4	0.065	0.417	6.22	0.1650	0.4058
3901	100	19.0	0.826	223	0.336	0.0530	0.1577	0.046	2060	1803	-12.5	1657	-19.6	0.064	0.358	6.34	0.1390	0.4068

```
902  100 19.0  0.819  246 0.344 0.0355 0.1032 0.069   2790     2500     -10.4    2412   -13.5 0.043 0.535  9.69  0.1315 0.4200
903  100 19.0  0.825  226 0.347 0.0265 0.0764 0.070   3115     2740     -12.0    3102    -0.4 0.032 0.717 13.09  0.1302 0.4206
904  100 19.0  0.825  216 0.351 0.0165 0.0470 0.108   3880     4442      14.5    4155     7.1 0.020 1.152 21.27  0.1272 0.4255
905  100 19.0  0.824  243 0.341 0.0415 0.1217 0.061   2465     2214     -10.2    2102   -14.7 0.050 0.458  8.22  0.1346 0.4138
906  100 19.0  0.727  232 0.346 0.0305 0.0882 0.044   2710     1897     -30.0    2332   -13.9 0.042 0.623 11.34  0.1154 0.4759
001  100 26.0  0.825  231 0.436 0.0290 0.0665 0.050   2295     1893     -17.5    2088    -9.0 0.035 0.897 15.03  0.1128 0.5285
002  100 26.0  0.822  220 0.434 0.0345 0.0795 0.039    225     1575     600.0    1849   721.8 0.042 0.754 12.58  0.1135 0.5280
201  100 45.0  0.814  219 0.439 0.0480 0.1093 0.017    584      681      16.6     509   -12.8 0.059 0.937  9.15  0.1901 0.5393
303  100 26.0  0.807  243 0.126 0.0370 0.2937 0.003    144      152       5.6      92   -36.1 0.046 0.703  3.41  1.3216 0.1561
304  100 26.0  0.806  246 0.128 0.0320 0.2500 0.004    155      182      17.4     111   -28.4 0.040 0.812  4.00  1.2791 0.1588
301  100 26.0  0.817  245 0.122 0.0470 0.3852 0.002    102      108       5.4      65   -36.6 0.058 0.553  2.60  1.4272 0.1493
302  100 26.0  0.816  241 0.124 0.0430 0.3468 0.003    122      125       2.5      76   -37.7 0.053 0.605  2.88  1.3798 0.1520
305  100 26.0  0.806  238 0.129 0.0295 0.2287 0.004    192      199       3.6     123   -35.9 0.037 0.881  4.37  1.2593 0.1600
306  100 26.0  0.807  246 0.133 0.0225 0.1692 0.006    225      275      22.0     172   -23.7 0.028 1.156  5.91  1.1862 0.1648
307  100 26.0  0.816  244 0.119 0.0505 0.4244 0.002     92       91      -1.6      55   -40.5 0.062 0.515  2.36  1.4982 0.1458

3702 LEE EDWARD T      100   000MIN 32SEC CØST$002.38 REM. TIME 0099MIN 28SEC
         $IBSYS                                                          $$

ØMPILE TIME          887     TØTAL TIME          1886
BJECT PRØG          1390     DATA STØRAGE         132     AVAILABLE CØRE     10121     SYMBØL TABLE          504

00MI 35SEC00900=
```

TABLE 5.7 Tabular Comparison of Sensitivity with EXLINE's Flat-Oval Tube Data

For definition of FORTRAN symbols, see Table 5.6

TABLE 5.7

TUBE	P	H	R	DEG	B	A	A/B	DEFLEC	EXP SENS	CAL SENS	DEVIATIØN	NSENS2	DEVIA2	A/R	H/A	B/A	RH/B**2	BR
1	410	30.8	1.646	2.564	0.335	0.092	0.274	0.072	1390	1226	-11.8	799	-42.5	0.056	0.336	3.65	0.4528	0.2033
2	510	36.8	1.625	2.517	0.337	0.075	0.223	0.067	1062	957	-9.9	632	-40.5	0.046	0.490	4.48	0.5278	0.2071
3	410	31.9	1.621	2.637	0.342	0.069	0.202	0.090	1738	1479	-14.9	1009	-41.9	0.043	0.462	4.96	0.4421	0.2110
4	200	26.4	1.619	2.373	0.344	0.079	0.229	0.050	2565	2012	-21.6	1380	-46.2	0.049	0.335	4.36	0.3620	0.2122
5	100	22.9	1.630	2.012	0.449	0.067	0.149	0.039	5990	4122	-31.2	3481	-41.9	0.041	0.342	6.70	0.1851	0.2755
6	40	9.5	1.684	1.815	0.551	0.073	0.132	0.039	40600	12037	-70.4	19264	-52.6	0.043	0.131	7.57	0.0528	0.3270
7	120	17.1	1.616	1.819	0.445	0.077	0.174	0.050	9260	5335	-42.4	4915	-46.9	0.048	0.221	5.74	0.1397	0.2752
8	810	40.0	1.636	2.719	0.323	0.083	0.255	0.082	633	650	2.7	416	-34.3	0.050	0.484	3.92	0.6257	0.1977
9	810	46.1	1.648	2.676	0.319	0.086	0.271	0.052	458	417	-9.0	262	-42.8	0.052	0.534	3.69	0.7470	0.1935
10	1000	49.8	1.621	2.709	0.316	0.081	0.255	0.053	343	346	0.9	217	-36.7	0.050	0.618	3.92	0.8105	0.1947
11	50	17.7	2.513	3.256	0.409	0.115	0.282	0.198	6510	6758	3.8	4726	-27.4	0.046	0.154	3.55	0.2664	0.1626
12	130	28.5	2.538	3.197	0.413	0.134	0.324	0.179	2190	2388	9.0	1544	-29.5	0.053	0.213	3.09	0.4247	0.1626
13	120	25.1	2.547	3.169	0.412	0.128	0.310	0.224	3100	3266	5.4	2146	-30.8	0.050	0.196	3.22	0.3759	0.1619
14	80	22.4	2.532	3.113	0.413	0.125	0.302	0.186	4070	4191	3.0	2803	-31.1	0.049	0.179	3.31	0.3320	0.1632
15	240	38.5	2.523	3.145	0.419	0.136	0.324	0.163	1100	1212	10.2	768	-30.2	0.054	0.284	3.09	0.5541	0.1660
16	160	30.4	2.563	3.192	0.416	0.133	0.319	0.199	2130	2141	0.5	1379	-35.3	0.052	0.229	3.13	0.4496	0.1624
17	200	36.3	2.540	3.154	0.420	0.131	0.312	0.165	1400	1459	4.2	931	-33.5	0.052	0.276	3.20	0.5219	0.1655
18	160	32.7	2.545	3.173	0.417	0.136	0.325	0.163	1740	1778	2.2	1138	-34.6	0.053	0.241	3.08	0.4784	0.1639
19	40	15.6	2.539	3.146	0.405	0.125	0.308	0.176	9690	7822	-19.3	5517	-43.1	0.049	0.125	3.25	0.2418	0.1594
20	80	18.6	2.543	3.145	0.408	0.127	0.310	0.260	6160	5772	-6.3	3943	-36.0	0.050	0.147	3.22	0.2839	0.1605
21	800	39.7	2.445	2.993	0.297	0.125	0.421	0.086	420	387	-7.9	240	-42.9	0.051	0.317	2.37	1.0997	0.1215
22	1000	59.9	2.484	3.097	0.288	0.118	0.409	0.033	112	112	0.0	68	-39.3	0.048	0.508	2.44	1.7877	0.1161
23	1000	52.3	2.492	3.137	0.297	0.113	0.381	0.059	196	196	0.0	119	-39.3	0.045	0.462	2.62	1.4746	0.1193
24	200	37.0	2.456	2.966	0.405	0.129	0.318	0.069	1400	1259	-10.1	799	-42.9	0.053	0.287	3.14	0.5526	0.1651
25	80	24.3	2.465	2.951	0.410	0.126	0.308	0.074	3500	3387	-3.2	2240	-36.0	0.051	0.192	3.25	0.3558	0.1665
26	120	30.8	2.510	2.971	0.420	0.114	0.271	0.145	2330	2385	2.4	1569	-32.7	0.045	0.271	3.69	0.4391	0.1672
27	200	46.4	2.515	3.232	0.425	0.128	0.300	0.096	775	838	8.1	529	-31.7	0.051	0.363	3.33	0.6452	0.1691
28	800	67.3	2.485	3.041	0.363	0.109	0.301	0.085	174	205	17.8	125	-28.2	0.044	0.616	3.32	1.2671	0.1462
29	40	24.2	2.498	3.074	0.413	0.113	0.273	0.082	3490	3855	10.5	2590	-25.8	0.045	0.214	3.66	0.3546	0.1653
30	400	64.8	2.514	3.084	0.439	0.112	0.254	0.092	349	430	23.2	271	-22.3	0.044	0.581	3.93	0.8449	0.1747
31	120	15.9	1.552	2.942	0.387	0.049	0.126	0.151	11600	7515	-35.2	6787	-41.5	0.032	0.324	7.91	0.1643	0.2497
32	120	16.2	1.540	2.910	0.388	0.048	0.123	0.145	11400	7376	-35.3	6652	-41.6	0.031	0.338	8.10	0.1658	0.2519
33	200	18.2	1.035	3.129	0.395	0.027	0.068	0.111	9690	4522	-53.3	5336	-44.9	0.026	0.677	14.68	0.1208	0.3815
34	200	17.4	1.047	2.955	0.395	0.030	0.075	0.100	10100	4396	-56.5	5437	-46.2	0.028	0.584	13.25	0.1169	0.3771
35	240	18.9	1.495	3.189	0.248	0.050	0.202	0.121	2730	2780	1.8	1912	-30.0	0.033	0.378	4.95	0.4613	0.1656
36	240	18.9	1.511	3.057	0.248	0.049	0.198	0.119	3090	2861	-7.4	1973	-36.1	0.032	0.386	5.06	0.4643	0.1641
37	320	19.6	1.098	2.636	0.255	0.030	0.117	0.101	3560	3158	-11.3	2358	-33.8	0.027	0.660	8.58	0.3317	0.2320
38	320	19.8	1.067	2.592	0.255	0.029	0.114	0.092	3380	3051	-9.7	2280	-32.5	0.027	0.680	8.75	0.3259	0.2386
39	200	22.5	1.000	2.553	0.317	0.040	0.127	0.059	4190	2319	-44.7	1835	-56.2	0.040	0.560	7.88	0.2243	0.3167
40	COMPUTER ERRØR IN EXLINE'S DATA																	
41	800	38.4	1.571	3.128	0.301	0.053	0.175	0.122	784	824	5.1	550	-29.8	0.034	0.727	5.71	0.6645	0.1918
42	800	38.7	1.583	3.475	0.301	0.058	0.191	0.130	677	754	11.4	499	-26.3	0.036	0.672	5.23	0.6757	0.1902
43	520	34.7	1.617	3.444	0.298	0.100	0.336	0.131	542	618	14.0	387	-28.6	0.062	0.347	2.98	0.6314	0.1844
44	520	34.8	1.623	3.405	0.299	0.100	0.335	0.129	551	618	12.2	386	-29.9	0.062	0.348	2.98	0.6335	0.1840
45	520	34.8	1.620	3.368	0.299	0.100	0.335	0.127	548	617	12.6	386	-29.6	0.062	0.348	2.98	0.6323	0.1843
46	520	34.7	1.620	3.374	0.299	0.100	0.335	0.128	540	622	15.2	389	-28.0	0.062	0.347	2.98	0.6305	0.1843
47	520	34.8	1.624	3.288	0.299	0.100	0.335	0.123	557	618	11.0	387	-30.5	0.062	0.348	2.98	0.6338	0.1839
48	520	34.9	1.625	3.346	0.299	0.100	0.335	0.125	551	613	11.3	384	-30.3	0.062	0.349	2.99	0.6365	0.1837
49	520	34.7	1.611	3.384	0.299	0.100	0.335	0.128	556	620	11.5	388	-30.2	0.062	0.347	2.98	0.6270	0.1854
50	520	34.9	1.618	3.339	0.299	0.100	0.335	0.124	546	612	12.1	383	-29.9	0.062	0.349	2.99	0.6337	0.1845

3702 LEE EDWARD T 100 001MIN 35SEC CØST$007.11 REM. TIME 0089MIN 18SEC

01MI 35SEC00900=

TABLE 5.8 Tabular Comparison of Sensitivity with MASON's Flat-Oval Tube Data

For definition of FORTRAN symbols, see Table 5.6

TABLE 5.8

TUBE	P	H	R	DEG	B	A	A/B	DEFLEC	EXP SENS	CAL SENS	DEVIATIØN	NSENS2	DEVIA2	A/R	H/A	B/A	RH/B**2	BR
21	30	12.0	1.620	228	0.407	0.1080	0.2654	0.095	8500	6225	-26.8	5740	-32.5	0.067	0.111	3.77	0.1174	0.2512
22	30	15.0	2.060	241	0.407	0.1200	0.2948	0.130	7200	6376	-11.4	4832	-32.9	0.058	0.125	3.39	0.1865	0.1976
25	60	17.0	1.620	228	0.408	0.1190	0.2917	0.103	4000	3678	-8.0	2899	-27.5	0.073	0.143	3.43	0.1654	0.2519
26	60	21.0	2.060	241	0.409	0.1250	0.3056	0.137	3800	3642	-4.2	2530	-33.4	0.061	0.168	3.27	0.2586	0.1985
29	100	21.0	1.620	228	0.412	0.1230	0.2985	0.124	2400	2660	10.8	1965	-18.1	0.076	0.171	3.35	0.2004	0.2543
30	100	26.0	2.060	241	0.413	0.1270	0.3075	0.156	2300	2479	7.8	1663	-27.7	0.062	0.205	3.25	0.3140	0.2005
43	500	14.0	0.710	245	0.134	0.0420	0.3134	0.076	930	851	-8.5	539	-42.0	0.059	0.333	3.19	0.5536	0.1887
44	400	14.0	0.710	238	0.140	0.0310	0.2214	0.085	1310	1227	-6.3	817	-37.6	0.044	0.452	4.52	0.5071	0.1972
45	200	14.0	0.720	250	0.146	0.0180	0.1233	0.078	2100	2121	1.0	1506	-28.3	0.025	0.778	8.11	0.4729	0.2028
46	2000	22.0	0.720	245	0.130	0.0360	0.2769	0.099	230	273	18.7	169	-26.5	0.050	0.611	3.61	0.9373	0.1806
47	1400	22.0	0.710	250	0.135	0.0230	0.1704	0.112	360	441	22.5	284	-21.1	0.032	0.957	5.87	0.8571	0.1901
50	5000	32.0	0.720	250	0.120	0.0350	0.2917	0.067	57	72	26.3	42	-26.3	0.049	0.914	3.43	1.6000	0.1667
51	5000	32.0	0.740	250	0.115	0.0460	0.4000	0.045	39	48	23.1	28	-28.2	0.062	0.696	2.50	1.7905	0.1554
53	4000	30.0	0.820	300	0.117	0.0480	0.4103	0.056	53	59	11.3	35	-34.0	0.059	0.625	2.44	1.7971	0.1427

03702 LEE EDWARD T 100 001MIN 30SEC CØST$006.79 REM. TIME 0093MIN 19SEC

TABLE 5.9 Tabular Comparison of Sensitivity with MASON's Elliptical Tube Data

For definition of FORTRAN symbols, see Table 5.6

TABLE 5.9

TUBE	P	H	R	DEG	B	A	A/B	DEFLEC	EXP SENS	CAL SENS	DEVIATIØN	NSENS2	DEVIA2	A/R	H/A	B/A	RH/B**2	B/R
19	30	10.0	0.970	233	0.273	0.0870	0.3187	0.071	10700	7644	-28.6	2859	-73.3	0.090	0.115	3.14	0.1302	0.2814
20	30	10.5	1.190	235	0.275	0.0840	0.3055	0.112	9800	9699	-1.0	3596	-63.3	0.071	0.125	3.27	0.1652	0.2311
23	60	14.0	0.970	233	0.275	0.0880	0.3200	0.081	5000	4327	-13.5	1606	-67.9	0.091	0.159	3.12	0.1796	0.2835
24	60	14.5	1.170	237	0.276	0.0870	0.3152	0.115	5000	5015	0.3	1931	-61.4	0.074	0.167	3.17	0.2227	0.2359
27	100	18.0	0.970	233	0.276	0.0840	0.3043	0.086	3000	2783	-7.2	1076	-64.1	0.087	0.214	3.29	0.2292	0.2845
28	100	18.0	1.170	237	0.274	0.0930	0.3394	0.110	3000	2896	-3.5	1184	-60.5	0.079	0.194	2.95	0.2805	0.2342
54	50	20.0	2.250	300	0.648	0.1230	0.1898	0.353	12300	15567	26.6	6164	-49.9	0.055	0.163	5.27	0.1072	0.2880
56	50	20.0	2.250	300	0.658	0.1500	0.2280	0.294	6500	12972	99.6	5172	-20.4	0.067	0.133	4.39	0.1039	0.2924
57	50	18.0	2.250	300	0.670	0.1560	0.2328	0.331	9600	14587	51.9	6066	-36.8	0.069	0.115	4.29	0.0902	0.2978
58	50	18.0	2.250	300	0.661	0.1520	0.2300	0.336	9900	14832	49.8	6117	-38.2	0.068	0.118	4.35	0.0927	0.2938
59	50	18.0	2.250	300	0.660	0.1540	0.2333	0.332	10400	14636	40.7	6026	-42.1	0.068	0.117	4.29	0.0930	0.2933
60	50	14.0	2.250	300	0.363	0.1190	0.3278	0.295	14000	13029	-6.9	5112	-63.5	0.053	0.118	3.05	0.2391	0.1613
61	50	12.5	2.250	300	0.420	0.1000	0.2381	0.558	17100	24619	44.0	9304	-45.6	0.044	0.125	4.20	0.1594	0.1867
62	50	13.0	2.250	300	0.418	0.1020	0.2440	0.508	17100	22413	31.1	8470	-50.5	0.045	0.127	4.10	0.1674	0.1858
63	50	13.0	2.250	300	0.419	0.1010	0.2411	0.514	16600	22696	36.7	8583	-48.3	0.045	0.129	4.15	0.1666	0.1862
65	50	13.0	2.250	300	0.418	0.1000	0.2392	0.517	17600	22823	29.7	8638	-50.9	0.044	0.130	4.18	0.1674	0.1858
66	50	20.0	2.250	300	0.642	0.1260	0.1963	0.342	14900	15090	1.3	5947	-60.1	0.056	0.159	5.10	0.1092	0.2853
67	50	20.0	2.250	300	0.642	0.1240	0.1931	0.347	15300	15326	0.2	6042	-60.5	0.055	0.161	5.18	0.1092	0.2853
68	50	20.0	2.250	300	0.642	0.1280	0.1994	0.337	15700	14862	-5.3	5856	-62.7	0.057	0.156	5.02	0.1092	0.2853
69	50	20.0	2.250	300	0.642	0.1260	0.1963	0.342	15100	15090	-0.1	5947	-60.6	0.056	0.159	5.10	0.1092	0.2853
70	50	20.0	2.250	300	0.642	0.1250	0.1947	0.345	15100	15207	0.7	5994	-60.3	0.056	0.160	5.14	0.1092	0.2853
71	50	20.0	2.250	300	0.640	0.1260	0.1969	0.341	15500	15050	-2.9	5923	-61.8	0.056	0.159	5.08	0.1099	0.2844
72	75	20.0	2.250	300	0.644	0.1230	0.1910	0.526	12600	15487	22.9	6115	-51.5	0.055	0.163	5.24	0.1085	0.2862
73	75	20.0	2.250	300	0.645	0.1210	0.1876	0.536	12200	15757	29.2	6227	-49.0	0.054	0.165	5.33	0.1082	0.2867
74	75	31.0	2.250	300	0.642	0.1320	0.2056	0.242	6290	7129	13.3	2695	-57.2	0.059	0.235	4.86	0.1692	0.2853
75	75	31.0	2.250	300	0.643	0.1330	0.2068	0.241	6290	7094	12.8	2681	-57.4	0.059	0.233	4.83	0.1687	0.2858
76	100	23.0	2.250	300	0.682	0.1110	0.1628	0.666	12800	14707	14.9	5765	-55.0	0.049	0.207	6.14	0.1113	0.3031
77	100	24.0	2.250	300	0.665	0.1310	0.1970	0.520	8390	11471	36.7	4415	-47.4	0.058	0.183	5.08	0.1221	0.2956
78	100	23.0	2.250	300	0.661	0.1320	0.1997	0.547	8700	12069	38.7	4671	-46.3	0.059	0.174	5.01	0.1184	0.2938
79	100	23.0	2.250	300	0.661	0.1310	0.1982	0.551	8390	12158	44.9	4706	-43.9	0.058	0.176	5.05	0.1184	0.2938
80	100	23.0	2.250	300	0.661	0.1310	0.1982	0.551	8960	12158	35.7	4706	-47.5	0.058	0.176	5.05	0.1184	0.2938
81	100	23.0	2.250	300	0.667	0.1410	0.2114	0.516	7820	11396	45.7	4430	-43.4	0.063	0.163	4.73	0.1163	0.2964
82	100	23.0	2.250	300	0.661	0.1440	0.2179	0.502	7690	11070	44.0	4288	-44.2	0.064	0.160	4.59	0.1184	0.2938
83	100	23.0	2.250	300	0.666	0.1440	0.2162	0.505	7790	11148	43.1	4331	-44.4	0.064	0.160	4.63	0.1167	0.2960
84	100	23.0	2.250	300	0.665	0.1440	0.2165	0.504	7820	11132	42.4	4322	-44.7	0.064	0.160	4.62	0.1170	0.2956
85	100	20.0	2.250	300	0.362	0.1140	0.3149	0.270	4420	5953	34.7	2617	-40.8	0.051	0.175	3.18	0.3434	0.1609
86	100	20.0	2.250	300	0.363	0.1140	0.3140	0.272	4400	6000	36.4	2633	-40.2	0.051	0.175	3.18	0.3415	0.1613
87	100	22.0	2.250	300	0.408	0.1030	0.2525	0.324	5800	7157	23.4	3053	-47.4	0.046	0.214	3.96	0.2974	0.1813
88	100	21.0	2.250	300	0.406	0.1090	0.2685	0.339	6190	7488	21.0	3138	-49.3	0.048	0.193	3.72	0.2866	0.1804
89	100	21.0	2.250	300	0.409	0.1020	0.2494	0.367	5850	8088	38.3	3398	-41.9	0.045	0.206	4.01	0.2825	0.1818
90	100	21.0	2.250	300	0.406	0.1040	0.2562	0.354	5900	7806	32.3	3287	-44.3	0.046	0.202	3.90	0.2866	0.1804
91	100	21.0	2.250	300	0.410	0.1010	0.2463	0.372	6190	8208	32.6	3447	-44.3	0.045	0.208	4.06	0.2811	0.1822
92	100	19.0	2.250	300	0.408	0.1120	0.2745	0.420	6290	9261	47.2	3746	-40.4	0.050	0.170	3.64	0.2568	0.1813
93	100	19.0	2.250	300	0.407	0.1130	0.2776	0.414	6010	9136	52.0	3697	-38.5	0.050	0.168	3.60	0.2581	0.1809
94	100	19.0	2.250	300	0.407	0.1120	0.2752	0.417	6140	9210	50.0	3730	-39.3	0.050	0.170	3.63	0.2581	0.1809
95	100	19.0	2.250	300	0.408	0.1130	0.2770	0.416	6010	9188	52.9	3713	-38.2	0.050	0.168	3.61	0.2568	0.1813
96	100	19.0	2.250	300	0.409	0.1100	0.2689	0.429	5940	9465	59.3	3830	-35.5	0.049	0.173	3.72	0.2556	0.1818
97	100	19.0	2.250	300	0.415	0.1010	0.2434	0.478	6690	10554	57.8	4275	-36.1	0.045	0.188	4.11	0.2482	0.1844
98	100	19.0	2.250	300	0.414	0.1010	0.2440	0.476	6690	10497	56.9	4257	-36.4	0.045	0.188	4.10	0.2494	0.1840
99	100	19.0	2.250	300	0.414	0.1010	0.2440	0.476	7060	10497	48.7	4257	-39.7	0.045	0.188	4.10	0.2494	0.1840
100	100	19.0	2.250	300	0.411	0.1070	0.2603	0.445	6430	9809	52.6	3970	-38.3	0.048	0.178	3.84	0.2531	0.1827
101	100	19.0	2.250	300	0.410	0.1070	0.2610	0.442	6400	9755	52.4	3953	-38.2	0.048	0.178	3.83	0.2543	0.1822
102	100	19.0	2.250	300	0.410	0.1070	0.2610	0.442	7000	9755	39.4	3953	-43.5	0.048	0.178	3.83	0.2543	0.1822
103	100	31.0	2.250	300	0.636	0.1260	0.1981	0.333	6350	7351	15.8	2782	-56.2	0.056	0.246	5.05	0.1724	0.2827
104	100	31.0	2.250	300	0.635	0.1290	0.2031	0.325	6010	7166	19.2	2713	-54.9	0.057	0.240	4.92	0.1730	0.2822

TUBE	P	H	R	DEG	B	A	A/B	DEFLEC	EXP SENS	CAL SENS	DEVIATIØN	NSENS2	DEVIA2	A/R	H/A	B/A	RH/B**2	H/R
105	100	31.0	2.250	300	0.638	0.1260	0.1975	0.335	6350	7388	16.3	2794	-56.0	0.056	0.246	5.06	0.1714	0.2836
106	100	31.0	2.250	300	0.638	0.1250	0.1959	0.337	6350	7444	17.2	2816	-55.7	0.056	0.248	5.10	0.1714	0.2836
107	100	31.0	2.250	300	0.636	0.1250	0.1965	0.336	6350	7407	16.6	2803	-55.9	0.056	0.248	5.09	0.1724	0.2827
108	100	31.0	2.250	300	0.636	0.1250	0.1965	0.336	6350	7407	16.6	2803	-55.9	0.056	0.248	5.09	0.1724	0.2827
109	100	31.0	2.250	300	0.637	0.1210	0.1900	0.347	6990	7658	9.6	2899	-58.5	0.054	0.256	5.26	0.1719	0.2831
110	100	31.0	2.250	300	0.638	0.1210	0.1897	0.348	7190	7677	6.8	2906	-59.6	0.054	0.256	5.27	0.1714	0.2836
111	100	31.0	2.250	300	0.638	0.1190	0.1865	0.353	7010	7800	11.3	2953	-57.9	0.053	0.261	5.36	0.1714	0.2836
112	100	30.0	2.250	300	0.640	0.1200	0.1875	0.374	7010	8247	17.6	3116	-55.5	0.053	0.250	5.33	0.1648	0.2844
113	100	30.0	2.250	300	0.641	0.1200	0.1872	0.375	6810	8267	21.4	3123	-54.1	0.053	0.250	5.34	0.1643	0.2849
114	250	40.0	2.250	300	0.642	0.1270	0.1978	0.514	3980	4533	13.9	1772	-55.5	0.056	0.315	5.06	0.2184	0.2853
115	250	40.0	2.250	300	0.640	0.1340	0.2094	0.484	3720	4276	14.9	1675	-55.0	0.060	0.299	4.78	0.2197	0.2844
116	250	56.0	2.250	300	0.676	0.1150	0.1701	0.305	1480	2696	82.2	1112	-24.9	0.051	0.487	5.88	0.2757	0.3004
117	250	56.0	2.250	300	0.644	0.1300	0.2019	0.240	1400	2122	51.6	905	-35.4	0.058	0.431	4.95	0.3038	0.2862
118	250	56.0	2.250	300	0.642	0.1320	0.2056	0.235	1430	2073	45.0	887	-38.0	0.059	0.424	4.86	0.3057	0.2853
119	250	56.0	2.250	300	0.643	0.1310	0.2037	0.238	1370	2097	53.1	896	-34.6	0.058	0.427	4.91	0.3048	0.2858
120	250	59.0	2.250	300	0.641	0.1290	0.2012	0.211	1430	1863	30.3	810	-43.4	0.057	0.457	4.97	0.3231	0.2849
121	250	27.0	2.250	300	0.366	0.0980	0.2678	0.371	3250	3276	0.8	1598	-50.8	0.044	0.276	3.73	0.4535	0.1627
122	250	27.0	2.250	300	0.365	0.0980	0.2685	0.368	3020	3247	7.5	1586	-47.5	0.044	0.276	3.72	0.4560	0.1622
123	250	27.0	2.250	300	0.365	0.0990	0.2712	0.365	3020	3219	6.6	1570	-48.0	0.044	0.273	3.69	0.4560	0.1622
124	500	63.0	2.250	300	0.632	0.0900	0.1424	0.479	1770	2113	19.4	938	-47.0	0.040	0.700	7.02	0.3549	0.2809
125	500	61.0	2.250	300	0.635	0.0930	0.1465	0.511	1850	2253	21.8	990	-46.5	0.041	0.656	6.83	0.3404	0.2822
126	500	73.0	2.250	300	0.631	0.1240	0.1965	0.245	740	1081	46.1	505	-31.8	0.055	0.589	5.09	0.4125	0.2804
127	500	73.0	2.250	300	0.631	0.1240	0.1965	0.245	770	1081	40.4	505	-34.4	0.055	0.589	5.09	0.4125	0.2804
128	500	73.0	2.250	300	0.631	0.1240	0.1965	0.245	740	1081	46.1	505	-31.8	0.055	0.589	5.09	0.4125	0.2804
129	500	73.0	2.250	300	0.631	0.1240	0.1965	0.245	740	1081	46.1	505	-31.8	0.055	0.589	5.09	0.4125	0.2804
130	500	39.0	2.250	300	0.362	0.0910	0.2514	0.278	1250	1228	-1.8	663	-47.0	0.040	0.429	3.98	0.6696	0.1609
131	500	39.0	2.250	300	0.362	0.0910	0.2514	0.278	1230	1228	-0.2	663	-46.1	0.040	0.429	3.98	0.6696	0.1609
132	500	39.0	2.250	300	0.362	0.0910	0.2514	0.278	1250	1228	-1.8	663	-47.0	0.040	0.429	3.98	0.6696	0.1609
133	1000	42.0	2.250	300	0.354	0.1040	0.2938	0.371	740	818	10.5	445	-39.9	0.046	0.404	3.40	0.7541	0.1573
134	1000	42.0	2.250	300	0.354	0.1030	0.2910	0.374	770	825	7.1	449	-41.7	0.046	0.408	3.44	0.7541	0.1573
135	1000	41.0	2.250	300	0.355	0.1040	0.2930	0.401	800	885	10.6	479	-40.1	0.046	0.394	3.41	0.7320	0.1578
136	1000	40.0	2.250	300	0.354	0.1040	0.2938	0.426	800	940	17.5	507	-36.6	0.046	0.385	3.40	0.7182	0.1573
137	1500	51.0	2.250	300	0.348	0.1160	0.3333	0.270	480	397	-17.3	221	-54.0	0.052	0.440	3.00	0.9475	0.1547
138	1500	51.0	2.250	300	0.349	0.1180	0.3381	0.269	480	395	-17.7	219	-54.4	0.052	0.432	2.96	0.9421	0.1551
139	1500	50.0	2.250	300	0.347	0.1180	0.3401	0.279	430	410	-4.7	227	-47.2	0.052	0.424	2.94	0.9343	0.1542
140	1500	52.0	2.250	300	0.347	0.1180	0.3401	0.249	400	366	-8.5	203	-49.2	0.052	0.441	2.94	0.9717	0.1542
141	1500	50.0	2.250	300	0.348	0.1200	0.3448	0.277	480	408	-15.0	226	-52.9	0.053	0.417	2.90	0.9290	0.1547
142	1500	47.0	2.250	300	0.345	0.0860	0.2493	0.433	510	636	24.7	358	-29.8	0.038	0.547	4.01	0.8885	0.1533
143	1500	48.0	2.250	300	0.345	0.0840	0.2435	0.415	510	611	19.8	345	-32.4	0.037	0.571	4.11	0.9074	0.1533
144	1500	46.0	2.250	300	0.345	0.0870	0.2522	0.456	510	670	31.4	376	-26.3	0.039	0.529	3.97	0.8696	0.1533
145	1500	47.0	2.250	300	0.340	0.0830	0.2441	0.423	480	622	29.6	352	-26.7	0.037	0.566	4.10	0.9148	0.1511
146	25	18.0	2.250	300	0.645	0.1080	0.1674	0.419	14500	20457	41.1	8300	-42.8	0.048	0.167	5.97	0.0973	0.2867
147	25	18.0	2.250	300	0.645	0.1060	0.1643	0.426	14600	20812	42.5	8454	-42.1	0.047	0.170	6.08	0.0973	0.2867
148	25	18.0	2.250	300	0.648	0.1080	0.1667	0.420	14000	20529	46.6	8350	-40.4	0.048	0.167	6.00	0.0965	0.2880
149	25	18.0	2.250	300	0.647	0.1080	0.1669	0.420	14300	20505	43.4	8333	-41.7	0.048	0.167	5.99	0.0967	0.2876
150	25	18.0	2.250	300	0.646	0.1050	0.1625	0.430	13500	21008	55.6	8550	-36.7	0.047	0.171	6.15	0.0970	0.2871
151	25	18.0	2.250	300	0.645	0.1070	0.1659	0.423	14300	20640	44.3	8376	-41.4	0.048	0.168	6.03	0.0973	0.2867
152	50	26.0	2.250	300	0.659	0.1130	0.1715	0.474	9100	11585	27.3	4399	-51.7	0.050	0.230	5.83	0.1347	0.2929
153	50	27.0	2.250	300	0.658	0.1140	0.1733	0.442	9100	10783	18.5	4081	-55.2	0.051	0.237	5.77	0.1403	0.2924
154	50	27.0	2.250	300	0.643	0.1060	0.1649	0.460	7500	11236	49.8	4242	-43.4	0.047	0.255	6.07	0.1469	0.2858
155	50	27.0	2.250	300	0.642	0.1070	0.1667	0.455	7200	11121	54.5	4195	-41.7	0.048	0.252	6.00	0.1474	0.2853
156	50	27.0	2.250	300	0.658	0.1070	0.1626	0.469	7200	11456	59.1	4338	-39.7	0.048	0.252	6.15	0.1403	0.2924
157	50	32.0	2.250	300	0.640	0.1030	0.1609	0.348	7200	8487	17.9	3221	-55.3	0.046	0.311	6.21	0.1758	0.2844
158	50	29.0	2.250	300	0.642	0.1040	0.1620	0.413	7700	10089	31.0	3810	-50.5	0.046	0.279	6.17	0.1583	0.2853
159	50	30.0	2.250	300	0.642	0.1030	0.1604	0.393	7200	9586	33.1	3625	-49.7	0.046	0.291	6.23	0.1638	0.2853

TUBE	P	H	R	DEG	B	A	A/B	DEFLEC	EXP SENS	CAL SENS	DEVIATIØN	NSENS2	DEVIA2	A/R	H/A	B/A	RH/B**2	H/R
160	100	27.0	2.250	300	0.648	0.1340	0.2068	0.740	4400	9034	105.3	3415	-22.4	0.060	0.201	4.84	0.1447	0.2880
161	100	28.0	2.250	300	0.652	0.1350	0.2071	0.697	5300	8510	60.6	3213	-39.4	0.060	0.207	4.83	0.1482	0.2898
162	100	27.0	2.250	300	0.652	0.1380	0.2117	0.725	5300	8845	66.9	3346	-36.9	0.061	0.196	4.72	0.1429	0.2898
163	100	37.0	2.250	300	0.636	0.0960	0.1509	0.553	4500	6757	50.2	2625	-41.7	0.043	0.385	6.63	0.2058	0.2827
164	100	38.0	2.250	300	0.635	0.0990	0.1559	0.509	4200	6211	47.9	2422	-42.3	0.044	0.384	6.41	0.2120	0.2822
165	100	38.0	2.250	300	0.635	0.1020	0.1606	0.495	4200	6048	44.0	2356	-43.9	0.045	0.373	6.23	0.2120	0.2822
166	100	38.0	2.250	300	0.635	0.0990	0.1559	0.509	4300	6211	44.4	2422	-43.7	0.044	0.384	6.41	0.2120	0.2822
167	250	60.0	2.250	300	0.630	0.0930	0.1476	0.470	1800	2295	27.5	1009	-43.9	0.041	0.645	6.77	0.3401	0.2800
168	250	59.0	2.250	300	0.629	0.0940	0.1494	0.483	1500	2359	57.3	1034	-31.1	0.042	0.628	6.69	0.3355	0.2796
169	250	61.0	2.250	300	0.628	0.0930	0.1481	0.447	1500	2183	45.5	967	-35.5	0.041	0.656	6.75	0.3480	0.2791
170	250	59.0	2.250	300	0.631	0.0940	0.1490	0.487	1500	2380	58.7	1041	-30.6	0.042	0.628	6.71	0.3334	0.2804
171	250	62.0	2.250	300	0.628	0.0930	0.1481	0.429	1500	2097	39.8	932	-37.9	0.041	0.667	6.75	0.3537	0.2791
172	250	60.0	2.250	300	0.630	0.0930	0.1476	0.470	1500	2295	53.0	1009	-32.7	0.041	0.645	6.77	0.3401	0.2800
173	500	99.0	2.250	300	0.616	0.0850	0.1380	0.253	820	616	-24.9	298	-63.7	0.038	1.165	7.25	0.5870	0.2738
176	500	72.0	2.250	300	0.629	0.1000	0.1590	0.552	820	1349	64.5	624	-23.9	0.044	0.720	6.29	0.4095	0.2796
178	500	76.0	2.250	300	0.624	0.0850	0.1362	0.541	800	1321	65.1	613	-23.4	0.038	0.894	7.34	0.4392	0.2773
179	500	77.0	2.250	300	0.623	0.0850	0.1364	0.520	800	1269	58.6	592	-26.0	0.038	0.906	7.33	0.4464	0.2769
180	500	76.0	2.250	300	0.624	0.0860	0.1378	0.535	800	1307	63.4	608	-24.0	0.038	0.884	7.26	0.4392	0.2773
181	500	76.0	2.250	300	0.624	0.0860	0.1378	0.535	790	1307	65.4	608	-23.0	0.038	0.884	7.26	0.4392	0.2773
182	500	76.0	2.250	300	0.624	0.0860	0.1378	0.535	790	1307	65.4	608	-23.0	0.038	0.884	7.26	0.4392	0.2773
193	1000	57.5	2.250	300	0.380	0.1310	0.3447	0.285	190	348	83.2	191	0.5	0.058	0.439	2.90	0.8959	0.1689
194	1000	66.0	2.250	300	0.375	0.1280	0.3413	0.186	190	226	18.9	126	-33.7	0.057	0.516	2.93	1.0560	0.1667
195	1000	68.0	2.250	300	0.376	0.1260	0.3351	0.174	190	212	11.6	119	-37.4	0.056	0.540	2.98	1.0822	0.1671
196	1000	55.0	2.250	300	0.337	0.0950	0.2819	0.278	390	339	-13.1	192	-50.8	0.042	0.579	3.55	1.0896	0.1498
197	1000	56.0	2.250	300	0.335	0.0970	0.2896	0.253	390	308	-21.0	175	-55.1	0.043	0.577	3.45	1.1227	0.1489
198	1000	56.0	2.250	300	0.335	0.0980	0.2925	0.251	390	306	-21.5	173	-55.6	0.044	0.571	3.42	1.1227	0.1489
199	1000	57.0	2.250	300	0.336	0.0910	0.2708	0.257	390	313	-19.7	178	-54.4	0.040	0.626	3.69	1.1360	0.1493
200	1000	54.0	2.250	300	0.336	0.0960	0.2857	0.287	390	350	-10.3	198	-49.2	0.043	0.563	3.50	1.0762	0.1493
201	1000	56.0	2.250	300	0.336	0.0940	0.2798	0.263	390	320	-17.9	182	-53.3	0.042	0.596	3.57	1.1161	0.1493
204	1000	58.0	2.250	300	0.331	0.0930	0.2810	0.226	280	276	-1.4	157	-43.9	0.041	0.624	3.56	1.1911	0.1471
205	1000	60.0	2.250	300	0.329	0.0930	0.2827	0.200	280	244	-12.9	139	-50.4	0.041	0.645	3.54	1.2472	0.1462
206	1000	59.0	2.250	300	0.329	0.0930	0.2827	0.210	170	256	50.6	146	-14.1	0.041	0.634	3.54	1.2264	0.1462
207	1000	59.0	2.250	300	0.330	0.0930	0.2818	0.213	280	259	-7.5	148	-47.1	0.041	0.634	3.55	1.2190	0.1467
208	1000	51.0	2.250	300	0.333	0.1080	0.3243	0.295	260	360	38.5	202	-22.3	0.048	0.472	3.08	1.0348	0.1480
209	1000	51.0	2.250	300	0.336	0.1060	0.3155	0.311	190	379	99.5	212	11.6	0.047	0.481	3.17	1.0164	0.1493
210	1000	50.0	2.250	300	0.334	0.1070	0.3204	0.319	360	389	8.1	218	-39.4	0.048	0.467	3.12	1.0085	0.1484
211	1000	51.0	2.250	300	0.335	0.1080	0.3224	0.302	340	368	8.2	206	-39.4	0.048	0.472	3.10	1.0225	0.1489
212	1000	51.0	2.250	300	0.334	0.1080	0.3234	0.298	360	364	1.1	204	-43.3	0.048	0.472	3.09	1.0286	0.1484
213	1000	48.0	2.250	300	0.288	0.0800	0.2778	0.267	390	325	-16.7	187	-52.1	0.036	0.600	3.60	1.3021	0.1280
214	1000	40.0	2.250	300	0.292	0.0860	0.2945	0.451	390	550	41.0	312	-20.0	0.038	0.465	3.40	1.0555	0.1298
215	1000	40.0	2.250	300	0.291	0.0900	0.3093	0.427	410	521	27.1	295	-28.0	0.040	0.444	3.23	1.0628	0.1293
216	1000	47.0	2.250	300	0.283	0.0820	0.2898	0.260	360	317	-11.9	182	-49.4	0.036	0.573	3.45	1.3204	0.1258
217	1000	40.0	2.250	300	0.291	0.0890	0.3058	0.432	390	526	34.9	298	-23.6	0.040	0.449	3.27	1.0628	0.1293
218	1000	55.0	2.250	300	0.331	0.1010	0.3051	0.246	230	300	30.4	169	-26.5	0.045	0.545	3.28	1.1295	0.1471
219	1000	56.0	2.250	300	0.330	0.1020	0.3091	0.229	230	279	21.3	158	-31.3	0.045	0.549	3.24	1.1570	0.1467
220	1000	57.0	2.250	300	0.330	0.1000	0.3030	0.221	190	269	41.6	152	-20.0	0.044	0.570	3.30	1.1777	0.1467
221	1000	58.0	2.250	300	0.329	0.1000	0.3040	0.208	210	253	20.5	143	-31.9	0.044	0.580	3.29	1.2056	0.1462
222	1000	58.0	2.250	300	0.329	0.1000	0.3040	0.208	210	253	20.5	143	-31.9	0.044	0.580	3.29	1.2056	0.1462
223	1000	60.0	2.250	300	0.332	0.0960	0.2892	0.202	210	246	17.1	139	-33.8	0.043	0.625	3.46	1.2248	0.1476
224	1000	59.0	2.250	300	0.332	0.0980	0.2952	0.208	210	253	20.5	144	-31.4	0.044	0.602	3.39	1.2044	0.1476
225	1000	59.0	2.250	300	0.331	0.0980	0.2961	0.206	210	250	19.0	142	-32.4	0.044	0.602	3.38	1.2117	0.1471
226	1000	64.0	2.250	300	0.367	0.1250	0.3406	0.192	180	233	29.4	130	-27.8	0.056	0.512	2.94	1.0691	0.1631
227	1000	68.0	2.250	300	0.365	0.1250	0.3425	0.157	150	191	27.3	107	-28.7	0.056	0.544	2.92	1.1484	0.1622
228	1000	68.0	2.250	300	0.365	0.1250	0.3425	0.157	170	191	12.4	107	-37.1	0.056	0.544	2.92	1.1484	0.1622
229	1000	73.0	2.250	300	0.361	0.1240	0.3435	0.123	130	150	15.4	84	-35.4	0.055	0.589	2.91	1.2603	0.1604
230	1000	74.0	2.250	300	0.363	0.1220	0.3361	0.123	150	149	-0.7	84	-44.0	0.054	0.607	2.98	1.2636	0.1613

CHAPTER 6

CONCLUSION, RECOMMENDATION AND PRELIMINARY DESIGN PROCEDURE

6.1 Conclusion of BOURDON Tube Study

In this study, three papers:

(1) WUEST, W., "Theory of High-Pressure BOURDON Tubes"

(2) ANDREEVA, L.E., "Elastic Elements of Instruments"

(3) DRESSLER, R., "Elastic Shell-Theory Formulation for BOURDON Tubes"

(References 1, 2 and 6 respectively) representative of the state-of-the-art of BOURDON tube theories have been reviewed.

The first of these by WUEST (based upon a plane strain elasticity problem) is primarily for thick-walled, flat-oval cross-sections with characteristic ratio λ less than 1.

i.e. $$\lambda = \frac{a^2}{dR} < 1$$

where a = average semi-major axis of the oval cross-section

d = wall thickness

R = mean or tube radius of curvature

This requirement is necessary for assumptions used in the analysis. With accurate experimental measurements (as suggested in WUEST's paper) good correlation (within 12%)

with theoretical results was illustrated by WUEST.

In contrast to WUEST's theory, ANDREEVA's approximation analysis (based on the RITZ's method) is derived for thin-walled BOURDON tubes. Both elliptical and flat-oval cross-sections are considered in the analysis.

As existing test results for thin-wall tubes (test data of KARDOS, MASON, EXLINE - References 3, 4, 5 respectively) are available for comparison, ANDREEVA's expressions for sensitivity were computer programmed in FORTRAN IV. The logic and listing of the procedure are attached in Appendix C.

The comparison of results with ANDREEVA's expressions and test data of KARDOS, MASON, and EXLINE indicates good correlation (a median line drawn through the experimental points will vary at approximately ±15% from the theoretical curve) for flat-oval cross-sections with $\frac{a}{R} < 0.2$ and $0.3 < \frac{Rh}{a^2} < 2$. For elliptic cross-sections, however, more scatter is evident. Possible reasons for this may be due to:

(a) variations in measurements

(b) inconsistencies in fabrication or test techniques

In the graphical representations of sensitivity $\frac{\Delta R}{R}\frac{E}{p}$ versus $\frac{Rh}{a^2}$, it can be observed that different curves can be ascribed to different values of the ratios: $\frac{a}{R}$ and $\frac{b}{a}$ - as were shown qualitatively by KARDOS in References 3 and 17.

Another form of graphical comparison was presented - $\frac{\Delta R}{R}\frac{E}{p}\frac{bh^3}{a^4}$ versus $\frac{Rh}{a^2}$. It can be seen that its scatter band

is exorbitantly wide, which suggests that possibly a better choice of parameters might reduce the scatter.

In DRESSLER's work a formulation, for BOURDON tubes with an elliptical cross-section, using thin elastic shell theory (based upon LOVE's shell equations, Reference 7) is presented. Although the formulation is essentially complete, there remains considerable task to arrive at the final form of the expressions as detailed in Table 4.2 and in the boundary conditions. As the equations are complicated and unwieldly, a complete derivation of the thin-elastic shell theory application to the BOURDON gage with an elliptical cross-section has been rehearsed, but with a different approach (Appendix A) in order to:

1. Check and complete the formulation as described by DRESSLER
2. Check and emphasize the assumptions and approximations on which the final expressions are based.

From this reanalysis the following remarks, on which the final expressions (Table 4.2) and boundary conditions are based, can be concluded:

1. Two possible thin, elastic, moment shell theories for BOURDON tubes with an elliptical cross section are noted:
   (a) "simplified" thin shell theory
   (b) "thin and shallow" shell or slightly curved

plate theory (as used in DRESSLER's formulation, Reference 6)

The "simplified" thin shell theory for BOURDON tubes with an elliptical cross-section is characterized with the following hypothesis and approximations:

(a) KIRCHHOFF Hypothesis

(b) LOVE's First Approximation

(c) ARON's Approximations for the curvature changes δK_{ij} $(i,j = 1,2)$

The "thin and shallow" shell or slightly curved plate theory for BOURDON tubes with an elliptical cross-section is characterized with the above hypothesis and approximations, and in addition, with the following assumptions:

(a) The vanishing of terms containing the transverse stress resultants Q_{i3} $(i = 1,2)$ in the first two force equilibrium equations is assumed

(b) Terms with the GAUSSIAN curvature as a factor are neglected

(c) Terms containing tangential displacements u and v in the rotation components ϕ_{i3} $(i = 1,2)$ are neglected - in plate theory tangential displacements, in ϕ_{i3}, are not involved

2. Because of the pronounced curvature at the end regions of the semi-major axis of the "elliptical" BOURDON tube (resulting in a very small radius of

curvature) the effect of moments on the transverse shear may be significant, therefore, the "simplified" thin shell theory (as stated above) is employed to obtain the final form of the expressions as illustrated in Table 4.2 and in the boundary conditions - see also H.L.LANGHAAR's, "Paradoxes in the Theories of Plates and Shells", Reference 9.

3. For the boundary conditions at the end plug of the BOURDON tube an alternate "simplified" condition (reasoned along a physical and geometrical basis) is offered over the natural conditions (based on a free-end condition) suggested by DRESSLER. A complete derivation of a more rigorous (but exact) nature, based upon the edge conditions at the junction of two shells (the BOURDON shell and the rigid movable end plug), is also presented (Appendix A).

6.2 Recommendation

Based upon this study the recommendations as listed hereunder may be prescribed:

1. To substantiate WUEST's thick-wall high pressure tube theory, test results for flat-oval cross-sections with λ less than 1 should be obtained.
2. For tubes with the characteristic ratio $0.3 < \frac{Rh}{a^2} < 2$

and $\frac{a}{R} < 0.2$, ANDREEVA's thin-walled flat-oval tube expression may be used for a preliminary design of BOURDON tubes.

3. More test data should be generated for:
   (a) thin-walled flat-oval tubes with characteristic ratio $\frac{Rh}{a^2} < 0.3$ and tubes with $\frac{a}{R} > 0.2$.
   (b) thin-walled elliptic tubes with all ranges of the various tube ratios.

   For both (a) and (b), it should be noted that the average value (say from five tests) at each increment of $\frac{Rh}{a^2}$, should be determined and used for comparison with theoretical results.

4. When comparing tube sensitivity performance characteristics, the following log-log graphical representation should be used for a meaningful interpretation of results:
   Sensitivity $\frac{\Delta R}{R}\frac{E}{p}$ vs $\frac{Rh}{a^2}$ with the constant ratio $\frac{a}{R}$ plotting for a family of curves $(\frac{b}{a})$ = constant as in (3) above, "average values" should be used.

5. Due to the complexity of the boundary conditions at the end plug or deflecting end and storage capacity limitation in electronic automatic computers two phases should be followed to the solution of the governing partial differential equations (Table 4.2)

and edge conditions of the BOURDON gage:

Phase 1 - Using Table 4.2 equations and the simplified BOUNDARY conditions at the end plug

Phase 2 - Using Table 4.2 equations and the non-simplified BOUNDARY conditions of the end-plug which involve integro-differential expressions.

6.3 Suggestions for a Preliminary Design of BOURDON Tubes

Two preliminary design procedures are suggested below. Both designs are for thin-wall tubes. For tubes with the ratio: $\frac{a^2}{Rh} << 1$, WUEST's form of analysis may be followed. The symbols used for the tube geometry in this section are as in ANDREEVA's analysis - see CHAPTER 3.

Design I

The given conditions or data of this design method are:

(1) ratios $\frac{b}{a}$ and $\frac{a}{R}$

(2) tube radius R

(3) Chart: $\frac{\Delta R}{R}\frac{E}{p}$ vs $\frac{Rh}{a^2}$ with the ratio group, $\frac{b}{a}$ and $\frac{a}{R}$.

In (1) above, the availability of tube stocks may determine the ratios. The value of R may be dictated by space limi-

tation. The chart of sensitivity $\frac{\Delta R}{R}\frac{E}{p}$ vs $\frac{Rh}{a^2}$ may be constructed through experimental testing of tubes or via ANDREEVA's equation (3.7).

Therefore, with the chart of sensitivity vs $\frac{Rh}{a^2}$, the sensitivity $(\frac{\Delta R}{R}\frac{E}{p})$ of the tube may be obtained for a thickness suitable for the pressure involved (see Reference 5). Thus all geometric dimensions of the tube are known. If desired, next, the tip travel of the tube may be found via expression (3.9).

Design II

Alternatively, one might desire to optimize a tube, say, for maximum sensitivity. Through this approach the basic concepts of optimization are used which include:

1. Optimization Function U

$$U = \text{Sensitivity} = \frac{\Delta R}{R}\frac{E}{p(1-\mu^2)}$$

$$= \frac{R^2}{bh}\left(1 - \frac{b^2}{a^2}\right)\frac{\alpha}{\beta+x^2}$$

2. Equality Constraints ψ_i[1]

$$\psi_1 = \frac{Rh}{a^2} \qquad \psi_3 = \frac{a}{R}$$

$$\psi_2 = \frac{a}{b}$$

---

[1] Additional constraints, such as stress constraints, may be incorporated. See Reference 2 for stress formulas. (These stress formulas are not very exact. However they provide an indication of the stress levels in the tube.)

3. Constraining Functions

(a) Ratio Constraints ψ_i

$$0.3 \leq \psi_1 \leq 2 \qquad 1.0 \leq \psi_2 \leq 8 \qquad 0.1 \leq \psi_3 \leq 0.2$$

Observe that these limits may be changed if applicable. These limits are results of findings of CHAPTER 5.

(b) Regional Constraints ϕ_i

$$L_R \leq R \leq U_R \qquad L_b \leq b \leq U_b$$

$$L_a \leq a \leq U_a \qquad L_h \leq h \leq U_h$$

Where L and U denote lower and upper limits respectively.

The method begins by calculating or generating trial values of the tube parameters (R, b, a and h) subjected to their "regional" constraints ϕ_i. Thence if the "ratio" constraints ψ_i are within range (if not, regenerate trial values of the tube parameters) a good point is generated and its optimization function U determined. Thereafter, depending on the strategy[2] used for convergence, an optimum tube is thus found.

---

[2] see J.N.SIDDALL, "Theory of Engineering Design", PART II, McMaster University, Hamilton, Ontario, Canada, 1967.

REFERENCES

1. WUEST, W., "Theory of High-Pressure BOURDON Tubes", ASME Paper No. 58-A-119, 1958.

2. ANDREEVA, L.E., "Elastic Elements of Instruments", Published by the ISRAEL program for Scientific Translations Chapter V11, 1966.

3. KARDOS, G., "Tests on Deflection of Flat-Oval BOURDON Tubes", ASME Paper No. 54-A-67, 1958.

4. MASON, H.G., "Sensitivity and Life Data on BOURDON Tubes", ASME Paper No. 54-A-169, 1954.

5. EXLINE, P.G., "BOURDON Tube Deflection Characteristics", Trans. ASME, Series D, Journal of Basic Engineering, vol. 82, 1960, pp. 887-893.

6. DRESSLER, R., "Elastic Shell-Theory Formulation for BOURDON Tubes", Transactions of the ASME, Journal of Basic Engineering, Dec. 1965.

7. LOVE, A.E.H., "A Treatise on the Mathematical Theory of Elasticity", Fourth Edition, 1927, Dover publication.

8. KOITER, W.T., "A Consistent First Approximation in the General Theory of Thin Elastic Shells", Proceedings of the Symposium on the Theory of Thin

Elastic Shells (DELFT, 24-26 August, 1959), North-Holland Publishing Company - Amsterdam.

9. LANGHAAR, H.L., "Paradoxes in the Theories of Plates and Shells",
Proceedings of the Second Southeastern Conference on Theoretical and Applied Mechanics (vol. 2), Atlanta, Georgia, March 5-6, 1964. Edited by W.A.Shaw, Pergamon Press.

10. WILLIS, A.P., "Vector Analysis with an Introduction to Tensor Analysis",
Dover Publication.

11. EISENHART, L.P., "A Treatise on the Differential Geometry of Curves and Surfaces",
Ginn and Co. (also published by Dover Publication).

12. ORAVAS, A.G., "Theory of Surface Structures",
unpublished lecture notes, McMaster University, Hamilton, Ontario, 1967.

13. NOVOZHILOV, V.V., "The Theory of Thin Shells",
P. Noordhoff Ltd., Groningen, The Netherlands, Second Edition, 1964, English Translation.

14. ZLASOV, V.Z., "General Theory of Shells and its Applications in Engineering",
NASA Technical Translation, April 1964, NASA TT F-99
Translation of "Obshchaya teoriya obolochek i yeye prilozheniya v tekhnike".

Gosudarstvennoye Izdatel'stvo Tekhniko - Teoreticheskoy Literatury, Moscow-Leningrad, 1949.

15. ORAVAS, A.G., "Continuum Mechanics", unpublished lecture notes, McMaster University, Hamilton, Ontario, 1968.

16. GOL'DENVEIZER, "Theory of Elastic Thin Shells", Pergamon Press, N.Y., 1961.

17. KARDOS, G., "Correlation and Analysis of BOURDON Tube Test Data", ASME Paper No. 68-WA/PT-1.

APPENDIX A

THIN-SHELL THEORY FOR BOURDON TUBE WITH AN ELLIPTICAL CROSS-SECTION

A.1 Introduction

In this section an elastic thin shell theory formulation for BOURDON tubes with an elliptic cross-section is detailed. The shell analysis approach used is that of References 12 and 15. To facilitate the analysis and comparison with Reference 6, symbols and conventions employed will be similar to those of References 6 and 12 where convenient.

A.2 Coordinate Systems

The coordinate systems used in the analysis are illustrated in Figure A.1: (a) a reference (or fixed) rectangular cartesian system

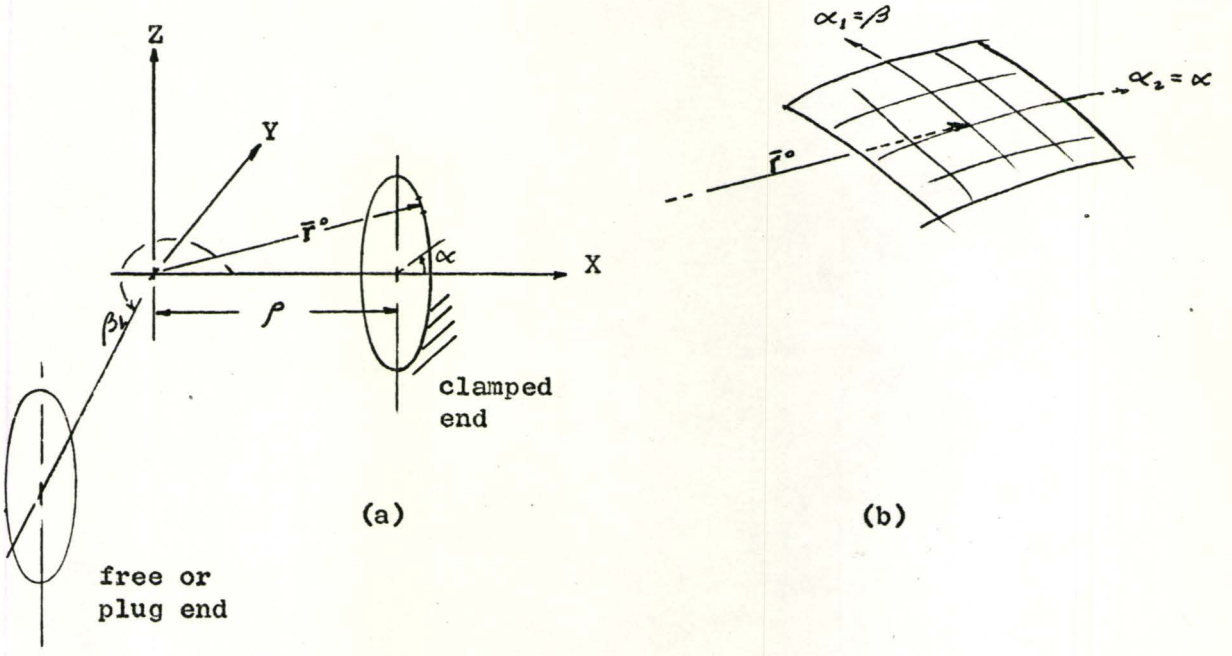

Figure A.1 - Coordinate Systems: (a) Reference System (X,Y,Z) (b) "Curvilinear Coordinate Net" System in the Surface

X,Y,Z with its origin located at a distance ρ from the centreline of the incomplete torus and (b) a "curvilinear coordinate net" traced out by the parametric variables α_1 and α_2 in the surface (which may be considered as the middle surface of the shell). The variables α_1 and

α_2 represent respectively the parameters β (the angle sweeping out the semi-torus) and α (the angle sweeping out the ellipse) of the shell cross-section.

In the application to the BOURDON gage the incomplete toroidal shell is clamped rigidly at one end (Figure A.1 (a)) and the plug or free end deflects as internal pressure is applied. Due to symmetry the deflection at the free end occurs in the X-Y plane.

Thus having defined the coordinate systems of the BOURDON gage, properties of the shell surface can now be developed.

A.3 Differential Geometry and Metrical Properties

Through the properties of the surface curves defined by the line β = constant or α = constant of the "coordinate net", a description of the shell surface can be determined. The curvilinear properties of the surface will include metrical coefficients, normal curvature, geodesic torsion, geodesic curvature, and Gaussian curvature.

As the position vector $\bar{r}^\circ$ defined from the origin of the reference coordinate system to the middle surface of the shell is of prime importance to the solution of the various curvilinear properties, a detail analysis of $\bar{r}^\circ$ follows.

To facilitate the analysis, $\bar{r}^\circ$ will be expressed in terms of Gaussian intrinsic surface coordinates, β and α (References 10, 11),

$$\bar{r}^\circ = x\bar{e}_x + y\bar{e}_Y + z\bar{e}_z$$

where,

$x = x(\beta, \alpha)$, $y = y(\beta, \alpha)$, $z = z(\beta, \alpha)$, are components in X,Y,Z directions respectively as a function of β ,α - in Reference 6 these are called parametric equations.

$\bar{e}_X$, $\bar{e}_Y$, $\bar{e}_Z$ are the unit base vectors of the reference coordinate system.

A.3.1 Position Vector $\bar{r}$•

From geometry an ellipse may be produced from two concentric circles of radii $\bar{b}$ and $\bar{a}$ (see Figure A.2). If a vertical line and

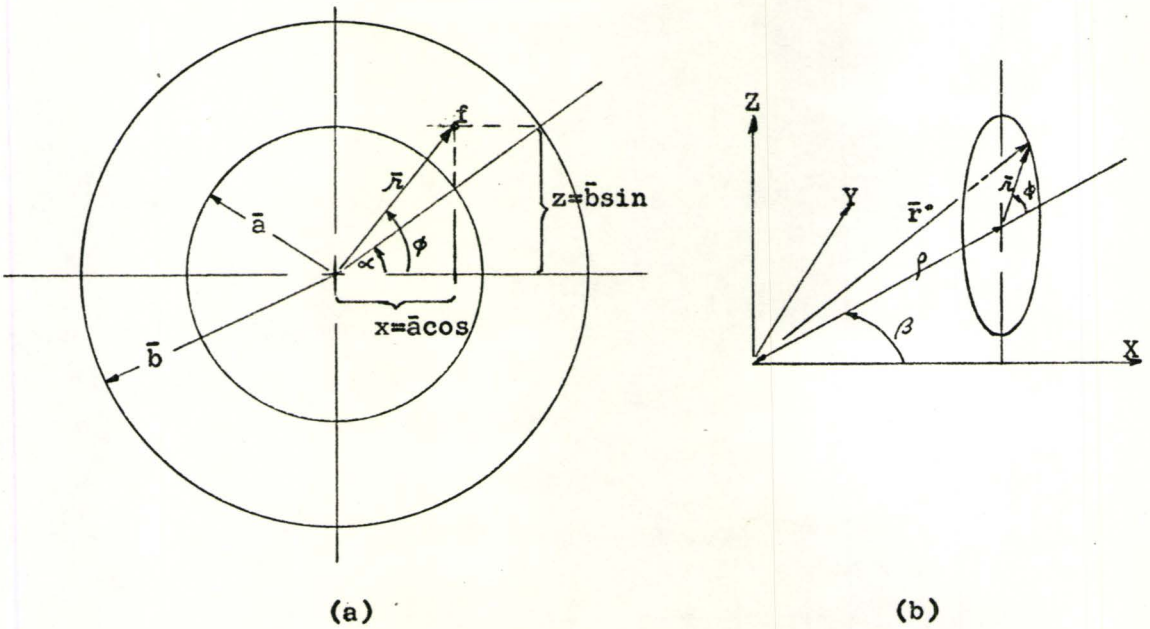

(a) (b)

Figure A.2 - Generation of an Ellipse

a horizontal line are drawn from the intersections of a radial line (with angle α) and the two circles, they will define a point f. The construction of a number of these points, such as f, will clearly map an ellipse with semi-major diameter $\bar{b}$ and semi-minor diameter $\bar{a}$.

With a local vector $\bar{r}$ of magnitude r at an angle ϕ to the shell surface, the position vector $\bar{r}^\circ$ may be expressed as

$$\bar{r}^\circ = (\rho + r\cos\phi)\cos\beta\ \bar{e}_x + (\rho + r\cos\phi)\sin\beta\ \bar{e}_Y + (r\sin\phi)\bar{e}_z$$

From Figure A.2(a), relations between ϕ and α can be observed,

$$r\sin\phi = \bar{b}\sin\alpha$$

$$r\cos\phi = \bar{a}\cos\alpha$$

Therefore,

$$\bar{r}^\circ = (\rho + \bar{a}\cos\alpha)\cos\beta\ \bar{e}_x + (\rho + \bar{a}\cos\alpha)\sin\beta\ \bar{e}_Y + (\bar{b}\sin\alpha)\bar{e}_z \qquad (A.1)$$

Thus any point on the BOURDON gage with an elliptical cross-section can be defined.

A.3.2 Differential Arc Lengths and Metrical Coefficients

Since $\bar{r}^\circ = \bar{r}^\circ(\alpha_1, \alpha_2)$, upon differentiation

$$d\bar{r}^\circ = \frac{\partial \bar{r}^\circ}{\partial \alpha_1} d\alpha_1 + \frac{\partial \bar{r}^\circ}{\partial \alpha_2} d\alpha_2 \qquad (A.2)$$

where $d\bar{r}^\circ$ denotes the differential increment in $\bar{r}^\circ$ which occurs in passing from a point p on the surface to an infinitely near surface point q (Figure A.3(a)).

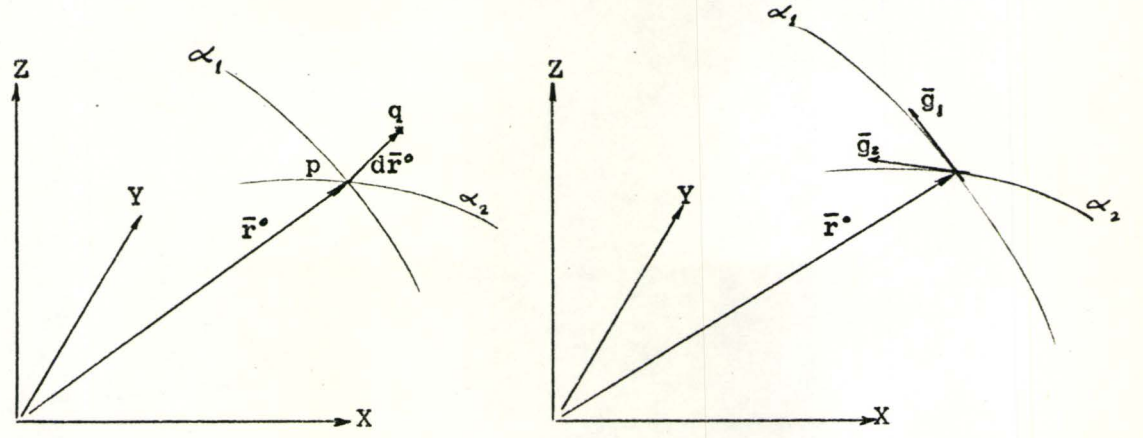

Figure A.3 - Arc Length and Metrics

The vectors $\partial\bar{r}^\circ/\partial\alpha_1$ and $\partial\bar{r}^\circ/\partial\alpha_2$ are tangential vectors to the α_1 and α_2 -curves respectively, in the directions of α_1 and α_2 increasing (Figure A.3(b)). These vectors are the metrics of the curves, and are denoted by $\bar{g}_1$ and $\bar{g}_2$ respectively, i.e.,

$$\bar{g}_1 = \partial\bar{r}^\circ/\partial\alpha_1 \quad , \quad \bar{g}_2 = \partial\bar{r}^\circ/\partial\alpha_2$$

Therefore equation (A.2) becomes,

$$d\bar{r}^{\circ} = \bar{g}_1 d\alpha_1 + \bar{g}_2 d\alpha_2 \qquad (A.3)$$

By forming the "dot" or scalar product of expression (A.3),

$$ds^2 = d\bar{r}^{\circ} \cdot d\bar{r}^{\circ}$$
$$= g_{11} d\alpha_1^2 + 2g_{12} d\alpha_1 d\alpha_2 + g_{22} d\alpha_2^2 \qquad (A.4)$$

where ds is the differential arc length (or the magnitude of $d\bar{r}^{\circ}$) and the metrical coefficients,

$$g_{11} = \bar{g}_1 \cdot \bar{g}_1 \quad , \quad g_{12} = \bar{g}_1 \cdot \bar{g}_2 \quad , \quad g_{22} = \bar{g}_2 \cdot \bar{g}_2 \qquad (A.5)$$

The first and third terms to the right of equation (A.4) represent the components of $d\bar{r}^{\circ}$ along the increasing directions of α_1, α_2 -curves. If ds_1 and ds_2 denote the corresponding magnitude of $d\bar{r}^{\circ}$, then

$$ds_1 = (g_{11})^{1/2} d\alpha_1 \quad , \quad ds_2 = (g_{22})^{1/2} d\alpha_2 \qquad (A.6)$$

The remaining term with g_{12} determines whether the parametric curves α_1 and α_2 are orthogonal. Since,

$$g_{12} = \bar{g}_1 \cdot \bar{g}_2$$
$$= /\bar{g}_1/ \ /\bar{g}_2/ \cos\angle \bar{g}_1 \bar{g}_2$$

Therefore

$$\cos\angle(\bar{g}_1, \bar{g}_2) = g_{12} / (/\bar{g}_1/ \; /\bar{g}_2/)$$

= zero if the angle between the vectors $\bar{g}_1$ and $\bar{g}_2$ is 90 degrees (i.e. $g_{12} = 0$)

where

$/\bar{g}_1/$ = magnitude of $\bar{g}_1$

$= (g_{11})^{1/2}$

and

$/\bar{g}_2/$ = magnitude of $\bar{g}_2$

$= (g_{22})^{1/2}$

Thus for the BOURDON gage with an elliptic cross-section, the following results can be verified:

with $\bar{r}^* = (\rho + \bar{a}\cos\alpha)\cos\beta\,\bar{e}_x + (\rho + \bar{a}\cos\alpha)\sin\beta\,\bar{e}_Y + (\bar{b}\sin\alpha)\bar{e}_z$

metrical coefficients,

$$\bar{g}_\beta = \bar{g}_1 = \partial\bar{r}^*/\partial\alpha_1 = \partial\bar{r}^*/\partial\beta = -(\rho + \bar{a}\cos\alpha)\sin\beta\,\bar{e}_x + (\rho + \bar{a}\cos\alpha)\cos\beta\,\bar{e}_Y$$

$$g_{\beta\beta} = g_{11} = \bar{g}_\beta \cdot \bar{g}_\beta = (\rho + \bar{a}\cos\alpha)^2 \qquad \text{(A.7)}$$

$$/\bar{g}_\beta/ = (g_{\beta\beta})^{1/2} = \rho + \bar{a}\cos\alpha$$

$$\bar{g}_\alpha = \bar{g}_2 = \partial \bar{r}^\circ / \partial \alpha_2 = \partial \bar{r}^\circ / \partial \alpha = -\bar{a} \sin\alpha \cos\beta \, \bar{e}_x - \bar{a} \sin\alpha \sin\beta \, \bar{e}_Y + \bar{b} \cos\alpha \, \bar{e}_z$$

$$g_{\alpha\alpha} = g_{22} = \bar{g}_\alpha \cdot \bar{g}_\alpha = \bar{a}^2 \sin^2\alpha + \bar{b}^2 \cos^2\alpha \qquad (A.8)$$

$$/\bar{g}_\alpha/ = (g_{\alpha\alpha})^{1/2} = (\bar{a}^2 \sin^2\alpha + \bar{b}^2 \cos^2\alpha)^{1/2}$$

$$g_{\beta\alpha} = g_{\alpha\beta} = \bar{g}_\beta \cdot \bar{g}_\alpha = \bar{g}_1 \cdot \bar{g}_2 = \bar{g}_2 \cdot \bar{g}_1 = 0$$

differential arc lengths,

$$ds_\beta = ds_1 = /\bar{g}_\beta / d\beta, \qquad ds_\alpha = ds_2 = /\bar{g}_\alpha / d\alpha \qquad (A.9)$$

Then since $g_{12} = 0$, the parametric curves β and α are orthogonal.

A.4 Surface Curves - Their Classification and Curvatures

Before discussing further properties of surface curves[1], it is convenient to introduce a mobile orthogonal unit vector triad[2] known as the RIBAUCOUR Triad (after Albert RIBAUCOUR in 1872), for each surface curve. For the α_1 and α_2-curves the RIBAUCOUR triads are repre-

---

[1] In a spatial curve the orthogonal unit vector triad is known as the FRENET triad. For the fundamental distinction between the two types of triads refer to Reference 12.

[2] c.f., Reference 6, the RIBAUCOUR Triad system is equivalent to the moving local coordinate system (x, y, z).

sented as $(\bar{e}_1, \bar{e}_b^1, \bar{e}_n)$ and $(\bar{e}_2, \bar{e}_b^2, \bar{e}_n)$ respectively (see Figure A.4).

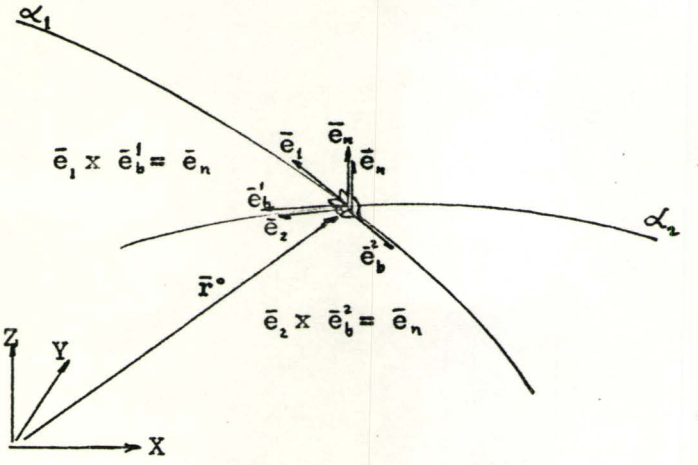

Figure A.4 - The RIBAUCOUR Triads, $(\bar{e}_1, \bar{e}_b^1, \bar{e}_n)$ and $(\bar{e}_2, \bar{e}_b^2, \bar{e}_n)$

They are defined and related to the position vector by the following relations,

$$\bar{e}_1 = \text{unit tangent vector to "line } \alpha_1 \text{"}$$
$$= \partial \bar{r}^\circ / \partial s_1 \qquad \text{(A.10)}$$

$$\bar{e}_2 = \text{unit tangent vector to "line } \alpha_2 \text{"}$$
$$= \partial \bar{r}^\circ / \partial s_2 \qquad \text{(A.11)}$$

These two unit vectors $\bar{e}_1$ and $\bar{e}_2$ define the surface tangent plane. Therefore the unit normal vector to this plane is,

$$\bar{e}_n = \bar{e}_1 \times \bar{e}_2 / (/\bar{e}_1 \times \bar{e}_2/) \qquad \text{(A.12)}$$

Finally the unit binormals to line α_1 and line α_2 are determined with the aid of the unit normal vector in accordance with the orthogonal dextral vector product rule,

$$\begin{aligned} \bar{e}_b^1 &= \text{unit binormal to "line } \alpha_1 \text{"} \\ &= \bar{e}_n \times \bar{e}_1 \\ \bar{e}_b^2 &= \text{unit binormal to "line } \alpha_2 \text{"} \\ &= \bar{e}_n \times \bar{e}_2 \end{aligned} \qquad \text{(A.13)}$$

If one of these triads is moved along the surface curve (say α_1), the triad must continuously reorientate in order that $\bar{e}_1$ may remain tangent to the curve, and that $\bar{e}_n$ may remain normal to the surface tangent plane - these characteristics apply to the other triad as well. This reorientation per unit arc-length can expressed as a rate of rotation vector, known as the CESARO vector (after Ernesto CESÀRO in 1896), in which its scalar coefficients along the triad's vector directions are the curvatures of the surface curve. In its most general form the CESÀRO vector is written as,

$$\bar{c}_i = k_i^{(t)} \bar{e}_i + k_i^{(n)} \bar{e}_b^i + k_i^{(g)} \bar{e}_n \qquad (i = 1,2) \qquad \text{(A.14)}$$

where

$k_i^{(t)}$ represents Geodesic Torsion for line α_i

$k_i^{(n)}$ represents Normal Curvature for line α_i

$k_i^{(g)}$ represents Geodesic Curvature for line α_i

Then by definition of the arc-length rate of rotation of the triad:

$$\partial/\partial s_i (\bar{e}_j) = \bar{c}_i \times \bar{e}_j \qquad \text{(Reference 12)}$$

It will be noted at this point that the following tensorial notation equivalents of the curvatures are (Reference 12):

$$\begin{aligned} k_1^{(t)} &= -k_{12} \\ k_2^{(t)} &= k_{21} \\ k_1^{(n)} &= k_{11} \\ k_2^{(n)} &= k_{22} \\ k_1^{(g)} &= k_{13} \\ k_2^{(g)} &= k_{23} \end{aligned} \qquad \text{(A.15)}$$

These tensorial equivalents will be used when convenient, in the analysis.

Therefore as exemplified above a knowledge of the scalar coefficients of the CESÀRO vectors provides a means to a graphic description of the surface at any point as the mobile triads move along the parametric curves.

In surface theory, curves are classified according to the vanishing of any one of the three curvature components of the CESÀRO vector:

a. Principal Line of Curvature - $k_i^{(t)} = 0$

then,

$$\bar{c}_i = k_i^{(n)} \bar{e}_b^i + k_i^{(g)} \bar{e}_n$$

Consequently, as the geodesic torsion vanishes the consecutive normals along the curve intersect.

b. Asymptotic Line - $k_i^{(n)} = 0$

then,

$$\bar{c}_i = k_i^{(t)} \bar{e}_i + k_i^{(g)} \bar{e}_n$$

c. Geodesic - $k_i^{(g)} = 0$

then,

$$\bar{c}_i = k_i^{(t)} \bar{e}_i + k_i^{(n)} \bar{e}_b^i$$

A Geodesic represents the "shortest curve" between two points in the surface.

The CESÀRO vector components may be evaluated in terms of the RIBAUCOUR triads according to the following relations: (for detailed proof see Reference 12)

$$k_i^{(t)} = \bar{e}_n \cdot \frac{\partial \bar{e}_b^i}{\partial s_i}$$

as $\bar{e}_n \cdot \bar{e}_b^i = 0$, then $\partial / \partial s_i (\bar{e}_n \cdot \bar{e}_b^i) = 0$

or $\bar{e}_n \cdot \partial / \partial s_i (\bar{e}_b^i) = -\bar{e}_b^i \cdot \partial / \partial s_i (\bar{e}_n)$

Therefore,

$$k_i^{(t)} = \bar{e}_n \cdot \frac{\partial \bar{e}_b^i}{\partial s_i} = -\bar{e}_b^i \cdot \frac{\partial \bar{e}_n}{\partial s_i}$$

Similarly,

$$k_i^{(n)} = \bar{e}_i \cdot \frac{\partial \bar{e}_n}{\partial s_i} = -\bar{e}_n \cdot \frac{\partial \bar{e}_i}{\partial s_i} \qquad \text{(A.16)}$$

and,

$$k_i^{(g)} = -\bar{e}_i \cdot \frac{\partial \bar{e}_b^i}{\partial s_i} = \bar{e}_b^i \cdot \frac{\partial \bar{e}_i}{\partial s_i}$$

In Figure A.5, the two RIBAUCOUR triads for the BOURDON tube

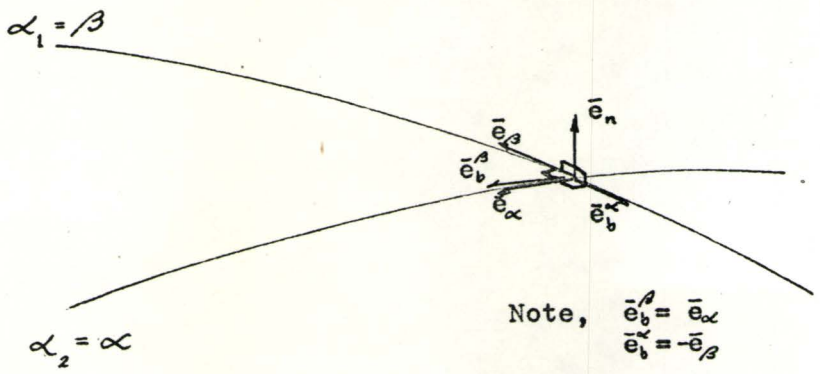

Figure A.5 - Orthogonal Parametric Lines and the RIBAUCOUR Triads

are shown to illustrate the relative orientation of the unit vectors. As the parametric curves $\alpha_1 = \beta$ and $\alpha_2 = \alpha$ were demonstrated to be

orthogonal, the binormals $\bar{e}_b^{\beta}$ and $\bar{e}_b^{\alpha}$ of the triads are:

$$\bar{e}_b^{1} = \bar{e}_2 \quad \text{or} \quad \bar{e}_b^{\beta} = \bar{e}_{\alpha}$$

and (A.17)

$$\bar{e}_b^{2} = -\bar{e}_1 \quad \text{or} \quad \bar{e}_b^{\alpha} = -\bar{e}_{\beta}$$

Therefore from equations (A.10) to (A.17):

Unit vectors of the RIBAUCOUR Triad

$$\bar{e}_{\beta} = \bar{e}_1 = \frac{\partial \bar{r}^{\circ}}{\partial s_{\beta}} = \frac{\bar{g}_{\beta}}{/\bar{g}_{\beta}/}$$

$$= -\sin\beta\, \bar{e}_x + \cos\beta\, \bar{e}_y$$

$$\bar{e}_{\alpha} = \bar{e}_2 = \partial \bar{r}^{\circ}/\partial s_{\alpha} = \frac{\bar{g}_{\alpha}}{/\bar{g}_{\alpha}/}$$

$$= \frac{-\bar{a}\sin\alpha\cos\beta\, \bar{e}_x - \bar{a}\sin\alpha\sin\beta\, \bar{e}_y + \bar{b}\cos\alpha\, \bar{e}_z}{(\bar{a}^2\sin^2\alpha + \bar{b}^2\cos^2\alpha)^{1/2}}$$

$$\bar{e}_n = \frac{\bar{e}_{\beta} \times \bar{e}_{\alpha}}{/\bar{e}_{\beta} \times \bar{e}_{\alpha}/} = \frac{\bar{e}_{\beta} \times \bar{e}_{\alpha}}{/\bar{e}_{\beta}/\ /\bar{e}_{\alpha}/\sin 90^{\circ}} = \bar{e}_{\beta} \times \bar{e}_{\alpha}$$

$$= \frac{\bar{b}\cos\alpha\cos\beta\, \bar{e}_x + \bar{b}\cos\alpha\sin\beta\, \bar{e}_y + \bar{a}\sin\alpha\, \bar{e}_z}{(\bar{a}^2\sin^2\alpha + \bar{b}^2\cos^2\alpha)^{1/2}}$$

For line β

$$k_{\beta}^{(t)} = \bar{e}_n \cdot \frac{\partial \bar{e}_b^{\beta}}{\partial s_{\beta}} = \bar{e}_n \cdot \frac{1}{/\bar{g}_{\beta}/} \frac{\partial \bar{e}_{\alpha}}{\partial \beta}$$

= 0 means, line β exhibits no twist.

$$k_{\beta}^{(n)} = -\bar{e}_n \cdot \frac{\partial \bar{e}_{\beta}}{\partial s_{\beta}} = -\bar{e}_n \cdot \frac{1}{|\bar{g}_{\beta}|} \frac{\partial \bar{e}_{\beta}}{\partial \beta}$$

$$= \frac{\bar{b} \cos\alpha}{(\rho + \bar{a} \cos\alpha)(\bar{a}^2 \sin^2\alpha + \bar{b}^2 \cos^2\alpha)^{1/2}}$$

Observe that $k_{\beta}^{(n)}$ is negative when $\pi/2 < \alpha < 3\pi/2$ and vanishes at $\alpha = \pi/2 \ , \ 3\pi/2$

i.e. at $\alpha = \pi/2$ and $3\pi/2$, $k_{\beta}^{(n)} = 1/R_{\beta} = 0$ or the radius of curvature, $R_{\beta} = \infty$.

$$k_{\beta}^{(g)} = \bar{e}_b^{\beta} \cdot \frac{\partial \bar{e}_{\beta}}{\partial s_{\beta}} = \bar{e}_{\alpha} \cdot \frac{1}{|\bar{g}_{\beta}|} \frac{\partial \bar{e}_{\beta}}{\partial \beta}$$

$$= \frac{\bar{a} \sin\alpha}{(\rho + \bar{a} \cos\alpha)(\bar{a}^2 \sin^2\alpha + \bar{b}^2 \cos^2\alpha)^{1/2}}$$

Note that $k_{\beta}^{(g)}$ is negative in the interval $\pi < \alpha < 2\pi$ and vanishes at $\alpha = \pi$ and 2π.

Then,

$$\bar{c}_{\beta} = k_{\beta}^{(n)} \bar{e}_{\alpha} + k_{\beta}^{(g)} \bar{e}_n$$

For line α

$$k_{\alpha}^{(t)} = \bar{e}_n \cdot \frac{\partial \bar{e}_b^{\alpha}}{\partial s_{\alpha}} = \bar{e}_n \cdot \frac{1}{|\bar{g}_{\alpha}|} \frac{\partial(-\bar{e}_{\beta})}{\partial \alpha}$$

= 0 means, line α exhibits no twist.

$$k_{\alpha}^{(n)} = \bar{e}_{\alpha} \cdot \frac{1}{|\bar{g}_{\alpha}|} \frac{\partial \bar{e}_n}{\partial \alpha}$$

$$= \frac{\bar{a}\,\bar{b}}{(\bar{a}^2 \sin^2\alpha + \bar{b}^2 \cos^2\alpha)^{3/2}}$$

$$k_{\alpha}^{(g)} = -\bar{e}_{\alpha} \cdot \frac{\partial \bar{e}_b^{\alpha}}{\partial s_{\alpha}} = -\bar{e}_{\alpha} \frac{1}{|\bar{g}_{\alpha}|} \frac{\partial (-\bar{e}_{\beta})}{\partial \alpha}$$

$= 0$ graphically, this means that as the RIBAUCOUR triad moves along the curve, line α does not deviate from the tangent directed along $\bar{e}_{\alpha}$ (as seen from a plan view of the surface) - see Figure A.6.

Then,

$$\bar{c}_{\alpha} = -k_{\alpha}^{(n)} \bar{e}_{\beta}$$

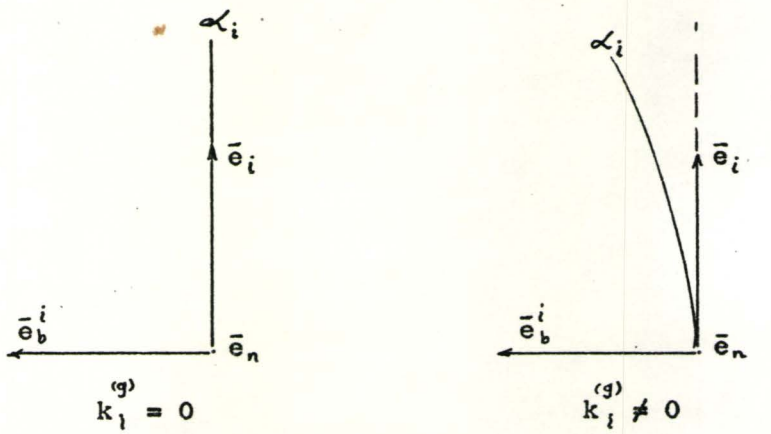

Figure A.6 - Plan View of RIBAUCOUR Triad: (a) $k_i^{(g)} = 0$, then Line α_i does not deviate from the Tangent directed along $\bar{e}_i$ (b) $k_i^{(g)} \neq 0$, then Line α_i deviates from the Tangent

Gaussian Curvature

With the CESARO vectors, representing the kinematic curvature vectors for all three curvatures of the surface, a total surface curvature per unit surface area can be defined. This total surface curvature per unit surface area or Gaussian curvature is defined as k_g, such that: (Reference 12)

$$k_g (\bar{e}_1 \times \bar{e}_2) = \bar{k}_1 \times \bar{k}_2 \qquad \text{(A.18)}$$

where $\bar{k}_i$ = the "pure curvature" or "curvature in the surface"

$$= \bar{e}_n \times \bar{c}_i \times \bar{e}_n \qquad (i = 1,2) \qquad \text{(A.19)}$$

By expanding the vector triple product in the last expression, $\bar{k}_i$ can be verified to be the surface component/or projection of $\bar{c}_i$ (i.e., $\bar{k}_i$ is the CESARO vector $\bar{c}_i$ with the normal component removed or, $\bar{k}_i = \bar{c}_i - (\bar{e}_n \cdot \bar{c}_i)\bar{e}_n$).

Therefore the "pure curvatures" for lines α_1 and α_2 are:

$$\bar{k}_1 = \bar{e}_n \times \bar{c}_1 \times \bar{e}_n = k_1^{(t)} \bar{e}_1 + k_1^{(n)} \bar{e}_b^1$$

$$\bar{k}_2 = \bar{e}_n \times \bar{c}_2 \times \bar{e}_n = k_2^{(t)} \bar{e}_2 + k_2^{(n)} \bar{e}_b^2$$

From equation (A.18),

$$k_g(\bar{e}_1 \times \bar{e}_2) = \bar{k}_1 \times \bar{k}_2$$

or $$k_g \sin\psi_{12}\ \bar{e}_n = \bar{k}_1 \times \bar{k}_2$$

where ψ_{12} is the angle between the tangent unit vectors $\bar{e}_1$ and $\bar{e}_2$. By performing the "Dot product" with $\bar{e}_n$,

$$k_g = 1/\sin\psi_{12}\ (\bar{k}_1 \times \bar{k}_2 \cdot \bar{e}_n)$$

Expanding the scalar triple product, k_g becomes:

$$k_g = (k_1^{(n)} k_2^{(n)} + k_1^{(t)} k_2^{(t)}) + (k_1^{(t)} k_2^{(n)} - k_1^{(n)} k_2^{(t)})\cot\psi_{12} \qquad \text{(A.20)}$$

Equation (A.20) is then the general expression for the Gaussian curvature, which is not frequently encountered; as coordinate lines of surfaces in most engineering applications (e.g. cylinders, spheres, etc.) can be classified as "Orthogonal, Principal Lines of Curvature" such as the BOURDON gage problem where the Gaussian curvature is merely the product of the normal curvatures.

i.e.,

$$k_g = k_\beta^{(n)} k_\alpha^{(n)}$$

$$= \bar{a}\,\bar{b}^2\cos\alpha\,/((\rho + \bar{a}\cos\alpha)(\bar{a}^2\sin^2\alpha + \bar{b}^2\cos^2\alpha)^2)$$

Observe that k_g is negative when $\pi/2 < \alpha < 3\pi/2$, and vanishes at $\alpha = \pi/2$ and $3\pi/2$ since $k_\beta^{(n)} = 1/R_\beta = 0$ or $R_\beta = \infty$.

A.5 Summary of Geometric and Vectorial Properties of the BOURDON Gage with an Elliptical Cross-Section

In summary, the properties of the BOURDON gage are, (with reference to Figure A.7):

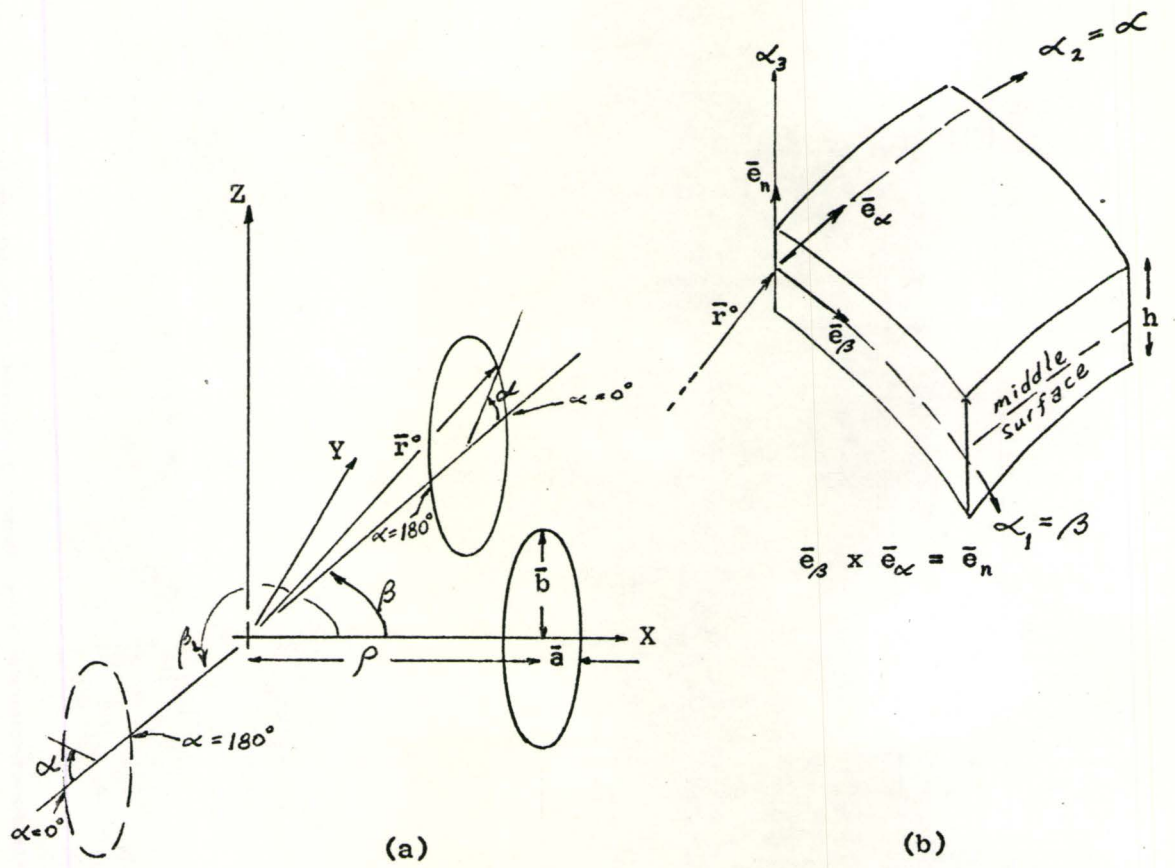

Figure A.7 - Geometric Properties of BOURDON Gage

Position Vector

$$\bar{r}^{\circ} = \bar{r}^{\circ}(\beta,\alpha) = (\rho + \bar{a}\cos\alpha)\cos\beta\,\bar{e}_x + (\rho + \bar{a}\cos\alpha)\sin\beta\,\bar{e}_Y + (\bar{b}\sin\alpha)\bar{e}_z$$

Metric Coefficients

$$/\bar{g}_\beta/ = (g_{\beta\beta})^{1/2} = \rho + \bar{a}\cos\alpha$$

$$/\bar{g}_\alpha/ = (g_{\alpha\alpha})^{1/2} = (\bar{a}^2\sin^2\alpha + \bar{b}^2\cos^2\alpha)^{1/2} \qquad \text{(A.21)}$$

$$g_{\beta\alpha} = g_{\alpha\beta} = 0$$

RIBAUCOUR Unit Vectors; $(\bar{e}_\beta\ ,\ \bar{e}_b^\beta\ ,\ \bar{e}_n)$, $(\bar{e}_\alpha\ ,\ \bar{e}_b^\alpha\ ,\ \bar{e}_n)$

$$\bar{e}_\beta = -\sin\beta\,\bar{e}_x + \cos\beta\,\bar{e}_Y$$

$$\bar{e}_\alpha = (g_{\alpha\alpha})^{-1/2}(-\bar{a}\sin\alpha\cos\beta\,\bar{e}_x - \bar{a}\sin\alpha\sin\beta\,\bar{e}_Y + \bar{b}\cos\alpha\,\bar{e}_z)$$

$$\bar{e}_n = (g_{\alpha\alpha})^{-1/2}(\bar{b}\cos\alpha\cos\beta\,\bar{e}_x + \bar{b}\cos\alpha\sin\beta\,\bar{e}_Y + \bar{a}\sin\alpha\,\bar{e}_z) \qquad \text{(A.22)}$$

$$\bar{e}_b^\beta = \bar{e}_\alpha \quad , \quad \bar{e}_b^\alpha = -\bar{e}_\beta$$

Curvatures and CESÀRO Vectors

a. Line β: $\quad k_\beta^{(t)} = 0$

$$k_\beta^{(n)} = \bar{b}\cos\alpha\,/(/\bar{g}_\beta//\bar{g}_\alpha/) \qquad \text{(A.23) cont'd}$$

$$k_{\beta}^{(g)} = \bar{a} \sin\alpha / (/\bar{g}_{\beta}//\bar{g}_{\alpha}/)$$

$$\bar{c}_{\beta} = k_{\beta}^{(n)} \bar{e}_{\alpha} + k_{\beta}^{(g)} \bar{e}_{n}$$

b. Line α:

$$k_{\alpha}^{(t)} = 0$$

$$k_{\alpha}^{(n)} = \bar{a}\, \bar{b} / (g_{\alpha\alpha})^{3/2} \qquad (A.23)$$

$$k_{\alpha}^{(g)} = 0$$

$$\bar{c}_{\alpha} = -k_{\alpha}^{(n)} \bar{e}_{\beta}$$

Gaussian Curvature of the Surface

$$k_{g} = \bar{a}\, \bar{b}^{2} \cos\alpha / (/\bar{g}_{\beta}/(g_{\alpha\alpha})^{2}) \qquad (A.24)$$

A.6 The Theory of Thin Elastic Shells with Application to the BOURDON Gage

Since 1888 when A.E.H. LOVE noted and corrected the inaccuracies in the work (a theory of thin elastic shell founded on the hypothesis of KIRCHHOFF (1850)) of G. ARON (1874), there evolved many versions of the theory of thin shells in analogy to the theory of plates of KIRCHHOFF. These theories, however, differ from the prototype, "the theory of LOVE", only by terms which are small and by variations in rigor - LOVE (as many theoreticians say) in his development is inconsistent with regard to small terms: some are retained and others which are of the same order of magnitude are rejected.

In these theories a shell is considered "thin" if the follow-

ing relation holds: (Reference 13)

$$\max (h/R) \leq 1/20$$

where,

h denotes the thickness of the shell

R denotes the radius of curvature (minimum)

It was W.T. KOITER (Reference 8) who in 1959 elucidated the "First Approximation" theory of LOVE and the theories of the other authors by comparing their strain energies. He proved that:

> LOVE's so-called first approximation for the strain energy, as the sum of stretching or extensional energy and bending or flexural energy, is a consistent first approximation, and that no refinement of this first approximation is justified, in general, if the basic LOVE-KIRCHHOFF assumptions (or equivalent assumptions) are retained.

In accordance with the analysis of KOITER, Les McLEAN in 1966 showed that the theory of thin shells as set out in Reference 12, of which this analysis of the BOURDON gage with an elliptical cross section is based upon, is consistent.

A.7 Assumptions and Hypothesis

In this analysis of the BOURDON gage the following assumptions and hypothesis will be used:

(a) The gage material is assumed to be homogenous, isotropic, thin, elastic and of constant thickness h.

(b) KIRCHHOFF-ARON Hypothesis

Straight-line elements of a shell to the middle surface which

are normal to the middle surface before deformation remain so after deformation and retain their lengths.

(c) LOVE's "First Approximation"

The "arc length" is not affected by changes in position, relative to the middle surface - consequently (as stated previously) the first approximation for the strain energy can be expressed as the sum of stretching energy and bending energy.

(d) The normal stresses acting on surface parallel to the middle surface are negligible as compared to the other normal stresses.

(e) ARON's Approximations for the curvature variations

The tangential displacement components of the middle surface are small (in comparison with the normal desplacement component) and may be neglected in all "curvature variation" expressions denoted by δk_{ij} , (i, j = 1, 2).

For an experimental confirmation of ARON's approximation, see Reference 14.

A.8 The Strain Tensor

In the general case, the strain tensor can be shown to be given by the relation (Reference 8)

$$\bar{\bar{\epsilon}} = \tfrac{1}{2}(\partial\bar{u}/\partial\bar{r} + \bar{u}\,\partial/\partial\bar{r} + \partial\bar{u}/\partial\bar{r} \cdot \bar{u}\,\partial/\partial\bar{r})$$

where,

$\bar{\bar{\epsilon}}$ denotes the Euler-Lagrange strain tensor usually represented as $\bar{\bar{\epsilon}}^{L}$

$\bar{u}$ denotes a unique smooth displacement vector function, evaluated from the kinematics of deformation and in accordance with the KIRCHHOFF-ARON hypothesis (Reference 12, pages 49 ,68), which equals $\bar{u}^{\circ} + \alpha_3 \delta \bar{e}_3$. $\bar{u}^{\circ}$ is the displacement vector of the middle surface = $u\,\bar{e}_1 + v\,\bar{e}_2 + w\,\bar{e}_3$ and $\delta \bar{e}_3$ is the first variation of the unit normal vector $\bar{e}_n$, evaluated from the postulate: that any quantity of the deformed configuration may be represented by the corresponding quantity in the undeformed configuration plus its (first)variation.

$\partial / \partial \bar{r}$ denotes the "directed derivative" for a parallel surface as defined by equation (4. 6. - 6.), Reference 12.

i.e.,

$$\partial / \partial \bar{r} = a_1 \bar{e}_1 \, \partial / \partial s_1 + a_2 \bar{e}_2 \, \partial / \partial s_2 + \bar{e}_3 \, \partial / \partial \alpha_3$$

with,

$$a_i = (1 + \alpha_3 k_{ii})^{-1}$$

For the linear case $\bar{\bar{\epsilon}}$ is reduced, by neglecting the quadratic term, to

$$\bar{\bar{\epsilon}} = \tfrac{1}{2}(\partial \bar{u} / \partial \bar{r} + \bar{u} \, \partial / \partial \bar{r})$$

John SCHROEDER, in 1964 (Reference 12, page 74) obtained the final form of the strain tensor for the parallel surface:

$$\begin{aligned}\bar{\bar{\epsilon}} = {} & (\phi_{11} + \alpha_3 \delta k_{11}) a_1 \bar{e}_1 \bar{e}_1 \\ & + (\phi_{12} + \phi_{21})/2 + \alpha_3/2(\delta k_{21} a_2 + \delta k_{12} a_1) \bar{e}_1 \bar{e}_2 \\ & + (\phi_{12} + \phi_{21})/2 + \alpha_3/2(\delta k_{21} a_2 + \delta k_{12} a_1) \bar{e}_2 \bar{e}_1 \\ & + (\phi_{22} + \alpha_3 \delta k_{22}) a_2 \bar{e}_2 \bar{e}_2\end{aligned} \tag{A.25a}$$

Then with LOVE's First Approximation (terms such as $(1 + \alpha_3 k_{ii})$ are approximately equal to 1), the linear strain tensor (equation A.25a) is reduced to the form: (Reference 12, page 75)

$$\bar{\bar{\epsilon}} = \bar{\bar{\epsilon}}^{\circ} + \alpha_3 \delta \bar{\bar{K}} \tag{A.25b}$$

where, $\bar{\bar{\epsilon}}^{\circ}$ denotes the dilatation strain tensor for the middle surface (i.e. at $\alpha_3 = 0$)

$\alpha_3 \delta \bar{\bar{K}}$ denotes the strain tensor for the shell due to the variation of the curvature tensor $\delta \bar{\bar{K}}$ of the middle surface.

In their explicit forms, $\bar{\bar{\epsilon}}^{\circ}$ and $\delta \bar{\bar{K}}$ may be shown as:

$$\bar{\bar{\epsilon}} = \begin{bmatrix} \phi_{11} \bar{e}_1 \bar{e}_1 + \frac{1}{2}(\phi_{12} + \phi_{21}) \bar{e}_1 \bar{e}_2 \\ + \frac{1}{2}(\phi_{21} + \phi_{12}) \bar{e}_2 \bar{e}_1 + \phi_{22} \bar{e}_2 \bar{e}_2 \end{bmatrix}$$

$$\delta \bar{\bar{K}} = \begin{bmatrix} \delta k_{11} \bar{e}_1 \bar{e}_1 + \frac{1}{2}(\delta k_{12} + \delta k_{21}) \bar{e}_1 \bar{e}_2 \\ + \frac{1}{2}(\delta k_{21} + \delta k_{12}) \bar{e}_2 \bar{e}_1 + \delta k_{22} \bar{e}_2 \bar{e}_2 \end{bmatrix} \tag{A.26}$$

The quantities ϕ_{ij} are defined as : Reference 12, page 47)

$$\phi_{ij} = \partial \bar{u}' / \partial s_i \cdot \bar{e}_j$$

or,

$$\begin{aligned}
\phi_{11} &= (\partial u/\partial s_1 - v\, k_{13} + w\, k_{11}) \\
\phi_{12} &= (\partial v/\partial s_1 + u\, k_{13} + w\, k_{12}) \\
\phi_{13} &= (\partial w/\partial s_1 - u\, k_{11} - v\, k_{12}) \\
\phi_{21} &= (\partial u/\partial s_2 - v\, k_{23} + w\, k_{21}) \\
\phi_{22} &= (\partial v/\partial s_2 + u\, k_{23} + w\, k_{22}) \\
\phi_{23} &= (\partial w/\partial s_2 - u\, k_{21} - v\, k_{22})
\end{aligned} \qquad \text{(A.27)}$$

Kinematically ϕ_{ij} $(i \neq j)$ is interpreted as the rotation of $\bar{e}_i$ towards $\bar{e}_j$ (about the axis $\bar{e}_k = \bar{e}_i \times \bar{e}_j$), during the process of deformation; the terms ϕ_{ii} represent longitudinal dilatations in the $\bar{e}_i$ direction. The quantities u, v, w are the deformation components of middle surface along the coordinate directions $(\alpha_1, \alpha_2, \alpha_3)$ respectively (refer to Figure A.7(b)).

The curvature variations δk_{ij} (Reference 12, equations (4.5.1. - 4.)) are expressed in terms of ϕ_{ij} and k_{ij} (see equations (A.15)). Then,

$$\delta k_{11} = -\partial \phi_{13}/\partial s_1 + k_{12}\phi_{12} + k_{13}\phi_{23}$$

$$\delta k_{12} = -\partial \phi_{23}/\partial s_1 - k_{11}\phi_{12} - k_{13}\phi_{13}$$

$$\delta k_{13} = \partial \phi_{12}/\partial s_1 - k_{11}\phi_{23} + k_{12}\phi_{13}$$

$$\delta k_{21} = -\partial \phi_{13}/\partial s_2 - k_{22}\phi_{21} + k_{23}\phi_{23} \qquad (A.28)^3$$

$$\delta k_{22} = -\partial \phi_{23}/\partial s_2 + k_{21}\phi_{21} - k_{23}\phi_{13}$$

$$\delta k_{23} = -\partial \phi_{21}/\partial s_2 - k_{21}\phi_{23} + k_{22}\phi_{13}$$

or, in terms of displacements equations (A.28) become:

$$\delta k_{\beta\beta} = \delta k_{11} = -(g_{\beta\beta})^{-1}\,\partial^2 w/\partial\beta^2 + k_\beta^{(n)}(g_{\beta\beta})^{-1/2}\partial u/\partial\beta + k_\beta^{(g)}\left((g_{\alpha\alpha})^{-1/2}\partial w/\partial\alpha - k_\alpha^{(n)} v\right)$$

$$\delta k_{\beta\alpha} = \delta k_{12} = -1/(|\bar{g}_\alpha||\bar{g}_\beta|)\,\partial^2 w/\partial\beta\partial\alpha + k_\alpha^{(n)}(g_{\beta\beta})^{-1/2}\partial v/\partial\beta - k_\beta^{(n)}\left((g_{\beta\beta})^{-1/2}\partial v/\partial\beta + k_\beta^{(g)} u\right) - k_\beta^{(g)}\left((g_{\beta\beta})^{-1/2}\partial w/\partial\beta - k_\beta^{(n)} u\right) \qquad (A.29)$$

$$\delta k_{\alpha\beta} = \delta k_{21} = -k_\beta^{(g)}(g_{\beta\beta})^{-1/2}\partial w/\partial\beta - 1/(|\bar{g}_\alpha||\bar{g}_\beta|)\,\partial^2 w/\partial\beta\partial\alpha + (g_{\alpha\alpha})^{-1/2}\partial(k_\beta^{(n)})/\partial\alpha\, u + k_\beta^{(n)}(g_{\alpha\alpha})^{-1/2}\partial u/\partial\alpha - k_\alpha^{(n)}(g_{\alpha\alpha})^{-1/2}\partial u/\partial\alpha$$

$$\delta k_{\alpha\alpha} = \delta k_{22} = (\bar{a}^2 - \bar{b}^2)\sin\alpha\cos\alpha/(g_{\alpha\alpha})^2\,\partial w/\partial\alpha - (g_{\alpha\alpha})^{-1}\partial^2 w/\partial\alpha^2 + (g_{\alpha\alpha})^{-1/2}\partial(k_\alpha^{(n)})/\partial\alpha\, v + k_\alpha^{(n)}(g_{\alpha\alpha})^{-1/2}\partial v/\partial\alpha$$

---

[3] δk_{13} and δk_{23} are shown here for completeness. They will not be directly involved in this particular analysis. Their uses occur in the kinematic compatibility equations of PETERSON-MAINARDI (Reference 12, page 85). Further, in these curvature changes, the effects of longitudinal dilatations ϕ_{ii} were neglected (Reference 12, page 57).

Thus with the aid of equations (A.9), (A.15), (A.21) to (A.23) the strain tensor components can be shown to be:

Strain tensor components at the middle surface

$$\epsilon^{\circ}_{\beta\beta} = (g_{\beta\beta})^{-1/2}\partial u/\partial\beta - k^{(g)}_{\beta} v + k^{(n)}_{\beta} w$$

$$\epsilon^{\circ}_{\alpha\alpha} = (g_{\alpha\alpha})^{-1/2}\partial v/\partial\alpha + k^{(n)}_{\alpha} w \qquad \text{(A.30)}$$

$$\epsilon^{\circ}_{\beta\alpha} = \epsilon^{\circ}_{\alpha\beta} = \tfrac{1}{2}\left((g_{\beta\beta})^{-1/2}\partial v/\partial\beta + (g_{\alpha\alpha})^{-1/2}\partial u/\partial\alpha + k^{(g)}_{\beta} u\right)$$

Strain tensor components of the curvature tensor $\delta\bar{\bar{K}}$

$$\delta K_{\beta\beta} = -(g_{\beta\beta})^{-1/2}\partial\phi_{13}/\partial\beta + k^{(g)}_{\beta}\phi_{23}$$

$$\delta K_{\alpha\alpha} = -(g_{\alpha\alpha})^{-1/2}\partial\phi_{23}/\partial\alpha \qquad \text{(A.31)}$$

$$2\delta K_{\beta\alpha} = 2\,\delta K_{\alpha\beta} = -(g_{\beta\beta})^{-1/2}\partial\phi_{23}/\partial\beta - k^{(g)}_{\beta}\phi_{13} - (g_{\alpha\alpha})^{-1/2}\partial\phi_{13}/\partial\alpha - k^{(n)}_{\alpha}\phi_{21} - k^{(n)}_{\beta}\phi_{12}$$

where the rotations ϕ_{ij} $(i \neq j)$ are,

$$\phi_{12} = (g_{\beta\beta})^{-1/2}\partial v/\partial\beta + k^{(g)}_{\beta} u$$

$$\phi_{21} = (g_{\alpha\alpha})^{-1/2}\partial u/\partial\alpha \qquad \text{(A.32)}$$

$$\phi_{23} = (g_{\alpha\alpha})^{-1/2}\partial w/\partial\alpha - k^{(n)}_{\alpha} v$$

$$\phi_{13} = (g_{\beta\beta})^{-1/2}\partial w/\partial\beta - k^{(n)}_{\beta} u$$

A.9 Strain Tensor Components of the Curvature Tensor $\delta\bar{\bar{K}}$ and the Curvature Variations δk_{ij} -with ARON's Approximations

Now since the BOURDON gage is sufficiently thin, the use of ARON's Approximations[4] for the curvature variations is assumed to be valid. Then the strain tensor components of the curvature tensor $\delta\bar{\bar{K}}$ and the variations of curvature δk_{ij} now become:

Strain tensor components of the curvature tensor $\delta\bar{\bar{K}}$ - with ARON's Approximations

$$\delta K_{\beta\beta} = -1/g_{\beta\beta}\ \partial^2 w/\partial\beta^2 + k_\beta^{(g)}(g_{\alpha\alpha})^{-1/2}\partial w/\partial\alpha$$

$$\delta K_{\alpha\alpha} = -1/g_{\alpha\alpha}\ \partial^2 w/\partial\alpha^2 + (\bar{a}^2 - \bar{b}^2)\sin\alpha\cos\alpha/(g_{\alpha\alpha})^2\,\partial w/\partial\alpha \qquad \text{(A.33)}$$

$$\delta K_{\beta\alpha} = \delta K_{\alpha\beta} = -1/(|\bar{g}_\alpha||\bar{g}_\beta|)\ \partial^2 w/\partial\beta\partial\alpha - k_\beta^{(g)}(g_{\beta\beta})^{-1/2}\partial w/\partial\beta$$

Variations of curvature δk_{ij} (i, j = 1, 2 or β, α respectively) - with ARON's Approximations

$$\delta k_{\beta\beta} = \delta k_{11} = -1/g_{\beta\beta}\ \partial^2 w/\partial\beta^2 + k_\beta^{(g)}(g_{\alpha\alpha})^{-1/2}\partial w/\partial\alpha$$

$$\delta k_{\alpha\alpha} = \delta k_{22} = -1/g_{\alpha\alpha}\ \partial^2 w/\partial\alpha^2 + (\bar{a}^2 - \bar{b}^2)\sin\alpha\cos\alpha/(g_{\alpha\alpha})^2\,\partial w/\partial\alpha$$

$$\delta k_{\beta\alpha} = \delta k_{\alpha\beta} = -1/(|\bar{g}_\alpha||\bar{g}_\beta|)\ \partial^2 w/\partial\beta\partial\alpha - k_\beta^{(g)}(g_{\beta\beta})^{-1/2}\partial w/\partial\beta \qquad \text{(A.34)}$$

---

[4] Experimental confirmation of ARON's Approximations may be found in Reference 14, page 336.

and observe that with ARON's Approximations,

$$\delta k_{\beta\alpha} = \delta k_{\alpha\beta}$$

Equations (A.34) therefore represent ARON's Approximations for the curvature variations. For the strain tensor components at the middle surface refer to equations (A.30).

A.10 The General Equilibrium Equations - For Orthogonal Parametric Coordinate Lines

From the First and Second Axioms of motion in absence of an electromagnetic field[5] the following equations of equilibrium can be shown to be:(References 12, 15)

$$-\int_v \rho_m \, d\bar{v}/dt \; dv + \int_v \bar{f} dv + \int_v \partial/\partial\bar{r} \cdot \bar{\bar{\sigma}} \, dv = 0$$

$$-\int_v (\bar{r} \times \rho_m \, d\bar{v}/dt) dv + \int_v \bar{r} \times \bar{f} dv - \int_v \partial/\partial\bar{r} \cdot (\bar{\bar{\sigma}} \times \bar{r}) dv = 0$$

---

[5] From the Second Axiom of Motion it can be shown that the stress tensor does not possess a vector invariant; then the stress tensor must be symmetric, i.e. $\bar{\bar{\sigma}} = \bar{\bar{\sigma}}_c$, where the subscript "c" represents the conjugate of $\bar{\bar{\sigma}}$. It should be noted that this symmetry condition will not be valid if the continuum is in an electromagnetic field, as additional terms for couple - stresses will exist (Reference 15).

where,

ρ_m denotes mass density (per unit volume)

$\bar{v}$ denotes velocity field relative to the fixed frame of reference

$\bar{f}$ denotes the body force intensity

$\bar{\bar{\sigma}}$ denotes the stress tensor

dv denotes the differential volume of the "free body" continuum

$\partial / \partial \bar{r}$ denotes the directed derivative; with $\bar{r}$ being the position vector to the differential volume element or to any parallel surface

Then, in accordance with the following:

(a) a static system

(b) the body force intensity $\bar{f}$ is considered negligible as compared to the surface forces

(c) the relations between ds_i^* of the parallel surface and ds_i of the middle surface,

$$ds_i^* = (1 + \alpha_3 k_{ii}) ds_i \qquad (i = 1, 2)$$

(d) the CESÀRO vectors for the case of orthogonal parametric coordinate lines,

$$\bar{c}_1 = -k_{12}\bar{e}_1 + k_{11}\bar{e}_2 + k_{13}\bar{e}_3$$

$$\bar{c}_2 = -k_{21}\bar{e}_1 + k_{21}\bar{e}_2 + k_{23}\bar{e}_3$$

and the relations:

$$\partial/\partial s_i(\bar{e}_j) = \bar{c}_i \times \bar{e}_j \qquad (i, j = 1, 2)$$

(e) the directed derivative $\partial/\partial\bar{r}$, as previously given, for surfaces other than the middle surface,

$$\partial/\partial\bar{r} = (1 + \alpha_3 k_{11})^{-1}\bar{e}_1\,\partial/\partial s_1 + (1 + \alpha_3 k_{22})^{-1}\bar{e}_2\,\partial/\partial s_2 + \bar{e}_3\,\partial/\partial\alpha_3$$

and the position vector to any parallel surface $\bar{r} = \bar{r}^\circ + \alpha_3\bar{e}_3$; $\bar{r}^\circ$ locates a point in the middle surface and $\alpha_3\bar{e}_3$ locates the parallel surface from the middle surface

(f) the PETERSON-MAINARDI equations for the case of orthogonal parametric coordinate lines - see footnote 3

(g) the stress tensor expressed in the trinomial form

$$\bar{\bar{\sigma}} = \bar{\sigma}_j\,\bar{e}_j \qquad (j = 1, 2, 3)$$

where the stress vector

$$\bar{\sigma}_j = \sigma_{ij}\,\bar{e}_i \qquad (\text{sum on } i = 1, 2, 3)$$

the general force and moment equilibrium equations for orthogonal parametric coordinate lines of a shell element may be derived: (Reference 12)

Equations of force equilibrium

From $\bar{e}_1$ - direction . . .

$$\partial F_{11}/\partial s_1 + \partial F_{21}/\partial s_2 + k_{11}F_{13} - k_{13}\left(F_{12} + F_{21} - 2k_{21}\int_{\alpha_3}\sigma_{11}\,\alpha_3\,d\alpha_3\right) + k_{23}\left(F_{11} - F_{22} - 2k_{21}\int_{\alpha_3}\sigma_{12}\,\alpha_3\,d\alpha_3\right) + k_{21}F_{23} - \partial k_{12}/\partial s_2\int_{\alpha_3}\sigma_{11}\,\alpha_3\,d\alpha_3 - \partial k_{21}/\partial s_1\int_{\alpha_3}\sigma_{12}\,\alpha_3\,d\alpha_3 + P_1 = 0 \qquad (A.35)$$

From $\bar{e}_2$ - direction . . .

$$\partial F_{12}/\partial s_1 + \partial F_{22}/\partial s_2 + k_{13}\left(F_{11} - F_{22} + 2k_{21}\int_{\alpha_3}\sigma_{12}\,\alpha_3\,d\alpha_3\right) + k_{23}\left(F_{21} + F_{12} - 2k_{21}\int_{\alpha_3}\sigma_{22}\,\alpha_3\,d\alpha_3\right) + k_{22}F_{23} + k_{12}F_{13} - \partial k_{12}/\partial s_2\int_{\alpha_3}\sigma_{12}\,\alpha_3\,d\alpha_3 - \partial k_{21}/\partial s_1\int_{\alpha_3}\sigma_{22}\,\alpha_3\,d\alpha_3 + P_2 = 0 \qquad (A.36)$$

From $\bar{e}_3$ - direction . . .

$$\partial F_{13}/\partial s_1 + \partial F_{23}/\partial s_2 - k_{13}\left(F_{23} - 2k_{21}\int_{\alpha_3}\sigma_{13}\,\alpha_3\,d\alpha_3\right) + k_{23}\left(F_{13} - 2k_{21}\int_{\alpha_3}\sigma_{23}\,\alpha_3\,d\alpha_3\right) - k_{11}F_{11} - k_{22}F_{22} - k_{12}\left(F_{12} + F_{21}\right) - \partial k_{12}/\partial s_2\int_{\alpha_3}\sigma_{13}\,\alpha_3\,d\alpha_3 - \partial k_{21}/\partial s_1\int_{\alpha_3}\sigma_{23}\,\alpha_3\,d\alpha_3 + P_3 = 0 \qquad (A.37)$$

Equations of moment equilibrium

From $\bar{e}_1$ - direction . . .

$$\partial M_{11}/\partial s_1 + \partial M_{21}/\partial s_2 - k_{13}\left(M_{12} + M_{21} + 2k_{21}\int_{\alpha_3}\alpha_3^2\,\sigma_{12}\,d\alpha_3\right) + k_{23}\left(M_{11} - M_{22} + 2k_{21}\int_{\alpha_3}\alpha_3^2\,\sigma_{22}\,d\alpha_3\right) - k_{12}M_{13} + F_{23} - \partial k_{12}/\partial s_2\int_{\alpha_3}\alpha_3^2\,\sigma_{12}\,d\alpha_3 + \partial k_{21}/\partial s_1\int_{\alpha_3}\alpha_3^2\,\sigma_{22}\,d\alpha_3 - M_2 = 0 \qquad (A.38)$$

From $\bar{e}_2$ - direction . . .

$$\partial M_{12}/\partial s_1 + \partial M_{22}/\partial s_2 + k_{13}(M_{11} - M_{22} + 2k_{21}\int_{\alpha_3} \alpha_3^2\, \sigma_{11}\, d\alpha_3) + k_{23}(M_{12} + M_{21} - 2k_{21}\int_{\alpha_3} \alpha_3^2\, \sigma_{12}\, d\alpha_3) + k_{21} M_{23} - F_{13} - \partial k_{12}/\partial s_2 \int_{\alpha_3} \alpha_3^2\, \sigma_{11}\, d\alpha_3 - \partial k_{21}/\partial s_1 \int_{\alpha_3} \alpha_3^2\, \sigma_{12}\, d\alpha_3 + M_1 = 0 \qquad (A.39)$$

where, the stress resultants F_{ij} and stress couples M_{ij} are expressed in terms of the stress components σ_{ij}, which act on the faces of an infinitesimal shell element (Figure A.8) - note, only $\overline{\sigma_1} = \sigma_{11}\bar{e}_1 + \sigma_{12}\bar{e}_2 + \sigma_{13}\bar{e}_3$ is shown to avoid confusion.[6]

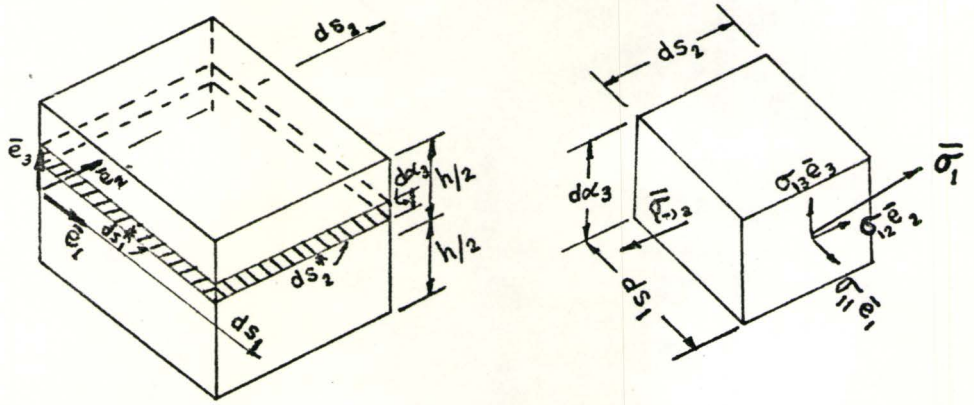

(a) (b)

Figure A.8 - (a) Semi-infinitesimal Segment of the Shell

(b) Infinitesimal Element of the Shell

---

[6] It can be observed from the "EULER Stress Principle for Contact Stress Vectors" that: $\overline{\sigma_{(-)i}} = -\overline{\sigma_i}$ $(i = 1, 2, 3)$
This proof was given by George HAMEL in 1908, as a consequence of the Fundamental Axiom of Motion for forces.

Therefore,

Stress Resultants

$$
\begin{aligned}
F_{11} &= \int_{\alpha_3} \sigma_{11}(1 + \alpha_3 k_{22})d\alpha_3 \\
F_{12} &= \int_{\alpha_3} \sigma_{12}(1 + \alpha_3 k_{22})d\alpha_3 \\
F_{13} &= \int_{\alpha_3} \sigma_{13}(1 + \alpha_3 k_{22})d\alpha_3 \\
F_{21} &= \int_{\alpha_3} \sigma_{21}(1 + \alpha_3 k_{11})d\alpha_3 \\
F_{22} &= \int_{\alpha_3} \sigma_{22}(1 + \alpha_3 k_{11})d\alpha_3 \\
F_{23} &= \int_{\alpha_3} \sigma_{23}(1 + \alpha_3 k_{11})d\alpha_3
\end{aligned}
\qquad \text{(A.40)}
$$

Stress Couples (the unit base vectors $\bar{e}_i$ are included to indicate the "directions" of the couples - in accordance with the Right-Hand Screw Rule)

$$
\begin{aligned}
M_{11}\bar{e}_1 &= -\int_{\alpha_3} \alpha_3 \sigma_{12}(1 + \alpha_3 k_{22})d\alpha_3 \bar{e}_1 \\
M_{12}\bar{e}_2 &= \int_{\alpha_3} \alpha_3 \sigma_{11}(1 + \alpha_3 k_{22})d\alpha_3 \bar{e}_2 \\
M_{13}\bar{e}_3 &= \int_{\alpha_3} \alpha_3 \sigma_{13}(1 + \alpha_3 k_{22})d\alpha_3 \bar{e}_3 \\
M_{21}\bar{e}_1 &= -\int_{\alpha_3} \alpha_3 \sigma_{22}(1 + \alpha_3 k_{11})d\alpha_3 \bar{e}_1 \\
M_{22}\bar{e}_2 &= \int_{\alpha_3} \alpha_3 \sigma_{21}(1 + \alpha_3 k_{11})d\alpha_3 \bar{e}_2 \\
M_{23}\bar{e}_3 &= \int_{\alpha_3} \alpha_3 \sigma_{23}(1 + \alpha_3 k_{11})d\alpha_3 \bar{e}_3
\end{aligned}
\qquad \text{(A.41)}
$$

where the limits of integration are $-h/2$ and $+h/2$.

And further, the remaining quantities, P_i and M_i, of the equilibrium equations are defined as:

P_i = the net boundary forces = $\sigma_{3i}(1 + \alpha_3 k_{11})(1 + \alpha_3 k_{22})\Big|_{\alpha_3}$

M_i = the net moments caused by the boundary forces

$= \alpha_3 \sigma_{31}(1 + \alpha_3 k_{11})(1 + \alpha_3 k_{22})\Big|_{\alpha_3}$

where $i = 1, 2, 3$

A.11 Stress Resultants and Stress Couples in Terms of the Strain Parameter Relations

With the aid of the following,

1. assumption (a), therefore the stress-strain relation for an isotropic, homogeneous Hookean material is used,

VIZ: $\bar{\bar{\sigma}} = 2\mu\bar{\bar{\epsilon}} + \lambda(\bar{\bar{\epsilon}} : \bar{\bar{1}})\bar{\bar{1}}$

or $\sigma_{ij}\bar{e}_i\bar{e}_j = 2\mu\epsilon_{ij}\bar{e}_i\bar{e}_j + \lambda(\bar{\bar{\epsilon}} : \bar{\bar{1}})\delta_{ij}\bar{e}_i\bar{e}_j$

where,

$\lambda = \nu E/((1 + \nu)(1 - 2\nu))$

$\mu = E/(2(1 + \nu))$

} denote the usual CAUCHY-LAMÉ elastic constants

ν denotes the POISSON's ratio

$\bar{\bar{1}}$ denotes the Identity tensor, $\bar{e}_\alpha\bar{e}_\alpha$

Kronecker delta, $\delta_{ij} = 1$ when $i = j$

$= 0$ when $i \neq j$

2. assumption (c), $\sigma_{33} = 0$

3. the strain tensor components (equations (A.25a))

the stress resultants F_{ij} (equations (A.40)) and stress couples M_{ij} (equations (A.41)) may be evaluated in terms of the strain parameter relations: (Reference 12, page 111)

Stress resultants

$$
\begin{aligned}
F_{11} &= Eh/(1-\nu^2)(\varepsilon_{11} + \nu\,\varepsilon_{22} + h^2/12\,\delta k_{11}(k_{22} - k_{11})) \\
F_{12} &= \mu h((\varepsilon_{12} + \varepsilon_{21}) + h^2/12\,\delta k_{12}(k_{22} - k_{11})) \\
F_{21} &= \mu h((\varepsilon_{12} + \varepsilon_{21}) - h^2/12\,\delta k_{21}(k_{22} - k_{11})) \\
F_{22} &= Eh/(1-\nu^2)(\varepsilon_{22} + \nu\,\varepsilon_{11} - h^2/12\,\delta k_{22}(k_{22} - k_{11}))
\end{aligned}
\qquad \text{(A.43)}
$$

Then by virtue of LOVE's First Approximation, equations (A.43) are simplified to,

$$
\begin{aligned}
F_{11} &= Eh/(1-\nu^2)(\varepsilon_{11} + \nu\,\varepsilon_{22}) \\
F_{12} &= Eh/(2(1+\nu))(\varepsilon_{12} + \varepsilon_{21}) \\
F_{21} &= Eh/(2(1+\nu))(\varepsilon_{12} + \varepsilon_{21}) \\
F_{22} &= Eh/(1-\nu^2)(\varepsilon_{22} + \nu\,\varepsilon_{11})
\end{aligned}
\qquad \text{(A.44)}
$$

Stress couples

$$
\begin{aligned}
M_{11} &= -\mu h^3/12\left(\left(\delta k_{12} + \delta k_{21}\right) + k_{22}\left(\phi_{12} + \phi_{21}\right)\right) \\
M_{12} &= Eh^3/\left(12(1-\nu^2)\right)\left(\delta k_{11} + \nu\,\delta k_{22} + \phi_{11}\left(k_{22} - k_{11}\right)\right) \\
M_{21} &= -Eh^3/\left(12(1-\nu^2)\right)\left(\delta k_{22} + \nu\,\delta k_{11} - \phi_{22}\left(k_{22} - k_{11}\right)\right) \\
M_{22} &= \mu h^3/12\left(\delta k_{21} + \delta k_{12} + k_{11}\left(\phi_{12} + \phi_{21}\right)\right)
\end{aligned}
\qquad \text{(A.45)}
$$

Then by virtue of LOVE's First Approximation equations (A.45) are simplified to,

$$
\begin{aligned}
M_{11} &= -Eh^3/\left(24(1+\nu)\right)\left(\delta k_{12} + \delta k_{21}\right) \\
M_{12} &= Eh^3/\left(12(1-\nu^2)\right)\left(\delta k_{11} + \nu\,\delta k_{22}\right) \\
M_{21} &= -Eh^3/\left(12(1-\nu^2)\right)\left(\delta k_{22} + \nu\,\delta k_{11}\right) \\
M_{22} &= Eh^3/\left(24(1+\nu)\right)\left(\delta k_{21} + \delta k_{12}\right)
\end{aligned}
\qquad \text{(A.46)}
$$

The other stress resultants, F_{13} and F_{23}, and stress couples, M_{13} and M_{23}, may be determined, if desired, by substituting the above expressions for F_{ij} and M_{ij} into the equilibrium equations (A.35), (A.36) and (A.38), (A.39).

A.12 Stress Resultants and Stress Couples in Terms of the Displacement Components u, v, w of the Middle Surface - with ARON's Approximations

In terms of the displacement components u, v, w and with ARON's Approximations for the curvature variations (equations (A.34)), the stress resultants (A.44) and stress couples (A.46) become:[7]

Stress resultants

$$F_{\beta\beta} = F_{11} = E'\big((g_{\beta\beta})^{-1/2}u_{,\beta} - k_{\beta}^{(g)}v + (k_{\beta}^{(n)} + \nu k_{\alpha}^{(n)})w + \nu(g_{\alpha\alpha})^{-1/2}v_{,\alpha}\big)$$

$$F_{\alpha\alpha} = F_{22} = E'\big((g_{\alpha\alpha})^{-1/2}v_{,\alpha} + (k_{\alpha}^{(n)} + \nu k_{\beta}^{(n)})w - \nu k_{\beta}^{(g)}v + \nu(g_{\beta\beta})^{-1/2}u_{,\beta}\big) \qquad (A.47)$$

$$F_{\beta\alpha} = F_{\alpha\beta} = F_{12} = F_{21} = E'(1-\nu)/2\big((g_{\beta\beta})^{-1/2}v_{,\beta} + (g_{\alpha\alpha})^{-1/2}u_{,\alpha} + k_{\beta}^{(g)}u\big)$$

Stress couples

$$M_{\beta\alpha} = M_{12} = D\big(-1/g_{\beta\beta}\,w_{,\beta\beta} + (k_{\beta}^{(g)}(g_{\alpha\alpha})^{-1/2} + \nu(\bar{a}^2 - \bar{b}^2)\sin\alpha\cos\alpha/(g_{\alpha\alpha})^2)w_{,\alpha} - \nu/g_{\alpha\alpha}\,w_{,\alpha\alpha}\big) \qquad (A.48)\ \text{cont'd}$$

---

[7] Note that partial derivatives may be denoted with a comma followed by a subscripted parameter β or α,

eg. $u_{,\beta} = \partial u/\partial\beta$, $u_{,\beta\alpha} = \partial^2 u/\partial\beta\partial\alpha$, etc.

$$M_{\alpha\beta} = M_{21} = -D\Big(-1/g_{\alpha\alpha}\, w_{,\alpha\alpha} + (\nu k_{\beta}^{(g)} (g_{\alpha\alpha})^{-1/2} + (\bar{a}^2 - \bar{b}^2)\sin\alpha\cos\alpha\,/(g_{\alpha\alpha}{}^{3})\Big)w_{,\alpha} - \nu/g_{\beta\beta}\, w_{,\beta\beta}\Big)$$

$$M_{\beta\beta} = M_{11} = D(1-\nu)\Big(1/(/\bar{g}_{\alpha}\,//\bar{g}_{\beta}\,/)w_{,\beta\alpha} + k_{\beta}^{(g)} (g_{\beta\beta})^{-1/2} w_{,\beta}\Big) \qquad \text{(A.48)}$$

$$M_{\alpha\alpha} = M_{22} = -M_{\beta\beta}$$

where,

$$E' = Eh/(1-\nu^2)$$

$$D = Eh^3/(12(1-\nu^2))$$

The curvatures and metrical coefficients are defined by equations (A.21) to (A.23). It is observed from above that due to the approximations imposed,

$$F_{\beta\alpha} = F_{\alpha\beta}$$

and therefore,

$$M_{\alpha\alpha} = -M_{\beta\beta}$$

A.13 The Governing Three Equilibrium Equations for the BOURDON Gage with an Elliptical Cross-Section

Rewriting the equilibrium equations (A.35) to (A.39) with the aid of the properties of the CESÀRO vectors (equations (A.23), equations (A.9), and a further assumption that no applied couple-stresses M_i are acting on the shell, the equations for the BOURDON gage become:

$$(g_{\beta\beta})^{-1/2}F_{11,\beta} + (g_{\alpha\alpha})^{-1/2}F_{21,\alpha} - k_{13}(F_{12} + F_{21}) + k_{11}F_{13} + P_1 = 0$$

$$(g_{\beta\beta})^{-1/2}F_{12,\beta} + (g_{\alpha\alpha})^{-1/2}F_{22,\alpha} + k_{13}(F_{11} - F_{22}) + k_{22}F_{23} + P_2 = 0$$

$$(g_{\beta\beta})^{-1/2}F_{13,\beta} + (g_{\alpha\alpha})^{-1/2}F_{23,\alpha} - k_{13}F_{23} - k_{11}F_{11} - k_{22}F_{22} + P_3 = 0 \qquad \text{(A.49a)}$$

$$(g_{\beta\beta})^{-1/2}M_{11,\beta} + (g_{\alpha\alpha})^{-1/2}M_{21,\alpha} - k_{13}(M_{12} + M_{21}) + F_{23} = 0$$

$$(g_{\beta\beta})^{-1/2}M_{12,\beta} + (g_{\alpha\alpha})^{-1/2}M_{22,\alpha} + k_{13}(M_{11} - M_{22}) - F_{13} = 0$$

Solving the last two equations for the stress resultants F_{13} and F_{23} give:

$$F_{13} = (g_{\beta\beta})^{-1/2}M_{12,\beta} + (g_{\alpha\alpha})^{-1/2}M_{22,\alpha} + k_{13}(M_{11} - M_{22})$$

$$F_{23} = -(g_{\beta\beta})^{-1/2}M_{11,\beta} - (g_{\alpha\alpha})^{-1/2}M_{21,\alpha} + k_{13}(M_{12} + M_{21}) \qquad \text{(A.49b)}$$

These are now substituted into the first three equilibrium equations[8] (A.49a) which then give: (using the β and α symbols)

$$(g_{\beta\beta})^{-1/2}F_{\beta\beta,\beta} + (g_{\alpha\alpha})^{-1/2}F_{\alpha\beta,\alpha} - k_{\beta}^{(g)}(F_{\beta\alpha} + F_{\alpha\beta})$$
$$+ k_{\beta}^{(n)}\left((g_{\beta\beta})^{-1/2}M_{\beta\alpha,\beta} + (g_{\alpha\alpha})^{-1/2}M_{\alpha\alpha,\alpha} + k_{\beta}^{(g)}(M_{\beta\beta} - M_{\alpha\alpha})\right) \qquad \text{(A.50) cont'd}$$
$$+ P_1 = 0$$

---

[8] As the curvature is large at the extremities of the cross-section the effects of the moments on the transverse shear may be significant, the "shallow shell" approximation of neglecting F_{i3} in the first two equilibrium equations will not be used (see also Reference 11).

$$
\begin{aligned}
&(g_{\beta\beta})^{-1/2} F_{\beta\alpha},_{\beta} + (g_{\alpha\alpha})^{-1/2} F_{\alpha\alpha},_{\alpha} + k_{\beta}^{(g)} (F_{\beta\beta} - F_{\alpha\alpha}) \\
&+ k_{\alpha}^{(n)} \big(-(g_{\beta\beta})^{-1/2} M_{\beta\beta},_{\beta} - (g_{\alpha\alpha})^{-1/2} M_{\alpha\beta},_{\alpha} + k_{\beta}^{(g)} (M_{\beta\alpha} + M_{\alpha\beta})\big) \\
&\qquad\qquad + P_2 = 0 \\
&(g_{\beta\beta})^{-1/2}\big((g_{\beta\beta})^{-1/2} M_{\beta\alpha},_{\beta} + (g_{\alpha\alpha})^{-1/2} M_{\alpha\alpha},_{\alpha} + k_{\beta}^{(g)} (M_{\beta\beta} - M_{\alpha\alpha})\big),_{\beta} \\
&+ (g_{\alpha\alpha})^{-1/2}\big(-(g_{\beta\beta})^{-1/2} M_{\beta\beta},_{\beta} - (g_{\alpha\alpha})^{-1/2} M_{\alpha\beta},_{\alpha} + k_{\beta}^{(g)} (M_{\beta\alpha} + M_{\alpha\beta})\big),_{\alpha} \\
&- k_{\beta}^{(g)}\big(-(g_{\beta\beta})^{-1/2} M_{\beta\beta},_{\beta} - (g_{\alpha\alpha})^{-1/2} M_{\alpha\beta},_{\alpha} + k_{\beta}^{(g)} (M_{\beta\alpha} + M_{\alpha\beta})\big) \\
&\qquad - k_{\beta}^{(n)} F_{\beta\beta} - k_{\alpha}^{(n)} F_{\alpha\alpha} + P_3 = 0
\end{aligned}
\qquad \text{(A.50)}
$$

Thus, it can be seen that the total criterion of equilibrium is contained in the three equations (A.50) remaining.

Finally, when equations (A.47) and (A.48) for the stress resultants F_{ij} and stress couples M_{ij} are substituted into the three equations of equilibrium (A.50), the equilibrium equations in terms of the displacement components u, v, w are obtained. Therefore listing the partial derivatives and their corresponding coefficients of each equation, they appear as follow:

Equilibrium equation in $\bar{e}_{\beta}$- direction

$$
\begin{aligned}
u,_{\beta\beta} \quad &: E'/g_{\beta\beta} \\
u,_{\alpha\alpha} \quad &: E'(1-\nu)/(2g_{\alpha\alpha}) \\
u,_{\alpha} \quad &: E'(1-\nu)/(2/\bar{g}_{\alpha}/)\big(-(\bar{a}^2 - \bar{b}^2)\sin\alpha\cos\alpha/(g_{\alpha\alpha})^{3/2} - k_{\beta}^{(g)}\big) \\
u \quad &: E'(1-\nu)/\big(-k_{\beta}^{(g)} k_{\beta}^{(g)} + \bar{a}\cos\alpha/(g_{\alpha\alpha}/\bar{g}_{\beta}/) \\
&\qquad - k_{\beta}^{(g)} (\bar{a}^2 - \bar{b}^2)\sin\alpha\cos\alpha/(g_{\alpha\alpha})^{3/2}\big)
\end{aligned}
\qquad \text{(A.51a) cont'd}
$$

$$v,_{\beta\alpha} : E'(1+\nu)/(2/\bar{g}_\alpha\,//\bar{g}_\beta\,/)$$

$$v,_{\beta} : E'k^{(g)}_{\beta}(\nu-3)/(2/\bar{g}_\beta\,/)$$

$$w,_{\beta\beta\beta} : -Dk^{(n)}_{\beta}/(g_{\beta\beta})^{3/2}$$

$$w,_{\beta\alpha\alpha} : -Dk^{(n)}_{\beta}/(g_{\alpha\alpha}/\bar{g}_\beta\,/)$$

(A.51a)

$$w,_{\beta\alpha} : Dk^{(n)}_{\beta}/(/\bar{g}_\alpha\,//\bar{g}_\beta\,/)(k^{(g)}_{\beta}+(\bar{a}^2-\bar{b}^2)\sin\alpha\cos\alpha/(g_{\alpha\alpha})^{3/2})$$

$$w,_{\beta} : E'(k^{(n)}_{\beta}+\nu k^{(n)}_{\alpha})/(g_{\beta\beta})^{1/2}+D(1-\nu)k^{(n)}_{\beta}/(g_{\alpha\alpha}/\bar{g}_\beta\,/)$$
$$(k^{(g)}_{\beta}(\bar{a}^2-\bar{b}^2)\sin\alpha\cos\alpha/(g_{\alpha\alpha})^{1/2}-\bar{a}\cos\alpha/(g_{\beta\beta})^{1/2})$$

$$P_\beta = 0$$

Equilibrium equilibrium equation in e_α - direction

$$u,_{\beta\alpha} : E'(1+\nu)/(2/\bar{g}_\alpha\,//\bar{g}_\beta\,/)$$

$$u,_{\beta} : E'k^{(g)}_{\beta}(3-\nu)/(2/\bar{g}_\beta\,/)$$

$$v,_{\beta\beta} : E'(1-\nu)/(2g_{\beta\beta})$$

$$v,_{\alpha\alpha} : E'/g_{\alpha\alpha}$$

$$v,_{\alpha} : -E'k^{(g)}_{\beta}/(g_{\alpha\alpha})^{1/2}-E'(\bar{a}^2-\bar{b}^2)\sin\alpha\cos\alpha/(g_{\alpha\alpha})^2$$

(A.51b) cont'd

$$v : -Ek^{(g)}_{\beta}k^{(g)}_{\beta}-E'\nu/(g_{\alpha\alpha})^{1/2}(\bar{a}\cos\alpha/(/\bar{g}_\alpha\,//\bar{g}_\beta\,/)$$
$$-k^{(g)}_{\beta}(\bar{a}^2-\bar{b}^2)\sin\alpha\cos\alpha/g_{\alpha\alpha})$$

$$w,_{\alpha\alpha\alpha} : -Dk^{(n)}_{\alpha}/(g_{\alpha\alpha})^{3/2}$$

$$w,_{\beta\beta\alpha} : -Dk^{(n)}_{\alpha}/(g_{\beta\beta}/\bar{g}_\alpha\,/)$$

$$w,_{\beta\beta} : -2Dk_{\beta}^{(g)} k_{\alpha}^{(n)} / g_{\beta\beta}$$

$$w,_{\alpha\alpha} : Dk_{\alpha}^{(n)} / g_{\alpha\alpha} \left(k_{\beta}^{(g)} + 3(\bar{a}^2 - \bar{b}^2)\sin\alpha\cos\alpha / (g_{\alpha\alpha})^{3/2}\right)$$

$$\begin{aligned} w,_{\alpha} : {} & Dk_{\alpha}^{(n)} / (g_{\alpha\alpha})^{1/2} ((\bar{a}^2 - \bar{b}^2)(\cos^2\alpha - \sin^2\alpha)/(g_{\alpha\alpha})^2 \\ & - k_{\beta}^{(g)} (1 + \nu)(\bar{a}^2 - \bar{b}^2)\sin\alpha\cos\alpha / (g_{\alpha\alpha})^{3/2} + k_{\beta}^{(g)} k_{\beta}^{(g)} \\ & - 4(\bar{a}^2 - \bar{b}^2)\sin^2\alpha\cos^2\alpha / (g_{\alpha\alpha})^3 + \nu \bar{a}\cos\alpha / (g_{\alpha\alpha} / \bar{g}_{\beta} /)) \end{aligned} \qquad \text{(A.51b)}$$

$$\begin{aligned} w : {} & E' k_{\beta}^{(g)} (k_{\beta}^{(n)} + \nu k_{\alpha}^{(n)}) - E' k_{\beta}^{(g)} k_{\alpha}^{(n)} - E' \nu \bar{b} \sin\alpha / (g_{\alpha\alpha} / \bar{g}_{\beta} /) \\ & - E'(\bar{a}^2 - \bar{b}^2)\sin\alpha\cos\alpha / (g_{\alpha\alpha})^{1/2} (3\bar{a}\bar{b} / (g_{\alpha\alpha})^{5/2} + \nu k_{\beta}^{(n)} / g_{\alpha\alpha}) \end{aligned}$$

$$P_{\alpha} = 0$$

Equilibrium equation in e_3-direction

$$u,_{\beta} : -E' (k_{\beta}^{(n)} + \nu k_{\alpha}^{(n)}) / (g_{\beta\beta})^{1/2}$$

$$v,_{\alpha} : -E' (k_{\alpha}^{(n)} + \nu k_{\beta}^{(n)}) / (g_{\alpha\alpha})^{1/2}$$

$$v : E' k_{\beta}^{(g)} (k_{\beta}^{(n)} + \nu k_{\alpha}^{(n)})$$

$$w,_{\beta\beta\beta\beta} : -D / (g_{\beta\beta})^2$$

$$w,_{\alpha\alpha\alpha\alpha} : -D / (g_{\alpha\alpha})^2 \qquad \text{(A.51c) cont'd}$$

$$w,_{\beta\beta\alpha\alpha} : -2D / (g_{\alpha\alpha} g_{\beta\beta})$$

$$w,_{\beta\beta\alpha} : 2D / g_{\beta\beta} ((\bar{a}^2 - \bar{b}^2)\sin\alpha\cos\alpha / (g_{\alpha\alpha})^2 - k_{\beta}^{(g)} / (g_{\alpha\alpha})^{1/2})$$

$$w,_{\alpha\alpha\alpha} : D / (g_{\alpha\alpha})^{3/2} (6(\bar{a}^2 - \bar{b}^2)\sin\alpha\cos\alpha / (g_{\alpha\alpha})^{3/2} + 2k_{\beta}^{(g)})$$

$$\begin{aligned} w,_{\beta\beta} : {} & Dk_{\beta}^{(g)} (3 - \nu)(\bar{a}^2 - \bar{b}^2)\sin\alpha\cos\alpha / (g_{\beta\beta} (g_{\alpha\alpha})^{3/2}) \\ & - 2Dk_{\beta}^{(g)} k_{\beta}^{(g)} (2 + 3\nu) / g_{\beta\beta} - D(3 - \nu)\bar{a}\cos\alpha / (g_{\alpha\alpha} (g_{\beta\beta})^{3/2}) \end{aligned}$$

$$
\begin{aligned}
w_{,\alpha\alpha} \;:\; & Dk_{\beta}^{(g)} k_{\beta}^{(g)} / g_{\alpha\alpha} + D\,\bar{a}\cos\alpha\,(1+\nu)/(|\bar{g}_{\beta}|(g_{\alpha\alpha})^{2}) \\
& - Dk_{\beta}^{(g)}(\bar{a}^{2}-\bar{b}^{2})\sin\alpha\cos\alpha\,(7+\nu)/(g_{\alpha\alpha})^{5/2} \\
& + 4D(\bar{a}^{2}-\bar{b}^{2})(\cos^{2}\alpha-\sin^{2}\alpha)/(g_{\alpha\alpha})^{3} \\
& - 19D(\bar{a}^{2}-\bar{b}^{2})^{2}\sin^{2}\alpha\cos^{2}\alpha/(g_{\alpha\alpha})^{4}
\end{aligned}
$$

$$
\begin{aligned}
w_{,\alpha} \;:\; & -3Dk_{\beta}^{(g)} k_{\beta}^{(g)}(\bar{a}^{2}-\bar{b}^{2})\sin\alpha\cos\alpha/(g_{\alpha\alpha})^{2} + Dk_{\beta}^{(g)} k_{\beta}^{(g)} k_{\beta}^{(g)}/(g_{\alpha\alpha})^{1/2} \\
& + 2Dk_{\beta}^{(g)}(\bar{a}^{2}-\bar{b}^{2})\sin^{2}\alpha\,(1+\nu)/(g_{\alpha\alpha})^{5/2} \\
& - Dk_{\beta}^{(g)}(\bar{a}^{2}-\bar{b}^{2})\cos^{2}\alpha\,(3+5\nu)/(g_{\alpha\alpha})^{5/2} \\
& + Dk_{\beta}^{(g)}\bar{a}\cos\alpha\,(1+\nu)/(|\bar{g}_{\beta}|(g_{\alpha\alpha})^{3/2}) \\
& + Dk_{\beta}^{(g)}(\bar{a}^{2}-\bar{b}^{2})^{2}\sin^{2}\alpha\cos^{2}\alpha\cdot(9+5\nu)/(g_{\alpha\alpha})^{7/2} \\
& + D/(g_{\alpha\alpha})^{1/2}(-4(\bar{a}^{2}-\bar{b}^{2})\sin\alpha\cos\alpha/(g_{\alpha\alpha})^{5/2} \\
& - 13(\bar{a}^{2}-\bar{b}^{2})^{2}\sin\alpha\cos\alpha(\cos^{2}\alpha-\sin^{2}\alpha)/(g_{\alpha\alpha})^{7/2} \\
& + 28(\bar{a}^{2}-\bar{b}^{2})^{3}\sin^{3}\alpha\cos^{3}\alpha/(g_{\alpha\alpha})^{9/2} - Dk_{\beta}^{(g)}\nu/(g_{\alpha\alpha})^{3/2}
\end{aligned}
\qquad \text{(A.51c)}
$$

$$
w \;:\; -E'(k_{\alpha}^{(n)} k_{\alpha}^{(n)} + k_{\beta}^{(n)} k_{\beta}^{(n)} + 2\nu k_{\alpha}^{(n)} k_{\beta}^{(n)})
$$

$$
P_3 = p
$$

Rearranging the equations (A.51) in a matrix form (as is done in Reference 14), a clearer picture of the system of three partial differential equations (with variable coefficients) in the three basic functions u, v, w can be observed. This system is presented in the form of Table A.1. In Table A.1, the unknown functions $u(\beta,\alpha)$, $v(\beta,\alpha)$, $w(\beta,\alpha)$ which are desired are the headings. The first three columns include the linear differential operators. The fourth column contains the free terms of the differential equations determined by the components P_{β}, P_{α}, P_3 of the external boundary or surface load.

TABLE A.1 – Governing Equations of the BOURDON Gage

$u(\beta,\alpha)$	$v(\beta,\alpha)$	$w(\beta,\alpha)$	Free Terms
$\frac{E'}{g_{\beta\beta}}\frac{\partial^2}{\partial\beta^2}+\frac{E'(1-\nu)}{2g_{\alpha\alpha}}\frac{\partial^2}{\partial\alpha^2}-\frac{E'(1-\nu)}{2\lvert\bar g_\alpha\rvert}\cdot\left[k_\beta^{(g)}+\frac{(\bar a^2-\bar b^2)\sin\alpha\cos\alpha}{(g_{\alpha\alpha})^{3/2}}\right]\frac{\partial}{\partial\alpha}+\frac{E'(1-\nu)}{2}\cdot\left[\frac{\bar a\cos\alpha}{g_{\alpha\alpha}\lvert\bar g_\beta\rvert}-\frac{k_\beta^{(g)}k_\beta^{(g)}}{}-\frac{k_\beta^{(g)}(\bar a^2-\bar b^2)\sin\alpha\cos\alpha}{(g_{\alpha\alpha})^{3/2}}\right]$	$\frac{E'(1+\nu)}{2\lvert\bar g_\alpha\rvert\lvert\bar g_\beta\rvert}\frac{\partial^2}{\partial\beta\partial\alpha}+\frac{E'k_\beta^{(g)}}{2\lvert\bar g_\beta\rvert}(\nu-3)\frac{\partial}{\partial\beta}$	$-\frac{D\,k_\beta^{(n)}}{(g_{\beta\beta})^{3/2}}\frac{\partial^3}{\partial\beta^3}-\frac{D\,k_\beta^{(n)}}{g_{\alpha\alpha}\lvert\bar g_\beta\rvert}\frac{\partial^3}{\partial\beta\partial\alpha^2}+\frac{D\,k_\beta^{(n)}}{\lvert\bar g_\alpha\rvert\lvert\bar g_\beta\rvert}\left[k_\beta^{(g)}+\frac{(\bar a^2-\bar b^2)\sin\alpha\cos\alpha}{(g_{\alpha\alpha})^{3/2}}\right]\frac{\partial^2}{\partial\beta\partial\alpha}+\left[\frac{E'}{\lvert\bar g_\beta\rvert}(k_\beta^{(n)}+\nu k_\alpha^{(n)})+\frac{D(1-\nu)k_\beta^{(n)}}{g_{\alpha\alpha}\lvert\bar g_\beta\rvert}\cdot\left(k_\beta^{(g)}\frac{(\bar a^2-\bar b^2)\sin\alpha\cos\alpha}{\lvert\bar g_\alpha\rvert}-\frac{\bar a\cos\alpha}{\lvert\bar g_\beta\rvert}\right)\right]\frac{\partial}{\partial\beta}$	P_β
$\frac{E'(1+\nu)}{2\lvert\bar g_\alpha\rvert\lvert\bar g_\beta\rvert}\frac{\partial^2}{\partial\beta\partial\alpha}-\frac{E'k_\beta^{(g)}(\nu-3)}{2\lvert\bar g_\beta\rvert}\frac{\partial}{\partial\beta}$	$\frac{E'(1-\nu)}{2\,g_{\beta\beta}}\frac{\partial^2}{\partial\beta^2}+\frac{E'}{g_{\alpha\alpha}}\frac{\partial^2}{\partial\alpha^2}+\left[-\frac{E'k_\beta^{(g)}}{\lvert\bar g_\alpha\rvert}-\frac{E'(\bar a^2-\bar b^2)\sin\alpha\cos\alpha}{(g_{\alpha\alpha})^2}\right]\frac{\partial}{\partial\alpha}-\left[E'k_\beta^{(g)}k_\beta^{(g)}+\frac{E'\nu}{\lvert\bar g_\alpha\rvert}\left(\frac{\bar a\cos\alpha}{\lvert\bar g_\alpha\rvert\lvert\bar g_\beta\rvert}-\frac{k_\beta^{(g)}(\bar a^2-\bar b^2)}{g_{\alpha\alpha}}\cdot\sin\alpha\cos\alpha\right)\right]$	$-\frac{D\,k_\alpha^{(n)}}{(g_{\alpha\alpha})^{3/2}}\frac{\partial^3}{\partial\alpha^3}-\frac{D\,k_\alpha^{(n)}}{\lvert\bar g_\alpha\rvert g_{\beta\beta}}\frac{\partial^3}{\partial\beta^2\partial\alpha}-\frac{2D\,k_\alpha^{(n)}k_\beta^{(g)}}{g_{\beta\beta}}\frac{\partial^2}{\partial\beta^2}+\frac{D\,k_\alpha^{(n)}}{g_{\alpha\alpha}}\left[k_\beta^{(g)}+\frac{3(\bar a^2-\bar b^2)\sin\alpha\cos\alpha}{(g_{\alpha\alpha})^{3/2}}\right]\frac{\partial^2}{\partial\alpha^2}+\left[\frac{E'}{\lvert\bar g_\alpha\rvert}(k_\alpha^{(n)}+\nu k_\beta^{(n)})+\frac{D\,k_\alpha^{(n)}}{\lvert\bar g_\alpha\rvert}\left(\frac{(\bar a^2-\bar b^2)(\cos^2\alpha-\sin^2\alpha)}{(g_{\alpha\alpha})^2}-\frac{k_\beta^{(g)}(1+\nu)(\bar a^2-\bar b^2)}{(g_{\alpha\alpha})^{3/2}}\cdot\sin\alpha\cos\alpha+k_\beta^{(g)}k_\beta^{(g)}-\frac{4(\bar a^2-\bar b^2)^2\sin^2\alpha\cos^2\alpha}{(g_{\alpha\alpha})^3}+\frac{\nu\,\bar a\cos\alpha}{g_{\alpha\alpha}\lvert\bar g_\beta\rvert}\right)\cdot\right]\frac{\partial}{\partial\alpha}+\left[E'k_\beta^{(g)}(k_\beta^{(n)}+\nu k_\alpha^{(n)})-E'k_\beta^{(g)}k_\alpha^{(n)}-\frac{E'\nu\,\bar b\sin\alpha}{g_{\alpha\alpha}\lvert\bar g_\beta\rvert}-\frac{E'(\bar a^2-\bar b^2)\sin\alpha\cos\alpha}{\lvert\bar g_\alpha\rvert}\left(\frac{3\bar a\,\bar b}{(g_{\alpha\alpha})^{5/2}}+\frac{\nu\,k_\beta^{(n)}}{g_{\alpha\alpha}}\right)\right]$	P_α
$-\frac{E'}{\lvert\bar g_\beta\rvert}(k_\beta^{(n)}+\nu k_\alpha^{(n)})\frac{\partial}{\partial\beta}$	$-\frac{E'}{\lvert\bar g_\alpha\rvert}(k_\alpha^{(n)}+\nu k_\beta^{(n)})\frac{\partial}{\partial\alpha}+\left[E'k_\beta^{(g)}\cdot(k_\beta^{(n)}+\nu k_\alpha^{(n)})\right]$	$-\frac{D}{(g_{\beta\beta})^2}\frac{\partial^4}{\partial\beta^4}-\frac{D}{(g_{\alpha\alpha})^2}\frac{\partial^4}{\partial\alpha^4}-\frac{2D}{g_{\alpha\alpha}g_{\beta\beta}}\frac{\partial^4}{\partial\beta^2\partial\alpha^2}+\frac{2D}{g_{\beta\beta}}\left[\frac{(\bar a^2-\bar b^2)\sin\alpha\cos\alpha}{(g_{\alpha\alpha})^2}-\frac{k_\beta^{(g)}}{\lvert\bar g_\alpha\rvert}\right]\frac{\partial^3}{\partial\beta^2\partial\alpha}+\frac{D}{(g_{\alpha\alpha})^{3/2}}\left[\cdot\frac{6(\bar a^2-\bar b^2)\sin\alpha\cos\alpha}{(g_{\alpha\alpha})^{3/2}}+2k_\beta^{(g)}\right]\frac{\partial^3}{\partial\alpha^3}+\left[\frac{D\,k_\beta^{(g)}(3-\nu)(\bar a^2-\bar b^2)}{(g_{\alpha\alpha})^{3/2}g_{\beta\beta}}\cdot\sin\alpha\cos\alpha-\frac{2D\,k_\beta^{(g)}k_\beta^{(g)}(2+3\nu)}{g_{\beta\beta}}-\frac{D(3-\nu)\bar a\cos\alpha}{g_{\alpha\alpha}(g_{\beta\beta})^{3/2}}\cdot\right]\frac{\partial^2}{\partial\beta^2}+\left[\frac{D\,k_\beta^{(g)}k_\beta^{(g)}}{g_{\alpha\alpha}}+\frac{D\,\bar a\cos\alpha(1+\nu)}{(g_{\alpha\alpha})^2\lvert\bar g_\beta\rvert}-\frac{D\,k_\beta^{(g)}(\bar a^2-\bar b^2)}{(g_{\alpha\alpha})^{5/2}}\cdot\sin\alpha\cos\alpha(7+\nu)+\frac{4D(\bar a^2-\bar b^2)}{(g_{\alpha\alpha})^3}(\cos^2\alpha-\sin^2\alpha)-\frac{19D(\bar a^2-\bar b^2)^2\sin^2\alpha\cos^2\alpha}{(g_{\alpha\alpha})^4}\right]\frac{\partial^2}{\partial\alpha^2}+\left[-\frac{3D\,k_\beta^{(g)}k_\beta^{(g)}(\bar a^2-\bar b^2)}{(g_{\alpha\alpha})^2}\cdot\sin\alpha\cos\alpha+\frac{D\,k_\beta^{(g)}k_\beta^{(g)}k_\beta^{(g)}}{\lvert\bar g_\alpha\rvert}+\frac{2D\,k_\beta^{(g)}(\bar a^2-\bar b^2)\sin^2\alpha(1+\nu)}{(g_{\alpha\alpha})^{5/2}}-\frac{D\,k_\beta^{(g)}(\bar a^2-\bar b^2)\cos^2\alpha(3+5\nu)}{(g_{\alpha\alpha})^{5/2}}+\frac{D\,k_\beta^{(g)}\bar a\cos\alpha(1+\nu)}{(g_{\alpha\alpha})^{3/2}\lvert\bar g_\beta\rvert}+\frac{D\,k_\beta^{(g)}(\bar a^2-\bar b^2)^2\sin^2\alpha\cos^2\alpha(9+5\nu)}{(g_{\alpha\alpha})^{7/2}}+\frac{D}{\lvert\bar g_\alpha\rvert}\left[-\frac{4(\bar a^2-\bar b^2)}{(g_{\alpha\alpha})^{5/2}}\cdot\sin\alpha\cos\alpha-\frac{13(\bar a^2-\bar b^2)^2\sin\alpha\cos\alpha(\cos^2\alpha-\sin^2\alpha)}{(g_{\alpha\alpha})^{7/2}}+\frac{28(\bar a^2-\bar b^2)^3\sin^3\alpha\cos^3\alpha}{(g_{\alpha\alpha})^{9/2}}\right]-\frac{D\,k_\beta^{(g)}\nu}{(g_{\alpha\alpha})^{3/2}}\left]\frac{\partial}{\partial\alpha}-E'\right[k_\alpha^{(n)}k_\alpha^{(n)}+k_\beta^{(n)}k_\beta^{(n)}+2\nu k_\alpha^{(n)}k_\beta^{(n)}\right]$	P_3

A.14 Reduction of the System of Three Differential Equations to the Familiar Straight Circular Cylinder Problem

Of interest is the reduction of the system of three differential equations (Table A.1 or equations (A.51)) to the familiar problem of the straight circular cylinder. This reduction also serves the purpose of checking for the correctness of the equations (A.51) to an extent (a further check can be accomplished with a dimensional analysis of each coeeficient). As given in Reference 12, the system of three partial differential equations (with constant coefficients) for the straight circular cylinder - (Figure A.9), appears as follows:

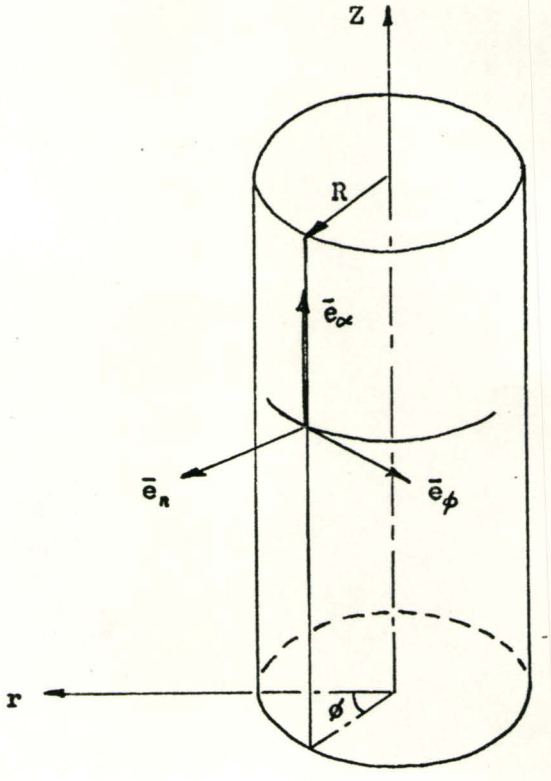

Figure A.9 - Coordinates and Properties of a Straight Circular Cylinder

$$u_{,\phi\phi} + (1-\nu)/2u_{,\alpha\alpha} + (1+\nu)/2v_{,\phi\alpha} + \nu w_{,\phi} = -R^2(1-\nu^2)/Eh\, P_\phi$$

$$(1+\nu)/2u_{,\phi\alpha} + (1-\nu)/2v_{,\phi\phi} + v_{,\alpha\alpha} + w_{,\alpha} = -R^2(1-\nu^2)/Eh\, P_\alpha \qquad (A.52)$$

$$\nu u_{,\phi} + v_{,\alpha} + h^2/(12R^2)(w_{,\phi\phi\phi\phi} + w_{,\alpha\alpha\alpha\alpha} + 2w_{,\phi\phi\alpha\alpha}) + w = R^2(1-\nu^2)/Eh\, P_3$$

By setting the following equivalence or properties to equations (A.51) or Table A.1:

$k^{(g)}_{\beta} = 0$

$k^{(n)}_{\beta} = 0$

$\bar{a} = \bar{b}$

$g_{\alpha\alpha} = g_{\beta\beta} = R^2$

$k^{(n)}_{\alpha} = 1/R$

$D = 0$ in the first two equilibrium equations

Set $\beta \to \emptyset$ in all partial derivative operators

the system of three partial differential equations for the BOURDON gage with an elliptic cross section can be transformed to equations (A.52) of the straight circular cylinder.

Thus the system of three differntial equations ((A.51) or Table A.1) may be considered verified.

A.15 Boundary Conditions

In order for the system of equations (A.51) or in Table A.1 to be determinate appropriate relations between the forces, moments, displacements or functions of these quantities at the edge or boundary of the shell must be specified. Considering the case where the boundaries coincide with the lines of curvature of the middle surface as this particular case is most often encountered in engineering practise. For the general case in which the edge boundary does not coincide with any coordinate lines on the surface LOVE in Reference 7, article 332, should be consulted.

It can be seen that (neglecting M_{13} as it did not enter into the equilibrium equations for the BOURDON gage) at the edge along α_1 = constant the stresses and moments required for the boundary conditions are:

$$F_{11} \quad , \quad F_{12} \quad , \quad F_{13} \quad , \quad M_{11} \quad , \quad M_{12}$$

From this it appears that five boundary conditions are necessary. However as in KIRCHHOFF's plate theory only four conditions are really required. The twisting couple M_{11}, in fact, can be replaced by corresponding, distributed, tangential and transverse forces (see Figure A.10) - i.e. statically equivalent forces.

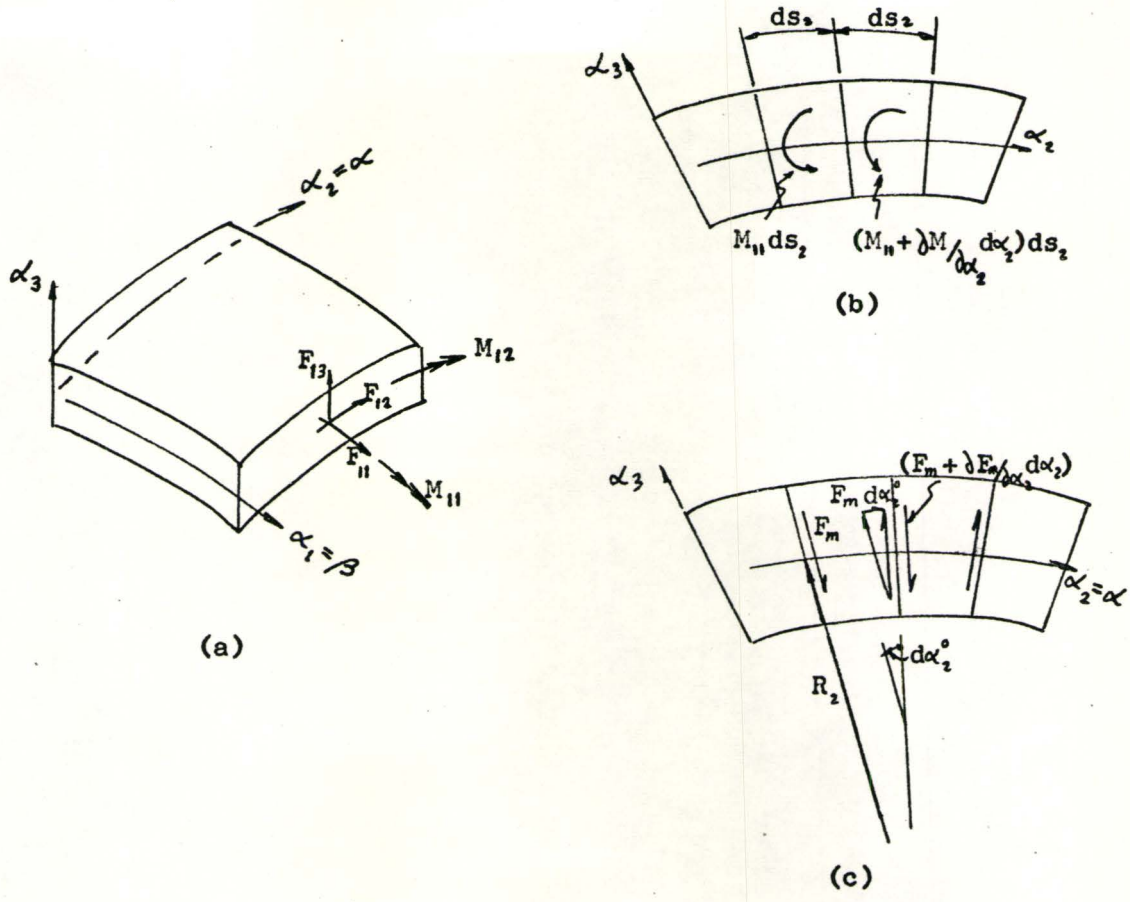

Figure A.10 - (a) Stress Resultants and Couples at an edge boundary coinciding with a coordinate line, α_1 = constant
(b) M_{11} along ds_2 or Twisting Moment ($M_{11}\,ds_2$)
(c) Corresponding Forces for M_{11}

Referring to Figure A.10(c), it can be observed that because of the curvature, there is a horizontal component (to be situated at the middle surface) of F_m directed positively in α_2 - direction which is designated by the force $F_m d\alpha_2^\circ$. This component $F_m d\alpha_2^\circ$ when combined with F_{12} will give an effective shear $F_{12\,eff}$ tangent to the edge,

i.e. $F_{12\,eff} = F_{12} + (F_m d\alpha_2^0)/ds_2$

(Note that $F_m d\alpha_2^0$ must be divided by ds_2, as the stress resultant F_{12} is per unit length)

Since $R_\alpha\, d\alpha_2^0 = ds_2$ and observing that $F_m ds_2 = M_{11} ds_2$:

$$F_{12\,eff} = F_{12} + (F_m R_\alpha^{-1}\, ds_2)/ds_2$$

Therefore,

$$F_{12\,eff} = F_{12} + M_{11}/R_\alpha \qquad (A.53)$$

Similarly, an effective transverse shear $F_{13\,eff}$ may be determined by writing the net vertical force at point A(Figure A.10(c)). It is observed that the difference between the forces F_m and $(F_m + (\partial F_m/\partial\alpha_2)\cdot d\alpha_2)$ is a net force $(\partial F_m/\partial\alpha_2)d\alpha_2$ acting in the negative α_3- direction. Combining this with F_{13} gives:

$$F_{13\,eff} = F_{13} - (\partial F_m/\partial\alpha_2)d\alpha_2/ds_2$$
$$= F_{13} - (\partial M_{11}/\partial\alpha_2)(d\alpha_2/ds_2$$

And by equations (A.9), $ds_i = (g_{ii})^{1/2} d\alpha_i$

Therefore,

$$F_{13\,eff} = F_{13} - (g_{22})^{-1/2}\partial M_{11}/\partial\alpha_2 \qquad (A.54)$$

Thus it follows from above that the four required boundary conditions,

$$F_{11}\ ,\ F_{12\,eff}\ ,\ F_{13\,eff}\ ,\ M_{12}$$

will completely determine the state of stress at the edge of the shell in the case of the edge or boundary coinciding with a coordinate line

(α_1 = constant) of the shell surface.

In an analogous manner, the boundary conditions along the edge of the shell prescribed by α_2 = constant are:

F_{22} , $F_{21\,eff}$, $F_{23\,eff}$, M_{21}

where,

$$F_{21\,eff} = F_{21} - M_{22}/R_1 \qquad (A.55)$$

$$F_{23\,eff} = F_{23} + (g_{11})^{-1/2}\,\partial M_{22}/\partial \alpha_1 \qquad (A.56)$$

However, it is often the case that other conditions may be prescribed instead of the above four conditions - depending on the type of constraint; for example at the junction of two shells: the BOURDON shell and the end plug. Other alternative but equivalent conditions may be through displacements, angles of rotation at the edge, or a combination of forces and displacements.

Observe that as LOVE's First Approximation is employed, it can be proved that

$$F_{12\,eff} = F_{12} \quad , \quad F_{21\,eff} = F_{21}$$

For the BOURDON gage then, the boundary conditions are as follows:

(a) At the clamped edge or regidly fixed edge of the gage

- at $\beta = 0^\circ$

(i) $u = 0$

(ii) $v = 0$

(iii) $w = 0$

(iv) $w_{,\beta} = 0$ (i.e. $\phi_{13} = 0$)

(b) From symmetry of the gage

- $\alpha = 0$ and π (refer to Figure A.7)

(i) $v = 0$

(ii) $w_{,\alpha} = 0$ (i.e. $\phi_{23} = 0$)

(iii) $F_{\alpha\beta} = 0$; or in terms of displacement

$$F_{\alpha\beta\,eff} = F_{\alpha\beta}$$
$$= 0$$
$$= E'(1 - \nu)/2\left((g_{\beta\beta})^{-1/2} v_{,\beta} + (g_{\alpha\alpha})^{-1/2} u_{,\alpha} + k^{(g)}_{\beta} u\right)$$
$$= 0$$

Then at $\alpha = 0$ and π, because of (i) above and $k^{(g)}_{\beta}$ vanishing,

$$F_{\alpha\beta} = u_{,\alpha}$$
$$= 0$$

(iv) $F_{\alpha 3\,eff} = 0$; or in terms of displacement equation (A.56) becomes:

$$F_{\alpha 3\,eff} = F_{\alpha 3} + (g_{\beta\beta})^{-1/2} M_{\alpha\alpha,\beta}$$
$$= 0$$

$$F_{\alpha 3\,eff} = -D/(g_{\alpha\alpha})^{3/2} w_{,\alpha\alpha\alpha} - D(2-\nu)/(g_{\beta\beta}/\bar{g}_{\alpha}/) w_{,\beta\beta\alpha}$$
$$- D(3-\nu) k_{\beta}^{(g)}/g_{\beta\beta}\, w_{,\beta\beta}$$
$$+ D/g_{\alpha\alpha}\,(k_{\beta}^{(g)} + 3(\bar{a}^2 - \bar{b}^2)\sin\alpha\cos\alpha/(g_{\alpha\alpha})^{3/2}) w_{,\alpha\alpha}$$
$$+ D(g_{\alpha\alpha})^{-1/2}(k_{\beta}^{(g)} k_{\beta}^{(g)} + (\bar{a}^2 - \bar{b}^2)(\cos^2\alpha - \sin^2\alpha)/(g_{\alpha\alpha})^2$$
$$- k_{\beta}^{(g)}(1+\nu)(\bar{a}^2 - \bar{b}^2)\sin\alpha\cos\alpha/(g_{\alpha\alpha})^{3/2}$$
$$- 4(\bar{a}^2 - \bar{b}^2)^2 \sin^2\alpha\cos^2\alpha/(g_{\alpha\alpha})^3$$
$$+ \nu\,\bar{a}\cos\alpha/(g_{\alpha\alpha}/\bar{g}_{\beta}/))w_{,\alpha}$$

Then at $\alpha = 0$ and π,

$$F_{\alpha 3\,eff} = w_{,\alpha\alpha\alpha}$$
$$= 0$$

(c) At the deflection or plug end of the gage

At the shell boundary $\beta = \beta_L$, the displacement components u, v and w must be such that they can be realized by a middle surface moving like a rigid body - as the shell is assumed rigidly attached to the rigid (non-deformable) and moving end plug.

For a rigid body (i.e. the end plug), the displacement vector $\bar{U}^p$ of its middle surface can be resolved into a translation part and a rotation part (see also Reference 16)

$$\bar{U}^p = \bar{U}_o^p + \bar{\phi}_o^p \times \bar{r} \qquad (A.57)$$

where,

$\bar{U}_o^p$ denotes the "translation" vector of the plug with components U_o, V_o, W_o

$= U_o \bar{e}_X + V_o \bar{e}_Y + W_o \bar{e}_Z$

$\bar{\phi}_o^p$ denotes the "rotation" vector of the plug with components

$\phi_X^\circ, \phi_Y^\circ, \phi_Z^\circ$

$= \phi_X^\circ \bar{e}_X + \phi_Y^\circ \bar{e}_Y + \phi_Z^\circ \bar{e}_Z$

$\bar{r}$ denotes the position vector of the end plug along the contour of the BOURDON shell at $\beta = \beta_L$

$= (\rho + \bar{a} \cos\alpha)\cos\beta_L \bar{e}_X + (\rho + \bar{a} \cos\alpha)\sin\beta_L \bar{e}_Y + (\bar{b} \sin\alpha)\bar{e}_Z$

By taking the "dot" product of the above expression with $\bar{e}_\beta$, $\bar{e}_\alpha$ and $\bar{e}_n$ the expressions for u, v and w of the BOURDON shell at the rigid boundary are realized:

$$u = \bar{U}^p \cdot \bar{e}_\beta = \bar{U}_o^p \cdot \bar{e}_\beta + (\bar{\phi}_o^p \times \bar{r}) \cdot \bar{e}_\beta$$

$$v = \bar{U}^p \cdot \bar{e}_\alpha = \bar{U}_o^p \cdot \bar{e}_\alpha + (\bar{\phi}_o^p \times \bar{r}) \cdot \bar{e}_\alpha \qquad (A.58)$$

$$w = \bar{U}^p \cdot \bar{e}_n = \bar{U}_o^p \cdot \bar{e}_n + (\bar{\phi}_o^p \times \bar{r}) \cdot \bar{e}_n$$

Expanding equations (A.58) with the aid of equations (A.21) and (A.22), noting that from symmetry of the motion $W_o, \phi_X^\circ, \phi_Y^\circ = 0$, u, v and w become (at $\beta = \beta_L$):

$$u = -\sin\beta_L U_o + \cos\beta_L V_o + (\rho + \bar{a} \cos\alpha)\phi_Z^\circ$$

$$v = -\bar{a} \sin\alpha \,/\!/\bar{g}_\alpha\,/\cos\beta_L U_o - \bar{a} \sin\alpha \,/\!/\bar{g}_\alpha\,/\sin\beta_L V_o \qquad (A.59)$$

$$w = \bar{b} \cos\alpha \,/\!/\bar{g}_\alpha\,/\cos\beta_L U_o + \bar{b} \cos\alpha \,/\!/\bar{g}_\alpha\,/\sin\beta_L V_o$$

Along the contour of the BOURDON shell at $\beta = \beta_L$, the continuity condition requires that the angular rotation of the normal about the line α be equal to the corresponding component of rotation of the rigid plug. This then represents the fourth boundary condition, or

$$\bar{\phi}_S \cdot \bar{e}_\alpha = \bar{\phi}_o^p \cdot \bar{e}_\alpha$$

where

$\bar{\phi}_S$ denotes the rotation vector of the BOURDON shell

$\bar{\phi}_o^p$ denotes the rotation vector of the end plug (as defined previously)

From an Euler-Cauchy (1828) kinematic model of deformation (Reference 15), the rotation vector of the BOURDON shell may be obtained. Expressing the Displacement Gradient (or linear Displacement Tensor) $\bar{\bar{u}} = \partial \bar{u} / \partial \bar{r}$ through tensor resolution into symmetric and antisymmetric parts:

$$\bar{\bar{u}} = \partial \bar{u} / \partial \bar{r} = \tfrac{1}{2}(\partial \bar{u} / \partial \bar{r} + \bar{u}\, \partial / \partial \bar{r}) + \tfrac{1}{2}(\partial \bar{u} / \partial \bar{r} - \bar{u}\, \partial / \partial \bar{r})$$

or

$$\partial \bar{u} / \partial \bar{r} = \bar{\bar{\epsilon}} + \bar{\bar{\phi}} \qquad \text{(A.60)}$$

The first term on the right side of expressions (A.60) is the familiar relative deformation of $d\bar{r}$ called the strain tensor $\bar{\bar{\epsilon}}$ (c.f. equation (A.25))and the other term $\bar{\bar{\phi}}$, called the rotation tensor, describes the rotational displacement of $d\bar{r}$ due to the displacement field $\bar{u}$.

It can be shown for the antisymmetric part that:

$$\bar{\bar{I}} \cdot \bar{\bar{\phi}} = \bar{\bar{I}} \cdot \tfrac{1}{2}(\partial \bar{u}/\partial \bar{r} - \bar{u}\,\partial/\partial \bar{r})$$

or

$$\bar{\bar{\phi}} = -\tfrac{1}{2}\,\bar{\bar{I}} \times \partial \times \bar{u}/\partial \bar{r}$$

Since half the curl of the displacement field $\bar{u}$ is equal to the rotation vector $(\bar{\phi}_s)$ of the field. That is,

$$(\tfrac{1}{2}\,\partial/\partial \bar{r} \times \bar{u}) = \bar{\phi}_s$$

Therefore,

$$\bar{\bar{\phi}} = -\bar{\bar{I}} \times \bar{\phi}_s$$

Equations (A.60) become:

$$\partial \bar{u}/\partial \bar{r} = \tfrac{1}{2}(\partial \bar{u}/\partial \bar{r} + \bar{u}\,\partial/\partial \bar{r}) - \bar{\bar{I}} \times \bar{\phi}_s$$

or

$$\bar{\bar{I}} \times \bar{\phi}_s = \tfrac{1}{2}(\bar{u}\,\partial/\partial \bar{r} - \partial \bar{u}/\partial \bar{r}) \qquad \text{(A.61)}$$

Let $\bar{\phi}_s = \phi_1 \bar{e}_1 + \phi_2 \bar{e}_2 + \phi_3 \bar{e}_3$

ϕ_1 and ϕ_2 represent the angular rotations of the normal about the lines α_1 and α_2 respectively. ϕ_3 is the angular rotation about the normal.

With $\bar{\bar{1}} = \bar{e}_1\bar{e}_1 + \bar{e}_2\bar{e}_2 + \bar{e}_3\bar{e}_3$, the left side of equation (A.61) becomes,

$$\bar{\bar{1}} \times \bar{\phi}_S = \begin{bmatrix} 0\,\bar{e}_1\bar{e}_1 - \phi_3\bar{e}_1\bar{e}_2 + \phi_2\bar{e}_1\bar{e}_3 \\ \phi_3\bar{e}_2\bar{e}_1 + 0\,\bar{e}_2\bar{e}_2 - \phi_1\bar{e}_2\bar{e}_3 \\ -\phi_2\bar{e}_3\bar{e}_1 + \phi_1\bar{e}_3\bar{e}_2 + 0\,\bar{e}_3\bar{e}_3 \end{bmatrix} \qquad (A.62)$$

Observe the antisymmetric characteristic of equation (A.62), i.e. $(T_{ij})_c = -T_{ji}$

The right side of equation (A.61) can be determined from the displacement tensor $\bar{\bar{u}} = \partial\bar{u}/\partial\bar{r}$ as given in Reference 12, page 72 (employing LOVE's First Approximation):

$$\partial\bar{u}/\partial\bar{r} = u_{rs}\bar{e}_r\bar{e}_s \qquad (r, s = 1, 2, 3)$$

and since

$\bar{u}\,\partial/\partial\bar{r} = (\partial\bar{u}/\partial\bar{r})_c$, the conjugate tensor:

$$\bar{u}\,\partial/\partial\bar{r} = u_{sr}\bar{e}_r\bar{e}_s \qquad (r, s = 1, 2, 3)$$

where

$$u_{11} = \phi_{11} + \alpha_3(-\partial\phi_{13}/\partial s_1 + k_{12}\phi_{12} + k_{13}\phi_{23})$$

$$u_{12} = \phi_{12} + \alpha_3(\partial\phi_{23}/\partial s_1 + k_{13}\phi_{13})$$

$$u_{13} = \phi_{13}$$

$$u_{21} = \phi_{21} + \alpha_3(-\partial\phi_{13}/\partial s_2 + k_{23}\phi_{23})$$

$$u_{22} = \phi_{22} + \alpha_3 (-\partial \phi_{23} / \partial s_2 + k_{21} \phi_{21} - k_{23} \phi_{13})$$

$$u_{23} = \phi_{23}$$

$$u_{31} = -\phi_{13}$$

$$u_{32} = -\phi_{23}$$

$$u_{33} = 0$$

Upon carrying out the operations as required by equation (A.61) and equating base vectors on both sides of the expression, the rotation components of the rotation vector $\bar{\phi}_S$ may be determined:

$$\phi_1 = \phi_{23}$$

$$\phi_2 = -\phi_{13}$$

$$\phi_3 = \tfrac{1}{2}(\phi_{12} - \phi_{21} + \alpha_3 (\partial \phi_{23} / \partial s_1 + \partial \phi_{13} / \partial s_2 + k_{13} \phi_{13} - k_{23} \phi_{23}))$$

Therefore, the rotation vector of the BOURDON shell $\bar{\phi}_S$ (at $\alpha_3 = 0$) becomes,

$$\bar{\phi}_S = \phi_{23} \bar{e}_1 - \phi_{13} \bar{e}_2 + \tfrac{1}{2}(\phi_{12} - \phi_{21}) \bar{e}_3$$

Thence from the continuity condition at $\beta = \beta_L$, the angular rotation of the normal about the line α is equal to the corresponding angular rotation of the rigid plug. Thus resolving the rotation vectors into the direction of $\bar{e}_2$ (or $\bar{e}_\alpha$):

$$\bar{\phi}_s \cdot \bar{e}_\alpha = \bar{\phi}_o^p \cdot \bar{e}_\alpha$$

or

$$-\phi_{13} = \bar{b} \cos\alpha \, // \bar{g}_\alpha \, // \phi_z^\circ$$

With ϕ_{13} as given by equation (A.32), then

$$(g_{\beta\beta})^{-1/2} \partial w / \partial \beta - k_\beta^{(n)} u = -\bar{b} \cos\alpha \, // \bar{g}_\alpha \, // \phi_z^\circ \qquad \text{(A.63)}$$

Equation (A.63) therefore expresses the continuity condition of angular rotations at the junction of two middle surfaces - the BOURDON shell at $\beta = \beta_L$ and the rigid end plug.

Hence the required four edge conditions are obtained. However three additional relations are necessary to determine the three constants U_o, V_o and ϕ_z° of the rigid end plug.

Since the rigid end plug must be in equilibrium with the "external" forces (in this case, the edge forces at the boundary of the BOURDON shell at $\beta = \beta_L$) the additional relations can be obtained from the usual static equilibrium conditions applied to the plug. A new local coordinate system (as suggested in Reference 6) x^*, y^*, z^* located at the center of the rigid plug is first defined (see Figure A.11).

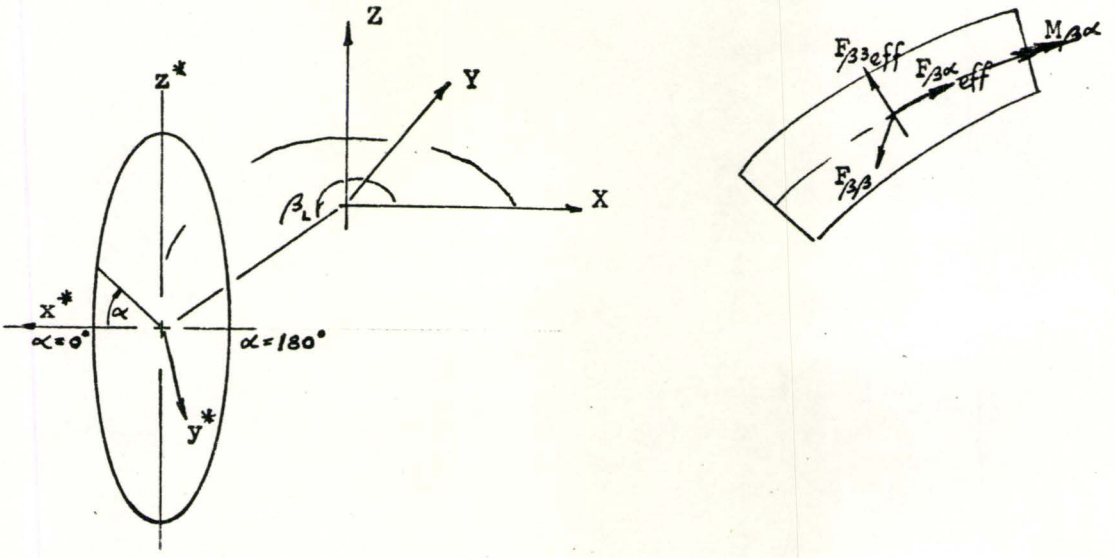

Figure A.11 - Local Coordinate System of Rigid End Plug

Its associated unit base vectors $\bar{e}_{x*}$, $\bar{e}_{y*}$ and $\bar{e}_{z*}$ can be easily determined from Figure A.11 by placing the RIBAUCOUR triad ($\bar{e}_{\beta}$, $\bar{e}_b^{\beta}$, $\bar{e}_n$) at, for example, $\alpha = 0$ and $\beta = \beta_L$ and observing the following correspondence:

$$\bar{e}_{x*} = \bar{e}_n \Big|_{\alpha = 0,\ \beta = \beta_L} = \cos\beta_L\, \bar{e}_X + \sin\beta_L\, \bar{e}_Y$$

$$\bar{e}_{y*} = \bar{e}_{\beta} \Big|_{\alpha = 0,\ \beta = \beta_L} = -\sin\beta_L\, \bar{e}_X + \cos\beta_L\, \bar{e}_Y \qquad \text{(A.64)}$$

$$\bar{e}_{z*} = \bar{e}_{\alpha} \Big|_{\alpha = 0,\ \beta = \beta_L} = \bar{e}_Z$$

With reference to Figure A.11, the six equilibrium conditions imposed on the rigid end plug are:

1. Σ forces (x*) = 0
2. Σ forces (y*) = 0
3. Σ forces (z*) = 0
4. Σ moments (x*) = 0
5. Σ moments (y*) = 0
6. Σ moments (z*) = 0

Because of the symmetry of the shell solution (Reference 6) automatic satisfaction of three of the six relations is obtained. Thus the three remaining relations to determine the constants U_o, V_o and ϕ_z^o of the rigid end plug are:

$$\begin{aligned} &\Sigma \text{ forces } (x^*) = 0 \\ &\Sigma \text{ forces } (y^*) = 0 \\ &\Sigma \text{ moments } (z^*) = 0 \end{aligned} \qquad \text{(A.65)}$$

From Figure A.11 it can be observed that in order to satisfy the first condition of (A.65), $F_{\beta\alpha eff}$ and $F_{\beta 3 eff}$ must be resolved in the direction of x^* and integrated along the contour ds_α : i.e.

$$2 \int_0^{\pi} F_{x^*} \, ds_\alpha = 0 \qquad @ \beta = \beta_L$$

where

$$F_{x^*} = -F_{\beta\alpha eff} \, \bar{e}_\alpha \cdot \bar{e}_{x^*} + F_{\beta 3 eff} \, \bar{e}_n \cdot \bar{e}_{x^*}$$

Since $ds_\alpha = |\bar{g}_\alpha| d\alpha$,

$$\int_0^\pi |\bar{g}_\alpha| (-F_{\beta\alpha\,eff} (\bar{e}_\alpha \cdot \bar{e}_{x^*}) + F_{\beta 3\,eff} (\bar{e}_n \cdot \bar{e}_{x^*})) d\alpha = 0 \qquad \text{(A.66)}$$

$$@\ \beta = \beta_L$$

The second relation is merely,

$$(\text{Area of Ellipse}) \cdot p - 2 \int_0^\pi F_{\beta\beta}\ ds_\alpha = 0$$

$$@\ \beta_L$$

or

$$(\text{Area of Ellipse}) \cdot p - 2 \int_0^\pi |\bar{g}_\alpha| F_{\beta\beta}\ d\alpha = 0 \qquad \text{(A.67)}$$

$$@\ \beta_L$$

The third relation consists of the moment resultant $M_{\beta\alpha}$ and that due to $F_{\beta\beta}$ about the z^* axis. Then,

$$\int_0^\pi M_{z^*}\, ds_\alpha = 0$$

$$@\ \beta_L$$

where

$$M_{z^*} = M_{\beta\alpha} (\bar{e}_\alpha \cdot \bar{e}_{z^*}) + F_{\beta\beta} (\bar{a} \cos\alpha)$$

or

$$\int_0^\pi |\bar{g}_\alpha| (M_{\beta\alpha} (\bar{e}_\alpha \cdot \bar{e}_{z^*}) + F_{\beta\beta}\, \bar{a} \cos\alpha) d\alpha \qquad \text{(A.68)}$$

$$@\ \beta = \beta_L$$

Observe that the following "dot" products of base vectors give:

$$(\bar{e}_\alpha \cdot \bar{e}_{x^*}) = -\bar{a} \sin\alpha \,/\!/\bar{g}_\alpha/$$

$$(\bar{e}_\alpha \cdot \bar{e}_{z^*}) = \bar{b} \cos\alpha \,/\!/\bar{g}_\alpha/ \qquad \text{(A.69)}$$

$$(\bar{e}_n \cdot \bar{e}_{x^*}) = \bar{b} \cos\alpha \,/\!/\bar{g}_\alpha/$$

Thus, equations (A.59), (A.63) and the additional relations (A.66), (A.67), (A.68) for the determination of U_o, V_o, ϕ_z^o constitute the boundary conditions at the junction of two shells - the BOURDON shell at $\beta = \beta_L$ and the rigid end plug.

(d) Alternatively a simplified approach to the edge conditions at $\beta = \beta_L$ may be :

(i) $\oint F_{\beta\beta}\, ds_\alpha = pdA$

approximating ds_α = perimeter of the ellipse

dA_n = area of the plug acted upon by the fluid pressure p

(ii) $\phi_{22} = (\bar{g}_{\alpha\alpha})^{-1/2} v_{,\alpha} + k_\alpha^{(n)} w = 0$

(iii) $\delta k_{\alpha\alpha} = -(\bar{g}_{\alpha\alpha})^{-1} w_{,\alpha\alpha} + (\bar{a}^2 - \bar{b}^2)\sin\alpha\cos\alpha/(g_{\alpha\alpha})^2 w_{,\alpha} = 0$

(iv) equation (A.68) with the approximation of ds_α as in (i) above.

Conditions (ii), (iii) and (iv) are reasoned upon a geometric and physical basis that the BOURDON shell is attached rigidly to an indeformable end-plug. Observe that the relations for u,

v, w and slope ϕ_{i3} are provided.

Thus with the above edge conditions, the system of three partial differential equations (A.51) or Table A.1 for the BOURDON tube with an elliptical cross-section is completely formulated.

APPENDIX B

TEST DATA

Table B.1 Test Data - KARDOS

Table B.2(a) Performance Data and Derived Constants - EXLINE

Table B.2(b) Physical and Dimensional Characteristics - EXLINE

Table B.3 Sensitivity and Life Data on BOURDON Tubes - MASON

Table B.1 Test data – KARDOS

TUBE NO.	MAT'L.	A INCHES	a INCHES	b INCHES	R_o INCHES	ϕ_o DEGREES	λ	μ_e	$4/p \times 10^6$ INCHES/PSI.	$\frac{\Delta RE}{RP}$	a/R_o
1001	N.S.C.	0.034	0.125	0.031	0.798	217°	1.74	0.248	9.89	70.5	.1566
1003	N.S.C.	0.034	0.127	0.0265	0.792	192°	1.67	0.208	12.1	86.4	.1604
1101	N.S.C.	0.032	0.125	0.0315	0.795	221°	1.63	0.252	11.9	83.5	.1572
1102	N.S.C.	0.032	0.128	0.025	0.790	224°	1.55	0.195	17.6	122.5	.1620
1103	N.S.C.	0.032	0.123	0.0355	0.801	217°	1.70	0.289	12.4	87.1	.1536
1201	N.S.C.	0.019	0.128	0.049	0.805	220°	0.934	0.383	49.2	342	.1590
1202	N.S.C.	0.019	0.131	0.0455	0.807	223°	0.894	0.339	57.5	379	.1623
1204	N.S.C.	0.019	0.137	0.0315	0.791	236°	0.800	0.230	91.5	602	.1732
1205	N.S.C.	0.019	0.139	0.0255	0.792	228°	0.778	0.184	109	743	.1755
1301	N.S.C.	0.021	0.114	0.030	0.793	236°	1.28	0.263	39.1	256	.1438
1302	N.S.C.	0.021	0.116	0.0255	0.786	217°	1.23	0.220	43.1	312	.1476
1401	N.S.C.	0.025	0.112	0.027	0.791	204°	1.58	0.241	18.8	159	.1416
1402	N.S.C.	0.025	0.110	0.032	0.797	216°	1.65	0.291	17.6	126	.1380
1501	N.S.C.	0.030	0.123	0.0355	0.799	223°	1.58	0.288	13.7	94.8	.1539
1502	N.S.C.	0.030	0.125	0.031	0.795	237°	1.53	0.248	16.9	110	.1572
1601	N.S.C.	0.008	0.137	0.044	0.797	229°	0.340	0.321	530	3570	.1719
1602	N.S.C.	0.008	0.144	0.0335	0.806	191°	0.312	0.233	652	5400	.1787
1701	N.S.C.	0.0145	0.137	0.037	0.798	238°	0.616	0.270	146	939	.1717
1702	N.S.C.	0.0145	0.139	0.0327	0.794	234°	0.595	0.235	184	1210	.1751
2001	N.S.C.	0.0115	0.140	0.0363	0.792	231°	0.465	0.259	274	1840	.1768
2002	N.S.C.	0.0115	0.138	0.0417	0.792	225°	0.478	0.302	212	1468	.1742
2101	N.S.C.	0.010	0.143	0.035	0.790	227°	0.386	0.245	483	3000	.1810
2102	N.S.C.	0.010	0.148	0.025	0.783	235°	0.358	0.169	736	4900	.1890
2103	N.S.C.	0.010	0.140	0.040	0.797	226°	0.407	0.288	423	2890	.1757
2105	N.S.C.	0.010	0.145	0.0305	0.810	218°	0.385	0.210	488	3415	.1790
2106	N.S.C.	0.010	0.152	0.019	0.791	236°	0.342	0.125	853	5610	.1922
2107	N.S.C.	0.010	0.136	0.0415	0.797	208°	0.431	0.327	265	1992	.1706
2202	N.S.C.	0.0135	0.156	0.0135	0.782	241°	0.193	0.0865	3230	21100	.1995
2401	N.S.C.	0.009	0.195	0.0195	0.806	239°	0.191	0.100	1900	12100	.2419
2402	N.S.C.	0.009	0.197	0.0145	0.806	231°	0.1872	0.0736	2160	14300	.2444
2801	T.B.	0.022	0.132	0.026	0.831	224°	1.05	0.197	84	309	.1588
2802	T.B.	0.022	0.132	0.031	0.834	226°	1.05	0.235	70.6	256	.1583
3001	T.B.	0.015	0.135	0.0275	0.807	226°	0.664	0.204	243	911	.1673
3002	T.B.	0.015	0.137	0.0230	0.822	228°	0.657	0.168	305	1112	.1667
3101	T.B.	0.018	0.139	0.0195	0.825	222°	0.769	0.140	212	793	.1685
3102	T.B.	0.018	0.137	0.0285	0.822	223°	0.789	0.208	132	493	.1667
3201	T.B.	0.010	0.142	0.0265	0.840	226°	0.417	0.187	882	3175	.1690
3202	T.B.	0.010	0.136	0.035	0.832	199°	0.450	0.257	606	2560	.1635
3203	T.B.	0.010	0.146	0.0155	0.834	211°	0.391	0.106	1250	4890	.1751
3204	T.B.	0.010	0.148	0.0105	0.847	224°	0.387	0.071	1700	6130	.1747
3301	T.B.	0.0125	0.141	0.021	0.818	205°	0.515	0.0887	583	2500	.1724
3302	T.B.	0.0125	0.138	0.026	0.825	224°	0.542	0.188	496	1838	.1673
3401	T.B.	0.0235	0.264	0.0337	0.849	231°	0.286	0.128	378	1320	.3110
3402	T.B.	0.0235	0.266	0.0282	0.844	195°	0.280	0.106	400	1709	.3152
3501	T.B.	0.0135	0.352	0.033	0.850	211°	0.0927	0.0938	1930	7420	.4141
3502	T.B.	0.0135	0.353	0.028	0.855	236°	0.0927	0.0794	2300	7780	.4129
3601	T.B.	0.0105	0.351	0.041	0.863	215°	0.0704	0.117	2520	9320	.4067
3602	T.B.	0.0105	0.354	0.0307	0.875	266°	0.0796	0.0668	3000	8960	.4046
3604	T.B.	0.0105	0.360	0.017	0.867	186°	0.0702	0.0472	3980	17650	.4152
3702	T.B.	0.0285	0.363	0.0637	0.827	210°	0.179	0.176	2560	1020	.4389
3801	T.B.	0.0225	0.342	0.0427	0.831	223°	0.1601	0.125	557	2060	.4116
3802	T.B.	0.0225	0.346	0.0327	0.834	226°	0.157	0.0945	643	2330	.4149
3803	T.B.	0.0225	0.350	0.0217	0.823	224°	0.151	0.062	732	2718	.4253
3804	T.B.	0.0225	0.336	0.054	0.828	233°	0.166	0.161	470	1671	.4058
3901	T.B.	0.019	0.336	0.053	0.826	223°	0.139	0.158	554	2060	.4068
3902	T.B.	0.019	0.344	0.0355	0.819	246°	0.132	0.103	821	2790	.4200
3903	T.B.	0.019	0.347	0.0265	0.825	226°	0.130	0.0764	850	3115	.4206
3904	T.B.	0.019	0.351	0.0165	0.825	216°	0.128	0.047	1010	3880	.4255
3905	T.B.	0.019	0.341	0.0415	0.824	243°	0.135	0.122	726	2465	.4138
3906	T.B.	0.019	0.346	0.0305	0.727	232°	0.116	0.0882	667	2710	.4759
4001	T.B.	0.026	0.436	0.029	0.825	231°	0.113	0.0665	640	2295	.5285
4002	T.B.	0.026	0.434	0.0345	0.822	220°	0.114	0.0795	587	225	.5280
4201	T.B.	0.045	0.439	0.048	0.814	219°	0.190	0.109	152	584	.5393
4301	Be Cu	0.026	0.122	0.047	0.817	245°	1.44	0.387	237	102.5	.1493
4302	Be Cu	0.026	0.124	0.043	0.816	241°	1.391	0.348	27.7	122	.1520
4303	Be Cu	0.026	0.126	0.037	0.807	243°	1.31	0.293	32.8	144	.1561
4304	Be Cu	0.026	0.128	0.032	0.806	246°	1.28	0.250	35.4	155	.1588
4305	Be Cu	0.026	0.129	0.0295	0.806	238°	1.26	0.229	42.8	192	.1600
4306	Be Cu	0.026	0.133	0.0225	0.807	246°	1.19	0.170	51.6	225.5	.1648
4307	Be Cu	0.026	0.119	0.0505	0.816	244°	1.49	0.423	21.3	92.5	.1458

TABLE B.2(a) PERFORMANCE DATA AND DERIVED CONSTANTS - EXLINE

Tube	Ro in.	ΔR in.	ΔR/Ro in.	φo rad.	-Δφ rad.	b/a	Roh/a²	ΔR/Ro E/P	bh³/a⁴ E/P	ΔR/Ro a/Ro
1	1.646	.034	.020	2.564	.050	.274	.453	.296	1390	.2033
2	1.625	.031	.019	2.517	.048	.223	.528	.308	1062	.2071
3	1.621	.041	.025	2.637	.065	.202	.442	.285	1738	.2110
4	1.619	.029	.018	2.373	.042	.229	.362	.265	2565	.2122
5	1.630	.035	.021	2.012	.042	.149	.185	.119	5990	.2755
6	1.684	.097	.057	1.815	.097	.132	.053	.027	40600	.3270
7	1.616	.063	.039	1.819	.066	.174	.140	.092	9260	.2752
8	1.636	.029	.018	2.719	.049	.255	.626	.308	633	.1977
9	1.648	.022	.013	2.676	.034	.271	.747	.374	458	.1935
10	1.621	.019	.012	2.709	.032	.255	.811	.341	343	.1947
11	2.513	.053	.021	3.256	.067	.282	.266	.149	6510	.1626
12	2.538	.048	.019	3.197	.060	.324	.425	.241	2190	.1626
13	2.547	.062	.024	3.169	.076	.310	.376	.217	3100	.1619
14	2.532	.052	.021	3.113	.063	.302	.332	.196	4070	.1632
15	2.523	.044	.017	3.145	.054	.324	.554	.276	1100	.1660
16	2.563	.056	.022	3.192	.067	.319	.450	.265	2130	.1624
17	2.540	.045	.018	3.154	.055	.312	.521	.282	1400	.1655
18	2.545	.045	.018	3.173	.055	.325	.478	.274	1740	.1639
19	2.539	.064	.025	3.146	.083	.308	.241	.171	9690	.1594
20	2.543	.078	.031	3.145	.096	.310	.282	.179	6160	.1605
21	2.445	.028	.012	2.993	.036	.421	1.098	.423	420	.1215
22	2.484	.010	.004	3.097	.012	.409	1.788	.407	112	.1161
23	2.492	.017	.004	3.137	.021	.381	1.475	.408	196	.1193
24	2.456	.024	.010	2.966	.028	.318	.553	.337	1400	.1651
25	2.465	.026	.010	2.951	.031	.308	.355	.225	3500	.1665
26	2.510	.045	.018	2.971	.050	.271	.439	.248	2330	.1672
27	2.515	.024	.010	3.232	.032	.300	.644	.303	775	.1691
28	2.485	.023	.009	3.041	.027	.300	1.275	.334	174	.1462
29	2.498	.022	.009	3.074	.026	.273	.355	.192	3490	.1653
30	2.514	.023	.009	3.084	.027	.254	.844	.285	349	.1747
31	1.552	.076	.049	2.942	.137	.126	.165	.092	11600	.2497
32	1.540	.074	.048	2.910	.133	.123	.165	.103	11400	.2519
33	1.035	.070	.068	3.129	.198	.068	.120	.065	9690	.3815
34	1.047	.074	.071	2.955	.194	.076	.117	.065	10100	.3771
35	1.495	.035	.023	3.189	.073	.202	.460	.244	2730	.1656
36	1.511	.039	.026	3.057	.077	.198	.464	.271	3090	.1641
37	1.098	.044	.040	2.636	.100	.117	.331	.189	3560	.2320
38	1.067	.041	.038	2.592	.094	.114	.327	.181	3380	.2386
39	1.000	.043	.043	2.553	.108	.127	.224	.190	4190	.3167
40	1.000	.034	.034			.129	.221	.143	3320	.
41	1.571	.034	.022	3.128	.059	.251	.663	.285	784	.1918
42	1.583	.031	.019	3.475	.066	.194	.681	.279	677	.1902
43	1.617	.029	.018	3.444	.061	.156	.632	.288	542	.1844
44	1.623	.030	.018	3.405	.062	.159	.633	.292	551	.1840
45	1.620	.030	.018	3.368	.060	.159	.632	.290	548	.1843
46	1.620	.030	.018	3.374	.060	.159	.630	.284	540	.1843
47	1.624	.030	.018	3.288	.059	.163	.633	.295	557	.1839
48	1.625	.030	.018	3.346	.061	.160	.637	.296	551	.1837
49	1.611	.030	.019	3.384	.060	.167	.627	.292	556	.1854
50	1.618	.029	.018	3.339	.059	.160	.634	.293	546	.1845

TABLE B.2(b) PHYSICAL AND DIMENSIONAL CHARACTERISTICS - EXLINE

Tube No.	Material	Max. P psi	E $\times 10^6$	a	b	h
1	Steel	410	28.5	.3346	.0916	.0308
2	Steel	510	28.5	.3366	.0751	.0368
3	"	410	28.5	.3420	.0690	.0319
4	"	200	28.5	.3436	.0788	.0264
5	"	100	28.5	.4491	.0670	.0229
6	"	40	28.5	.5507	.0727	.0095
7	"	120	28.5	.4448	.0775	.0171
8	"	810	28.5	.3234	.0826	.0400
9	"	810	28.5	.3189	.0864	.0461
10	"	1000	28.5	.3156	.0806	.0498
11	Bronze	50	15.5	.4086	.1151	.0177
12	"	130	15.5	.4127	.1337	.0285
13	"	120	15.5	.4124	.1279	.0251
14	"	80	15.5	.4133	.1248	.0224
15	"	240	15.5	.4187	.1357	.0385
16	"	160	15.5	.4163	.1328	.0304
17	"	200	15.5	.4203	.1313	.0363
18	"	160	15.5	.4171	.1356	.0327
19	"	40	15.5	.4047	.1247	.0156
20	"	80	15.5	.4082	.1267	.0186
21	316 SS	800	28	.2971	.1251	.0397
22	"	1000	28	.2885	.1180	.0599
23	"	1000	28	.2973	.1133	.0523
24	"	200	28	.4055	.1290	.0370
25	"	80	28	.4103	.1263	.0243
26	"	120	15.5	.4196	.1136	.0308
27	"	200	15.5	.4253	.1278	.0464
28	"	800	15.5	.3633	.1093	.0673
29	"	40	15.5	.4129	.1129	.0242
30	"	400	15.5	.4391	.1116	.0648
31	Steel	120	28.5	.3875	.0490	.0159
32	"	120	28.5	.3879	.0479	.0162
33	"	200	28.5	.3949	.0269	.0182
34	"	200	28.5	.3948	.0298	.0174
35	"	240	28.5	.2475	.0500	.0189
36	"	240	28.5	.2480	.0490	.0189
37	"	320	28.5	.2547	.0297	.0196
38	"	320	28.5	.2546	.0291	.0198
39	BeCo	200	19.5	.3167	.0402	.0225
40	"	200	19.5	.3169	.0409	.0222
41	Steel	800	28.5	.3013	.0528	.0384
42	"	800	28.5	.3011	.0576	.0387
43	Bronze	520	15.5	.2981	.1001	.0347
44	"	520	15.5	.2986	.1001	.0348
45	"	520	15.5	.2986	.1001	.0348
46	"	520	15.5	.2986	.1001	.0347
47	"	520	15.5	.2986	.1001	.0348
48	"	520	15.5	.2985	.1000	.0349
49	"	520	15.5	.2986	.1001	.0347
50	"	520	15.5	.2985	.1000	.0349

Table B.3 Sensitivity and Life Data on BOURDON Tubes - MASON

1. Specimen number, e.g., 160 S 002: The first figure is the manufacturer's pressure rating p in psi, the letter is the coil type (C = cee, S = flat spiral, H = helical) and the last figure is a serial number, assigned by the subcommittee.

2. Stock description: Wall thickness h in mils followed by an abbreviation for the material: BC = beryllium copper, Bz = bronze, CM = chrome-molybdenum steel, CRS = corrosion-resistant steel, CS = carbon steel, PB = phosphor bronze, S = steel, TM = trumpet metal.

3. Coil description: Radius R_o in inches, angle ϕ_o in degrees; no allowance has been made for end fittings.

4. Cross-section description, Fig. 2: Major semiaxis a at mid-wall, mils; minor semiaxis b at mid-wall, mils; approximate shape E = elliptical, F = flat oval, D = dee.

5. Pressure sensitivity $k_1 = (-\Delta\phi/\phi)(E/p)$, dimensionless; modulus E, unless otherwise noted, is taken from Giacobbe and Bounds (6); angle changes computed from travel as Δx, Δy, or $\sqrt{\Delta x^2 + \Delta y^2}$ are noted.

6. Life, 10^{-3} N cycles; from 0 to rated pressure p unless otherwise noted, and to fracture, unless otherwise noted.

7. Pulsation stress (maximum fiber stress) developed on life test, 10^{-3} S psi.

8. Parameters Rh/a^2, b/a, $a^2/10^2h^2$, $10^6bh^3/a^4$, all dimensionless; useful for comparison with various theories (5).

ASME Research Committee on Mechanical Pressure Elements

Data Form No. 1: Pressure-responsive Bourdon Tube

H.L.M.—Revised May 24, 1954

(1) Type: Helix or (flat) spiral . or cee

(2) Material: alloy ; composition %
Young's modulus E = psi; Poisson's ratio ν =

(3) Stock before coiling: temper ; hardness
nominal grain size mm; supplied by

(4) Heat and stress treatment after coiling:

(5) Fittings soldered or brazed or welded

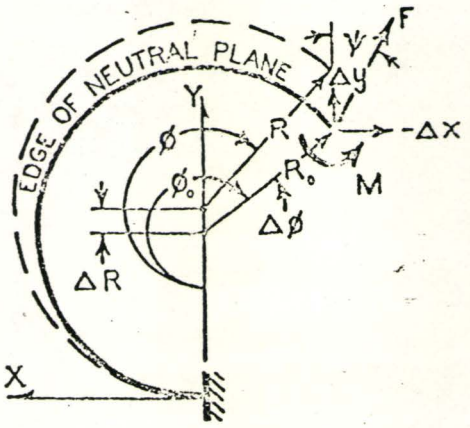

Fig. 1 Coil Geometry

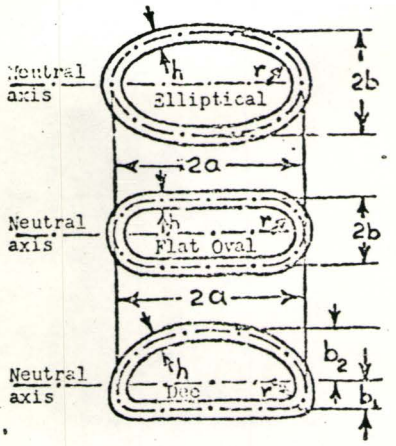

Fig. 2 Cross Sections

(6) Cross-section: elliptical or flat oval or dee Dimensions after coiling, h = a = b = b_1 = b_2 = r =
Sketch deviations if any from sections shown above.

(7) Radius and total angular length of innermost coil, R_{01} = in., ϕ_{01} = deg; ratio of effective (unstiffened) length of n coils to their total length = ;
for spirals supply also R_{02}, ϕ_{02}, ... R_{0n}, ϕ_{0n}

(8) Max. useful pressure diff'c p = psi; set of %, fatigue life of cycles, and nonlinearity (0 to 100% range) of % appear at temperature of deg F and this pressure difference.

(9) Pressure sensitivity, per psi: in radius, $\Delta R/R_0 p$ = psi^{-1}, or in angle $-\Delta\phi/\phi_0 p$ = psi^{-1}, or in deflection $\sqrt{\Delta x^2 + \Delta y^2}/R_0 p$ = psi^{-1}; specify tip constraint, if any.

(10) Spring compliance, lb-in^{-1}, under pure moment M or lb^{-1} under pure force F; angle ψ = deg, at pressure p = psi: in radius $\Delta R/R_0 M$ = or $\Delta R/R_0 F$ = or in angle $\Delta\phi/\phi_0 M$ = or $\Delta\phi/\phi_0 F$ = , or in deflection $\sqrt{\Delta x^2 + \Delta y^2}/R_0 M$ = or $\sqrt{\Delta x^2 + \Delta y^2}/R_0 F$ = ; specify tip constraint, if any.

(11) Remarks

TABLE GEOMETRY, PRESSURE SENSITIVITY, LIFE

Specimen		Stock		Coil		Section		Press. Sens.	Puls. Stress	Life	Parameters			
p	#	h	Mtl.	R_o	ϕ_o	a	b	$-\frac{\Delta\phi}{\phi}\frac{E}{p}$	$10^{-3}S$	$10^{-3}N$	$\frac{Rh}{a^2}$	$\frac{b}{a}$	$\frac{a^2}{10^2h^2}$	$\frac{10^6bh^3}{a^4}$
100	C 001	25	PB	2.55	255	825 x250	E	2620	3		.09	.30	10.9	8.4

Serial 001 is phosphor bronze of 95 Cu, 5 Sn, 0.2 P; $(\Delta R/R)(E/p) = 2760$. Stock from Mackenzie Walton, half hard, Rockwell B-78, avg. grain size 0.886 mm. Heat treated after coiling, 500F for 1 hr, to Rockwell B-97. Soldered fittings. Section E or F, effective ϕ_o=248. Set < 0.05% at 70F.

160	S 002	18	BC	See		200 x 25	F	1485		1000[a]	.35	.12	1.23	91
230	S 003	20	BC	note		200 x 27	F	1030		"	.39	.14	1.00	135
300	S 004	22	BC	below		200 x 29	F	790		"	.43	.14	.82	193
370	S 005	24	BC			200 x 31	F	640		"	.46	.16	.69	268
510	S 006	28	BC			200 x 35	F	465		"	.54	.18	.51	480

Serials 2 to 6 are beryllium copper of 1.0-2.15 Be, 0.35 Co, bal. Cu; E=19x10^6, ν =0.3; 4.5 turn spirals of 1600°, with uniformly spaced radii, innermost 0.5" to outermost 1.0", fixed at outer end, 20° rotation at inner end, mean radius R_o taken as 0.77". Stock is solution annealed to Rockwell 30T46-60 before coiling; heattreated at 650 ± 5 F for 60 ± 5 min. after coiling. Fittings silver soldered.
Note a: For 1% set; 0% nonlinearity; 80°F.

90	H 007	11.5*TB	0.95*	1440	386*x 33*	F	2660	39	200[b]	.07	.09	1.12	2.3
120	H 008	12.5*TB	0.95*	1440	387*x 34*	F	2000	45	"	.08	.09	.96	3.0
270	H 009	18* TB	0.96*	1440	393*x 43*	F	886	52	"	.11	.11	.48	10.5
275	H 010	21* TB	1.57*	1440	383*x 63*	F	871	40	"	.22	.16	.33	27.1
500	H 011	16* TB	1.05*	3240	244*x126*	F	210	27	"	.24	.52	.23	146
200	H 012	21* TB	0.97*	810	635*x 42*	F	2100	68	"	.05	.07	.91	2.4

Serials 7 to 12 are trumpet brass of 81-82 Cu, 0.75-1.5 Sn, 0.05 max P, 0.05 max Fe, bal Zn, E=15x10^6, ν =0.33. Tip is constrained to radius R_o. Stock from American Brass Co. and Mackenzie Walton, cold drawn, hardness under .020" 15T-82 to 89, 30T-62 to 72, grain size .010-.030 mm. Heat treated at 480 F for 1 hr, furnace cooled with nitrogen. Fittings soldered. Nonlinearity 1/2% on #11, 1% on #7 to 10, 1 1/2% on #12.
Note b: For set of 1/2%, room temp.

30	C 019	10* TB	0.97	233	273 x 87	E	10700	-	-	.13	.32	7.4	15.8
30	C 020	10.5*TB	1.19	235	275 x 84	E	9800	-	-	.16	.31	6.9	18.3
30	C 021	12* PB	1.62	228	407 x108	F	8500	-	-	.12	.27	11.4	9.5
30	C 022	15* PB	2.06	241	407 x120	F	7200	-	-	.19	.29	7.4	14.7

#19,20 are trumpet brass; Cu 81, Sn 1, Zn 18; E=15x10^6 psi, G=6x10^6 psi, ν =0.25.
#21,22 are phosphor bronze, grade A; Cu 95.5, Sn 4.5; E=16x10^6 psi, G=6.25x10^6 psi, ν =0.28.
#19,21,22 have brazed fittings, #20 has soldered fittings. Not pulsed. $\Delta\phi/\phi$ based on chordal travel; data averaged from two independent testing laboratories.

60	C 023	14* TB	0.97	233	275 x 88	E	5000	-	-	.18	.32	3.8	42.2
60	C 024	14.5*TB	1.17	237	276 x 87	E	5000	-	-	.22	.32	3.6	45.7
60	C 025	17* PB	1.62	228	408 x119	F	4000	-	-	.17	.29	5.7	21.2
60	C 026	21* PB	2.06	241	409 x125	F	3800	-	-	.26	.31	3.8	41.4

#23,24 are trumpet brass; Cu 81, Sn 1, Zn 18; E=15x10^6 psi, G=6x10^6 psi, ν =0.25. #25,26 are phosphor bronze, grade A; Cu 95.5, Sn 4.5; E=16x10^6 psi, G=6.25x10^6 psi, ν =0.28.
#23,25,26 have brazed fittings, #24 has soldered fittings. Not pulsed. $\Delta\phi/\phi$ based on chord; data averaged from two independent testing laboratories.

TABLE (*continued*)

Specimen		Stock		Coil		Section	Press. Sens.	Puls. Stress	Life	Parameters			
p	#	h	Mtl.	R_o	ϕ_o	a b	$\frac{-\Delta\phi}{\phi}\frac{E}{p}$	$10^{-3}S$	$10^{-3}N$	$\frac{Rh}{a^2}$	$\frac{b}{a}$	$\frac{a^2}{10^2h^2}$	$\frac{10^6bh^3}{a^4}$
100	C 027	18*	TB	0.97	233	276 x 84 E	3000	-	-	.23	.30	2.3	84.5
100	C 028	18*	TB	1.17	237	274 x 93 E	3000	-	-	.28	.34	2.3	96.6
100	C 029	21*	PB	1.62	228	412 x123 F	2400	-	-	.20	.30	3.8	39.3
100	C 030	26*	PB	2.06	241	413 x127 F	2300	-	-	.31	.31	2.5	76.6
#27,28 are trumpet brass; Cu 81, Sn 1, Zn 18; E=15x10^6 psi, G=6x10^6 psi, ν=0.25. #29,30 are phosphor bronze, grade A; Cu 95.5, Sn 4.5; E=16x10^6 psi, G=6.25x10^6 psi, ν=0.28. #27, 29,30 have brazed fittings, #28 has soldered fittings. $\Delta\phi/\phi$ based on chord; data averaged from two independent testing laboratories.													
200	C 031	21*	TB	1.00	232	254 x 48 D	1410			.32	.19	1.5	105
200	C 032	23*	PB	1.18	234	255 x 48 D	1390			.42	.19	1.2	136
200	C 033	30*	PB	1.62	221	412 x129 D	1400			.29	.31	1.9	122
200	C 034	35*	PB	2.05	242	416 x123 D	1240			.42	.30	1.4	176
600	C 035	34*	TB	1.00	230	264 x 53 D	506			.49	.20	.6	431
600	C 036	36*	PB	1.19	234	262 x 56 D	430			.62	.21	.5	550
600	C 037	43*	PB	1.60	226	340 x 82 D	512			.60	.24	.6	588
600	C 038	48*	PB	2.00	244	344 x 85 D	408			.82	.25	.5	678
1000	C 039	41*	TB	1.02	230	264 x 56 D	270			.60	.21	.4	796
1000	C 040	42*	PB	1.20	235	266 x 54 D	304			.71	.20	.4	764
1000	C 041	54*	PB	1.62	226	352 x 88 D	277			.70	.25	.4	912
1000	C 042	58*	PB	2.02	244	350 x 87 D	246			.96	.25	.4	1150
Serials 31 to 42 made from elliptical tubing, flattened to D-shape in coiling; neutral axis assumed central. Data are averaged from two independent testing laboratories; $\Delta\phi/\phi$ based on chord. Rated pressure applied just before deflection test, #31-42. Serials 31,33-42 are silver soldered or brazed; #32 is soft soldered. Serials 31, 35, 39 are trumpet brass; Cu 81, Sn 1, Zn 18; E=15x10^6 psi, G=6x10^6 psi, ν=0.25. Serials 32-34, 36-38, 40-42 are phosphor bronze grade A; Cu 95.5, Sn 4.5; E=16x10^6 psi, G=6.25x10^6 psi, ν=0.28.													

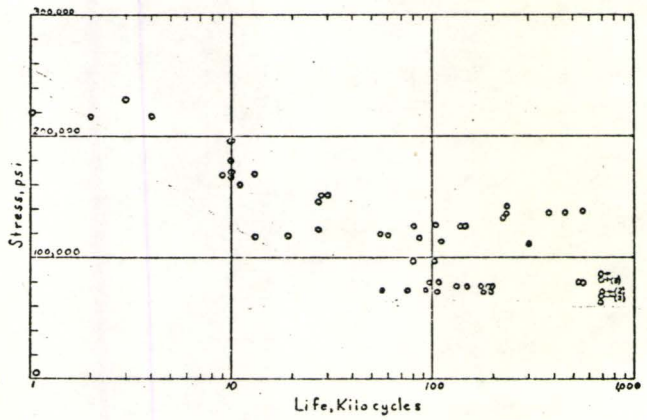

FIG. 4 FATIGUE OF STEEL BOURDON TUBES

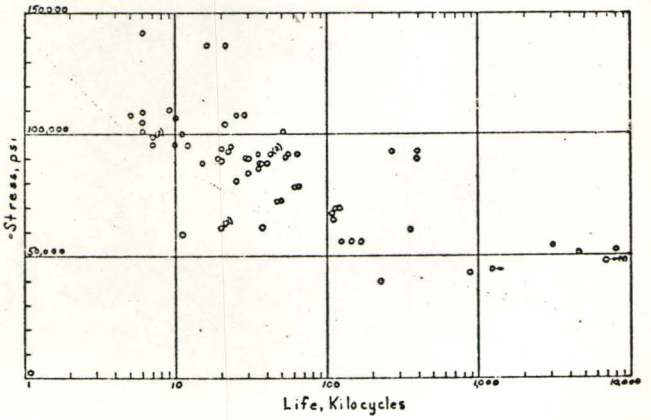

FIG. 5 FATIGUE OF PHOSPHOR-BRONZE BOURDON TUBES

TABLE (*continued*)

Specimen p # NT	Stock h	Mtl.	Coil R_o	ϕ_o	Section a x b	Press. Sens. $\frac{-\Delta\phi}{\phi}\frac{E}{p}$	Puls. Stress $10^{-3}S$	Life $10^{-3}N$	Parameters $\frac{Rh}{a^2}$	$\frac{b}{a}$	$\frac{a^2}{10^2h^2}$	$\frac{10^6bh^3}{a^4}$
500 C 043	14	BC	0.71	245	134 x 42 F	930	-	-	.56	.33	..96	356
400 C 044	14	BC	0.71	238	140 x 31 F	1310	-	-	.51	.22	1.00	221
200 C 045	14	BC	0.72	250	146 x 18 F	2100	-	-	.48	.12	1.08	108
2000 C 046	22	BC	0.72	245	130 x 36 F	230	-	-	.93	.28	.35	1340
1400 C 047	22	BC	0.71	250	135 x 23 F	360	-	-	.85	.17	.38	738
800 C 048	22	BC	0.75	248	141 x F	560	-	-	.83	.08	.41	
5000 C 049	32	BC	0.73	248	127 x F	91	-	-	1.44	.17	.16	
5000 C 050	32	BC	0.72	250	120 x 35 F	57	-	-	1.59	.29	.14	5500
5000 C 051	32	BC	0.74	250	115 x 46 F	39	-	-	1.78	.40	.13	8500
4000 C 052	30	BC	0.80	300	124 x F	97	-	-	1.56	.24	.17	
4000 C 053	30	BC	0.82	300	117 x 48 F	53	-	-	1.80	.41	.15	6840
#43 to 53 are beryllium copper; assume E=19.5x10^6 psi.												
50 C 054	20	CM	2.25*	300*	648 x123 E	12300	80	535	.11	.19	10	5.59
" C 055	-	CM	"	"	648 x126 E	13400	-	167	-	.19	-	
" C 056	20	CM	"	"	658 x150 E	6500	112	301[f]	.10	.23	11	6.35
" C 057	18	CM	"	"	670 x156 E	9600	136	233[f]	.09	.23	14	4.51
" C 058	18	CM	"	"	661 x152 E	9900	-	-	.09	.23	14	4.61
" C 059	18	CM	"	"	660 x154 E	10400	133	225[f]	.09	.23	13	4.74
" C 060	14	CM	"	"	363 x119 E	14000	79	551[f]	.24	.33	7	18.7
" C 061	12.5	CM	"	"	420 x100 E	17100	87	684	.16	.24	11	6.26
" C 062	13	CM	"	"	418 x102 E	17100	82	684	.17	.24	10	7.35
" C 063	13	CM	"	"	419 x101 E	16600	82	684	.17	.24	10	7.21
" C 064	-	CM	"	"	418 x100 E	17300	-	684	-	.24	-	
" C 065	13	CM	"	"	418 x100 E	17600	82	684	.17	.24	10	7.20
" C 066	20	CM	"	"	642 x126 E	14900	76	131	.11	.20	10	5.92
" C 067	20	CM	"	"	642 x124 E	15300	76	148	.11	.19	10	5.84
" C 068	20	CM	"	"	642 x128 E	15700	76	196	.11	.20	10	6.03
" C 069	20	CM	"	"	642 x126 E	15100	-	-	.11	.20	10	5.92
" C 070	20	CM	"	"	642 x125 E	15100	76	190	.11	.19	10	5.89
" C 071	20	CM	"	"	640 x126 E	15500	76	175	.11	.20	10	5.95
#54 to 71 are chrome-molybdenum steel; assume E=28.5x10^6 psi. Life test on #61 to 65 stopped at 684,000 cycles. $\Delta\phi/\phi$ based on Δy. #54-56 nearly like #66-73.												
Note f: Pulsated at 50% overpressure.												
75 C 072	20	CM	2.25*	300*	644 x123 E	12600	117, 40[g]	86	.11	.19	10.4	5.73
" C 073	20	CM	"	"	645 x121 E	12200	117, 39[g]	86	.11	.19	10.4	5.61
" C 074	31	CM	"	"	642 x132 E	6290	40[g]	-	.17	.21	4.3	23.1
" C 075	31	CM	"	"	643 x133 E	6290	38[g]	-	.17	.21	4.3	23.2
#72 to 75 are chrome-molybdenum steel; assume E=28.5x10^6 psi; $\Delta\phi/\phi$ based on Δy.												
Note g: Using Stress-coat. #72-73 nearly like #54-56, #66-71.												

Serials 43 to 53: Stock by Superior Tube Co., R30T-65, grain size 0.035 mm. Heat treated after coiling at 550-600 F for 2 hours.

TABLE (continued)

Specimen		Stock		Coil		Section		Press. Sens.	Puls. Stress	Life	Parameters			
p	#	h	Mtl.	R_o	ϕ_o	a	b	$-\frac{\Delta\phi}{\phi}\frac{E}{p}$	$10^{-3}S$	$10^{-3}N$	$\frac{Rh}{a^2}$	$\frac{b}{a}$	$\frac{a^2}{10^2h^2}$	$\frac{10^6bh^3}{a^4}$
100	C 076	23	CM	2.25*	300*	682	x111 E	12800	142	235	.11	.16	8.8	6.23
"	C 077	24	CM	"	"	665	x131 E	8390	118, 41g	60	.12	.20	7.5	9.21
"	C 078	23	CM	"	"	661	x132 E	8700	127, 41g	144	.12	.20	8.3	8.34
"	C 079	23	CM	"	"	661	x131 E	8390	127	81	.12	.20	8.3	8.29
"	C 080	23	CM	"	"	661	x131 E	8960	127	103	.12	.20	8.3	8.29
"	C 081	23	CM	"	"	667	x141 E	7820	-	-	.12	.21	8.4	8.62
"	C 082	23	CM	"	"	661	x144 E	7690	-	-	.12	.22	8.3	9.12
"	C 083	23	CM	"	"	666	x144 E	7790	-	-	.12	.22	8.4	8.80
"	C 084	23	CM	"	"	665	x144 E	7820	-	-	.12	.22	8.3	8.94
"	C 085	20	CM	"	"	362	x114 E	4420	-	-	.34	.32	3.3	53.5
"	C 086	20	CM	"	"	363	x114 E	4400	-	-	.34	.31	3.3	53.8
"	C 087	22	CM	"	"	408	x103 E	5800	64	684	.30	.25	3.4	39.4
"	C 088	21	CM	"	"	406	x109 E	6190	68	684	.28	.27	3.8	37.2
"	C 089	21	CM	"	"	409	x102 E	5850	71	684	.28	.25	3.8	33.8
"	C 090	21	CM	"	"	406	x104 E	5900	69	684	.28	.26	3.8	35.6
"	C 091	21	CM	"	"	410	x101 E	6190	71	684	.28	.25	3.8	33.2
"	C 092	19	CM	"	"	408	x112 E	6290	-	-	.25	.27	4.6	28.0
"	C 093	19	CM	"	"	407	x113 E	6010	-	-	.25	.28	4.6	28.4
"	C 094	19	CM	"	"	407	x112 E	6140	-	-	.25	.27	4.6	28.0
"	C 095	19	CM	"	"	408	x113 E	6010	-	-	.25	.28	4.6	28.2
"	C 096	19	CM	"	"	409	x110 E	5940	-	-	.26	.27	4.6	26.8
"	C 097	19	CM	"	"	415	x101 E	6690	-	-	.25	.27		25.5
"	C 098	19	CM	"	"	414	x101 E	6690	-	-	.25	.24		23.6
"	C 099	19	CM	"	"	414	x101 E	7060	-	-	.25	.24		23.6
"	C 100	19	CM	"	"	411	x107 E	6430	-	-	.25	.26		25.2
"	C 101	19	CM	"	"	410	x107 E	6400	-	-	.25	.26		25.2
"	C 102	19	CM	"	"	410	x107 E	7000	-	-	.25	.26		25.2
#76 to 102 are X4130 steel; assume E=28.5x10^6 psi; $\Delta\phi/\phi$ based on Δy. Life test on #87 to 91 stopped at 684,000 cycles.														
100	C 103	31	CM	2.25*	300*	636	x126 E	6350	72	105	.17	.20	4.2	23
"	C 104	31	CM	"	"	635	x129 E	6010	72	196	.17	.20	4.2	24
"	C 105	31	CM	"	"	638	x126 E	6350	72	180	.17	.20	4.2	22
"	C 106	31	CM	"	"	638	x125 E	6350	-	-	.17	.20	4.2	22
"	C 107	31	CM	"	"	636	x125 E	6350	-	-	.17	.20	4.2	23
"	C 108	31	CM	"	"	636	x125 E	6350	-	-	.17	.20	4.2	23
"	C 109	31	CM	"	"	637	x121 E	6990	73	56	.17	.19	4.2	22
"	C 110	31	CM	"	"	638	x121 E	7190	73	75	.17	.19	4.2	22
"	C 111	31	CM	"	"	638	x119 E	7010	74	93	.17	.19	4.2	21
"	C 112	30	CM	"	"	640	x120 E	7010	79	107	.16	.19	4.6	19
"	C 113	30	CM	"	"	641	x120 E	6810	79	97	.16	.19	4.6	19
#103 to 113 are chrome-molybdenum steel; assume E=28.5x10^6 psi; $\Delta\phi/\phi$ based on Δy.														

TABLE (*continued*)

Specimen p	#	Stock h	Mtl.	Coil R_o	ϕ_o	Section a	b	Press. Sens. $\frac{-\Delta\phi}{\phi}\frac{E}{p}$	Puls. Stress $10^{-3}S$	Life $10^{-3}N$	Parameters $\frac{Rh}{a^2}$	$\frac{b}{a}$	$\frac{a^2}{10^2h^2}$	$\frac{10^6bh^3}{a^4}$
250	C 114	40	CM	2.25*	300*	642	x127 E	3980	120,37g	55	.22	.20	2.6	48
"	C 115	40	CM	"	"	640	x134 E	3720	118,35g	19	.22	.21	2.6	51
"	C 116	56	CM	"	"	676	x115 E	1480	-	-	.28	.17	1.5	94
"	C 117	56	CM	"	"	644	x130 E	1400	137	379	.30	.20	1.3	133
"	C 118	56	CM	"	"	642	x132 E	1430	138	556	.31	.21	1.3	136
"	C 119	56	CM	"	"	643	x131 E	1370	137	453	.30	.20	1.3	134
"	C 120	59	CM	"	"	641	x129 E	1430	126	138	.32	.20	1.2	155
"	C 121	27	CM	"	"	366	x 98 E	3250	98	101	.45	.27	1.8	107
"	C 122	27	CM	"	"	365	x 98 E	3020	-	-	.46	.27	1.8	107
"	C 123	27	CM	"	"	365	x 99 E	3020	98	80	.46	.27	1.8	108
#114 to 123 are chrome-molybdenum steel; assume E=28.5x10^6 psi; $\Delta\phi/\phi$ based on Δy.														
#117-120 pulsated at 500 psi.														
500	C 124	63	CM	2.25*	300*	632	x 90 E	1770	36g	7	.35	.14	1.0	142
"	C 125	61	CM	"	"	635	x 93 E	1850	117,37g	13	.34	.15	1.0	146
"	C 126	73	CM	"	"	631	x124 E	740	84	-	.41	.22	0.8	296
"	C 127	73	CM	"	"	631	x124 E	770	-	-	.41	.22	0.8	296
"	C 128	73	CM	"	"	631	x124 E	740	-	-	.41	.22	0.8	296
"	C 129	73	CM	"	"	631	x124 E	740	-	-	.41	.22	0.8	296
"	C 130	39	CM	"	"	362	x 91 E	1250	113	110	.67	.25	0.9	314
"	C 131	39	CM	"	"	362	x 91 E	1230	-	-	.67	.25	0.9	314
"	C 132	39	CM	"	"	362	x 91 E	1250	-	-	.67	.25	0.9	314
#124 to 132 are chrome-molybdenum steel; assume E=28.5x10^6 psi; $\Delta\phi/\phi$ based on Δy.														
1000	C 133	42,48	CM	2.25*	300*	354	x104 E	740	151	30	.81	.29	.62	600
"	C 134	42,49	CM	"	"	354	x103 E	770	146	27	.83	.29	.59	635
"	C 135	41,47	CM	"	"	355	x104 E	800	124	27	.79	.29	.51	547
"	C 136	40,49	CM	"	"	354	x104 E	800	151	28	.81	.29	.62	600
#133 to 136 are chrome-molybdenum steel; assume E=28.5x10^6 psi; $\Delta\phi/\phi$ based on Δy. Outer wall thinner than inner wall.														
1500	C 137	51	CM	2.25*	300*	348	x116 E	480	168	9	.95	.33	.47	1040
"	C 138	51	CM	"	"	349	x118 E	480	166	10	.94	.34	.47	1060
"	C 139	50	CM	"	"	347	x118 E	430	169	10	.93	.34	.48	1000
"	C 140	52	CM	"	"	347	x118 E	400	160	11	.97	.34	.45	1130
"	C 141	50	CM	"	"	348	x120 E	480	169	13	.93	.34	.48	1010
"	C 142	47	CM	"	"	345	x 86 E	510	221	1	.89	.25	.54	640
"	C 143	48	CM	"	"	345	x 84 E	510	216	2	.91	.24	.52	660
"	C 144	46	CM	"	"	345	x 87 E	510	231	3	.86	.25	.57	570
"	C 145	47	CM	"	"	340	x 83 E	480	216	4	.92	.24	.52	640
#137 to 145 are chrome-molybdenum steel; assume E=28.5x10^6 psi; $\Delta\phi/\phi$ based on Δy.														

TABLE *(continued)*

Specimen		Stock		Coil		Section		Press. Sens.	Puls. Stress	Life	Parameters			
p	#	h	Mtl.	R_o	ø	a	b	$\frac{-\Delta\phi}{\phi}\frac{E}{p}$	$10^{-3}S$	$10^{-3}N$	$\frac{Rh}{a^2}$	$\frac{b}{a}$	$\frac{a^2}{10^2h^2}$	$\frac{10^6bh^3}{a^4}$
25	C 146	18	PB	2.25*	300*	645	x108 E	14500	48	684	.097	.17	12.8	3.63
"	C 147	18	PB	"	"	645	x106 E	14600	48	684	.097	.16	12.8	3.56
"	C 148	18	PB	"	"	646	x108 E	14000	48	684	.097	.17	13.0	3.59
"	C 149	18	PB	"	"	647	x108 E	14300	48	684	.097	.17	13.0	3.59
"	C 150	18	PB	"	"	646	x105 E	13500	-	-	.097	.16	13.0	3.50
"	C 151	18	PB	"	"	645	x107 E	14300	-	-	.097	.17	12.8	3.60
#146 to 151 are phosphor bronze; assume E=15.5x10^6 psi; $\Delta\phi/\phi$ based on Δy. Life test stoped at 684,000 cycles.														
50	C 152	26	PB	2.25*	300*	659	x113 E	9100	54	3040	.14	.17	6.4	10.5
"	C 153	27	PB	"	"	658	x114 E	9100	51	4565	.14	.18	6.0	11.9
"	C 154	27	PB	"	"	643	x106 E	7500	-	-	.15	.16	6.2	12.2
"	C 155	27	PB	"	"	642	x107 E	7200	-	-	.15	.17	6.2	12.3
"	C 156	27	PB	"	"	658	x107 E	7200	52	799	.14	.16	6.0	11.2
"	C 157	32	PB	"	"	640	x103 E	7200	39	224	.18	.16	4.0	20.1
"	C 158	29	PB	"	"	642	x104 E	7700	44	1224	.16	.16	4.9	14.8
"	C 159	30	PB	"	"	642	x103 E	7200	43	870	.16	.16	4.6	16.3
#152 to 159 are phosphor bronze; assume E=15.5x10^6 psi; $\Delta\phi/\phi$ based on Δy. Life test on #158 stopped at 1,224,000 cycles.														
100	C 160	27	PB	2.25*	300*	648	x134 E	4400	93	265	.14	.21	5.8	15
"	C 161	28	PB	"	"	652	x135 E	5300	90	386	.15	.21	5.5	18
"	C 162	27	PB	"	"	652	x138 E	5300	93	391	.14	.21	5.9	17
"	C 163	37	PB	"	"	636	x 96 E	4500	61	352	.21	.15	3.0	30
"	C 164	38	PB	"	"	635	x 99 E	4200	56	169	.21	.16	2.8	33
"	C 165	38	PB	"	"	635	x102 E	4200	56	145	.21	.16	2.8	34
"	C 166	38	PB	"	"	635	x 99 E	4300	56	125	.21	.16	2.8	33
#160 to 166 are phosphor bronze; assume E=15.5x10^6 psi; $\Delta\phi/\phi$ based on Δy.														
250	C 167	60	PB	2.25*	300*	630	x 93 E	1800	-	-	.34	.15	1.1	127
"	C 168	59	PB	"	"	629	x 94 E	1500	69	113	.34	.15	1.1	125
"	C 169	61	PB	"	"	628	x 93 E	1500	65	110	.35	.15	1.1	135
"	C 170	59	PB	"	"	631	x 94 E	1500	70	119	.35	.15	1.1	121
"	C 171	62	PB	"	"	628	x 93 E	1500	62	37	.35	.15	1.0	145
"	C 172	60	PB	"	"	630	x 93 E	1500	68	107	.34	.15	1.1	127
#167 to 172 are phosphor bronze; assume E=15.5x10^6 psi; $\Delta\phi/\phi$ based on Δy.														
500	C 173	99	PB	2.25*	300*	616	x 85 E	820	59	11	.59	.14	.39	570
"	C 174	-	PB	"	"	-	x - E	850	-	-	-	-	-	-
"	C 175	-	PB	"	"	-	x - E	850	-	-	-	-	-	-
"	C 176	72	PB	"	"	629	x100 E	820	96	12	.41	.16	.76	420
"	C 177	73	PB	"	"	630	x101 E	-	93	22	.41	.16	.74	400
"	C 178	76	PB	"	"	624	x 85 E	800	92	42	.44	.14	.67	400
"	C 179	77	PB	"	"	623	x 85 E	800	92	55	.45	.14	.66	390
"	C 180	76	PB	"	"	624	x 86 E	800	92	63	.44	.14	.67	400
"	C 181	76	PB	"	"	624	x 86 E	790	92	43	.44	.14	.67	400
"	C 182	76	PB	"	"	624	x 86 E	790	91	53	.44	.14	.67	390
Phosphor bronze, E=15.5x10^{6}psi; $\Delta\phi/\phi$ based on Δy.														

TABLE *(continued)*

Specimen p	#	Stock h	Mtl.	Coil R_o	ϕ_o	Section a	b	Press. Sens. $-\frac{\Delta\phi}{\phi}\frac{E}{p}$	Puls. Stress $10^{-3}S$	Life $10^{-3}N$	Parameters $\frac{Rh}{a^2}$	$\frac{b}{a}$	$\frac{a^2}{10^2h^2}$	$\frac{10^6bh^3}{a^4}$
500	- 183	41.5	-	-	-	338 x105	E	-	-	13	-	.31	.65	580
"	- 184	48	-	-	-	335 x101	E	-	-	32	-	.30	.49	890
"	- 185	47	-	-	-	334 x104	E	-	-	46	-	.31	.51	870
"	- 186	48	-	-	-	333 x105	E	-	-	88	-	.32	.48	960
"	- 187	48	-	-	-	335 x105	E	-	-	120	-	.31	.49	920
"	- 188	48	-	-	-	- x101	E	-	-	46	-	-	-	-
"	- 189	48	-	-	-	- x102	E	-	-	52	-	-	-	-
"	- 190	48	-	-	-	- x105	E	-	-	52	-	-	-	-
"	- 191	49	-	-	-	339 x 91	E	-	-	49	-	.27	.48	810
"	- 192	41	-	-	-	342 x 94	E	-	-	14	-	.27	.69	470
#183,188,189 and 190 are "double tubes".														
1000	C 193	57.5	PB	2.25*	300*	380 x131	E	190	101	58	.90	.34	.44	1190
"	C 194	66	PB	"	"	375 x128	E	190	78	61	1.06	.34	.32	1900
"	C 195	68	PB	"	"	376 x126	E	190	78	63	1.11	.34	.31	1970
"	C 196	55	PB	"	"	337 x 95	E	390	101	6	1.09	.28	.37	1230
"	C 197	56	PB	"	"	335 x 97	E	390	99	7	1.12	.29	.36	1380
"	C 198	56	PB	"	"	335 x 98	E	390	99	7	1.12	.29	.36	1390
"	C 199	57	PB	"	"	336 x 91	E	390	96	10	1.04	.27	.35	1330
"	C 200	54	PB	"	"	336 x 96	E	390	107	10	1.08	.29	.39	1190
"	C 201	56	PB	"	"	336 x 94	E	390	100	11	1.12	.28	.36	1270
"	C 202	59	PB	"	"	333 x 94	E	-	90	19	1.20	.28	.32	1570
"	C 203	57.5	PB	"	"	332 x 93	E	-	94	20	1.17	.28	.33	1470
"	C 204	58	PB	"	"	331 x 93	E	280	90	30	1.19	.28	.32	1480
"	C 205	60	PB	"	"	329 x 93	E	280	84	30	1.17	.28	.30	1660
"	C 206	59	PB	"	"	329 x 93	E	170	86	35	1.16	.28	.31	1660
"	C 207	59	PB	"	"	330 x 93	E	280	88	37	1.22	.28	.31	1660
"	C 208	51	PB	"	"	333 x108	E	260	108	5	1.03	.32	.43	1160
"	C 209	51	PB	"	"	336 x106	E	190	109	6	1.02	.32	.43	1090
"	C 210	50	PB	"	"	334 x107	E	360	110	9	1.01	.32	.44	1070
"	C 211	51	PB	"	"	335 x108	E	340	108	25	1.02	.32	.43	1150
"	C 212	51	PB	"	"	334 x108	E	360	108	28	1.03	.32	.43	1150
"	C 213	48	PB	"	"	288 x 80	E	390	105	6	1.31	.28	.36	1260
"	C 214	40	PB	"	"	292 x 86	E	390	142	6	1.06	.29	.53	760
"	C 215	40	PB	"	"	291 x 90	E	410	137	16	1.06	.31	.53	810
"	C 216	47	PB	"	"	283 x 82	E	360	104	21	1.32	.29	.36	1320
"	C 217	40	PB	"	"	291 x 89	E	390	137	21	1.06	.31	.53	800
"	C 218	55	PB	"	"	331 x101	E	230	96	7	1.13	.30	.36	1390
"	C 219	56	PB	"	"	330 x102	E	230	95	23	1.16	.30	.35	1430
"	C 220	57	PB	"	"	330 x100	E	190	90	29	1.18	.30	.33	1590
"	C 221	58	PB	"	"	329 x100	E	210	88	36	1.21	.30	.32	1690
"	C 222	58	PB	"	"	329 x100	E	210	88	40	1.21	.30	.32	1690
"	C 223	60	PB	"	"	332 x 96	E	210	88	15	1.22	.29	.31	1700
"	C 224	59	PB	"	"	332 x 98	E	210	89	20	1.20	.29	.32	1640
"	C 225	59	PB	"	"	331 x 98	E	210	92	35	1.21	.30	.33	1560
"	C 226	64	PB	"	"	367 x125	E	180	81	25	1.07	.34	.33	2280
"	C 227	68	PB	"	"	365 x125	E	150	73	49	1.15	.34	.29	2280
"	C 228	68	PB	"	"	365 x125	E	170	73	47	1.15	.34	.29	2860
"	C 229	73	PB	"	"	361 x124	E	130	62	20	1.26	.34	.24	2860
"	C 230	74	PB	"	"	363 x122	E	150	62	20	1.26	.34	.24	2800

#193 to 230 are phosphor bronze; assume $E=15.5\times10^6$ psi; $\Delta\phi/\phi$ based on Δy; #208 to 212 were heat treated.

TABLE *(continued)*

Specimen			Stock		Coil		Section	Press. Sens.	Puls. Stress	Life	Parameters			
p	#	h	Mtl.	R_o	ø	a	b	$\frac{-\Delta ø}{ø}\frac{E}{p}$	$10^{-3}S$	$10^{-3}N$	$\frac{Rh}{a^2}\cdot\frac{b}{a}$		$\frac{a^2}{10^2h^2}$	$\frac{10^6bh^3}{a^4}$
1000	C 231	46	CM	2.25*	300*	238 x 94	E	180	180	10	1.8	.39	.27	2810
1000	C 232	43,45	CM	"	"	240 x 93	E	190	197	10	1.7	.39	.30	2400
3000	C 233	24*	BC	.841*	255*	127*x	48*E	-	-	-	1.2	.38	.28	2400
3000	C 234	24*	BC	.837*	252*	125*x	50*E	-	-	-	1.3	.40	.27	3000
300	C 235	18*	PB	.848*	249*	188*x	52*-	-	-	-	.44	.28	1.09	260
200	C 236	16*	PB	.842*	249*	189*x	53*E	-	-	-	.36	.28	1.40	154
200	C 237	20*	Bz	.845*	249*	250*x	55*E	-	-	-	.26	.22	1.56	105
200	C 238	19*	Bz	1.13*	220*	183*x	49*E	-	-	-	.64	.27	.93	297
200	C 239	16*	Bz	.663*	219*	252*x	61*F	-	-	-	.17	.24	2.48	61
400	H 240	14*	Bz	.850*	600*	117*x	31*F	-	-	-	.84	.26	.70	400
100	C 241	10*	Bz	.742*	257*	187*x	27*E	-	-	-	.20	.14	3.5	19
65	C 242	8*	Bz	.800*	257*	185*x	47*E	-	-	-	.19	.25	5.4	20
25	C 243	8*	Bz	.829*	275*	298*x	59*-	-	-	-	.07	.20	13.9	3.1
20	C 244	10*	Bz	.829*	275*	297*x	58*-	-	-	-	.09	.20	7.6	6.3
275	H 245	6*	S	.390	See	99*x	27*F	2000			.24	.27		61
2000	H 246	15.7*	S	.390	Note	109*x	35*F	330			.52	.32		960
3000	H 247	16*	S	.390	Below	107*x	37*F	275			.54	.35		1155
4360	H 248	20.5*	S	.380		109*x	37*F	131			.66	.34		2260
9250	H 249	26.5*	S	.380		111*x	42*F	62			.82	.38		5150
100	H 250	12	PB	.781	1800	185 x	27 F	3440			.27	.15	2.38	40
200	H 251	16	PB	.781	1800	185 x	25 F	1890			.37	.14	1.34	88
400	H 252	20	PB	.781	1800	182 x	23 F	1030			.47	.13	.83	168
600	H 253	24	PB	.781	1800	180 x	20 F	665			.58	.11	.56	263
1000	H 254	25	BC	.781	1800	170 x	20 F	686			.68	.12	.46	374
300	H 255	16	CRS	.781	1800	180 x	15 F	2335			.39	.08	1.26	58
800	H 256	24	CRS	.781	1800	175 x	20 F	654			.61	.11	.53	295

231,232 are chrome molybdenum steel; assume E=28.5x10^6 psi; $\Delta ø/ø$ based on Δy; inner wall .045, outer wall .043. # 54 to 232 were pulsed at 120 cpm, with arrangements to prevent tubes from heating at tip end. Internal radius at end of major diameter of section is changed by suppliers when forming tube, to give performance desired.

#245-249 from Wolf (9), 30 to 40 turn helices.

#250-253 are phosphor bronze grade A: Cu 95, Sn 5, Pb .035; E=15.5x10^6; Rockwell B80. Formed and has silver soldered fittings; then stress relieved 8 hours at 300°F.

#254 is beryllium copper: Be 1.70 to 1.90, Ni+Co .60, balance Cu. E=18.5x10^6; 1/4 hard (Rockwell B 70 to 75). Formed and has silver soldered fittings; then is heat treated 3 hours at 600°F. Hardness after heat treatment, Rockwell C 35.

#255,256 are type 316 stainless steel: Cr 17, Ni 13, Mo 2.5. E=28x10^6; Rockwell B 80. Formed and has welded fittings; then is stress relieved 8 hours at 600°F.

Acknowledgment

For the painstaking work of reducing these data and plotting the graphs, acknowledgment is due in part to Mr. Jenny of the subcommittee, and in larger part to Leonard Mordfin, Robert Czorny, and Nazz Viola, of the Engineering Mechanics Section, National Bureau of Standards, whose assistance was secured by financial support to RCMPE from Engineering Foundation, Inc.

Thanks are due J. R. Keim, secretary of RCMPE, for the correction of major errors in Table 1 of the preprint.

Bibliography

1 "Die Bewegungslehre von Rohrenfedern," by W. Wuest, *Zeitschrift für Instrumentenkunde*, vol. 63, 1943, pp. 416–428.

2 "A Dimensional Analysis Approach to Bourdon Tube Design," by K. Goitein, *Instrument Practice*, vol. 6, 1952, pp. 748–755.

3 "Theories on Pressure Measurement With Bourdon Tubes," by F. B. Jennings and J. T. Duane, unpublished report, General Electric Company.

4 "Bibliography on Bourdon Tubes & Bourdon Tube Gages," by L. Van der Pyl, ASME Paper 53–IRD-1, September, 1953.

5 "Theories on Bourdon Tubes," by F. B. Jennings, report to RCMPE, June 21, 1954, and ASME paper 54—A-168, published in this issue, pp. 55–64.

6 "Selecting and Working Bourdon-Tube Materials," by J. B. Giacobbe and A. M. Bounds, *Instrument Manufacturing*, vol. 20, 1952, pp. 130–132, 136–137.

7 "Stress and Deformations of Toroidal Shells of Elliptical Cross Sections," by R. A. Clark, T. I. Gilroy, and E. Reissner, *Journal of Applied Mechanics*, Trans. ASME, vol. 74, 1952, pp. 37–48.

APPENDIX C

COMPUTER PROGRAM - FOR TABLES 5.6, .7, .8, .9

Symbols Used in Program

Fortran	Theory
X(I)	Values of ratio a/b of Table 3.1
YA(I), YB(I)	Values of α and β of Table 3.1
NT	Number of test data
NTUBE	Tube identification or no.
PR	Pressure, psi
B	Semi-major axis of tube cross-section, inch
A	Semi-minor axis of tube cross-section, inch
T	Tube wall thickness, mils
R	Tube radius, inch
DEGREE	Central angle of tube, degree
POISN	Poisson's ratio,
E	Elastic modulus, psi
EXPT	Experimental sensitivity
DEFLEC	Tube and deflection (equation 3.9), inch
SENSI	Sensitivity (thin-walled, equation 3.7)
DEVIA	Percent deviation of SENSI from EXPT
SENS2	Sensitivity (thick-walled, equation 3.8)
DEVIA2	Percent deviation of SENS2 from EXPT

```
$JOB            003702 LEE EDWARD T     100    010    030
$IBJOB          NODECK
$IBFTC
      DIMENSION X(11),YA(11),YB(11),DA(11,2),DB(11,2)
C     DEFLECTION ANALYSIS OF THE BOURDON GAGE WITH A FLAT-OVAL CROSS
C     SECTION BASED ON MINIMIZATION OF POTENTIAL ENERGY AS PRESENTED IN
C     THE WORK OF L. E. ANDREEVA
C
C     COMPUTATIONS USING KARDOS' DATA
      L=11
      NDEL=2
C     VALUES OF X AND YA AND YB ARE READ
      READ (5,101) (X(I),I=1,L)
  101 FORMAT (11F5.0)
      READ (5,102) (YA(I),I=1,L)
  102 FORMAT (11F5.0)
      READ (5,102) (YB(I),I=1,L)
      LL=L-1
C     DIFFERENCE TABLES ARE CONSTRUCTED TO THE NDEL-TH DIFFERENCE
      DO 20 K=1,NDEL
      DO 10 N=1,LL
      IF (K .GT. 1) GO TO 9
      NN=N+1
      DA(N,K)=YA(NN)-YA(N)
      DB(N,K)=YB(NN)-YB(N)
      GO TO 10
    9 KK=K-1
      NN=N+1
      DA(N,K)=DA(NN,KK)-DA(N,KK)
      DB(N,K)=DB(NN,KK)-DB(N,KK)
   10 CONTINUE
      LL=LL-1
   20 CONTINUE
C     PARAMETERS ALPHA AND BETA WILL NOW BE DETERMINED USING EVERETT'S
C     INTERPOLATION FORMULA (NEGLECTING THIRD AND HIGHER ORDER DIFF.)
C     HEADINGS WILL NOW BE PRINTED
      WRITE (6,201)
  201 FORMAT (1X,4HTUBE,3X,1HP,4X,1HH,5X,1HR,4X,3HDEG,4X,1HB,5X,1HA,4X,
     13HA/B,2X,6HDEFLEC,2X,8HEXP SENS,2X,8HCAL SENS,1X,9HDEVIATION,1X,
     26HNSENS2,1X,6HDEVIA2,2X,3HA/R,2X,3HH/A,2X,3HB/A,3X,7HRH/B**2,3X,
     32HBR//)
      DO 500 NGAGE=1,NT
      READ (5,103) NTUBE,PR,T,B,A,R,DEGREE,POISN,E,EXPT
  103 FORMAT (I5,7F5.0,F10.0,F5.0)
   25 AB=A/B
      BA=B/A
      IF (BA .GT. 5.0) GO TO 34
      H=0.5
      IF (BA .GT. 1.5) GO TO 30
      P=(BA-X(1))/H
      Q=1.0-P
      ALPHA=Q*YA(1)+P*YA(2)-P*Q/2.0*DA(1,2)
      BETA=Q*YB(1)+P*YB(2)-P*Q/2.0*DB(1,2)
      GO TO 40
   30 IF (BA .GT. 2.0) GO TO 31
      P=(BA-X(2))/H
      Q=1.0-P
      ALPHA=Q*YA(2)+P*YA(3)-P*Q/2.0*DA(1,2)
      BETA=Q*YB(2)+P*YB(3)-P*Q/2.0*DB(1,2)
```

```
      GO TO 40
   31 H=1.0
      IF (BA .GT. 3.0) GO TO 32
      P=(BA-X(3))/H
      Q=1.0-P
      ALPHA=Q*YA(3)+P*YA(4)-P*Q/2.0*DA(3,2)
      BETA=Q*YB(3)+P*YB(4)-P*Q/2.0*DB(3,2)
      GO TO 40
   32 IF (BA .GT. 4.0) GO TO 33
      P=(BA-X(4))/H
      Q=1.0-P
      ALPHA=Q*YA(4)+P*YA(5)-P*Q/2.0*DA(4,2)
      BETA=Q*YB(4)+P*YB(5)-P*Q/2.0*DB(4,2)
      GO TO 40
   33 IF (BA .GT. 5.0) GO TO 34
      P=(BA-X(5))/H
      Q=1.0-P
      ALPHA=Q*YA(5)+P*YA(6)-P*Q/2.0*DA(4,2)
      BETA=Q*YB(5)+P*YB(6)-P*Q/2.0*DB(4,2)
      GO TO 40
   34 H=1.0
      IF (BA .GT. 6.0) GO TO 35
      P=(BA-X(6))/H
      Q=1.0-P
      ALPHA=Q*YA(6)+P*YA(7)-P*Q/2.0*DA(5,2)
      BETA=Q*YB(6)+P*YB(7)-P*Q/2.0*DB(5,2)
      GO TO 40
   35 IF (BA .GT. 7.0) GO TO 36
      P=(BA-X(7))/H
      Q=1.0-P
      ALPHA=Q*YA(7)+P*YA(8)-P*Q/2.0*DA(7,2)
      BETA=Q*YB(7)+P*YB(8)-P*Q/2.0*DB(7,2)
      GO TO 40
   36 IF (BA .GT. 8.0) GO TO 37
      P=(BA-X(8))/H
      Q=1.0-P
      ALPHA=Q*YA(8)+P*YA(9)-P*Q/2.0*DA(7,2)
      BETA=Q*YB(8)+P*YB(9)-P*Q/2.0*DB(7,2)
      GO TO 40
   37 IF (BA .GT. 9.0) GO TO 38
      P=(BA-X(9))/H
      Q=1.0-P
      ALPHA=Q*YA(9)+P*YA(10)-P*Q/2.0*DA(8,2)
      BETA=Q*YB(9)+P*YB(10)-P*Q/2.0*DB(8,2)
      GO TO 40
   38 IF (BA .GT. 10.0) GO TO 39
      P=(BA-X(10))/H
      Q=1.0-P
      ALPHA=Q*YA(10)+P*YA(11)-P*Q/2.0*DA(9,2)
      BETA=Q*YB(10)+P*YB(11)-P*Q/2.0*DB(9,2)
      GO TO 40
   39 ALPHA=.267
      BETA=.114
   40 GAMA=DEGREE/(180.0/3.14159)
      NDEGRE=DEGREE
C     CONVERT UNITS TO INCHES
      T=T*0.001
      CC=(1.0-COS(GAMA))**2
```

```
      SS=(GAMA-SIN(GAMA))**2
      G=(CC+SS)**0.5
      XX=R*T/(B**2)
      D1=(1.0-POISN**2)/E
      D2=R**3/(A*T)*(1.0-1.0/(BA**2))
      D3=G*ALPHA/(BETA+XX**2)
      DEFLEC=PR*D1*D2*D3
      SENSI=R**2/(A*T)*(1.0-1.0/(BA**2))*ALPHA/(BETA+XX**2)
      BR=B/R
      AR=A/R
      HA=T/A
      NPR=PR
      NSENSI=SENSI
      DEVIA=(FLOAT(NSENSI)-EXPT)*100.0/EXPT
      NEXP=EXPT
C     CALCULATIONS FOR THICK WALLED CROSS SECTIONS
C     VALID FOR LARGE AXIS RATIOS, B/A
      C=(3.0/(R**2*T**2))**.25
      CB=C*B
      SH=SINH(CB)
      CH=COSH(CB)
      SI=SIN(CB)
      CO=COS(CB)
      CX=1.0/CB*(SH**2+SI**2)/(SH*CH+SI*CO)
      SENS2=R**2/(A*T)*(1.0-CX)/(CX+T**2/(12.0*A**2))
      NSENS2=SENS2
      DEVIA2=(FLOAT(NSENS2)-EXPT)*100.0/EXPT
C     RE-CONVERT UNITS TO MILS
      T=T*1000.0
      WRITE (6,205) NTUBE,NPR,T,R,NDEGRE,B,A,AR,DEFLEC,NEXP,NSENS
     1I,DEVIA,NSENS2,DEVIA2,AR,HA,BA,XX,BR
  205 FORMAT (1X,I4,I5,F5.1,F7.3,I5,F6.3,F7.4,F7.4,F6.3,I8,I10,F10.1,
     1I8,F7.1,F6.3,F6.3,F6.2,F8.4,F7.4)
  500 CONTINUE
      STOP
      END
$ENTRY
1.0001.5  2.0  3.0  4.0  5.0  6.0  7.0  8.0  9.0  10.0
 .637 .594 .548 .480 .437 .408 .388 .372 .360 .350 .343
 .096 .110 .115 .121 .121 .121 .121 .120 .119 .119 .118
 1001  100 34.0 .125 .031 .798  217  .28  27       70.5
 1003  100 34.0 .127.0265 .792  192  .28  27       86.4
 1101  100 32.0 .125.0315 .795  221  .28  27       83.5
 1102  100 32.0 .128 .025 .790  224  .28  27      122.5
 1103  100 32.0 .123.0355 .801  217  .28  27       87.1
 1201  100 19.0 .128 .049 .805  220  .28  27      342.
 1202  100 19.0 .131.0455 .807  223  .28  27      379.
 1204  100 19.0 .137.0315 .791  236  .28  27      602.
 1205  100 19.0 .139.0255 .792  228  .28  27      743.
 1501  100 30.0 .123.0355 .799  223  .28  27       94.8
 1502  100 30.0 .125 .031 .795  237  .28  27      110.
 1601  100  8.0 .137 .044 .797  229  .28  27     3570.
 1602  100  8.0 .144.0335 .806  191  .28  27     5400.
 1701  100 14.5 .137 .037 .798  238  .28  27      939.
 1702  100 14.5 .139.0327 .794  234  .28  27     1210.
 2001  100 11.5 .140.0363 .792  231  .28  27     1840.
 2002  100 11.5 .138.0417 .792  225  .28  27     1468.
 2101  10010.0 .143 .035 .790   227  .28  27     3000.
```

Example Data

```
 2102   10010.0   .148  .025  .783   235   .28   27        4900.
 2103   10010.0   .140  .040  .797   226   .28   27        2890.
 2105   10010.0   .145 .0305  .810   218   .28   27        3415.
 2106   10010.0   .152  .019  .791   236   .28   27        5610.
 2107   10010.0   .136 .0445  .797   208   .28   27        1992.
 2801   100 22.0  .132  .026  .831   224   .25   15         309.
 2802   100 22.0  .132  .031  .834   226   .25   15         256.
 3001   100 15.0  .135 .0275  .807   226   .25   15         911.
 3002   100 15.0  .137 .0230  .822   228   .25   15        1112.
 3101   100 18.0  .139 .0195  .825   222   .25   15         793.
 3102   100 18.0  .137 .0285  .822   223   .25   15         493.
 3301   100 12.5  .141  .021  .818   205   .25   15        2500.
 3302   100 12.5  .138  .026  .825   224   .25   15        1838.
$IBSYS
```